FRIVET: *fim* Recombinase *in vivo* Expression Technology

Robert J O Quantrell

Ph.D

University of Edinburgh

2007

Declaration

I hereby declare that this thesis has been composed by myself and has not been accepted in any previous applications for a degree at this or any other university. The work described herein has been performed by me, except where expressly indicated otherwise. All sources of information have been specifically acknowledged, and verbatim extracts have been distinguished.

10th December 2007

Abstract

Classic techniques designed to understand bacterial gene regulation *in vitro* are still used today to elucidate genetic mechanisms and pathways. However as much as we can learn from *in vitro* studies of bacterial behaviour, it is impossible to fully recreate the complex and multifaceted environment the bacterium faces *in vivo*. To this end the development of techniques to allow us to study gene regulation *in vivo* is important as these can then be applied to dissect bacterial pathogenesis and should uncover novel therapeutic targets.

Recombinase *in vivo* expression technology (RIVET) provides a heritable irreversible marker of gene activity in the host and has been applied recently to discover genes important for bacterial virulence in the host. The aim of this project was to develop a novel RIVET system using genes from the enterohaemorrhagic *Escherichia coli* O157:H7 (EHEC) *fim* operon and the beta-lactamase reporter gene (*bla*). This system was named FRIVET (*fim* recombinase *in vivo* expression technology)

The basis to FRIVET is a completely synthetic operon placed in single copy in the EHEC chromosome at the *fim* locus. The arabinose (*ara*) inducible promoter was tested in the system initially to validate the system *in vitro*. The key aim of these *in vitro* tests was to understand the working tolerances of the FRIVET operon and define appropriate control points. Emphasis was placed on 'setting' the system and controlling the levels of recombination achieved.

Construction of the FRIVET operon on allelic exchange vectors and subsequent exchange into a Shiga-like toxin negative EHEC strain was successful. *In vitro* tests using the *ara* promoter proved the system functioned as intended and was experimentally stable. When EHEC promoters, in particular *LEE5*, were tested *in vitro*, considerable difficulty was encountered in controlling levels of recombination and setting the system to the off status. This is essential for any use of the system to examine gene expression *in vivo*. Therefore the emphasis of future work must be on defining appropriate measures for controlling *in vitro* activity of chosen promoters when preparing constructs for *in vivo* challenges.

With appropriate modifications the FRIVET system has the potential to produce valuable data about EHEC gene expression in the host and therefore to contribute to our understanding of the complex regulation required to establish colonisation, maintain infection and induce pathology *in vivo*.

Abbreviations

A/E – Attaching and effacing

cat – Chloramphenicol acetyltransferase

Cif – Cycle inhibition factor

CT – Cholera toxin

efa-1 – EHEC *f*actor for adherence

EHEC – Enterohaemorrhagic *Escherichia coli*

EPEC – Enteropathogenic *Escherichia coli*

ETT2 - *E. coli* type III secretion system 2

FAE – Follicle associated epithelium

FRIVET – *fim* recombinase *in vivo* expression technology

Gb3 – Globotriaosylceramide

GI – Gastrointestinal

HC – Haemorrhagic colitis

HUS – Haemolytic uraemic syndrome

i.v.i – *in vivo* induced

IHF – Integration host factor

IVET – *in vivo* expression technology

LEE – Locus of enterocyte effacement

ler – LEE encoded regulator

LFR – Left flanking region

LPF – Long polar fimbriae

Lrp – Leucine responsive regulatory protein

Map – Mitochondrial associated protein

nle – Non LEE encoded

N-WASP - Neural Wiskott-Aldrich syndrome protein

ORF – Open reading frame

PCR – Polymerase chain reaction

RBS – Ribosome binding site

RFR – Right flanking region

RIVET – Recombinase *in vivo* expression technology

SAP – Shrimp alkaline phosphatase

SIVET – Selectable *in vivo* expression technology

STM – signature tagged mutagenesis

Stx – Shiga-like toxin

T3SS – Type III secretion system

TCP – Toxin co regulated pilus

TIR – Translocated Intimin receptor

TR – Terminal Rectum

TTP - Thrombocytopaenic purpura

UPEC – Urinary pathogenic *Escherichia coli*

Acknowledgements

I would like to thank Dr David Gally for his advice, support and direction during the production of this thesis and Dr Andrew Roe for his time and effort spent monitoring my work in the laboratory. I would also like to thank the various members of the ZAP lab who have helped in many areas and made my time there so much more enjoyable. I am also extremely grateful to Nicola, for providing moral support and motivation.

Table of Contents

List of Figures

List of Tables

Chapter 1

Introduction

Introduction overview

The introduction to this thesis will be divided into three distinct sections. Section 1.1 will outline *Escherichia coli* O157:H7; its pathogenesis and the major virulence factors deployed in its natural host as a commensal and in humans as a pathogen. Section 1.2 will focus on the *fim* operon, an important fimbrial cluster in uro-pathogenic *Escherichia coli*. The FRIVET system is constructed using a number of important genes from the *fim* operon. Section 1.3 describes *in vivo* expression technology and its evolution over the past decade. Section 1.4 outlines the *fim* recombinase *in vivo* expression technology (FRIVET) system and details its construction methods and uses. Section 1.5 summarises the main aims of the thesis.

1.1.1 – *Escherichia coli* O157:H7

Escherichia coli O157:H7 is a serotype of Enterohaemorrhagic *Escherichia coli* (EHEC) responsible for sporadic outbreaks of gastro-intestinal disease in humans. It was first identified and associated with human disease in 1982 in an outbreak in the USA (Riley *et al,* 1983). Since then outbreaks of haemorrhagic colitis (HC) and diarrhoea associated with *E. coli* O157:H7 have occurred mainly in Europe, Japan and North America and *E. coli* O157:H7 has emerged as a major cause of diarrhoeal illness and paediatric renal failure. *E. coli* O157:H7 associated deaths are thought to be in the region of 60 from 74,000 cases per annum (Mead *et al*, 1999).

The main routes of infection are faecal contamination of food or dairy products, direct contact with colonised ruminants and water supply contamination. The largest *E. coli* O157:H7 outbreak to date occurred in Sakai, Japan in 1996 with over 6000 school children infected. The outbreak was associated with faecal contaminated white radish sprouts from a single farm (Michino *et al,* 1999). However, person to person spread can also occur in outbreaks (Naylor *et al*, 2005). Patients that develop HC can develop more

serious sequelae such as haemolytic uraemic syndrome (HUS) and thrombocytopaenic purpura (TTP). The prevalence of HUS appears to be higher in the young and the elderly. The natural reservoir of *E. coli* O157:H7 is the ruminant, and recently the terminal rectum (TR) has been identified as a specific colonisation site of attachment for *E. coli* O157:H7 (Naylor *et al*, 2003). Experimental and natural infection studies in cattle results in the efficient colonisation of the intestinal tract and persistent shedding of *E. coli* O157:H7 in the faeces for several weeks post inoculation (Naylor *et al,* 2003; Wray *et al* 2000). Importantly, *E. coli* O157:H7 colonisation and infection in cattle seems to be asymptomatic except in very young calves (Dean-Nystrom *et al*, 1997).

To date the complete genome sequences of two *E. coli* O157:H7 strains have been reported. The first sequenced strain was isolated from the *E. coli* O157:H7 disease outbreak in 1983 termed *E. coli* O157 EDL933 (Perna *et al.*, 2001), the second sequenced strain was responsible for the large outbreak previously mentioned in Japan in 1996, termed *E. coli* O157 Sakai (Hayashi *et al.*, 2001).

The molecular mechanisms utilised by *E. coli* O157:H7 to colonise the ruminant host are not fully understood to date. *E. coli* O157:H7 is able to form distinct attaching and effacing lesions (A/E) on tissue culture cells (Nataro and Kaper, 1998) and intestinal epithelium *in vitro* (Phillips *et al,* 2000) characterised by localised clearance of brush border microvilli, actin cytoskeleton recruitment, pedestal formation and intimate bacterial attachment. Recent studies have also demonstrated that *E. coli* O157:H7 forms A/E lesions at the TR site of colonisation (Naylor *et al*, 2005). Important virulence factors involved in this process will be discussed in detail below. Briefly, the intimate attachment seen in A/E lesions is a result of a translocated effector protein inserting itself into the host cell membrane and acting as a receptor for the bacterial adhesin, intimin. As a consequence of this interaction the effector protein was termed the translocated intimin receptor (Tir). Studies have shown that (a) Intimin is an important adhesin for colonisation in a variety of ruminant models (Cornick *et al,* 2002; Dean-Nystrom *et al*, 1998; Woodward *et al*, 2003) and (b) mutations in Tir impact on calf colonisation (Vlisidou *et al*, 2006), suggesting a vital role for these proteins in

ruminant colonisation and a strong link between the formation of A/E lesions and ruminant persistence. Other T3SS secreted proteins and their role in host colonisation and pathogenesis will be discussed below.

The importance of other bacterial proteins in *E. coli* O157:H7 host persistence continues to be elucidated. Conflicting data on the importance of ToxB, a homologue of Efa1(EHEC factor for adherence) from EHEC O111:H-, as an important colonisation factor on cultured epithelial cell lines but not in ruminant infection studies has been published (Stevens *et al*, 2004; Tatsuno *et al*, 2001). Much of the work into *E. coli* O157:H7 genes involved in colonisation has focused on a small subset of potentially important virulence genes encoding a bacterial type III secretion system (T3SS) and an array of regulators, effectors and adhesins. Recently, a signature tagged mutagenesis study revealed 59 genes required for intestinal colonisation in young calves, many of which associated with the T3SS. *E. coli* O157:H7 appears to contain 2 distinct sets of genes encoding the structural genes for a T3SS:

- The LEE - Locus of Enterocyte Effacement
- ETT2 – *E. coli* type III secretion system 2

The importance of the LEE in *E. coli* O157:H7 pathogenesis is well documented and will be discussed below. The function of ETT2 however is less well understood. Although it appears to be non-functional as a T3SS, studies have shown that mutations in ETT2 regulatory genes appear to upregulate genes on the LEE (Zhang *et al,* 2004). This indicates a level of cross talk between regulators from distinct gene clusters.

1.1.2 – The Locus of Enterocyte Effacement (LEE)

The formation of A/E lesions by *E. coli* O157:H7 is a complex process with multiple levels of regulation. The translocation of key effector proteins responsible for the A/E histopathology is carried out by the T3SS. Bacterial T3SS utilise a multiprotein basal

apparatus spanning the inner and outer membranes, and a 'needle' complex, extending from the basal apparatus, which injects proteins into the host cell. The genes encoding the *E. coli* O157:H7 T3SS are contained on a 43kb pathogenicity island termed the Locus of Enterocyte Effacement (LEE). The LEE was first described in Enteropathogenic *E. coli* (EPEC) (McDaniel *et al*, 1995) and was sequenced shortly afterwards (Elliot *et al*, 1998). The *E. coli* O157:H7 LEE contains a substantially lower GC content (39% vs. 51%) than the rest of the *E. coli* O157:H7 chromosome suggesting the acquisition of the LEE by horizontal gene transfer (Khan *et al*, 2003). Although similar in structure and function there are two main differences associated with the EPEC LEE and the *E. coli* O157:H7 LEE. Firstly studies have shown the cloned LEE from EPEC confers the ability to form A/E lesions in *E. coli* K12 but the LEE from *E. coli* O157:H7 is unable to confer this ability to the same strain (Elliot *et al,* 1999). Additionally the *E. coli* O157:H7 LEE is larger than its EPEC version due to the presence of a 7.5kb prophage at the right hand end (Perna *et al*, 1998). The importance of this prophage in determining the regulation of the *E. coli* O157:H7 LEE is yet to be elucidated.

A total of 41 open reading frames (ORF's) have been discovered in the *E. coli* O157:H7 LEE (Perna *et al,* 1998) and the majority are organised into 5 distinct operons: LEE1, LEE2, LEE3, LEE4 and *tir*. However other genes known to have a role in the formation of A/E lesions and the regulation of the LEE lie outwith this pathogenicity island and will be discussed below. The LEE is shown diagrammatically in Fig 1.1.

The LEE1, LEE2 and LEE3 operons contain the genes encoding the structural proteins required for the T3SS basal apparatus (Elliot *et al,* 1998). It has been postulated that *E. coli* O157:H7 can differentially regulate the LEE operons to create a 'primed' state, in which the bacterium produces the T3SS basal apparatus but represses the production of secreted effector proteins. The T3SS is represented diagrammatically in Fig 1.2.

Fig 1.1

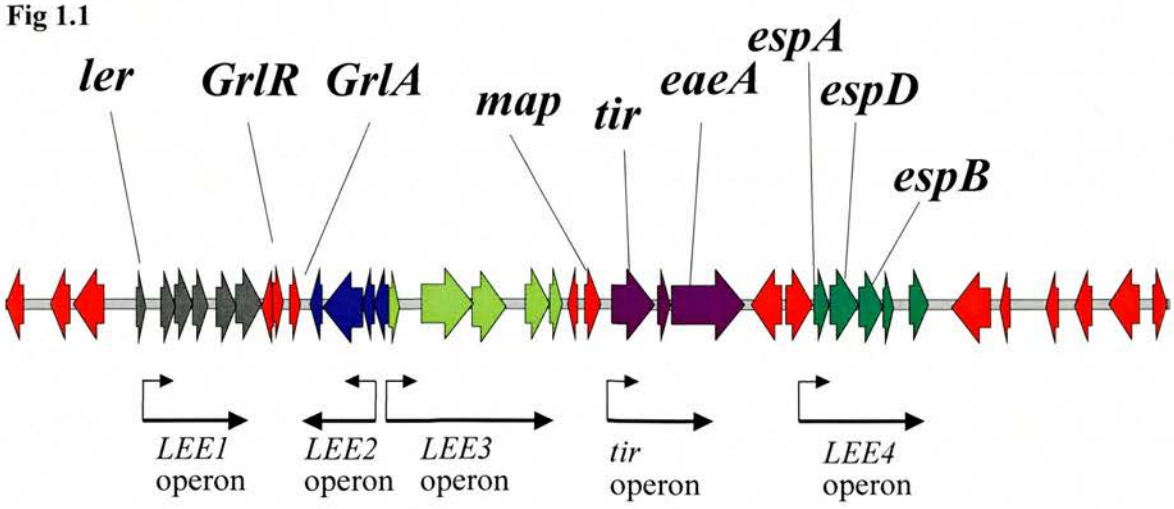

EDL933 LEE

Genetic organisation of the LEE pathogenicity island from *E. coli* O157:H7

1.1.3 – Ler – LEE Encoded Regulator

The first gene in the LEE1 operon is *ler* (LEE encoded regulator). Ler, an H-NS homologue, acts as a positive regulator of the LEE2, LEE3 and *tir* operons as well positively regulating its own expression by removing H-NS repression of the LEE, an action that seems to require GrlA and upstream IHF binding (Laaberki *et al,* 2006; Elliot *et al*, 2000; Bustamante *et al*, 2001; Mellies *et al*, 1999; Friedberg *et al*, 1999). It also seems that *ler* can respond to adverse environmental changes through the activity of the stress response sigma factor RpoS in conjunction with the non coding RNA DsrA (Laaberki *et al*, 2006) as well as the quorum sensing molecule QseA (Sperandio *et al*, 2002). The regulation of the LEE via *ler* is represented in Fig 1.3.

Fig 1.2

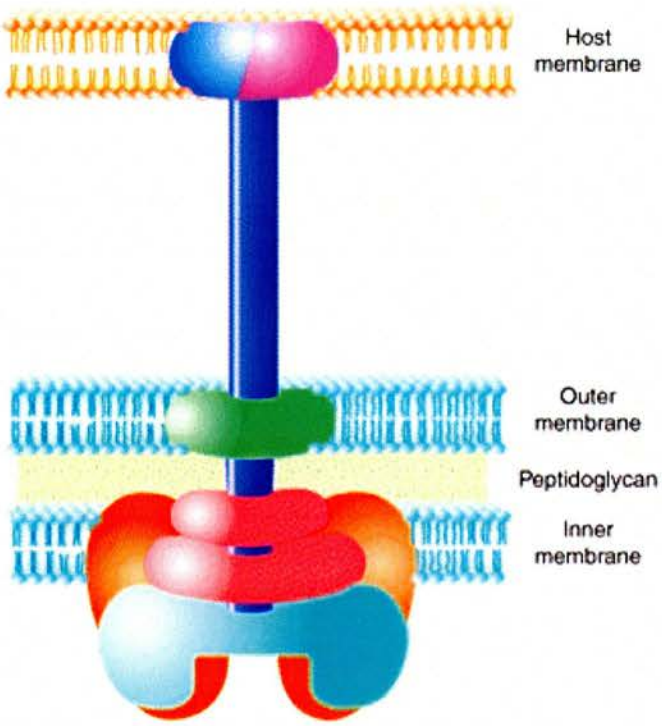

The type III secretion system (T3SS) from *E. coli* O157:H7. The basal apparatus and needle complex is comprised of proteins encoded by the LEE. The LEE also encodes translocated effector proteins that can be secreted through the needle complex and into the host cell. EspA forms a hollow protein filament extending from the needle complex. EspB and EspD form a pore in the host cell surface

Fig 1.3

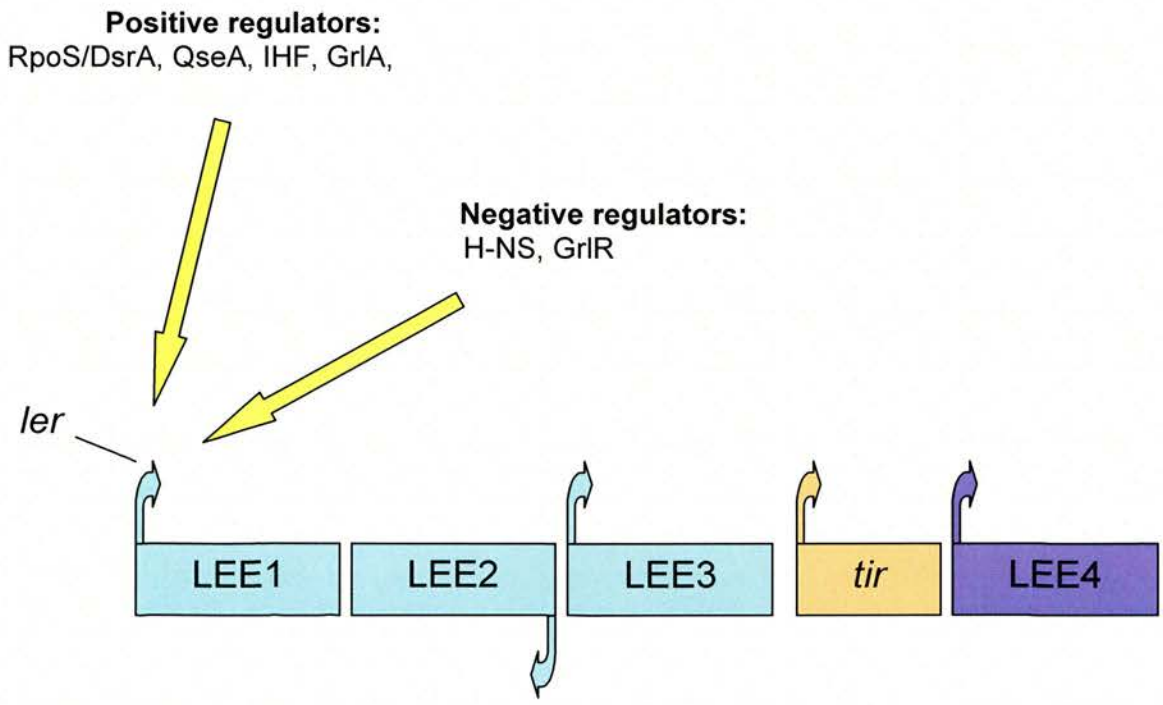

Positive and negative regulators of the *ler* gene. The yellow arrows represent factors that influence *ler* expression. The direct consequence of *ler* expression is the upregulation of the LEE1, LEE2 and LEE3 operons and the production of the T3SS. LEE4 and *tir* are also upregulated by Ler, although to a lesser extent than LEE1, LEE2 and LEE3.

1.1.4 – LEE4 Operon

The LEE4 operon encodes the translocated bacterial proteins EspA, EspD, EspB and EspF as well as the cytoplasmic protein SepL, and the T3SS needle complex protein, EscF. The EspA protein forms a hollow filament that elongates the needle complex on the T3SS and allows the efficient secretion of the other LEE4 translocated proteins EspB and EspD into the host cell (Knutton *et al*, 1998). EspB and EspD have been shown to be targeted to the host cell membrane by EPEC and EHEC and the proteins are thought to form a pore in the host cell membrane that completes the conduit from the bacterial T3SS

via the EspA filament through which translocated proteins can pass (Wachter *et al,* 1999, Wolff *et al*, 1998, Kresse *et al,* 1999, Daniell *et al,* 2001).

The *sepL, espA, espB* and *espD* genes are transcribed from a single promoter at *sepL* and the resultant RNA is subject to post-transcriptional regulation (Roe *et al* 2003). This post transcriptional control of LEE4 effector proteins was revealed by comparing transcription activity from the LEE4 promoter and the production of EspA filaments. Whilst the expression of the LEE4 promoter remained stable the expression of EspA filaments was heterogenous (Roe et al 2003). Additionally, *espADB* mRNA levels were measured and found to be inversely proportional to EspA and EspD production. That is, the cells secreting low amounts of EspA and EspD contained higher levels of *espADB* mRNA, providing further evidence of the post transcriptional control of LEE4.

It is clear therefore that the LEE4 operon is under an alternative control procedure to the LEE1,2,3 operons. This indicates a stratagem employed by the bacterium where the basal apparatus of the T3SS may be constructed already following Ler activation of the LEE1,2,3 operons but the secretion of effector proteins and the formation of the EscF needle and EspA hollow filament takes place at another time point and under different control. The use of *in vivo* expression technologies will help us to elucidate these levels of control.

1.1.5 – LEE5 Operon

The LEE5 operon comprises of the *tir*, *cesT* and *eae* genes encoding for the Tir, CesT and intimin proteins respectively and is transcribed from a single promoter at *tir* (Sanchez-SanMartin *et al*, 2001). Intimin is an outer membrane surface protein that binds to Tir on the surface of the host cell (Kenny *et al*, 1997).

There are at least five antigenically distinct subtypes of intimin: α, β, γ, δ, and ε, each exhibiting sequence variation in their C-terminal cell binding domains (Adu-Bobie *et al,*

1998) and tissue specific tropism (Reece *et al*, 2001). *E. coli* O157:H7 expresses Intimin γ, a subtype shown to effect tropism to follicle associated epithelium (FAE) in humans and cattle (Phillips *et al,* 2000; Naylor *et al*, 2003). Additionally the role of intimin as an adhesin for host cell receptors such as nucleolin (Sinclair and O' Brien, 2002) has been shown and there is speculation that intimin may act as the initial adhesin for *E. coli* O157:H7 colonisation in the host, although the mechanisms of intimin binding *in vivo* to host cell receptors is not well known. The 'middle' gene in the *tir* operon encodes the chaperone, CesT which has been shown to interact with Tir, enabling efficient transfer through the T3SS (Elliot *et al*, 1999; Creasey *et al* 2003)

Tir has been shown to be translocated into the host cell via the T3SS where it inserts into the host cell membrane and binds to intimin expressed on the bacterial cell surface The Intimin-Tir interaction is required for the subsequent actin cytoskeleton rearrangement and pedestal formation characteristic of A/E lesions (Kenny *at al,* 1997). Actin re-organisation proceeds as Tir couples with N-WASP (neural Wiskott-Aldrich syndrome protein), a process that requires the bacterial translocated protein, TccP (Tir-cytoskeleton coupling protein, aka $EspF_u$) (Campellone *et al,* 2004; Garmendia *et al,* 2004), although *in vivo* studies have shown that *tccP* mutants can form A/E lesions to some extent suggesting an alternative pathway for actin recruitment by Tir in the host cell (Vlisidou *et al*, 2006).

Tir has been shown to be essential for intestinal colonization in *E. coli* O157:H7 rabbit models (Ritchie *et al* 2003) bovine calf and lamb models (Vlisidou *et al,* 2006) and in rabbit EPEC models (Marches *et al* 2000). A recent study has shown that *E. coli* O157:H7 shows heterogenous expression of the *tir* operon and that the same subset of cells expressing *tir* also express intimin on their cell surface (Roe *et al*, 2004), this co-ordinate expression shows that intimin is only expressed on the cell surface when Tir is being produced, suggesting that the main function of intimin is an adhesin for Tir, and not as an initial adhesin for *E. coli* O157:H7 colonisation. Furthermore the same study showed that the subset of bacterial cells expressing *tir* were the same subset of cells that produced EspA filaments on their cell surface and furthermore, it is likely that factors

outside the LEE are responsible for this regulatory control (Roe *et* al, 2004). This provides important evidence that the expression of the LEE4 and the *tir* operons are co-ordinately controlled at the single cell level.

Interestingly, EPEC does not appear to exhibit the same heterogeneity of expression for LEE4 and *tir*, rather EPEC *tir* expression was homogenous for a given population. The differences in LEE4 and *tir* regulation between the two strains may be caused by the ETT2, which is present in *E. coli* O157:H7, but absent in EPEC (Roe *et al*, 2004).

1.1.6 – Map (mitochondrial-associated protein)

The *map* gene is transcribed from a different promoter to that of the *tir* operon (Kenny and Jepson, 2000). Map is a translocated effector protein, secreted into the host cell via the T3SS and the activity of CesT. In EPEC it has been shown to target the host cell mitochondria where it disrupts mitochondrion activity (Kenny and Jepson, 2000). The precise function of Map in *E. coli* O157:H7 pathogenesis *in vivo* is yet to be determined. Transcription studies in *E. coli* O157:H7 using *gfp* have shown the same heterogenous expression for *map* as for LEE4 and *tir*; however unlike LEE4 and *tir*, which appear to be co-ordinately controlled, the subpopulation expressing *map* was different to the subpopulation expressing LEE4 and *tir* (Roe *et al*, 2004) indicating different timing of *map* activation in the overall colonisation process. This result also indicates that *map* is under the control of a different regulatory pathway than *tir* and LEE4.

1.1.7 – Other LEE encoded effector proteins

Other translocated effector proteins encoded on the LEE include: EspF; EspH, EspG and EspZ/SepZ. EspF has shown to have a role in EPEC in disrupting barrier function in host cells and in inhibiting macrophage uptake (Quitard *et al*, 2006), however the role of EspF in *E. coli* O157:H7 is less clear (Viswanathan *et al*, 2004). Studies have shown a similar

function but redundancy of EspF via extra non LEE coded factors again highlighted the different modes of regulation for EPEC and *E. coli* O157:H7. EspH appears to play a key role in action cytoskeleton modulation (Tu, *et al*, 2003). EspG does not seem to be involved directly in A/E lesion formation but has shown to be responsible for disruption of the host cell microtubules (Shaw *et al*, 2005).

A role for EspZ (renamed from SepZ) in *E. coli* O157:H7 pathogenesis is yet to be determined, but in EPEC EspZ has been shown to be localized beneath pedestals in proximity to Tir. However, EspZ translocation is thought to occur after pedestal formation and is not essential for Tir activity (Kanack *et al*, 2005).

1.1.8 – Non-LEE encoded effector proteins

As well as the LEE encoded effectors, a variety of non LEE encoded virulence factors for *E. coli* O157:H7 and EPEC have been characterised. Cycle inhibition factor (Cif) has been shown to disrupt the host cell growth cycle and modulates the host cell actin cytoskeleton (Marches *et al*, 2003), but does not appear to be required for A/E lesion formation.

The *nleA* (Non-LEE encoded) gene is present in *E. coli* O157:H7 on a prophage and is not required for A/E lesion formation but seems to have a tropism to the host cell golgi apparatus (Gruenheid *et al*, 2004). Interestingly *nleA* was found to be present in 86% of clinical EHEC isolates (Mundy *et al*, 2004). The aforementioned TccP (EspFu) is also present on a prophage and recently another prophage encoded effector protein, EspJ was found to play a role in host persistence, but not A/E lesion formation (Dahan *et al* 2005). A recent study on the Sakai genome elucidated 39 putative Nle's (Tobe *et al*, 2006), indicating that *E. coli* O157:H7 has a large array of effector proteins, many as yet uncharacterised.

1.1.9 – *E. coli* O157:H7 adhesins

The precise role of adhesins in the pathogenesis of *E. coli* O157:H7 is still unclear. It is logical to presume that initial attachment to preferred tissue types or sites by *E. coli* O157:H7 may be mediated by fimbrial adhesins, with the formation of A/E lesions perhaps a direct consequence of bacterial binding. However as yet the fimbriae involved are unknown.

The sequencing of two *E. coli* O157:H7 strains has identified at least 16 putative fimbrial clusters. Some of these such as the type 1 fimbrial operon, are well characterised, and many clusters are at least partially conserved in other *E. coli* strains. In a recent study analysing *E. coli* O157:H7 fimbrial operons only four clusters were found that were specific to *E. coli* O157:H7 (Low *et al*, 2006). Of the four clusters, the functions of two are unknown. The remaining two clusters show similarity to the long polar fimbriae (LPF) described initially in *Salmonella enterica* serovar Typhimurium (S. Typhimurium) (Baumler and Heffron, 1995). LPF in S. Typhimurium have been shown to mediate attachment to the follicle associated epithelium (FAE) of murine Peyer's patches (Baumler *et al*, 1996). FAE is present at the terminal rectum of cattle, and therefore it may be possible that LPF in *E. coli* O157:H7 mediates initial binding to the FAE at this site but to date there is no evidence that this occurs *in vivo*.

A signature tagged mutagenesis (STM) study on *E. coli* O157:H7 in calves highlighted an *E. coli* O157:H7 gene showing homology to a fimbrial usher that lay within a cluster designated *loc8,* also shown to be important in calf colonisation (Dziva *et al*, 2004). A recent study has characterized this cluster (renamed F9) in *E. coli* O157:H7. Induction of F9 expression led to increased binding to bovine GI tissue for *E. coli* K12, but reduced binding for *E. coli* O157:H7, perhaps as a result of the induced F9 fimbriae interfering with T3SS formation and/or function (Low *et al*, 2006).

1.1.10 – Shiga Toxin

The main virulence factor for *E. coli* O157:H7 for human infections is shiga toxin (Stx) and it is this toxin that is responsible for the serious symptoms of *E. coli* O157:H7 infection such as HUS and HC (Nataro and Kaper, 1998). There are two types of Stx: Stx1 and Stx2 and both are encoded on lysogenic phages. This fact, coupled with the discovery that Stx can be detected in cattle faeces (Ball *et al*, 1994) seems to suggest a role for Stx in the successful colonisation of cattle, despite the apparent lack of pathogenicity shown by *E. coli* O157:H7 in this host. EHEC strains may carry and express only Stx1, only Stx2 or both. Stx toxins are compound toxins formed of a 32kDa 'A' subunit and a pentameric 'B' subunit made up of 7.7kDa monomers. The A subunit is the active domain entering the host cell and inhibiting protein synthesis and the B subunit mediates binding to specific receptors on the host and aids translocation of the toxin into the host cell (O'Loughlin and Robins-Browne, 2001).

Stx has been shown to bind to a specific glycolipid receptor: globotriaosylceramide (Gb3) on the host cell surface (Lingwood, 1996). As a result of this specific binding the distribution of Gb3 receptors is crucially important. The development of HUS in patients infected with *E. coli* O157:H7 is due to the renal damage caused by the shiga toxin and it is no surprise that renal tissue has a high concentration of Gb3 receptors. Significantly the different infection paths of *E. coli* O157:H7 in cattle and humans may be partly caused by variation in Gb3 receptor level expression. Studies have shown that while human intestinal tissue does not express high levels of Gb3, tissue types in the cattle intestinal tract have been shown to express Gb3 (Hoey *et al*, 2002). The expression of Gb3 at these sites in cattle may prevent dissemination of Stx to sub epithelial areas, exposing the host to Stx mediated tissue damage.

It is clear that Stx has an important role to play in both human disease and cattle colonisation. Key factors such as the distribution of Gb3 receptors and the different immunomodulatory effects shown by Stx between hosts may explain the differences seen in *E. coli* O157:H7 pathogenicity in cattle and humans. Recent work has indicated that

Stx increases *E. coli* O157:H7 binding in mice intestine (Robinson *et* al, 2006) and downregulates interleukin expression on bovine epithelial cells (Mahajan, A. personal communication). Studies indicate this could be due to an increase in a eukaryotic receptor for intimin (Robinson *et al*, 2006).

1.2.1 – The *fim* operon

Attachment to host tissue is a key step in bacterial pathogenesis. Bacterial pathogens have acquired a wide range of adhesins that can be expressed at the appropriate time during the infection process. *Escherichia coli* can produce over 15 different fimbrial adhesins depending on serotype and pathotype. In the case of uro-pathogenic *E. coli* (UPEC) adhesins are key virulence factors that allow the bacterium to bind specific receptors on the urinary epithelium and resist removal during urination. One of the main fimbrial adhesins associated with UPEC is type 1 fimbriae, which bind to α-D-mannose receptors and mediate binding and invasion of bladder epithelial cells (Martinez *et al*, 2000).

Bacterial cells have also been shown to express type 1 fimbriae at crucial stages of a murine model of cystitis, in a recent study cystitis strains mutated for type 1 fimbrial production were attenuated in a murine cystitis model (Snyder *et al,* 2006) and bacterial cells made constitutive for type 1 fimbriae were more pathogenic (Gunther *et al* 2002). Bacterial attachment via type 1 fimbriae has been shown to induce IL-8 secretion in mucosal cells, indicating a pro inflammatory response from the host to these organelles (Godaly *et al* 1998) and studies have provided a link between type 1 fimbrial expression and Crohn's disease (Boudeau *et al*, 2001).

Type 1 fimbriae, like many *E. coli* expressed fimbrial adhesins, exhibits phase variation. Phase variation means that at a particular point in time only a subset of the bacterial population will express the fimbriae leading to a heterogeneous population. The biological significance of this process for the bacterium is still a topic of debate. The

population as a whole can remain 'primed' for attachment at any one time without the danger of complete eradication by the host's immune defences. If the population was homogenous in either way, the bacteria may miss an opportunity to bind to host cells by not having the fimbriae expressed on their surface or alternatively may be cleared from the host completely if the entire population expressed the adhesin.

Type 1 fimbriae are encoded by the *fim* operon located at 98 minutes on the *E. coli* K-12 chromosome. *E .coli* O157:H7 possesses the *fim* operon but does not express the fimbriae due to a 16bp deletion in the *fimS* region (Roe *et al,* 2001). The *fim* operon is polycistronic, containing nine genes, seven of which encode for structural or export components (*fimAICDFGH*), the remaining two: *fimB* and *fimE*, encode site specific recombinases that regulate expression of the operon. In between the regulators and the structural genes is a 314bp invertible DNA element known as the *fim* switch that can be in the 'on' or 'off' orientation. Importantly, the *fim* switch contains a promoter at one end so that in one orientation (on) it can drive expression of downstream genes. FimB and FimE invert the *fim* switch and in the on orientation the *fimA-H* operon is expressed, whereas in the opposite (off) orientation the promoter points away from *fimA* and directs the transcription of a rapidly degraded antisense copy of *fimE*. The genetic organisation of the *fim* operon in the 'on' orientation is shown in Figure 1.4.

Fig 1.4

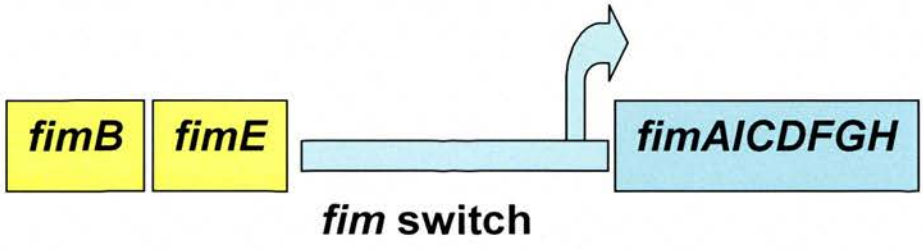

Genetic organisation of the *fim* operon on the *E. coli* chromosome. *fimB* and *fimE* are the site specific recombinase genes that regulate the orientation of the *fim* switch. The promoter embedded in the *fim* switch (shown here in the 'on' orientation) directs transcription of the downstream structural genes: *fimA-H*.

The inversion of the *fim* switch is under the direct control of the two site specific recombinases encoded by *fimB* and *fimE* (Klemm. 1986), the inversion from 'on' to 'off' is predominately controlled by FimE whereas FimB mediates inversion in both directions (Gally *et al.* 1996). FimB and FimE belong to the lambda integrase family of site specific recombinases and share 52% amino acid identity, indicating evolution from the same ancestor (Blomfield, 2001). Each recombinase contains a tetrad of conserved amino acids and mutations of these amino acids result in loss of activity (Burns *et al* 2000, Smith and Dorman, 1999).

In addition to the activity of the two recombinases, *fim* switch inversion is also controlled by two site specific DNA binding proteins: IHF (integration host factor) and Lrp (Leucine responsive regulatory protein) but inversion appears to be repressed by HNS (Spears *et al.* 1986). In rich culture media at 37^0C FimB mediated inversion occurs at a frequency of between 10^{-3} and 10^{-4} per cell per generation. FimE mediated inversion is much more frequent in the range of 0.3 per cell per generation (Gally *et al.* 1993) in rich media. Thus in *E. coli* K-12 MG1655 high frequencies of inversion from 'on' to 'off' result in a largely afimbriate population in the order of 3% (Blomfield *et al* 1993), however incubation in static culture selects for fimbriate bacteria that allow the bacterial population to form a pellicle, or surface layer, using cell-cell type 1 fimbriae-mediated binding.

The *fim* switch invertible element is flanked by two 9bp inverted repeats, termed IRL and IRR. FimB and FimE bind to these half sites, and, via the formation of Holliday intermediates, catalyse the recombination of the *fim* switch. Other DNA binding proteins are important for this activity. IHF binds to two distinct sites within the *fim* region. The first site is near the IRR and is thought to introduce a sharp bend in the DNA bringing the inverted repeats closer together (Blomfield *et al* 1997). The second site is outwith the *fim* switch and is located between the IRL and the 3' end of *fimE*. As this site is not involved with DNA looping much speculation has arisen about its function. The effect of IHF binding to this site is thought to play a part in determining FimB specificity (Blomfield 2001) but inconsistencies in various studies attempting to elucidate this could be

attributed to HNS binding at a site overlapping with this IHF site as it is known that HNS does play a role in determining FimB specificity (O' Gara and Dorman, 2000).
Mutations in the *ihf* genes have a 15,000 fold effect on *fimE* mediated inversion compared to an 80 fold effect on *fimB* mediated inversion (Blomfield *et al* 1997), but interestingly mutations in the IHF binding sites have a similar effect for *fimB* recombination as with the mutation of the *ihf* genes, but show much less of an effect on *fimE* recombination. The binding sites of IHF are shown in Figure 1.5.

The other main DNA binding protein associated with *fim* inversion is Lrp. Inversion of the *fim* element is stimulated by branched chain amino acids particularly leucine and requires the binding/unbinding of Lrp to three sites within the *fim* switch (Gally *et al*, 1993, Roesch and Blomfield, 1998). The binding of Lrp to two sites (sites 1 and 2) activates FimB and FimE recombination in a similar manner to IHF by introducing bends in the DNA, but Lrp binding to the third site (site 3) has been shown to inhibit *fim* switching (Roesch and Blomfield, 1998). Studies have shown that leucine promotes the dissociation of Lrp from site 3, presumably to allow recombination in the presence of exogenous amino acids. Additionally, mutations in site 3 that prevent Lrp binding result in high levels of recombination, even in the absence of amino acids (Roesch and Blomfield, 1998) indicating a loss of amino acid regulation of *fim* switch inversion. The Lrp binding sites are shown in Figure 1.5.

The DNA binding protein, HNS, is an important element in the control of *fim* switching. Mutations in *hns* result in increased *fimE* and *fimB* transcription levels (Olsen *et al*, 1998; Olsen and Klemm, 1994) indicating HNS acts as an inhibitor of *fim* recombinase gene expression and HNS has been shown to bind to *fimE* and *fimB* promoter regions (Olsen *et al*, 1998). Studies have also shown that HNS represses the transcription of *lrp* (Oshima *et al*, 1995).

Fig 1.5

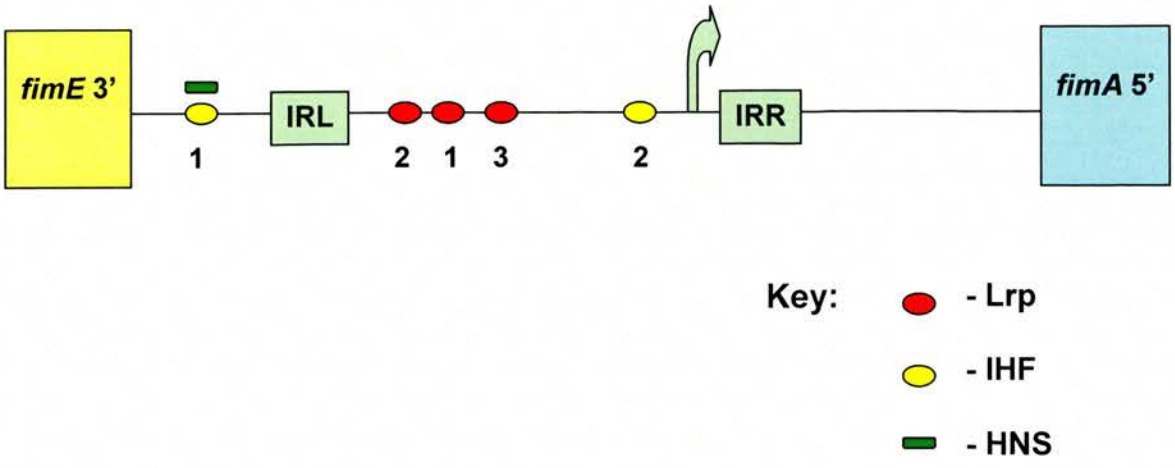

Binding sites of Lrp, IHF and HNS to the *fim* switch region. The *fim* switch is shown in the 'on' orientation.

It has been found that *fimB* has two distinct promoter sites (Schwan *et al,* 1994). The presence of two promoters could be strain specific. Additional levels of control of *fimB* expression have been found and lie far outside the characterised *fim* region. A recent study has shown the importance of the large (1.4kb) intergenic region upstream of *fimB* including the *yjhATS* operon. Researchers found distant 'cis' acting regulatory elements were essential in *fimB* expression. Mutations in various regions elucidated two regions lying over 500bp upstream of *fimB* that control FimB mediated recombination via repression of *fimB* expression. Additional sequences proximal to *yjhA* were also shown to be important (El-Labany *et al*, 2003).

N-acetylneuraminic acid (sialic acid) was also shown to suppress *fimB* expression (El-Labany *et al*, 2003). It is hypothesised that the bacterium recognizes and responds to sialic acid, by suppressing type 1 fimbrial production, therefore limiting potential clearance by the host immune system. Further research by the same group has shown the differential binding to regions 1 and 2 by two distinct regulators: NanR and NagC. NanR is responsive to sialic acid, whereas NagC is responsive to GlcNAc, a metabolite of sialic

acid. The two regulators have also been shown to provide methylation protection at both regions respectively (Sohanpal *et al*, 2004). Bacterial cells are unable to synthesise sialic acid, but can freely scavenge GlcNAc from the environment or synthesise it from sialic acid, alternatively the bacterium can recycle cell wall components including GlcNAc. Sialic acid is released as part of the host inflammatory response potentially providing the bacteria with a marker for the host immune response. Therefore signals arising from within the cell and from the environment are both part of the same regulatory circuit. The level of *fimB* transcription is tightly controlled as part of a complex regulation map in order to suppress the pro inflammatory response to the production of type 1 fimbriae. It seems logical that bacteria would have evolved to limit type 1 fimbrial expression to when necessary, i.e.when presented with the target receptor of choice.

The high frequency of FimE mediated recombination compared to the relatively low frequency of recombination for FimB, means that any slight drop in the levels of FimE recombination would markedly effect the 'off' to 'on' recombination balance. FimB acts to turn the cell from 'off' to 'on' and FimE activity defines the period of time the *fim* switch remains 'on'. It must be surmised therefore that *fimE* would be under very tight regulation.

It has been shown that the transcription of *fimE* can inhibit the frequency of FimB mediated recombination (O' Gara and Dorman, 2000), a level of control that requires HNS, and that the transcription of *fimE* is increased when the *fim* switch is in the 'on' orientation but levels of FimE activity are undetectable when the *fim* switch is in the 'off' orientation (Kulasekara and Blomfield, 1999). Essentially the orientation of the *fim* switch changes the stability of the *fimE* transcript. This effect, termed 'orientational control' (Kulasekara and Blomfield, 1999), no doubt exists to minimise the exposure of a bacterial cell to the host immune system by keeping the population largely afimbriate.

Bacterial cells initially switch from the 'off' to the 'on' orientation resulting in the fimbriae being produced and raising levels of *fimE* transcription. FimE levels will be low at this point but as the levels of FimE start to rise transcription of the *fim* structural genes

will be inhibited by FimE mediated switching from 'on' to 'off' and by direct transcriptional inhibition in 'on' cells. In the 'off' orientation *fimE* transcription levels will drop off, the bacterial cell will stop producing the fimbrial structural genes and the population as a whole will become more afimbriate. The control of *fim* expression therefore involves strong *fimE* feedback control to alter *fim* switching and phase variation levels.

1.2.2 – Bacterial adhesin 'cross-talk'

The large number of adhesins deployed by *E. coli* can depend on the pathotype and these are associated with certain serotypes. The sequenced UPEC strain CFT073 for example has been shown to contain as many as 12 fimbrial clusters (Snyder *et al*, 2005).

The ability of a bacterial population to respond to different environments and to change phenotype in response to new environmental factors can be extremely important in setting up a successful colonisation or infection. Bacteria that can deploy a number of different adhesins depending on environmental signals will have a significant advantage in survival in a new host compared to bacteria that have lost the ability to produce multiple different surface adhesins.

For the bacteria that have a number of functional adhesins, the regulatory circuits between these genetic loci are of importance. Producing fimbriae and other surface structures has a high energy cost for the bacterium and it would be disadvantageous to produce all the adhesins it can, all the time. Whilst it is important for the bacterial population as a whole to generate adhesin and antigenic heterogeneity, an individual bacterium must tightly regulate it's surface structures to ensure the optimum combination is produced to allow successful proliferation in the host.

The regulation or 'cross-talk' between fimbrial adhesins is dependant on environmental signals as well as regulatory genes present in the fimbrial loci themselves. It is more

efficient for the bacterium to produce a regulator that acts in a positive manner on its own set of adhesin genes but also acts to suppress or upregulate other fimbrial cluster genes.

In the case of type 1 fimbriae the regulatory product from the *pap* operon: PapB, has been shown to suppress *fim* switching by acting directly to inhibit FimB mediated switching, whilst increasing *fimE* expression *in vitro* (Holden *et al*, 2001; Xia *et al*, 2000). The *pap* operon contains genes encoding for P pili and is also subject to phase variation, although via *dam* methylation at key GATC sequences rather than an invertible element as with *fim*. As PapB acts to upregulate the production of its native P pili, the cross-talk net result is the production of P pili and the switching off of type 1 fimbrial production. Array studies have also shown that during UTI infection type 1 fimbriae are upregulated but P pili are downregulated, suggesting 'cross-talk' during the infection process (Snyder *et al*, 2004).

The same group has shown recently that type 1 fimbriae can have regulatory affects on the *pap* operon using phase locked 'on' mutants of UPEC strain CFT073 in microarray assays (Snyder *et al*, 2005). This result is not surprising as the negative cross-talk exhibited by the *pap* operon on the *fim* operon may be reciprocated to some degree. The actual mechanism by which the *fim* operon inhibts P pili production remains to be elucidated, but as with the *pap* operon regulator PapB, the *fim* recombinases: FimB and FimE are likely to be involved, with some evidence pointing to a role for FimE (Snyder *et al*, 2005).

Whilst understanding the regulation of type 1 fimbriae and P pili is important in our search for key virulence factors in a pathogens genome, we must also seek to understand the regulatory networks and circuits that each adhesin cluster may be a part of. Individually each cluster has complex regulatory pathways that govern the production of their specific surface structure; however regulators and genes from these operons may also play a crucial role in the regulatory pathways of other adhesin clusters.

In this way a bacterial cell can respond to environmental signals in a co-ordinated and energy efficient manner. Perhaps, more importantly, the bacterial population as a whole can maintain antigenic heterogeneity, a state that may be essential for evading the host immune system and for establishing and maintaining a successful infection.

1.3.1 – *in vivo* Expression Technology

Our increased knowledge of bacteria and their pathogenesis over the last century has mainly been due to defined experiments designed to study bacteria under laboratory controlled conditions. As such, control of the bacterial environment has allowed researchers to glean the maximum amount of data from each experiment and to construct hypotheses that can be proven or not in a defined manner. Bacterial responses to changes in their environment such as iron depletion and pH (Olson, E.R., 1993) have identified virulence factors essential for bacterial survival and persistence in the host.

It is clear however that even the more complex *in vitro* experiments cannot recreate the complexity and dynamics of an *in vivo* habitat. For bacteria to be successful in a particular biological habitat, complex regulatory systems have evolved at a genetic level and such complexity may be beyond the scope of laboratory based assays to unravel. Genes that have little or no activity in a laboratory screen may be critical to the persistence of the bacterium in the host, likewise, genes that appear vital in an *in vitro* assay may well play little or no role *in vivo*.

To this end, strategies for studying bacterial genetics *in vivo* have become important. Advances in gene fusion and reporter fusion technology allow researchers to analyse gene function 'quietly' without significant disruption to the fitness of the bacterium. Researchers have used this technology to design novel systems for isolating genes activated *in vivo*.

In vivo expression technology (IVET) was first described in 1987. A group from the UK successfully used a promoterless chloramphenicol resistance gene and a promoter trap

library of the plant pathogen *Xanthomonas campestris* to identify genes activated *in vivo* (Osbourn *et al* 1987).

The first use of IVET for an animal pathogen was in 1993 when Mahan *et al* defined a promoter trap system resulting in the identification of *Salmonella* Typhimurium genes expressed *in vivo* (Mahan *et al* 1993). The basis behind this form of IVET was the use of compromised strains carrying mutations in genes responsible for the biosynthesis of purines: the *purA* gene. The attenuated strain is not able to grow in the *in vivo* environment unless this gene is expressed. A promoter trap library was used to create gene fusions with a promoterless *purA* gene. Promoters induced in the environment now allow the expression of the *purA* gene and can complement the deficiency. To ensure that the induced promoter was not constitutively expressed, the *lacZ* gene was linked to the fusion to allow screening of the recovered bacteria for *in vitro* expression. Bacteria that produced beta-galactosidase were discarded from the study. Thus only genes that were *in vivo* induced (i.v.i.) were included in the final analysis. Importantly this form of IVET established three principles:

- The *purA* and *lacZ* fusion must be stably inserted in single copy into the *Salmonella typhimurium* chromosome. This avoids the inherent problems with using reporter strains carrying multicopy plasmids.
- A functional copy of the wild type virulence gene must be retained so as not to affect the fitness of the bacterium in the environment.
- To ensure only i.v.i. genes are analysed, a reporter gene for screening promoter activity *in vitro* must be used.

This form of IVET is characterised by its auxotrophy based selection. Many IVET studies followed that used this selection method, all of which required the complementation of a promoterless gene essential for survival in the environment. Another example of *purA* IVET was used to identify i.v.i. genes in a murine model of *Pseudomonas aeruginosa* (Handfield *et al* 2000). The difficulty in obtaining *purA* mutants in some bacteria has led to the use of other essential genes for auxotrophy IVET.

Genes such as *galU* (Lai *et al* 2001) and *inhA* (Dubnau *et al* 2002) required for galactose metabolism and mycolic acid biosynthesis respectively have been used to identify i.v.i. genes. Genes that are involved in pathogenesis have also been used as a reporter and screening method, for example the *hly* gene in *Listeria monocytogenes* (Gahan and Hill, 2000). The obvious specific disadvantage of auxotrophy IVET is the need to construct an auxotrophic mutant, which may be extremely difficult for some bacteria.

The original IVET experiment (Osbourn *et al* 1987) used a promoterless chloramphenicol acetyltransferase (*cat*) gene as a marker of *in vivo* induced expression. IVET based on antibiotic resistance is an important variant that expands the range of bacteria that can be used (Rediers et al 2005). The *cat* gene was also used in IVET studies of *Shigella flexneri* (Bartoleschi et al 2002), *Yersinia enterocolitica* (Young and Miller, 1997) and *Helicobacter pylori* (Angelini et al., 2004) amongst others.

A promoterless *tet* gene was used in an IVET study on *Porphyromonas gingivalis* (Wu et al., 2002). Antibiotic resistance IVET bypasses the need for an auxotrophic mutant and allows the temporal study of expressed i.v.i. genes but brings disadvantages of its own, chiefly the need to administer the antibiotic to the host system during the experiment. The administering of an antibiotic to the host may alter the environment enough to give false readings for the bacteria, the host itself may be affected by the antibiotic as can be the case with plants (Osbourn et al., 1987) and achieving the correct concentration of antibiotic at the relevant sites may be difficult.

A disadvantage with both auxotrophy and antibiotic resistance IVET is the inability to identify genes that are expressed weakly or temporally during the experiment. Such genes never survive the rigorous selection required in the environment and are missed in any subsequent screen. Bacterial persistence and infection is a complex process genetically, requiring many levels of control. Certain genes may be of vital importance to this process yet remain undiscovered if using traditional IVET systems.

1.3.2 – Recombinase *in vivo* Expression Technology

As such a major modification was made to the IVET method. In 1995 a research group produced a publication outlining this new method (Camilli and Mekalanos, 1995). They described using a promoterless site specific DNA resolvase, TnpR under control of a promoter trap library. If expressed, the resolvase would mediate recombination between two *res1* sites, removing the DNA between the sites. Using a murine model of *Vibrio cholerae* infection the group placed a tetracycline resistance gene in between the *res1* sites. Expressed promoters drove production of TnpR, which mediated recombination at the *res1* sites, removing the tetracycline resistance gene resulting in a permanent and heritable marker of promoter activity. Replica plating could now determine any tetracycline sensitive strains. To isolate only i.v.i genes, tetracycline was used as a selection pressure during the construction of the strains. This ensured that any constitutively expressed promoters would be removed from the study before inoculating the mice.

This new form of IVET was named recombinase based *in vivo* expression technology (RIVET) and is represented diagrammatically in Figure 1.6. The RIVET method has also been used to isolate i.v.i. genes in *Staphylococcus aureus* infection of mice (Lowe et al., 1998).

As RIVET was developed it was found that the lack of a positive selection method meant the laborious task of replica plating the recovered strains to look for sensitivity to the antibiotic selection. The addition of a second reporter gene that could be used for positive selection solved this problem. Merrell et al used the *sacB* gene (Merrell and Camilli, 2000), the product of which (levansucrase) converts sucrose into the toxic levan form, placed alongside the *tet* gene in between the *res1* sites to create a *res1-tet-sacB-res1* cassette. Bacteria that expressed the resolvase during the study will gain the ability to grow on sucrose containing media having lost the *sacB* gene.

Fig 1.6

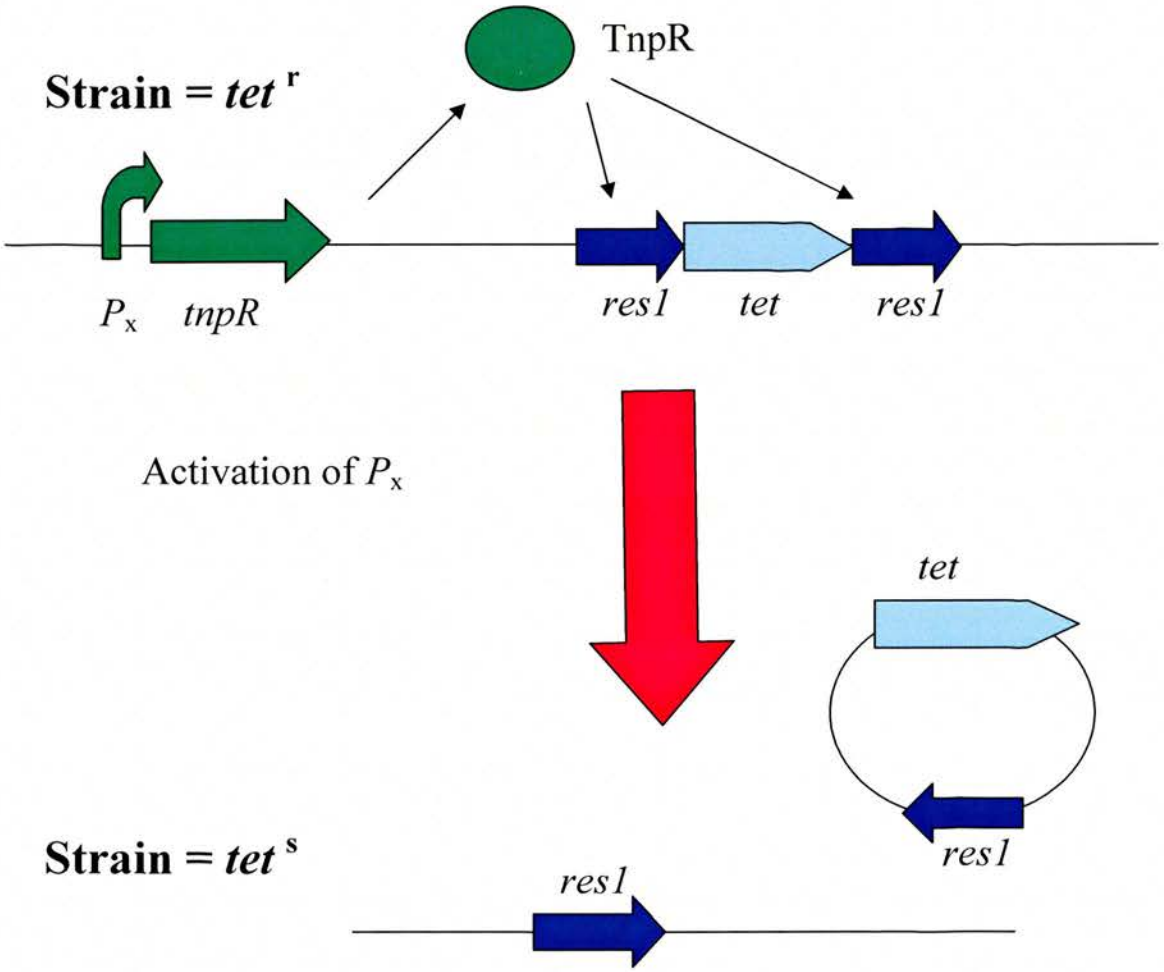

Diagrammatic representation of a RIVET experiment. Expression from Px produces TnpR. TnpR mediates recombination between the *res1* sites, excising the *tet* gene. The strain is now tetracycline sensitive.

Other research groups have used a *cat* gene, disrupted by the *tet* gene flanked with *res* sites. Strains expressing TnpR during the study will excise the *tet* cassette and become chloramphenicol resistant, quiescent strains will retain the resistance to tetracycline.

This new form of RIVET, called selectable *in vivo* expression technology (SIVET) was used to study induced lysogens of shiga toxin (STX) in shiga toxin producing *Escherichia coli* strains (STEC). By using SIVET the researchers could count proportions of a population that had expressed the *tnpR* gene under the phage promoter

Pr. The advantage of using a positive selection method when searching for a very low percentage of resolution (as with spontaneously induced prophages) is clearly demonstrated in this study as researchers could screen populations for chloramphenicol resistance. Using standard culture conditions the researchers found a spontaneous induction rate of 1 in 20 000 lysogens carrying the Stx-1 encoding phage and 1 in 7000 carrying the Stx-2 encoding phage per cell generation (Livny and Friedman, 2004), a figure greater than that of non STX encoding phages. The methodology of SIVET is represented diagrammatically in Figure 1.7.

Fig 1.7

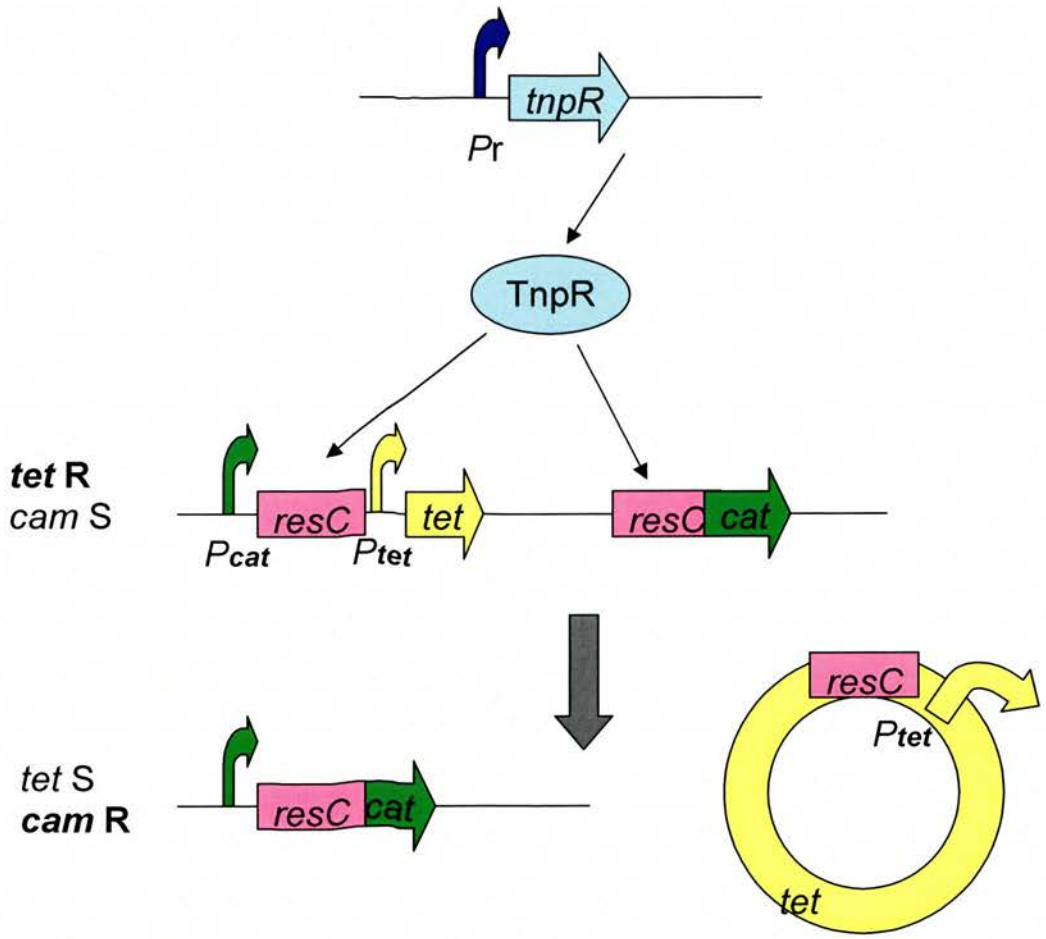

Selectable *in vivo* expression technology (SIVET) overview

RIVET is a much more sensitive method than auxotrophy IVET or antibiotic resistance IVET. Promoters that are weakly expressed or temporally controlled can still be studied. The other main disadvantage with RIVET however was the loss of potentially important genes during the construction process. Due to the systems sensitivity any virulence genes that also have activity *in vitro* will result in a strain that resolves before inoculation and cannot be constructed. Missing these genes out during the *in vivo* screen could lead to difficulties in unravelling the complex genetic cascades used by the bacterium in the environment.

Researchers working with the water-borne pathogen *Vibrio cholerae* were faced with the problem that two of the well known virulence genes for *V. cholerae* infection: cholera toxin (CT) and toxin co-regulated pilus (TCP) are produced *in vitro*. In order to proceed with *in vivo* studies using the respective subunit genes: *ctxA* and *tcpA* the researchers developed a 'tuned' RIVET system. (Lee *et al* 1999) By modifying the ribosome binding site (RBS) of the *tnpR* gene the researchers were able to suppress translation initiation at the RBS for any transcription level. Using an oligonucleotide primer, single nucleotide changes at three positions in the RBS were generated using PCR. The resulting library was screened using the iron repressible *irgA* promoter. This was cloned upstream of *tnpR* within the genome of a *V. cholerae* strain containing the *res1-tet-res1* cassette. The resultant library was then cultured in the presence of varying iron concentrations. Three strains were isolated that gave reduced resolution compared to wild type. Each strain was used to test the *ctxA* and *tcpA* promoters in LB broth and AKI broth, a medium that is known to induce the *V. cholerae toxR* regulon (Iwanaga et al., 1986). One of the strains tested did not resolve in LB broth but did resolve in AKI broth, and as a result was chosen for the study (Lee et al., 1999).

Previous forms of IVET were distinctly promoter 'hunting' methods. By using promoter trap libraries, novel *i.v.i* genes could be found. However this form of 'tuneable' RIVET allows researchers to investigate the importance of specific bacterial promoters *in vivo* and study the interplay between specific promoters and other virulence genes.

Researchers could now ask specific questions of virulence genes and their individual roles within an infection model.

The use of 'tuneable' RIVET as a screening method was outlined in 2005. Researchers used the same principles as the 'tuneable' RIVET but used a promoter trap library of *V. cholerae* to screen for *i.v.i.*genes in a murine model of infection (Osorio et al., 2005). Two main modifications were made. Firstly the *tet* gene previously flanked by the *res1* sites was omitted and replaced with two new reporter genes: *neo* and *sacB*. The *neo* gene confers resistance to Kanamycin and the *sacB* gene has been described above. This allowed researchers to select positively for resolved strains by growing on sucrose containing media after recovery. Strains still in possession of a *sacB* gene will be unable to grow. Sucrose resistant strains can then be tested for sensitivity to Kanamycin. The addition of this secondary selectable reporter removes the tedious negative screening associated with earlier RIVET studies using replica plating.

The second modification in this study was a preselection step designed to eliminate partially resolved strains. Each starting fusion strain was grown in LB overnight to stationary phase and diluted serially onto sucrose and non sucrose containing LB. Only strains resolved to less than 0.1% were included in the study. This new form of tuned RIVET dispenses with many of the drawbacks of the original form of RIVET whilst still retaining the ability to identify low level or transiently expressed *i.v.i.* genes. Only 35% of recovered resolved strains in the original RIVET study were true *i.v.i* genes (Camilli and Mekalanos, 1995) whereas 85% of the recovered strains were true *i.v.i.* genes in the tuned form of RIVET (Osorio et al., 2005).

RIVET has also been used to identify the regulators of virulence genes. By using the tuned RIVET method with key *V. cholerae* promoters: *toxT* and *ctxA*, as seen previously (Lee et al., 1999) and STM technology, researchers were able to screen *V. cholerae* strains for regulators of these two known virulence genes (Lee et al., 2001).

1.4 – *fim* Recombinase *in vivo* Expression Technology

IVET and RIVET have proven to be useful tools to help unravel bacterial activity *in vivo*. A well established animal model and ease of genetic manipulation has allowed such activity to be elucidated in a wide range of bacteria. Using the principles of IVET and RIVET, I propose a different method of RIVET, for use with *Escherichia coli* O157:H7 and its natural ruminant bovine host. This new method: *fim* recombinase *in vivo* expression technology (FRIVET) utilises genes taken from the *fim* operon in *E.coli* with an antibiotic reporter system. By using *fim* operon genes under the control of specific EHEC promoters, FRIVET could allow more control and flexibility than previous IVET or RIVET methods.

Two key alleles from the *fim* operon are used: *fimB* and *fimS*. As has been mentioned previously *fimS* (also referred to as the *fim* switch) is an invertible DNA element containing a promoter sequence for downstream *fim* structural genes. These structural genes are only transcribed when *fimS* is in the correct orientation ('on'), a factor partially under the control of *fimB*, a site-specific recombinase that binds to *fimS* causing inversion primarily from 'off' to 'on'.

By using a promoterless *fimB* gene fused transcriptionally to a variety of EHEC promoters we can control the inversion of *fimS* and consequently the transcription of any downstream genes. In place of the *fim* structural genes we will place the antibiotic resistance gene *bla* (producing beta-lactamase, conferring resistance to ampicillin) as a reporter gene for the FRIVET system.

The EHEC promoters to be used will attempt to cover a wide range of the EHEC virulence determinants. As such we will use a number of key promoters from the LEE which have been shown to be important for EHEC virulence and pathogenesis. Additionally we will use promoters for EHEC specific adhesin clusters, flagella regulation and other EHEC promoters that may generate interesting data *in vivo*.

Each FRIVET construct will first be engineered on a temperature sensitive allelic exchange vector. Once the final construct is made with the correct promoter in place upstream of *fimB* the construct will be placed in single copy at the *fim* locus in place of the native *fim* operon in the category 2 Shiga toxin negative strain: ZAP193.

Importantly the deletion of the *fim* operon and thus the ability to produce type 1 fimbriae from our FRIVET strains will not have a negative impact on the bacterium's pathogenicity in the host animal. Studies have shown that despite possessing a copy of the *fim* operon, *E. coli* O157:H7 does not produce type 1 fimbriae due to a 16bp deletion in the *fimS* region (Roe *et al,* 2001). We can confidently surmise therefore that type 1 fimbriae do not play a role in *E. coli* O157:H7 pathogenesis and that our FRIVET strains will not be impaired in their ability to adhere to host cell tissue due to the *fim* operon deletion. However we must also be aware that the *fim* operon contains two site specific recombinases: *fimB* and *fimE.* There is no evidence to suggest that FimB and FimE production is deficient in *E. coli* O157:H7 and therefore these proteins may play a role in the regulation of other fimbrial operons or regulatory networks that are as yet unknown.

The basic FRIVET assay will proceed as follows:

- Activation of the specific promoter will result in FimB production
- FimB will mediate the inversion of the 'off' *fimS* to the 'on' state
- The promoter in *fimS* is now 'lined up' and can now direct transcription of the *bla* gene conferring ampicillin resistance on the cell
- Bacteria can be recovered and analysed by direct plating onto media with and without ampicillin to obtain the percentage of the population resistant to ampicillin
- This figure will correlate with the transcriptional activity of *fim*B and its EHEC promoter during the assay

The FRIVET assay is shown diagrammatically in Figure 1.8.

Fig 1.8

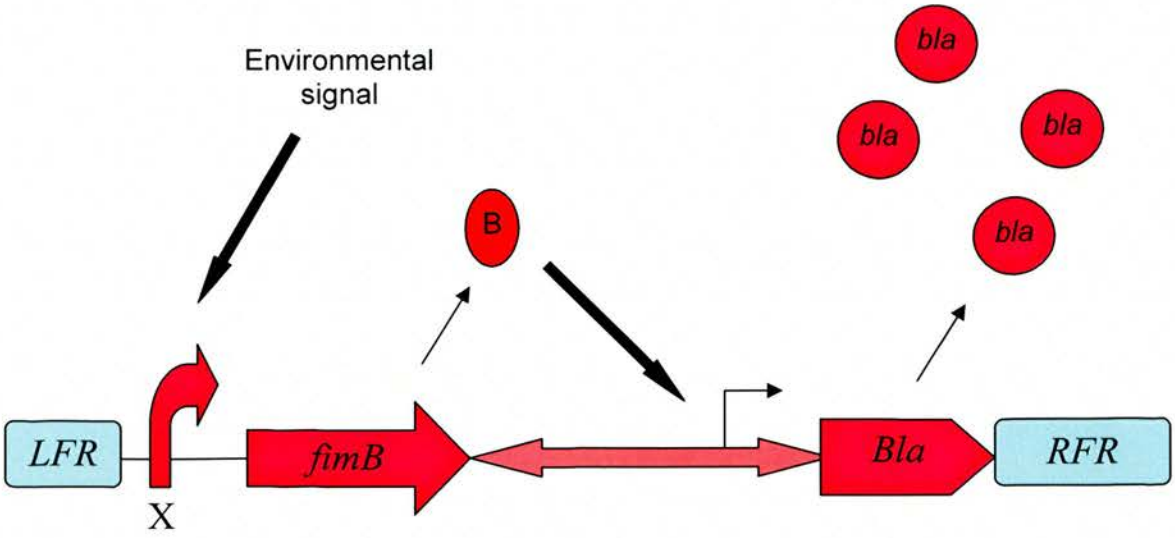

Diagrammatic representation of the FRIVET assay. Signals act on promoter X resulting in transcription of *fimB*. FimB can then mediate recombination of *fimS* from the 'off' orientation to the 'on' orientation. The promoter in *fimS* can now direct transcription of the downstream *bla* gene. The cell now becomes ampicllin resistant.

A key part of the FRIVET system is the ability to control the orientation of *fimS* as desired. Obviously there is a need to have the switch locked in the 'off' orientation at the start of the experiment, but the ability to control *fimS* orientation at other times has many advantages. A feature of the RIVET method is the non-reversible nature of the resolution event. After the excision of the *res1-tet-res1* cassette the bacterium becomes tetracycline sensitive and remains so until manipulated otherwise. Thus each bacterium has one chance to record the activity of its *tnpR* gene.

As an example, the extra level of control inherent to the FRIVET system will enable the orientation of the switch to be reset for the whole population at any given timepoint. After inoculating the animal model orally, an early time point sample is taken from a point high in the gastro-intestinal (GI) tract and analysed for ampicillin resistance. At the same point the orientation of the *fim* switch is reset to 'off' for the remaining population

still present in the animal model. Over the time course of a natural bacterial infection and persistence study this process can be repeated all the way down the GI tract to the terminal recto-anal junction, the identified site of EHEC colonisation (Naylor *et al*, 2003). A comparison between ampicillin resistance percentages at time/position point A can be compared with time/position point B, C, D etc. This will allow conclusions to be made regarding the necessary signals for that specific EHEC promoter being present in different areas of the GI tract.

Each FRIVET construct can therefore provide a stable and hereditable readout of promoter expression during a study but unlike RIVET the readout is not irreversible, but can be controlled to fit the studies hypotheses. As such it will provide greater flexibility than conventional RIVET for elucidating EHEC promoter activity *in vivo*.

The control of *fimS* orientation during an experiment will need an extra gene in the FRIVET system. Studies have shown the complex interaction between the Type 1 fimbrial operon and the regulators of the *E. coli pap* operon. The *pap* operon contains genes encoding P fimbriae in urinary pathogenic *E. coli* and has been shown to be important in the development of pyelonephritis but its role is not fully understood. As with type 1, the *pap* operon is phase variable but under DAM methylase control.

The effect of one of the *pap* operons regulators: PapB, and cross-talk with type 1 fimbriae has been studied previously (Holden *et al*, 2001, Xia *et al*, 2000). PapB acts to inhibt FimB mediated switching, although the mechanism for this action is not yet fully understood, it is thought to be due to direct binding to the *fim* switch. Due to this we can deploy PapB as our 'control' gene in order to lock our FRIVET *fim* switch in the present orientation, allowing us to lock the switch in the 'off' orientation whilst preparing the inoculum as well as locking the switch in the position it is recovered in. This is an important point as any unwanted FimB activity after recovery of the strain will result in an artificially high ampicillin resistance proportion.

To induce PapB, we will utilise the IPTG inducible promoters: *lac*UV5 and Ptac. Constructs will be made for both promoters and placed in single copy at the *lac* locus in the FRIVET strains. To 'reset' the *fim* switch during an experiment we can utilise the *fimE* gene. FimE acts to turn the *fim* switch from the 'on' orientation to the 'off' orientation. By placing *fimE* under the same IPTG control instead of *papB* we can create FRIVET strains designed to monitor a particular promoter's activity at points along the GI tract.

By creating dual single copy strains we will avoid problems associated with maintaining plasmids in our strains during *in vivo* assays whilst allowing full control over the inoculum and the recovered strains.

The FRIVET system will provide an alternative to existing IVET and RIVET systems as well as improving on their overall design. Its strengths lie in studying specific promoters in their natural *in vivo* environment without the need for mutagenesis or overly toxic reporter systems. The additional levels of control incorporated into the FRIVET system sets it apart from existing IVET systems. Instead of having a defined start and finish, FRIVET assays can be monitored at different time points and locations during the infection process. Complex temporal regulation between promoters can be unravelled and the process of attachment, immune evasion and proliferation can be elucidated. The simplicity in screening the recovered bacteria for their promoter activity will allow higher volumes of assays to be carried out and large amounts of data to be analysed.

1.5 – Thesis aims

The main aims of this thesis can be split into three distinct parts:

1) The construction of a working FRIVET synthetic operon. Using genes from the *fim* operon and the *bla* gene, we must demonstrate that the *fim* switch is invertible and that the promoter within *fimS* can direct transcription of *bla*

2) The *in vitro* testing of the FRIVET system. This will start with the functional testing of the operon itself using an inducible test promoter to define the working limits of the operon and appropriate control methods. Secondly we must define a suitable and reproducible screening system

3) The construction of experimental FRIVET strains for *in vivo* use. The *E. coli* O157:H7 promoters initially used will be: *lee5; fliC; lpf1* and *loc8*. The resulting FRIVET strains will be assessed *in vitro* to determine the operons functionality using various media and on cell lines.

To use constructed FRIVET strains in an *in vivo* experiment. The animal model and strain to be used will be decided closer to the time. Current animal models such as the sheep gut loop (ligated chambers in the ascending spiral colon) may be deployed.

The final aim of the study is to functionally prove that the FRIVET system can be used as an indicator of promoter activation in an *in vivo* environment. Ideally a FRIVET *in vivo* experiment would involve inoculation of a natural bovine host with a FRIVET test strain. Samples of bacteria collected and plated on SmacNal plates (Sorbitol MaConkey Nalidixic acid) would be analysed for ampicillin resistance levels. The prescence of ampicillin resistant colonies would indicate the activation of the FRIVET system post inoculation.

In this assay we can analyse the past activation of a promoter in the experimental setting. The specific targeting of complex regulatory pathways and precise temporal gene activation may however lie outwith the scope of this system as any data recorded for the assay would give us a promoter activation record without drawing accurate conclusions on the specific relevance of that activation regarding *E. coli* O157:H7 pathogenesis in the host. Further *in vivo* assays could involve post mortem collection of bacterial samples at various lengths along the GI tract. This assay could yield basic temporal data with regard to FRIVET activation.

Chapter 2

Materials & Methods

2.1 - Table of Strains

Strain	Description
ZAP193	NCTC12900, *stx*$^-$, *nal*^{r}
ZAP193 *sac/kan*	ZAP 193 Δ*lac sac/kan*
ZAP1	*E. coli* O157:H7 Redhouse dairy outbreak strain human isolate
E. coli AAEC185	F$^-$ λ^- *supE44 hsdR17 mcrA mcrB endA1 thi*$^{-1}$ Δ(*fimBEACDFGH*) Δ*recA* (Blomfield *et al.*, 1991)
E. coli AAEC189	AAEC185 Δ*lacZ* (Blomfield *et al.*, 1991)
E.coli MG1655	F- λ- *ilvG rfb50 rph1* (Guyer, 1980)
ZAP541	ZAP193 *lac*UV5::*pap*B
ZAP542	ZAP541 Δ*fim sackan*
ZAP543	ZAP542 *ara*::*fim*B::*fim*S::*bla* (pRQ15) *fim*S 'off' orientation
ZAP544	ZAP193 Ptac::*pap*B
ZAP545	ZAP544 Δ*fim sackan*
ZAP546	ZAP545 *ara*::*fim*B::*fim*S::*bla* (pRQ15) *fim*S 'off' orientation
ZAP547	ZAP193 Δ*fim*
ZAP548	ZAP547 *ara*::*fim*B::*fim*S::*bla* (pRQ15) *fim*S 'off' orientation
ZAP550	ZAP545 *lee5*::*fim*B::*fim*S::*bla* (pRQ101)

2.2 - Table of Plasmids

Name	Description	Source
pRQ1	pAJR26 containing *lac*UV5 promoter	This study
pRQ2	pRQ1 containing *fim*E cloned upstream of *lac*UV5 promoter	This study
pRQ3	pIB307 containing *fim* region left flanking region (LFR) from ZAP193	This study
pRQ4	pRQ3 containing *fim* region right flanking region (RFR) from ZAP193	This study
pRQ40	pRQ4 containing *sackan* cassette for allelic exchange	This study
pRQ5	pIB307 containing *fim* region LFR from ZAP1	This study
pRQ6	pRQ5 containing *fim* region RFR from ZAP1	This study
pRQ7	pRQ6 containing *sackan* cassette for allelic exchange	This study
pRQ8	pAJR26 containing *lac*UV5::*pap*B fusion cut from pHMG88	This study
pRQ10	pACYC184 containing *lac*UV5 promoter	This study
pRQ11	pRQ4 containing *fim*B from ZAP193	This study
pRQ12	pRQ11 containing *fim* switch from pMM36	This study
pRQ13	pRQ12 containing *bla* from pUC18	This study
pRQ15	pRQ13 containing *ara* promoter from pBAD18 to create *ara::fimB* fusion	This study
pRQ16	pRQ11 containing *fim* switch from NEC120	This study
pRQ17	pRQ16 containing *bla* from pUC18	This study
pRQ18	pRQ17 containing *ara* promoter from pBAD18 to create *ara::fimB* fusion	This study
pRQ19	pAJR26 containing Ptac promoter from pACTAC	This study
pRQ20	pRQ19 containing *papB* from MG1655 downstream of Ptac promoter to create Ptac::*papB* fusion	This study
pRQ23	pRQ11 containing *fim* switch from pJL2	This study
pRQ24	pRQ23 containing *bla* from pUC18	This study
pRQ101	pRQ13 containing *lee5* promoter from ZAP193 to create *lee5::fimB* fusion	This study
pRQ102	pRQ13 containing *fliC* promoter from pTOPO lab clone to create *fliC::fimB* fusion	This study
pRQ103	pRQ24 containing *lee5* promoter from ZAP193 to create *lee5::fimB* fusion	This study

Name	Description	Source
pRQ104	pRQ24 containing *lpf1* promoter from ZAP193 to create *lpf1::fimB* fusion	This study
pRQ105	pRQ24 containing *loc8* promoter from ZAP193 to create *loc8::fimB* fusion	This study
pRQ30	pACYC::*gfp*+ containing *ara* promoter from pBAD18 to create *ara::gfp*+ fusion	This study
pACTAC::*fimE*	pACTAC vector with *fimE* from MG1655 cloned downstream of Ptac promoter	This study
pBAD18	*E. coli* plasmid cloning vector, containing MCS downstream of the *araBAD* promoter, allowing insertion of a gene with expre controlled by arabinose induction	(Guzman *et al.*, 1995)
pACYC184	*E. coli* plasmid cloning vector, low copy number. Cm^r,	(Sambrook, 1989)
pIB307	pMAK705 based allelic exchange vector, temperature sensitive replicon	(Blomfield *et al.*, 1991)
pMM36	pACYC184, *fimS* in on orientation	(McClain *et al*, 1991)
pUC18	Small, high copy number cloning vector for *E. coli*	(Yanisch-Perron *et al, 1985*)
pHMG88	pACYC184, *lac*UV5::*papB*	(Forsman *et al*, 1989)
pAJR26	pIB307 derivative containing the *lacI* and *lacA* genes of ZAP193	A.Roe
pAJR27	pIB307 derivative containing the *lacI* and *lacA* genes of ZAP1	A.Roe
pACTAC	pACYC184 containing Ptac promoter	J.Emerson

2.3 - Table of Primers

Name	Sequence
PapB 3	gccggatccatatatccaggggcc
PapB 4	ccaggatccccggaatgccataat
FRIVET Bla Diag	ctgcaggcatcgtggtg
FRIVET FimS Diag	cgttataccgccagtaatg
FimS 5'V1	ccagatctggaaccgtaatgtatactcatc
Bla 3'	ccggatccgtaaacttggtctgacagttacc
RFR 1	ccggatccgcattgctaatgcaggtacg
RFR 2	aactgcaggcgatgttctatgaagtggc
LFR 1	gggggagctcccggataagtcttgttgtcg
LFR 2	ccggatcccctgatggcgggtaaacac
LFR up 5'	cccaacgatgaacgttatcacg
Bla 5' *Bam*HI	ccggatcccgctcatgagacaataaccctg
FimS 3'	ccggatcccagaacaacgattgccagag
FimB 5'	ccagatctttggtaccgctaatctagaacagctagtgcgcgtctg
FimB 3'	ccggatcccaccatccctggtatctcaac
FimS 5' *Bam*HI	ccggatcccagaacaacgattgccagag
FimE 5' *Eco*RV	gcggatatccagttaggagtactactattgtg
FimE 1	ccggatcccagttaggagtactactattgtg
FimE 2	ccggatccgacagtttggccccaattgtc
ara 5' *Xba*I	gctctagagccaccagatgggcattaaacg
ara 3' *Xba*I	gctctagagggtatggagaaacagtagagag
ara 5' *Bam*HI	ccggatccgccaccagatgggcattaaacg
LacUV5 1	ccagatctgggcagtgagcgcaacgc

Name	**Sequence**
FliC *Xba*I 3'	cctctagagggtttccacccgt
LPF1 5'	gctctagaggtcagtgagttcttcgg
LPF1 3'	gctctagacgacaactttgaaggaagg
LEE5 5'	gctctagaccagacgaagatgatagaac
LEE5 3'	gctctagagtatggtatacagcacgtag
5' Ptac *Xba*I	gctctagactgtgcaggtcgtaaatcac
3' Ptac *Xba*I	gctctagagtgaaattgttatccgctcac
Loc8 5'	gctctagagccatataaaccattagtagcc
Loc8 3'	gctctagaatgtttgactttcataattctcc
5' GFP *Bam*/*Kpn*/SD	ccggatccccgggtaccggaggccaccatggtgagcaagggcg
5'IRL *Kpn*I	ccggtacctaaatacaagacaattgggg
3' IRR *Bam*HI	ccggatccccaaaagatgaaacatttgggg
3' IRR *Kpn*I	ccggtaccccaaaagatgaaagatttgggg
5' IRL *Bam*HI	ccggatcctaaatacaagacaattgggg
3' GFP+ fuse	ccgtatgtagcatcaccttcac
lacA 3' down	catgccggatgcggctaatg
lacI up 5'	cgccttatggcatgatagcg

2.4 Media and Reagents

LB Medium

10g NaCl

10g Peptone

5g Yeast extract

1000ml distilled H_2O

Antibiotics, when required, were added after sterilisation at the following final concentrations:

Ampicillin	$50\mu gml^{-1}$ (10μgml-1 for FRIVET assays)
Kanamycin	$25\mu gml^{-1}$
Chloramphenicol	$12.5\mu gml^{-1}$
Tetracycline	$25\mu gml^{-1}$
Nalidixic acid	$5\mu gml^{-1}$

LB Agar

10g NaCl

10g Peptone

5g Yeast extract

1000ml distilled H_2O

Antibiotics, when required, were added after sterilisation at the following final concentrations:

Ampicillin	$50\mu gml^{-1}$
Kanamycin	$25\mu gml^{-1}$
Chloramphenicol	$12.5\mu gml^{-1}$
Tetracycline	$25\mu gml^{-1}$
Nalidixic acid	$5\mu gml^{-1}$

LB Sucrose plates (6% w/v)

10g peptone

5g yeast extract

12.5g Bacto-agar

850ml dH_2O, autoclave

Add 50g Sucrose to 150ml dH_2O, filter sterilise, and add to LB

M9 Medium

56.4g M9 minimal salts

10ml 1M $MgSO_4$

2ml 1M $CaCl_2$

20ml 50X non-essential amino acids

10ml 100X non-essential amino acids

10ml 20% w/v glucose/glycerol

1000ml dH_2O

Filter sterilize

SOC recovery medium (sigma)

2% Tryptone

0.5% Yeast extract

8.6mM NaCl

2.5mM KCL

20mM $MgS0_4$

20mM Glucose

10X TBE buffer

108g Tris base

55g Orthoboric acid

9.8g Na_2EDTA

1000ml dH_2O

Phosphate buffered saline

10 PBS tablets (Sigma UK) in 1000ml dH_2O

TFBI buffer

2.94g $KC_2H_3O_2$

1.47g $CaCl_2.2H_2O$

7.45g KCl

150ml 15% v/v glycerol

Make up to 900ml with sterile dH_2O, autoclave

Add 45ml 1M $MnCl_2$ to solution. Store at -20°C

TFBII buffer

11.03g $CaCl_2$

0.75g KCl

150ml 15% v/v glycerol

2.093g MOPS

Make up to 1000ml with sterile dH_2O, autoclave. Store at -20°C

2.5 – Biochemical Techniques

2.5.1 - Poly Acrylamide Gel Electrophoresis

A 5% v/v acrylamide gel was prepared as follows: 7.75ml of sterile distilled H_2O was pippetted into a sterile sterilin. 1.25ml 40% v/v acyrlamide/bis and 1ml of 10 X TBE was added. A BIORAD mini gell apparatus (Biorad, UK) was setup according to manufacturer's instructions and filled with 1 X TBE running buffer. Before pouring 100µl fresh Ammonium persulfate (APS) and 5µl TEMED were added to the gel mix. Using a 10ml syringe the gel was poured and left to set. Samples were added and run at 100V for approx. 50 minutes.

2.5.2 - Fluorstar measurement

Bacteria containing Fluorescent protein plasmids were grown in selected media to desired OD_{600}, and 20µl of culture was placed in 1 well of a black, flat bottomed 96 well plate (Nunc, UK) alongside dH_2O as a blank. The plate was transferred to the Fluostar Fluorimeter (BMG, UK) at 37^0C and measurements were taken according to manufacturer's protocol. A plasmid containing a promoterless *gfp+* gene was used as a negative control to set the gain for the experiment.

2.6 – Molecular Biology Techniques

2.6.1 – Polymerase chain reaction (PCR)

Template for PCR reactions was prepared by suspending a single bacterial colony in 100µl of dH_20 and boiling for 5 minutes. The lysate was pulsed 13,000rpm in a microcentrifuge for 10 sec. For PCR reactions using plasmid template a dilution of 1µl of 1/100 plasmid preparation was used. PCR's were carried out in 50µl reaction volumes containing 1µl of template, 5 µl of dNTP mix, 100pmol of each primer, 5 µl of 10 X PCR buffer with 1.5mM $MgCl_2$ (Roche, UK), and 2.5U of *Taq* DNA polymerase (Roche, UK). PCR was carried out using a Hybaid Thermocycler, and cycling conditions were as follows: denaturation at 94^0C for 4 min, followed by 30 cycles of denaturation at 94^0C for 45 sec, annealing at specific temperature for 45 sec, and extension at 72^0C for 60 sec, with a final extension at 72^0C for 10 min. Products were then held at 4^0C or stored at -20^0C.

2.6.2 - Agarose Gel Eletrophoresis

A 0.8% w/v agarose gel was made by addition of 0.4g molecular grade agarose (Sigma, UK) to 50ml of 1 X TBE. The solution was boiled in a microwave for 90 sec, allowed to cool to approximately 60^0C, and 1 µl of 1M Ethidium bromide added. The gel was then poured into a gel cassette with comb (SLS, UK). Once the gel was set, it was placed in an electrophoresis tank filled with 1 X TBE. For PCR diagnostics 2µl of PCR product was added to 7µl of MQ H_2O and 1µl of 10 X DNA loading buffer (Invitrogen, UK). For restriction endonuclease analysis 9µl of DNA sample was added to 1µl of 10 X DNA loading buffer (Invitrogen, UK), and the sample loaded onto the gel alongside a DNA marker, either 100bp ladder or a 1kb ladder (Invitrogen, UK). Electrophoresis was performed at 100V for approximately 30 minutes. The gel was visualised using the UV setting on a Flowgen MultiImage cabinet using image capture software (Flowgen, UK).

2.6.3 - Plasmid Purification

Bacteria were grown overnight in 5ml LB with appropriate antibiotic at 37°C at 200rpm. A Qiagen Qiaprep Spin mini prep kit (Qiagen, UK) was used according to the manufacturer's instructions. For pIB307 and related plasmids 5ml of overnight culture was used. For medium and high copy number plasmids 1.5ml was used. All plasmid preps were eluted in a final volume of 50µl MQ H_2O and stored at -20°C.

2.6.4 - DNA Purification from Enzymatic Analysis

DNA was purified from enzymatic reactions using the Qiagen Qiaprep spin DNA purification kit (Qiagen, UK) according to the manufacturer's instructions. For initial restriction reactions purified DNA was eluted in 40µl MQ H_2O. Subsequent restriction reactions were eluted at a volume of 10µl less than the starting volume of 40µl.

2.6.5 - DNA Purification from Agarose Gels

DNA was excised from agarose gels with a scalpel after visualisation on a UV transilluminator (SLS, UK). The DNA was then extracted using the Qiagen Qiaprep spin Gel purification kit (Qiagen, UK) according to manufacturer's instructions. Purified DNA was eluted in 30µl of dH_2O.

2.7 - DNA Manipulation

2.7.1 - Digestion of DNA with Restriction Endonucleases

For cloning, DNA restriction reactions were carried out in 50µl volumes containing 20µl DNA, 24µl dH_2O, 5µl reaction buffer, and 1µl enzyme. Digests were incubated at 37^0C water bath for 2 hours, purified using the Qiagen Qiaprep spin DNA purification kit (Qiagen, UK) and eluted in 40µl MQ H_2O. For restriction with a second enzyme 4µl reaction buffer and 1µl enzyme was added prior to incubation at 37^0C for 2 hours. Reaction was purified again and eluted in 30µl MQ H_2O.

For diagnostic purposes, reactions were carried out in 10µl volumes, containing 8µl purified plasmid, 1µl of restriction enzyme (New England Biolabs, UK) and 1µl of reaction buffer (NEB, UK). Digests were incubated in a 37^0C water bath for 2 hours and visualized on an agarose gel.

2.7.2 - De-phosphorylation of DNA

Shrimp Alkaline Phosphatase (SAP) was used to dephosphorylate digested plasmid DNA to prevent the plasmid self-ligating in ligation reactions. To dephosphorylate DNA, 1µl of SAP (NEB, UK) was added to restriction enzyme digest reactions for the final 30 mins at 37^0C prior to the final purification step.

2.7.3 - Ligation of DNA fragments

Digested DNA fragments and plasmids were visualised on a 0.8% w/v agarose gel. Using the HindIII DNA ladder (Invitrogen, UK) concentration of DNA was approximately calculated to give a 3:1 ratio of DNA fragment to plasmid in a 10µl ligation reaction containing 1µl of T4

DNA ligase (NEB, UK) and 1µl of 10 X ligase reaction buffer (NEB, UK). The reaction was incubated at 15°C overnight.

2.8 – Genetic Manipulations

2.8.1 - Preparation of chemically competent cells

From a fresh overnight culture bacteria were inoculated into 50ml LB at 37^{0}C shaking at 200rpm until an OD_{600} of 0.8. Culture was transferred to a 50ml falcon tube and cooled on ice for 5 minutes. Bacteria were harvested at 4,000rpm for 10 minutes at 4^{0}C, and re-suspended in 10ml of ice cold TFBI by gentle agitation. The cells were then harvested by centrifugation at 4,000rpm for 10 mins at 4^{0}C and gently suspended in 2ml of ice cold TFBII. Competent cells were stored at -20^{0}C

2.8.2 - Preparation of electro-competent cells

From a fresh overnight culture bacteria were inoculated into 50ml LB at 37^{0}C shaking at 200rpm until an OD_{600} of 0.8. Culture was transferred to a 50ml falcon tube and cooled on ice for 5 minutes. Bacteria were harvested at 4,000rpm for 10 minutes at 4^{0}C, and re-suspended in 25ml of ice cold 10% v/v glycerol. Bacteria were harvested as above and re-suspended in 12.5ml of ice cold 10% v/v glycerol, then harvested again and re-suspended in 2ml of 10% v/v glycerol. Competent cells were stored at -20^{0}C.

2.8.3 - Transformation of chemically competent cells

20µl of ligation reaction, or 1µl of purified plasmid, was transferred into an aliquot of 100µl competent cells and incubated on ice for 30 minutes in a glass test tube. The mixture was then transferred to a 42^{0}C water bath for 60s, and then placed on ice. 250µl of SOC was added to the mixture and incubated at 37^{0}C (30^{0}C for temperature sensitive plasmids) at 80rpm for 2 hours.

200µl of the transformation reaction was then plated out onto LB plates with appropriate antibiotic selction and incubated overnight at 37^0C (30^0C for temperature sensitive plasmids).

2.8.4 - Transformation of electro-competent cells

1µl of purified plasmid was added to 80µl of competent cells, and incubated on ice for 5 minutes. The mixture was transferred to a 1.5ml electroporation cuvette (Flowgen, UK) and electroporated at 2.5kV. 1ml SOC was added immediately, and the suspension transferred to a 1.5ml eppendorf tube. The reaction was incubated at 37^0C (30^0C for temperature sensitive plasmids) at 200rpm for 1 hour. 200µl was plated onto LB plates with appropriate antibiotic selection and incubated overnight at 37^0C (30^0C for temperature sensitive plasmids).

2.8.5 - Allelic exchange

Allelic exchange strains containing the *sackan* cassette were made electrocompetent, and transformed with the allelic exchange plasmid, with recovery of transformants at 30^oC on LB Chloramphenicol (LBC) and LB Kanamycin (LBK) plates. Ten colonies confirmed as successful transformants were used to inoculate 50ml of LBC, and logarithmic growth was maintained for 48 hours at 42^0C with shaking at 200rpm. At this stage a diagnostic PCR can be performed for primary integrates. After 48 hrs, a 1:500 dilution was made in LB and logarithmic growth was maintained for 48 hours at 30^0C with shaking at 200rpm. After 48 hours, the suspension was serially diluted and 200µl of 10^{-5} and 10^{-6} dilutions were used to seed LB sucrose plates, which were incubated at 30^0C for 24 hours. Succesful colonies on the LB sucrose plates (indicating loss of the *sacB* gene) were replica plated onto LBC, LBK, and LB agar plates. Colonies which were sensitive to chloramphenicol and kanamycin were analysed with PCR to confirm exchange of the required DNA fragment with the *sackan* cassette. The newly created strains were cultured and stored at -70^0C. This method is an extrapolation of methodology published previously (Blomfield *et al,* 1991).

2.9 - FRIVET Techniques

2.9.1 - FRIVET 'on' to 'off' switching assay

A confirmed 'on' colony is cultured in the presence of arabinose at a concentration of 0.04% w/v to late exponential phase. The culture is then serially diluted in PBS and plated onto LB agar for overnight incubation. Individual 'on' or 'off' colonies are serially diluted in PBS and replica plated onto LB/LBA plates. The 'off' colonies can be isolated and stored at -70^{0}C.

2.9.2 - FRIVET ampicillin resistance assay *in vitro*

From an overnight culture 50ml of appropriate media was inoculated to an OD(600) of 0.05. Arabinose was added at varying concentrations. The control flask has no inducer added. At required timepoints 100µl samples were taken, diluted serially and 100µl plated onto LB plates and LB ampicillin (10µgl^{-}1). Plates were incubated at 37^{0}C overnight. The colonies on each plate were counted to give the relevant ampicillin resistant % for that flask.

2.10 – Large intestine ligated gut loop assay

Each sheep was determined free from *E. coli* O157:H7 by examining faecal samples before surgery using selective CHROM-agar (CHROMagar Microbiology, France). Each sheep was sedated as described (Wales, A.D., *et al*, 2002). Briefly, each lamb was pre-treated with Xylazine (Rompun 2%, Bayer) and then anaethetised with a combination of diazepam (Valium, Roche) and ketamine (Ketaset, Fort Dodge) given intravenously. After intubation, anaesthesia was maintained by inhalation with isoflourene in oxygen. Twelve ligated intestinal loops, each roughly 10cm long were created by tying pairs of encircling braided nylon ligatires around the spiral colon, maintaining the mesenteric blood supply to each individual segment. A 2ml sample of each inoculum was injected

into each loop with a 25 gauge needle. The injection site was sealed by thermocautery. After inoculation, the intestine was replaced in the abdomen and the incision closed with sutures. The sheep was maintained under anaesthesia. After 6h the ligated segments were excised. The sheep was then killed with pentobarbitone. After removal from the animal each loop was placed in PBS prior to processing.

Each loop in turn was isolated and cut open to reveal the faecal matter and endothelial lining. The faecal matter and other loop contents were resuspended in PBS and serially diluted in PBS before spread plating on SmacNal and SmacNalAmp plates. The endothelial lining was scraped off using a spatula. After resuspension in PBS, the scrapings were serially diluted in PBS and plated on SmacNal and SmacNalAmp plates. Plates were incubated overnight at 37^0C before counting the proportion of ampicillin resistant colonies in each sample.

Chapter 3

Construction of the FRIVET system

3.1 – Deletion of *fim* region from strains ZAP193 and ZAP1

The *fim* region will be deleted from strains ZAP1 and ZAP193 using an allelic exchange vector containing *fim* flanking regions of homology on either side of the *sac/kan* cassette. The flanking regions will be cloned into pIB307 one at a time and a separate exchange vector will be constructed for each strain as flanking regions may contain sequence differences. The *sac/kan* cassette will be used to allow exchange of the full FRIVET constructs at a later date. An outline of the cloning strategy can be seen in Fig 3.2

As previously discussed the *E coli* O157:H7 *fim* operon contains a 16bp deletion in the *fimA* gene that results in the inability to express type 1 fimbriae (Roe *et al,* 2001). Therefore, crucially, by deleting this region we are not affecting the bacterium's natural ability to bind receptors or aid in pathogenesis in the host. However as *E. coli* O157:H7 does contain both characterised and uncharacterised fimbrial clusters, we must be aware that other genes within the *fim* operon may potentially play a role outside of the *fim* operon and that deletion of these genes may have consequences *in vivo* for the pathogenicity of the bacterium.

The region of homology downstream of *fimH* was designated the right flanking region (RFR) and was defined as starting immediately after the stop codon for *fimH.* As has been discussed the region of homology upstream of the *fim* operon, designated the left flanking region (LFR) must contain the necessary *fimB* control elements upstream of the *fim* operon. Therefore the start of the LFR can be defined as being approximately 700bp upstream of the *fimB* transcriptional start site. The organisation of the regions of homology can be seen in Fig 3.1

Fig 3.1

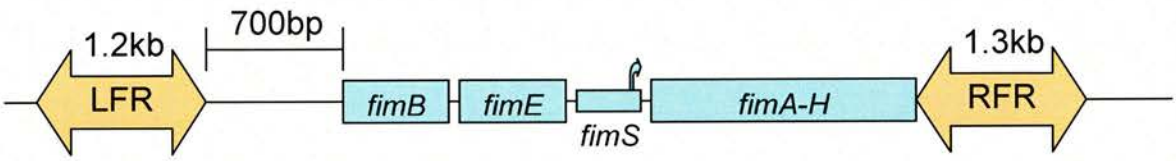

Diagram outlining the positions of the LFR and RFR relative to *fimB* and *fimH* for the FRIVET system

3.2 – FRIVET cloning strategy

Fig 3.2

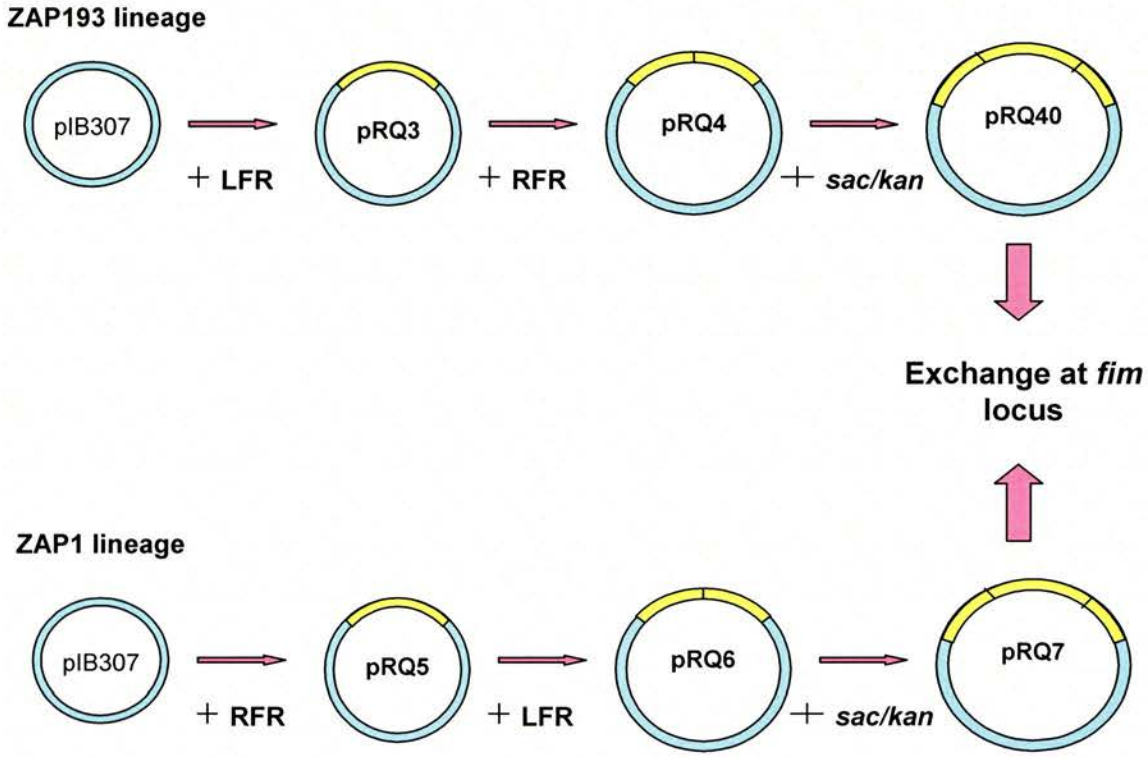

Cloning strategy used for creation of *fim* deletion vectors using temperature sensitive allelic exchange vector pIB307 as a template. Vectors were constructed in AAEC189 prior to single copy exchange into FRIVET strains.

Exchanging the *sac/kan* cassette at the *fim* locus will allow us to conduct a further exchange at this site. Using the same flanking regions of homology FRIVET constructs can be assembled between the LFR and RFR and exchanged into the *fim* locus.

3.3– Cloning the *fim* operon left flanking region from ZAP193 into pIB307

The LFR of the *fim* operon was amplified by PCR from ZAP 193 with primers LFR1 and LFR2 This fragment was digested with *Bam*HI and *Sac*I and ligated into the temperature sensitive exchange vector pIB307 between the *Bam*HI and *Sac*I restriction sites. The pIB307 vector contains a single *Bam*HI site and linearizes at 4.2kb. The cloning of the LFR from ZAP193 introduces an extra 1.2kb. When putative clones are digested with *Bam*HI (Fig 3.3a) three clones (#1, #4, #6) linearized at 5.4kb.

To confirm the cloning of the LFR into pIB307 an *Ava*II digest was performed on clones #1, #4, #6 and a putative negative #2 using pIB307 as a negative control (Fig 3.3b). The LFR introduces a novel *Ava*II site. All four clones produced 2 bands at 1.7kb and 3.7kb against the pIB307 single band at 4.2kb indicating the insertion of the LFR into pIB307 at the correct site. Clone #2 produces the correct banding pattern for the *Ava*II digest but does not seem to linearize any larger than pIB307 and was excluded from further study. Clone #6 was taken forward and designated pRQ3 (Fig 3.3c).

Fig 3.3a

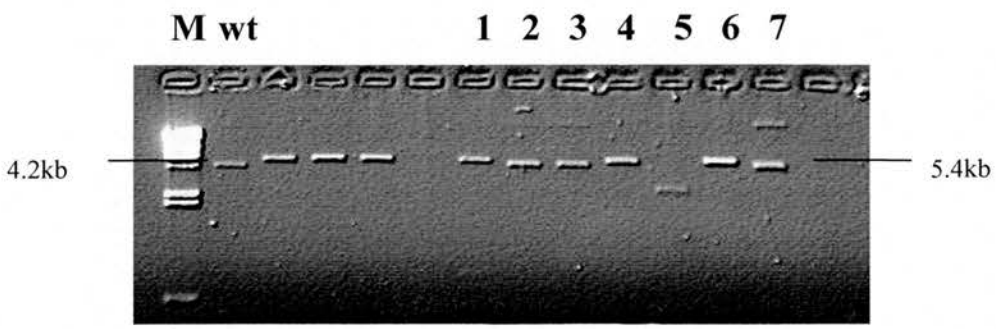

***Bam*HI digest of seven putative clones containing the LFR from ZAP193 compared against pIB307 (wt). Clones #1, #4 and #6 linearize 1.2kb larger than wt. M = *Hind*III ladder.**

Fig 3.3b

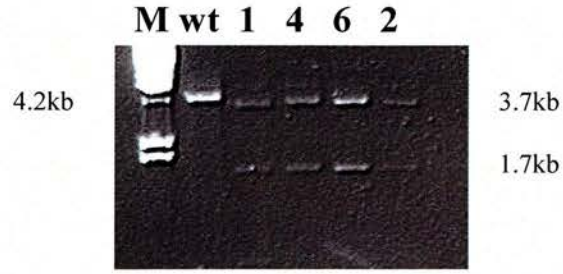

***Ava*II digest of clones #1, #4 and #6 against pIB307 and putative negative clone, #2 and pIB307 (wt). Clones #1, #4, #6 and #2 all produced 2 bands compared to wt, consistent with the cloning of the LFR into pIB307. M = *Hind*III ladder.**

Fig 3.3c

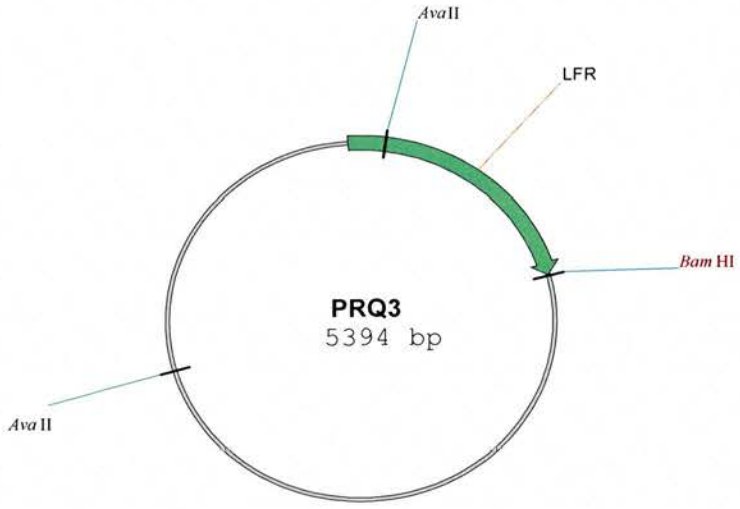

Vector map of pRQ3 showing the cloned LFR from strain ZAP193 and its novel *Ava*II site inserted into pIB307.

3.4- Cloning the *fim* operon right flanking region from ZAP193 into pRQ3

The RFR from ZAP193 *fim* operon was amplified by PCR using primers RFR 1 and RFR 2. The resulting fragment was digested with *Pst*I and *Bam*HI.and cloned into pRQ3 at the *Bam*HI and *Pst*I restriction sites.

Eight putative clones were subsequently analysed by restriction digest. The RFR introduces a novel *Ava*II site and all eight clones produced three bands at 1.7kb, 2.1kb and 2.8kb (Fig 3.4b) compared to pRQ3 that produces two bands at 1.7kb and 3.7kb. This indicates the correct cloning of the RFR into pRQ3. Clone #1 was taken forward and designated pRQ4 (Fig 3.4a).

Fig 3.4a

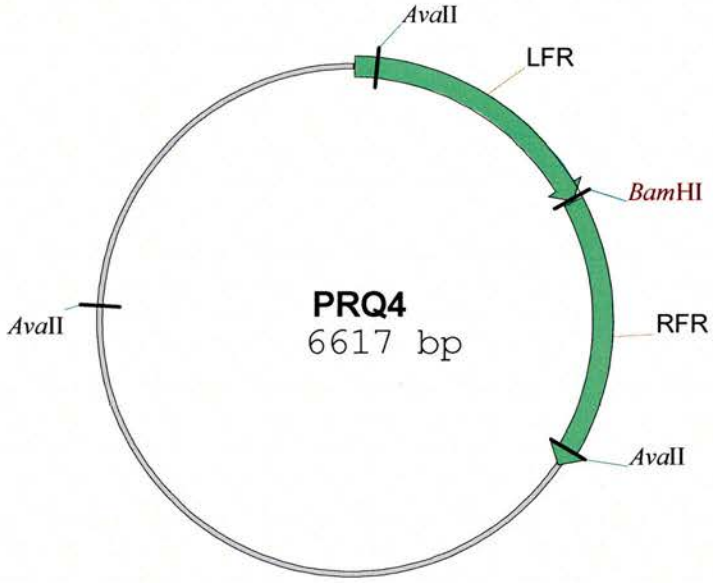

Vector map of pRQ4 containing both the LFR and RFR from strain ZAP193 showing two novel *Ava*II sites.

Fig 3.4b

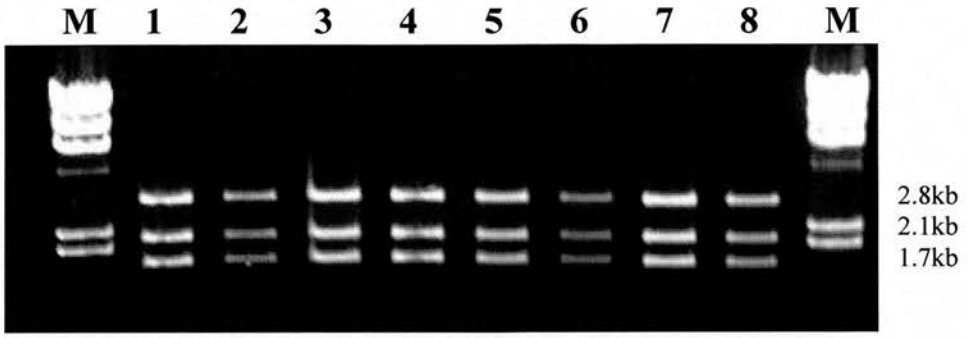

***Ava*II restriction analysis of eight putative pRQ3 clones containing the cloned RFR from strain ZAP193. All eight clones exhibit the expected banding pattern of 1.7kb, 2.1kb and 2.8kb for a correct orientational insertion of the RFR. M = 1kb ladder.**

3.5– Insertion of the *sac/kan* cassette between the LFR and RFR of pRQ4

The *sac/kan* cassette was gel excised from pDG28 and ligated into pRQ4 at the *Bam*HI restriction site. Two putative clones were digested with *Bam*HI to excise the *sac/kan* cassette (Fig 3.5a). One of the clones (#2) produced a band at 3.9kb, corresponding to the correct size for the *sac/kan* cassette and 6.6kb corresponding to the pRQ4 backbone. *E. coli* MG1655 strain AAEC189 was transformed with clone #2 and conferred kanamycin resistance, confirming the correct cloning of the *sac/kan* cassette into pRQ4. Clone #2 was designated pRQ40 (Fig 3.5b)

Fig 3.5a

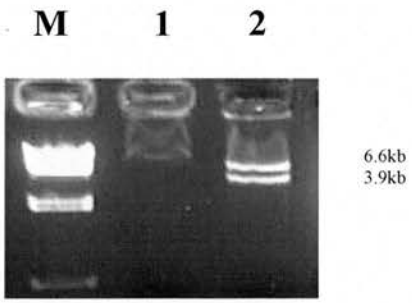

***Bam*HI excision analysis of two putative clones containing the *sac/kan* cassette from pDG28. Clone #2 excises a band at 3.9kb, the expected size for the *sac/kan* cassette. M = *Hind*III ladder.**

Fig 3.5b

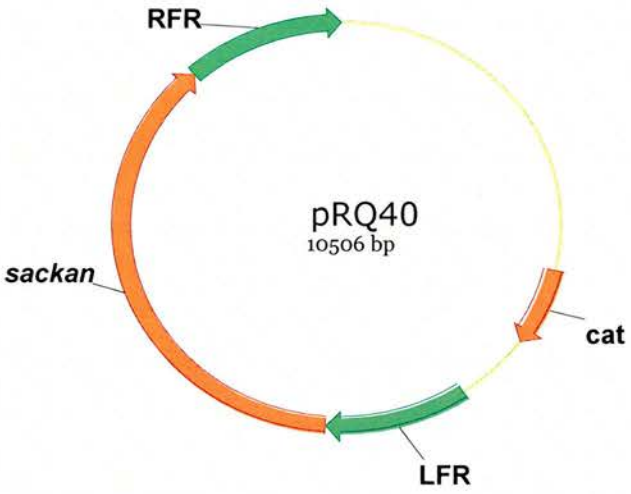

Diagrammatic representation of pRQ40 with the *sac/kan* cassette cloned between the LFR and RFR

3.6 - Cloning the *fim* operon right flanking region from ZAP1 into pIB307

The RFR of the *fim* operon from ZAP1 was amplified by PCR using primers RFR 1 and RFR 2. This fragment was digested with *Bam*HI and *Pst*I and ligated into pIB307 between the *Bam*HI and *Pst*I restriction sites.

Three putative clones were subject to restriction analysis with *Bam*HI and *Ava*II and compared against pIB307 (wt) (Fig 3.6a). All three clones linearized at 5.5kb compared to 4.2kb for wild type pIB307 indicating the cloning of 1.3kb extra DNA. To confirm the extra DNA cloned was the RFR an *Ava*II digest was performed. All three clones produced 2 bands at 2.8kb and 2.7kb. The RFR introduces a novel *Ava*II site compared to pIB307 which linearizes at 4.2kb with a single *Ava*II site. All three clones therefore contain the RFR in the correct orientation. Clone #1 was taken forward and designated pRQ5 (Fig 3.6b).

Fig 3.6a

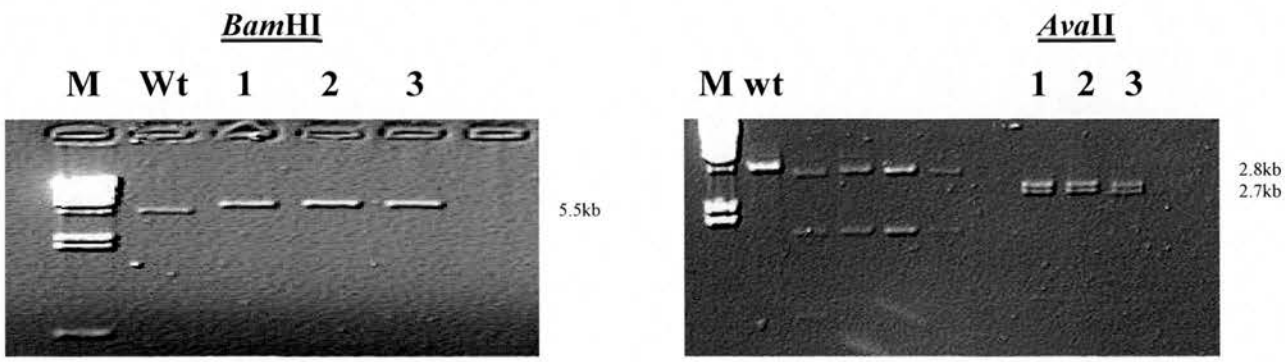

Three putative clones containing the RFR from ZAP1 digested using *Bam*HI and *Ava*II compared against pIB307 (wt). All three clones linearize 1.3kb larger than wt when digested with *Bam*HI and produce two bands of 2.8kb and 2.7kb compared to one band of 5.5kb when digested with *Ava*II. M = *Hind*III ladders.

Fig 3.6b

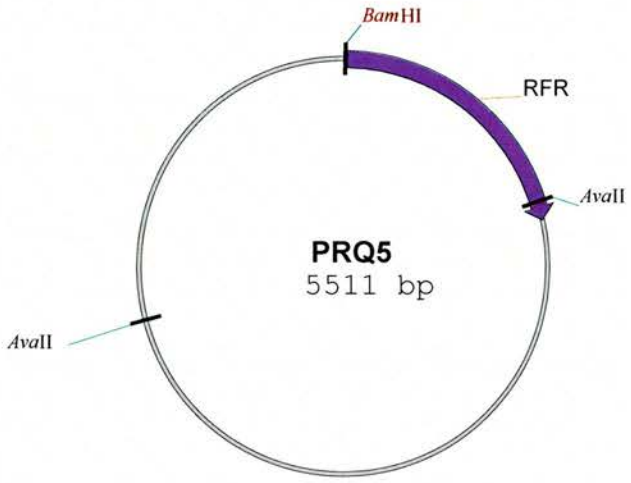

Vector map of pRQ5 showing the additional *Ava*II site on the RFR cloned from ZAP1 into pIB307.

3.7 - Cloning the *fim* operon left flanking region from ZAP1 into pRQ5

The LFR from the ZAP1 *fim* operon was amplified by PCR with the primers LFR 1 and LFR 2. The PCR product was digested with *Sac*I and *Bam*HI and was ligated into pRQ5 between the *Bam*HI and *Sac*I restriction sites.

Twelve putative clones were analysed by restriction digest with *Ava*II. The correct cloning of the LFR into pRQ5 would result in three bands at 1.7kb, 2.1kb and 2.8kb when digested with *Ava*II. Nine of the twelve putative clones produced three bands of 2.8kb, 2.1kb and 1.7kb (Fig 3.7a). Clones #4 and #7 produced an identical banding pattern to pRQ5 of 2.7kb and 2.8kb.

To confirm the LFR/RFR orientation was correct, a diagnostic PCR was performed on three putative correct clones (clones #1, #2, #3) and one putative negative clone (#7) across both flanking regions using the LFR 5' primer and the RFR 3' primer (Fig 3.7c). Clones #1, #2 and #3 produced a PCR product at the predicted length of 2.3kb.
Clone #7 did not produce a PCR product using the LFR/RFR primers. This confirmed the correct cloning of the LFR into pRQ5 and clone #1 was taken forward and designated pRQ6 (Fig 3.7b).

Fig 3.7a

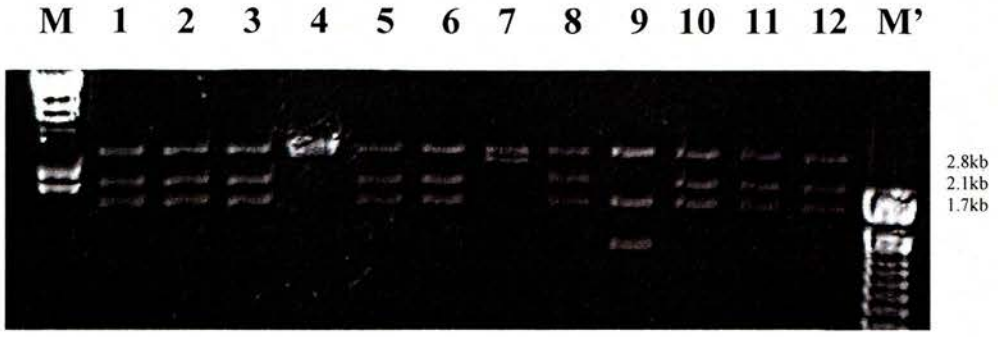

An *Ava*II digest of twelve putative constructs containing the LFR cloned upstream of the RFR in pRQ5. Clones #1-3, #5-6, #8 and #10-12 all exhibit the expected banding pattern for a correct orientational insertion of the LFR into pRQ5. M = *Hind*III ladder; M' = 100bp ladder

Fig 3.7b

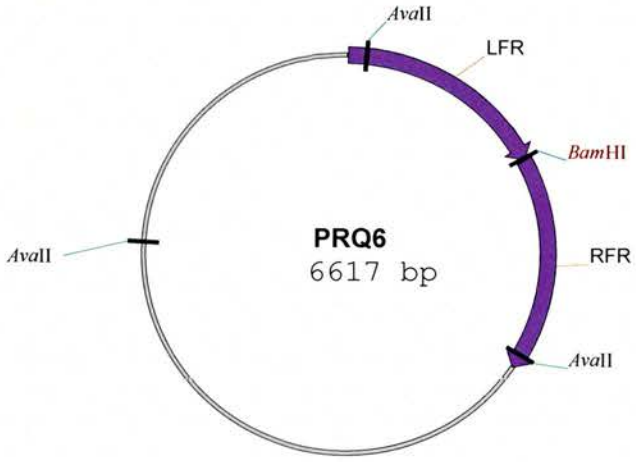

Vector map of pRQ6 containing the LFR cloned upstream of the RFR. The LFR introduces a novel *Ava*II site.

Fig 3.7c

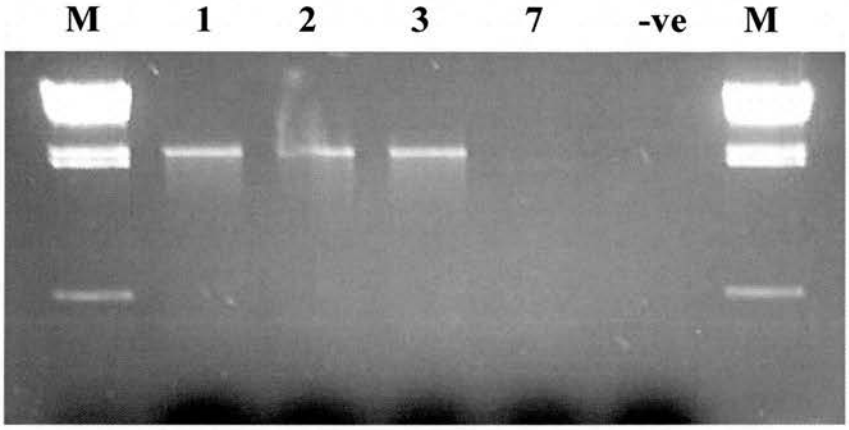

PCR using primers LFR1 and RFR2 on putative clones containing the LFR and RFR from ZAP1. Clones #1-3 all produced bands for the LFR/RFR PCR product. Clone #7 failed to produce a band using these primers. Lane 5 (-ve) is the negative PCR control. M = *Hind*III ladder

3.8– Cloning the *sac/kan* cassette between the LFR and RFR of pRQ6

The *sac/kan* cassette was excised from plasmid pDG28 using *Bam*HI and subsequently ligated into pRQ6 at the *Bam*HI restriction site.

Two putative clones were subjected to *Bam*HI restriction analysis. Clone #1 produced two bands at 6.6kb and 3.9kb indicating the excision of the *sac/kan* cassette (data not shown). Clone #1 also conferred kanamycin resistance to *E. coli* MG1655 strain AAEC189 when transformed. Clone #1 was designated pRQ7 (Fig 3.8).

Fig 3.8

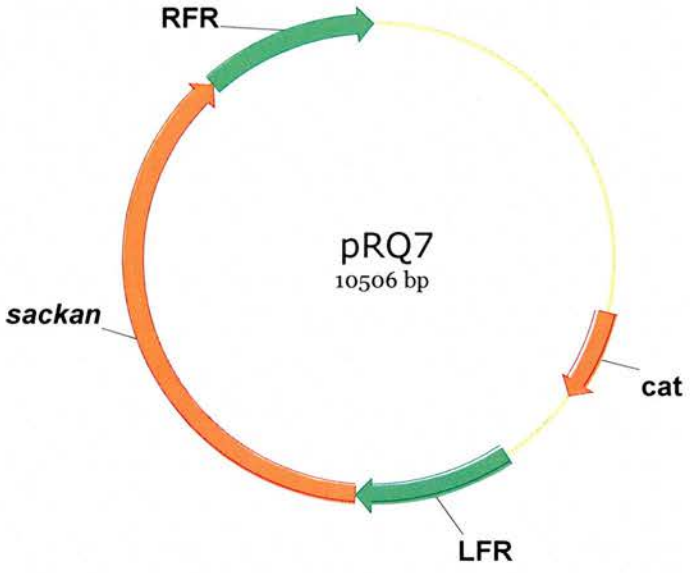

Vector map of pRQ7 showing the *sac/kan* cassette cloned between the LFR and RFR in pRQ6 between two *Bam*HI sites.

3.9– Deletion of the *fim* region from ZAP541

Strain ZAP541 was transformed with the temperature sensitive allelic exchange vector pRQ40. The exchange of the *sac/kan* cassette conferred kanamycin resistance and sucrose sensitivity onto ZAP541. Analysis was performed on two kanamycin resistant strains that showed impaired growth on sucrose media by PCR using primers *fimS* V1 5' and *fimS* 3' to confirm the deletion of the *fim* switch (Fig 3.9). *E. coli* strain MG1655 is used as a positive control in lane 3. Strain #1 was designated ZAP542.

Fig 3.9

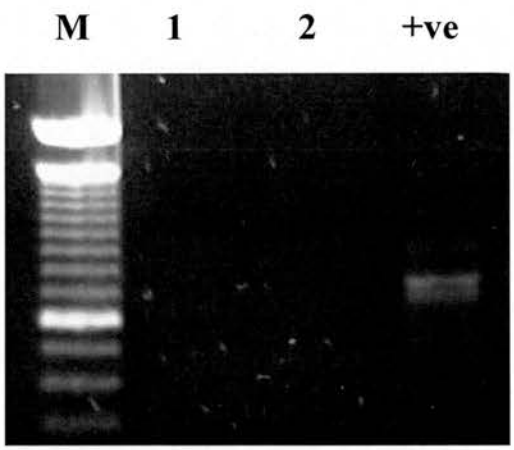

Diagnostic PCR on two *fim* region deleted strains. The PCR is specific for the *fim* switch. Both strains fail to produce a PCR product. Lane 3 contains the positive control *E. coli* MG1655 and produced a band at the expected size for the *fim* switch. M = 100bp ladder.

3.10– Construction of the FRIVET synthetic operon

The backbone of the FRIVET system is a synthetic operon containing three genes: *fimB, fimS* and *bla*. A genetic map of the FRIVET operon is shown in Figure 3.10a. A promoterless copy of *fimB* will be used for its ability to drive inversion of the *fim* switch from the 'off' to the 'on' orientation.

The *fim* switch contains a promoter that, in the 'on' orientation drives transcription of downstream genes, in the *fim* operon these are the *fim* structural genes, in the FRIVET system we will use the reporter gene *bla*, the product of which confers ampicillin resistance upon the cell.

Fig 3.10a

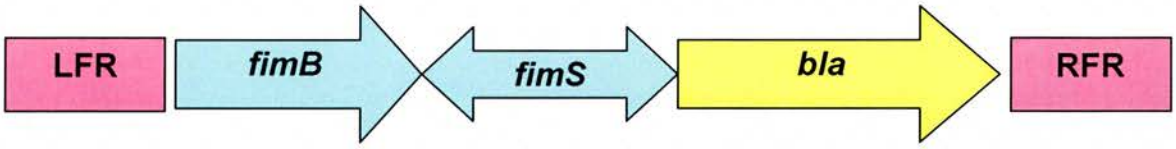

Gene map showing the organisation of the three genes in the FRIVET synthetic operon. The FRIVET operon is constructed between the LFR and RFR for subsequent allelic exchange.

Construction of the FRIVET backbone will take place on the allelic exchange vector pRQ4. All three genes will be cloned between the LFR and RFR on pRQ4 at an intergenic *Bam*HI site in a sequential manner, *fimB* first, followed by *fimS* and *bla*. All cloning steps will be carried out in the Δ*fim E. coli* strains AAEC185 and AAEC189.

The promoterless *fimB* gene will be amplified from MG1655 and the *bla* gene will be amplified from the vector pUC18. The 5' primer for *fimB* contains a novel *Xba*I site for subsequent cloning of the *ara* and other promoters for FRIVET assays.

The *fimS* region will be amplified from three distinct vectors/strains. Each of the three switch regions will be cloned downstream of *fimB* to create three distinct lineages:

- A locked 'on' variant of the switch from vector pMM36
- A locked 'off' variant of the switch from vector pJL2
- A variant with a slower rate of *fimB* mediated switching from strain NEC120

The *fim* switch in strain NEC120 contains an extra base 'T' in the IRR that results in a 30 fold reduction in *fimB* mediated switching (Leathart and Gally, 1998). The cloning strategy for creating the FRIVET backbone and its three *fimS* lineages are summarized in Figure 3.10b

Fig 3.10b

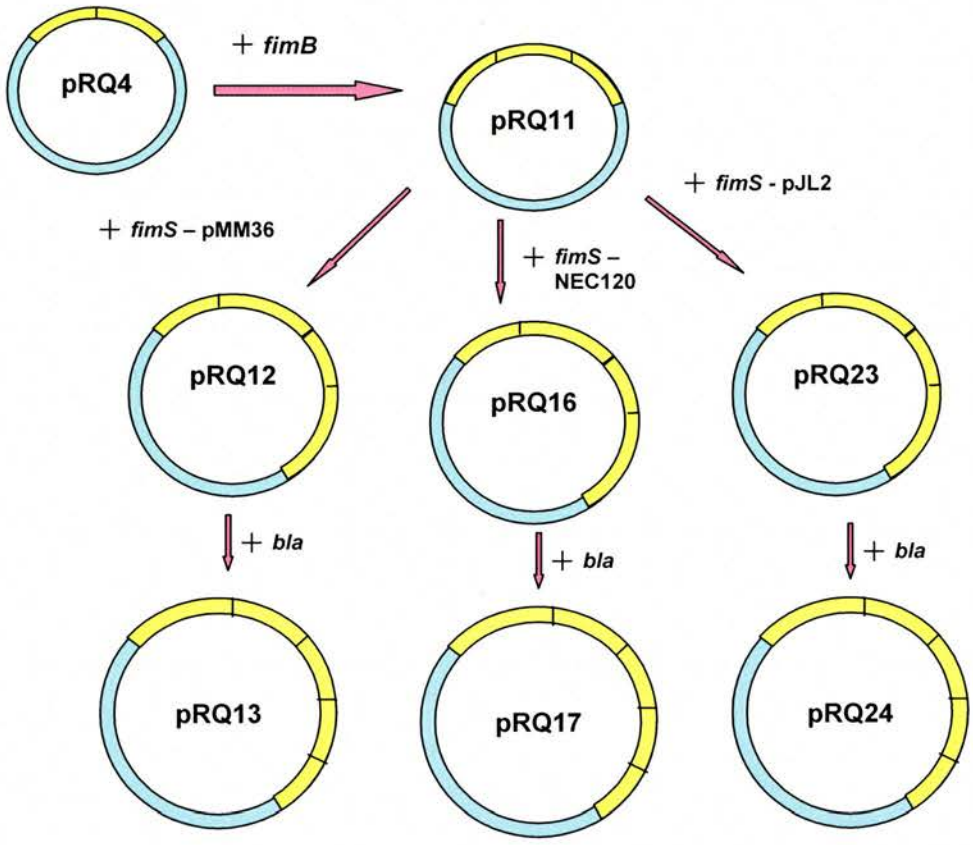

Cloning strategy used to construct the FRIVET backbone lineages using the genes: *fimB*, *fimS* and *bla*. pRQ4 was used as the template and vectors were constructed in strain AAEC189.

3.11 - Cloning the *fimB* gene from MG1655 between the LFR and RFR on pRQ4

The *fim*B gene was amplified from *E.coli* MG1655 using primers *fimB* 5' and *fimB* 3'. The resulting fragment was digested with *Bgl*II and *Bam*HI and ligated with pRQ4. The correct cloning of the *fimB* gene into pRQ4 will change the *Ava*II restriction pattern from 1.7kb, 2.1kb and 2.8kb for pRQ4 to 1.7kb, 2.8kb and 2.8kb for pRQ4 + *fimB*.

Five putative clones were analysed by *Ava*II restriction digest (Fig 3.11b). Clone #4 produced three bands of 1.7kb, 2.8kb and 2.8kb indicating the insertion of a DNA fragment identical in size to *fimB*. To confirm the extra DNA as being the *fimB* gene a specific PCR was performed using primers *fimB* 5' and *fimB* 3' using *E. coli* MG1655 as a positive control (+) (Fig 3.11c). Clone 4 produced a PCR product for *fimB* and was designated pRQ11 (Fig 3.11a)

Fig 3.11a

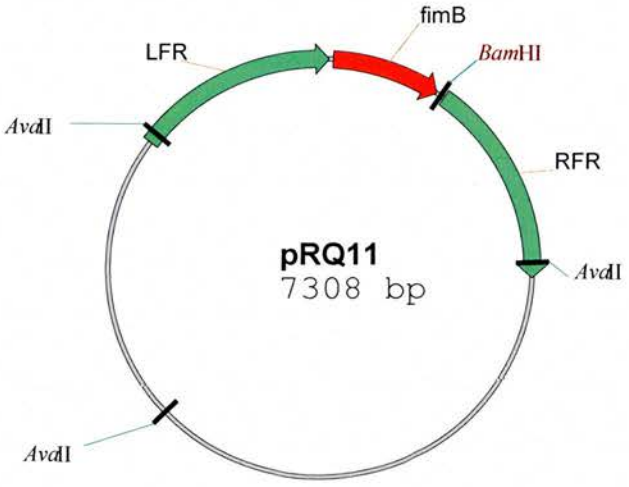

Vector map of pRQ11 showing *fimB* cloned between the LFR and RFR and a *Bam*HI restriction site downstream of *fimB* for subsequent cloning of *fimS* and *bla*.

Fig 3.11b

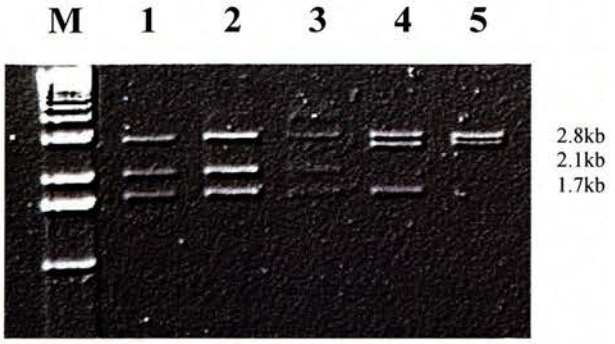

***Ava*II restriction digest of five putative clones of pRQ11. Clone #4 produces a banding pattern indicating the cloning of a *fimB* sized DNA fragment. Clones #1-#3 produce banding patterns identical to pRQ4. M = 1kb Ladder.**

Fig 3.11c

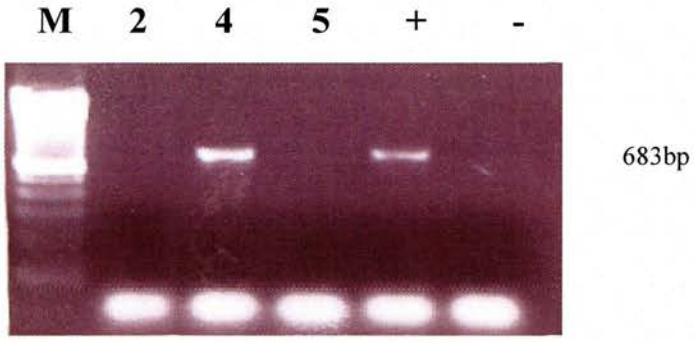

***fim*B specific PCR on clones #2, #4, and #5. The positive control (+) is an MG1655 DNA prep, the negative control (-) is water. Clone #4 is confirmed as containing *fimB*. M = 100bp ladder.**

3.12 – Cloning the *fimS* region from pMM36 into pRQ11

The *fimS* region was amplified from plasmid pMM36 using primers *fimS* 5' V1 and *fimS* 3'. pMM36 contains a copy of *fimS* locked in the 'on' orientation. The resulting fragment was digested with *Bgl*II and *Bam*HI and ligated with pRQ11.

An *Ava*II digest of 3 putative clones against pRQ11 showed two clones (#2 and #3) producing a banding pattern of 1.7kb, 2.8kb and 3.5kb (Fig 3.12a). This banding pattern corresponds to the insertion of DNA of roughly 700bp into pRQ11.

To confirm the extra DNA as *fimS* and to check its orientation a specific PCR was performed using the primer combinations (1) LFR1 and *fimS* 5' and (2) RFR2 and *fimS* 5' (Fig 3.12c). The first primer set was specific for a *fimS* insertion in the reverse orientation with the *Bam*HI site adjacent to *fimB* and the promoter in *fimS* directed upstream towards *fimB*. The second primer set was specific for *fimS* downstream of *fimB* with the *fimS* promoter pointing downstream away from *fimB* into the RFR.

Clones #2 and #3 produced a PCR product of the expected size with primer set 1 and clone #1 produced a PCR product for primer set 2. However the *Ava*II banding pattern for #1 suggests an insertion of a fragment of DNA larger than 700bp. As this result could not be readily explained, clones #1 was discarded and clone #2 designated pRQ12 (Fig 3.12b)

Fig 3.12a

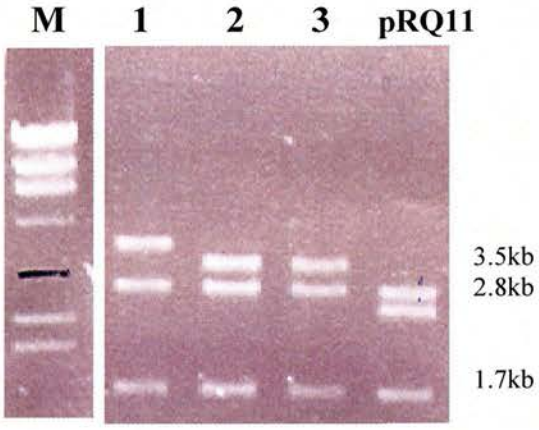

***Ava*II digest of three putative clones of pRQ12. #2 and #3 produce banding patterns indicating the cloning of an extra ~700bp DNA. M = 1kb Ladder**

Fig 3.12b

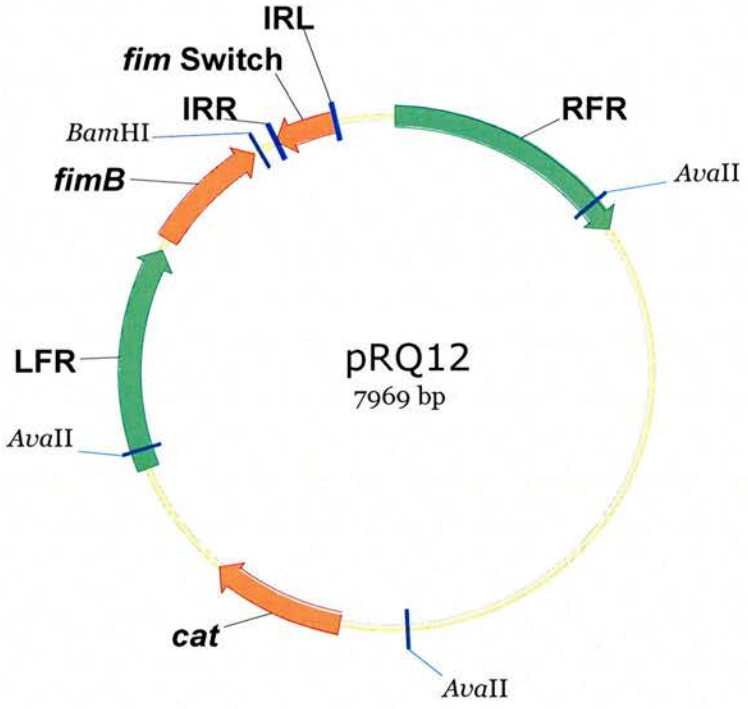

Vector map of pRQ12 showing the *fimS* region cloned downstream of *fimB*. The promoter in *fimS* is poining upstream into *fim*B.

Fig 3.12c

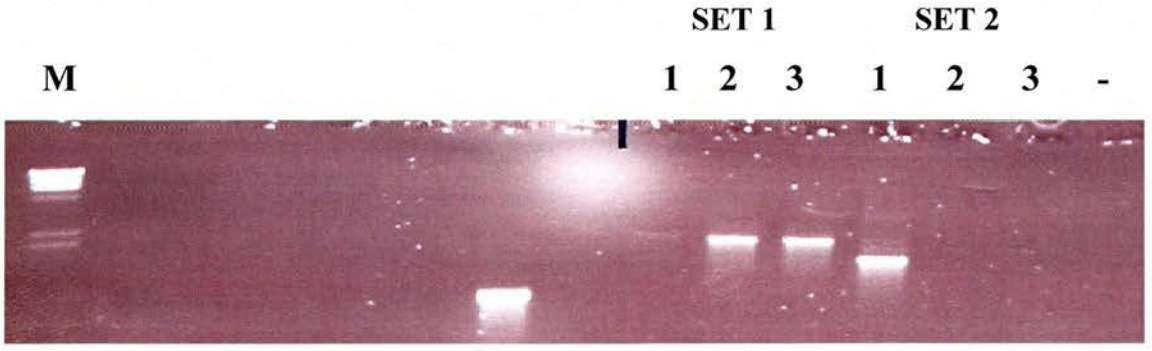

Diagnostic PCR to confirm the cloning of the *fimS* region into pRQ12 and to check its orientation respective to *fimB*. Clones #2 and #3 produce PCR products of the expected length confirming the cloning of the *fimS* region into pRQ11. M = *Hind*III ladder

3.13 – Cloning the *bla* gene into pRQ12 to create a transcriptional fusion with the promoter in *fimS*.

The *bla* gene was amplified from pUC18 using primers *bla* 5' *Bam*HI and *bla* 3'. The PCR product was digested with *Bam*HI and cloned downstream of *fimS* to create a transcriptional fusion with the *fimS* promoter. As the *bla* gene was cloned in using *Bam*HI sites the orientation of *bla* was confirmed by patching successful ligation reactions onto LBA and LBC plates. Six clones were found to be resistant to ampicillin.

To confirm these six clones had the correct *fimS::bla* transcriptional fusion construct an *Ava*II digest was performed on the six putative clones using two ampicillin sensitive clones and pRQ12 as controls (Fig 3.13b). The *bla* gene contains an *Ava*II site, thus correctly cloning the *bla* gene into pRQ12 in the correct orientation respective to fimS will result in an *Ava*II banding pattern of 2.8kb, 2.5kb, 1.9kb and 1.7kb. Clones #1 and #2 match this expected banding pattern. The two ampicillin sensitive controls C1 and C2 match the *Ava*II banding pattern for pRQ12. Clones #3 - #6 were ampicillin resistant but do not show the expected *Ava*II banding pattern.

To further confirm the *fimS::bla* fusion a PCR was performed using the 5' *fimS* V1 primer and the *bla* 3' primer (Fig 3.13a). Clones #1 and #2 produced a PCR product of the expected length confirming the creation of the *fimS::bla* fusion. Clones #3-#6, C1 and C2 did not produce a PCR product at the expected length and were discarded. Clone #1 was subsequently designated pRQ13 (Fig 3.13c)

Additionally pRQ13 was sequenced across the region spanning from the LFR to the RFR to confirm the genetic organisation of the FRIVET operon. Analysis of the sequence data showed no disruption of any of the ORF's in the FRIVET operon (data not shown).

Fig 3.13a

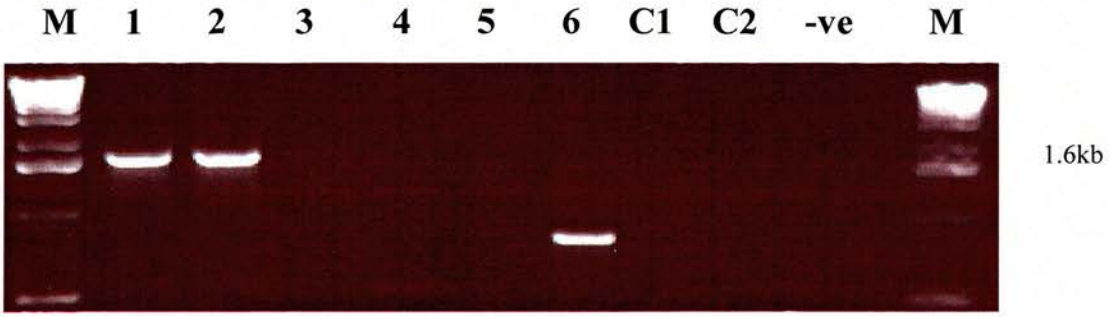

Fusion PCR specific for the *fimS*::*bla* construct. Clones #1 and #2 produced a PCR product of the expected length at 1.6kb. M = 1kb Ladder

Fig 3.13b

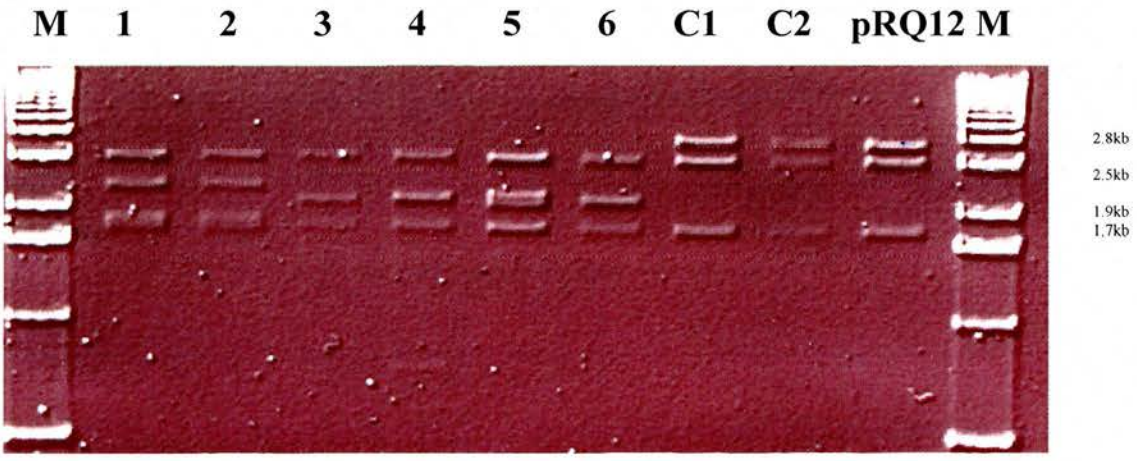

***Ava*II digest of six ampicillin resistant pRQ13 clones, #1 and #2 exhibit the correct banding pattern for a DNA fragment insertion next to *fimS*. M = 1kb ladder**

Fig 3.13c

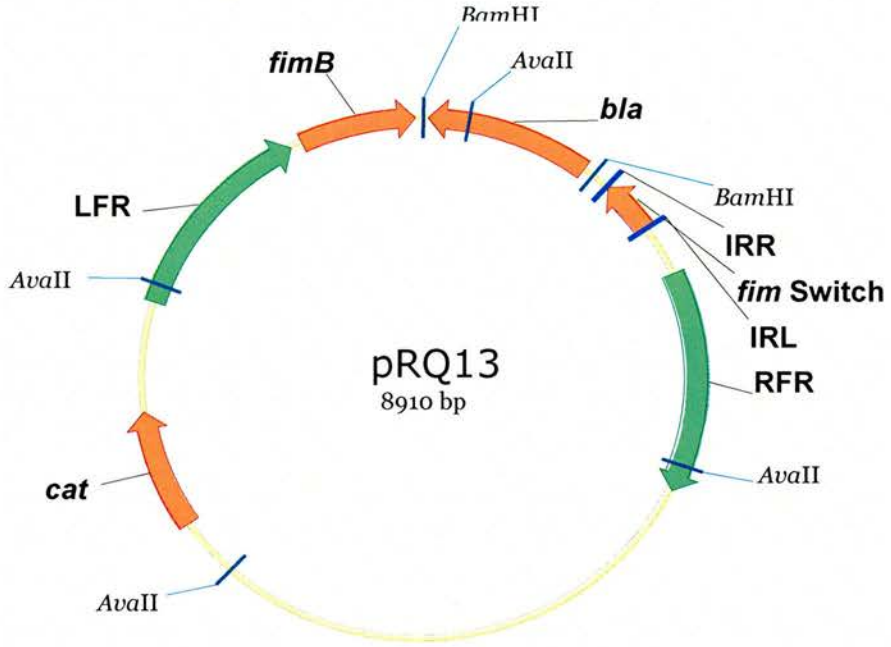

Vector map of pRQ13 showing the *fimS::bla* fusion construct downstream of *fimB* and the novel *Ava*II restriction site within *bla*.

3.14 – Cloning the *fimS* region from strain NEC120 into pRQ11

The *fim* switch region was amplified from *E. coli* strain NEC120 using primers *fimS* V1 5' and *fimS* 3' and the PCR fragment was digested with *Bgl*II and *Bam*HI before ligation with pRQ11.

Seven putative clones were analysed by *Ava*II restriction digest (Fig 3.14a). A correct insertion of *fimS* would result in an *Ava*II banding pattern of 3.5kb, 2.8kb and 1.7kb against 2.8kb, 2.8kb and 1.7kb for pRQ11. Figure 12b shows clones #2 and #3 with the expected banding pattern for a *fimS* insertion between the LFR and RFR. To confirm the presence of *fimS* and to check its orientation respective to *fimB*, a diagnostic PCR was performed using on clones #2 and #3 using two sets of primers: (1) *fimB* 5' and *fimS* 3'; (2) *fimB* 5' and *fimS* V1 5' (figure 3.14c). Clones #1 and #11 were used as negative controls and water was used as a PCR control (-) (Fig 3.14c)

Clone #3 produced a positive PCR product with primer set (1) and clone #2 produced a positive PCR with primer set (2) indicating both orientations of *fimS* were represented. Clone #3 was taken subsequently designated pRQ16 (Fig 3.14b).

Fig 3.14a

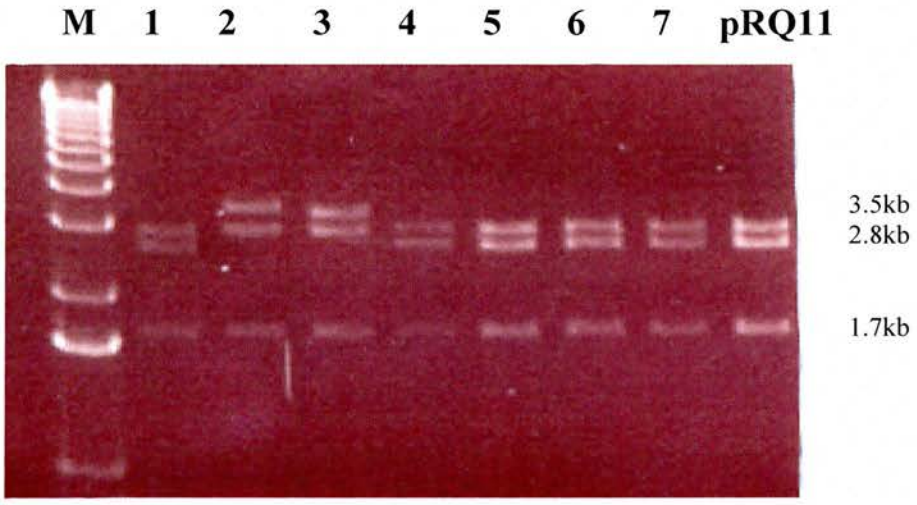

***Ava*II restriction digest on seven putative pRQ16 clones. Compared to pRQ11, clones #2 and #3 produce banding patterns indicating the insertion of *fimS* sized DNA fragment between the LFR and RFR. M = 1kb Ladder**

Fig 3.14b

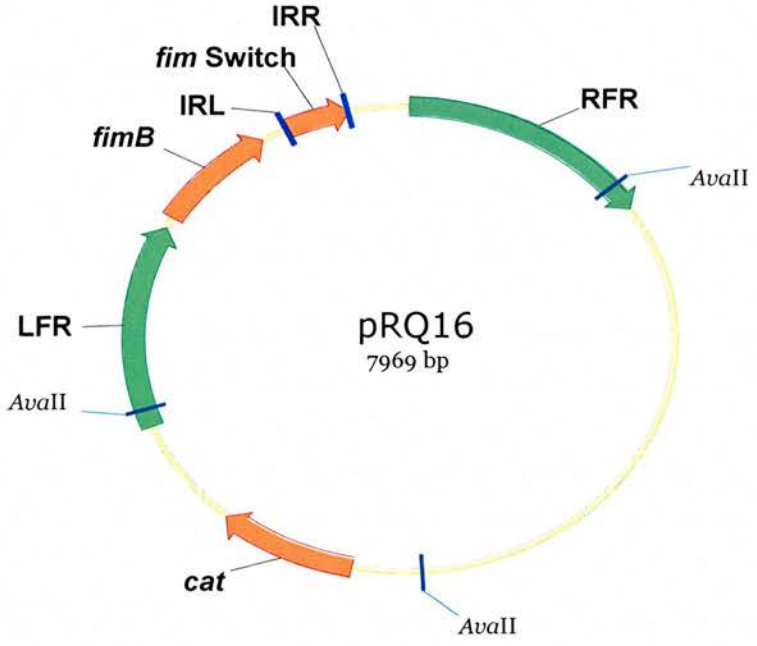

Vector map of pRQ16 showing the orientation of the *fimS* region after cloning downstream of *fimB*.

Fig 3.14c

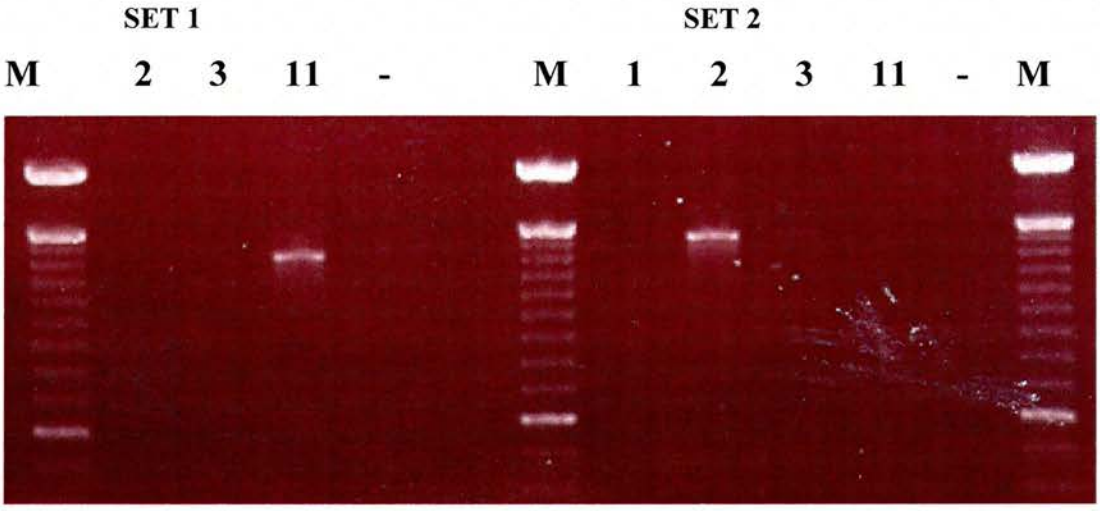

PCR using *fimB* and *fimS* primers to confirm the orientation of *fimS* repective to *fimB*. Clone #3 and clone #2 contain different orientations of *fimS*. M = 100bp Ladder

3.15 - Cloning *bla* into pRQ16 downstream of *fimS*

The *bla* gene was amplified from pUC18 using primers *bla* 5' *Bam*HI and *bla* 3' and the resulting PCR product was digested with *Bam*HI and ligated with pRQ16. Eight putative clones were analysed by *Bam*HI restriction digest to attempt to excise the *bla* gene. Only clone #6 excised a band at the expected size for the *bla* gene (Fig 3.15b).

To confirm *bla* orientation in clone #6 a PCR was performed using two sets of primers: (1) *fimS* V1 5' and *bla* 5'; (2) *bla* 5' and RFR2 (Fig 3.15c). Clone #6 produced a PCR product of the expected size for a *fimS::bla* fusion using primer set (2), confirming the correct orientation of *bla* respective to *fimS*. Clone #6 was subsequently designated pRQ17 (Fig 3.15a)

Fig 3.15a

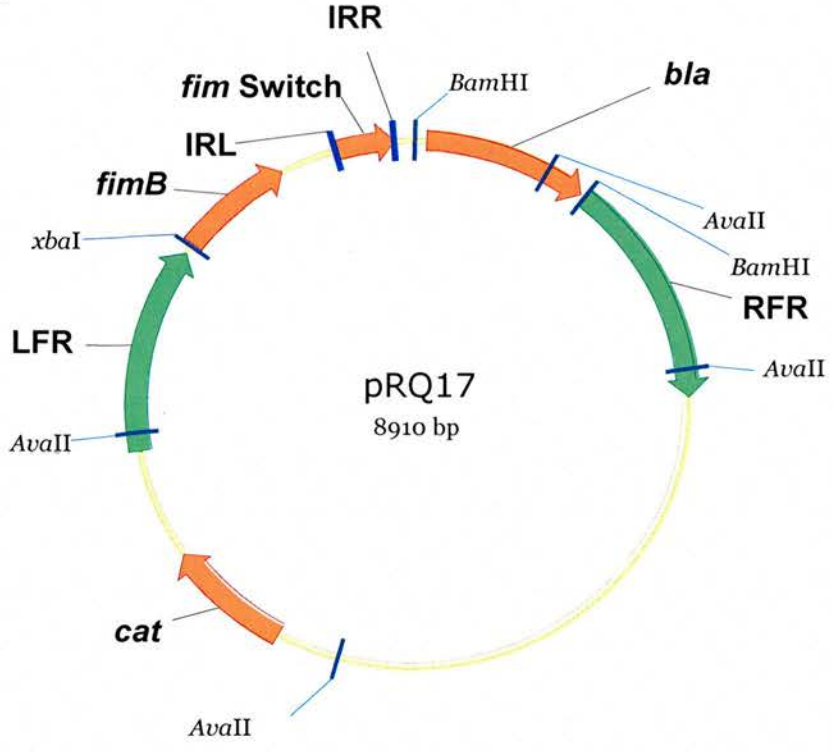

Vector map of pRQ17 showing the orientation of the *fimS::bla* fusion and the *Xba*I restriction site in *fimB* for subsequent promoter cloning. The *Bam*HI sites flanking the *bla* gene are also shown.

Fig 3.15b

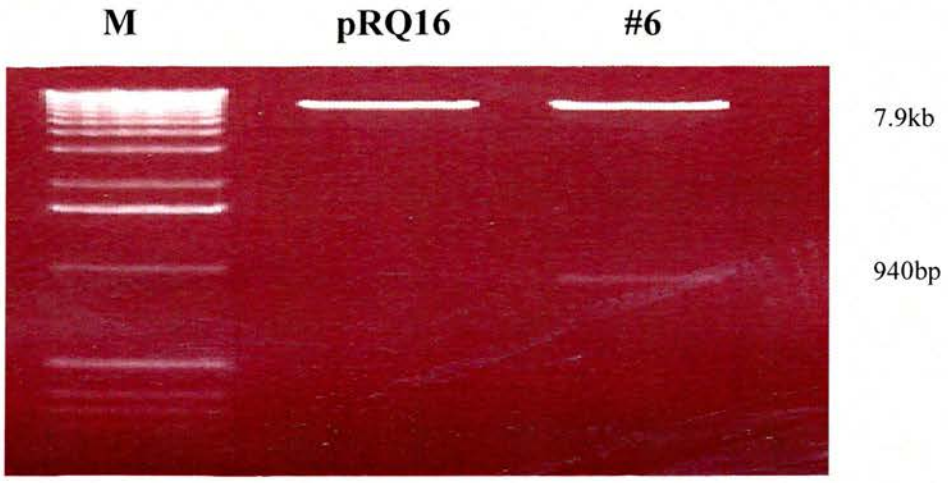

***Bam*HI restriction digest on clone #6 compared to parent vector pRQ16. A band of 950bp is excised, indicating the cloning of *bla* into pRQ16. M = *HinD*III ladder.**

Fig 3.15c

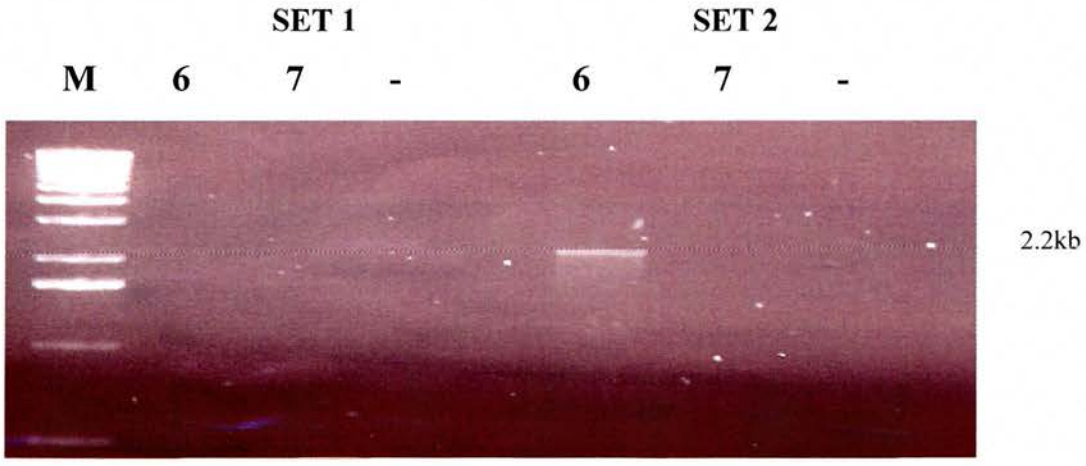

Diagnostic PCR on clones #6 and #7 using two sets of primers. Clone #7 failed to excise a band in the *Bam*HI restriction assay and is included as a negative control. Clone #6 produces a band of the expected size using primer set 2, confirming the cloning of *bla* in the correct orientation respective to *fimS*. As expected clone #7 failed to produce a PCR product. Water is used as a negative PCR control (-). M = 1kb Ladder

3.16 - Cloning *fimS* from pJL2 into pRQ11

The *fimS* region was amplified from pJL2 using the primers *fimS* V1 5' and *fimS* 3' and the resulting fragment digested with *Bgl*II and *Bam*HI before ligation with pRQ11 at the *Bam*HI site downstream of *fimB*.

A single putative clone was digested with *Ava*II and its banding pattern compared with pRQ11 (Fig 3.16b). The clone produced a banding pattern of 1.7kb, 2.8kb and 3.2kb corresponding with the expected jump in size of the 2.8kb band in pRQ11 from2.8kb to 3.2kb indicting an extra 400bp of DNA inserted between the *Ava*II sites.

To confirm the presence of the *fimS* region, and to identify its orientation, a diagnostic PCR was performed using 2 sets of primers: (1) *fim*B 5' and *fimS* 3' new; (2) *fimB* 5' and *fimS* V1 5' (Fig 3.16c). A PCR product of the expected size (1.3kb) was produced using primer set 1. Clone #1 was designated pRQ23 (Fig 3.16a).

Fig 3.16a

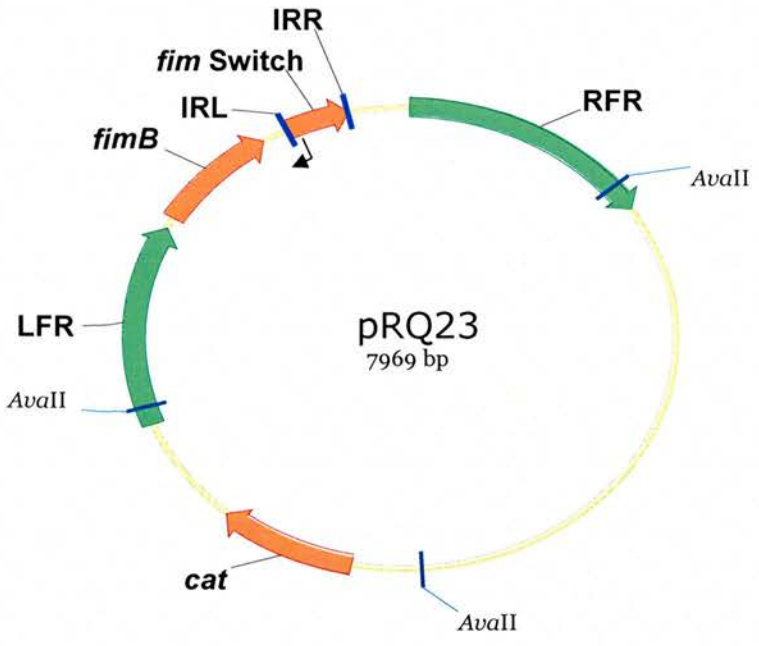

Vector map of pRQ23. The *fimS* region is cloned from pJL2 downstream of *fimB* increasing the distance between the *Ava*II sites on the LFR and RFR.

Fig 3.16b

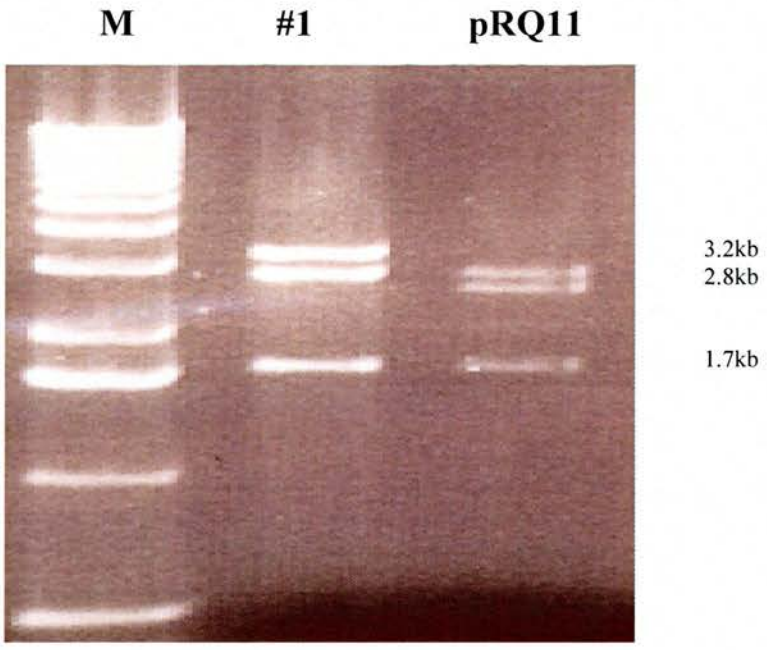

***Ava*II digest on a single putative clone compared against pRQ11. The 2.8kb band in pRQ11 has risen to 3.2kb, indicating the presence of an extra 400bp. M = 1kb ladder**

Fig 3.16c

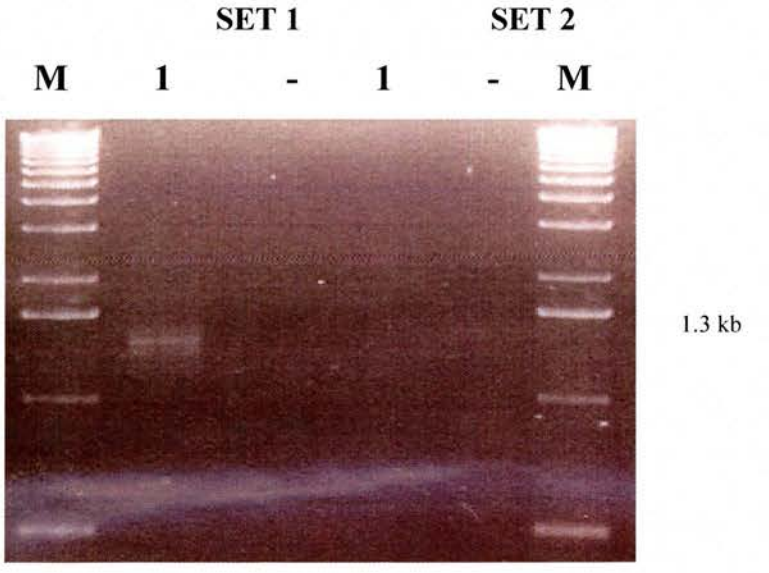

PCR using two sets of primers to confirm the orientation of *fimS* respective to *fimB*. Clone #1 produces a PCR product at the expected size with primer set 1 indicating the cloning of *fimS* in the orientation seen in Fig 13a. M = 1kb ladder

3.17 - Cloning the *bla* gene downstream of *fimS* in pRQ23

The *bla* gene was amplified from the vector pUC18 using primers *bla* 5' *Bam*HI and *bla* 3' and the resulting PCR product digested with *BamHI* and ligated with pRQ23.
Eight putative clones were subjected to *Ava*II restriction analysis and compared against pRQ23 (Fig 3.17b). Clone #7 produced a banding pattern of 1.3kb, 1.7kb, 2.8kb and 3kb (the 2.8kb and 3kb bands are seen as a doublet). This corresponds to the expected banding pattern for clones containing the *fimS::bla* fusion as the *bla* gene contains a novel *Ava*II site at its 3' end thereby increasing the number of bands from three in pRQ23 to four in a pRQ23::*bla* clone.

To confirm the cloning of the *bla* gene a *Bam*HI excision was performed on clone #7 and compared with clone #6 and pRQ23 (Fig 3.17c). As expected, a band was excised from clone #7 but not from clone #6 or pRQ23 that matched the correct size for the *bla* gene. Clone #7 was subsequently designated pRQ24 (Fig 3.17a).

Fig 3.17a

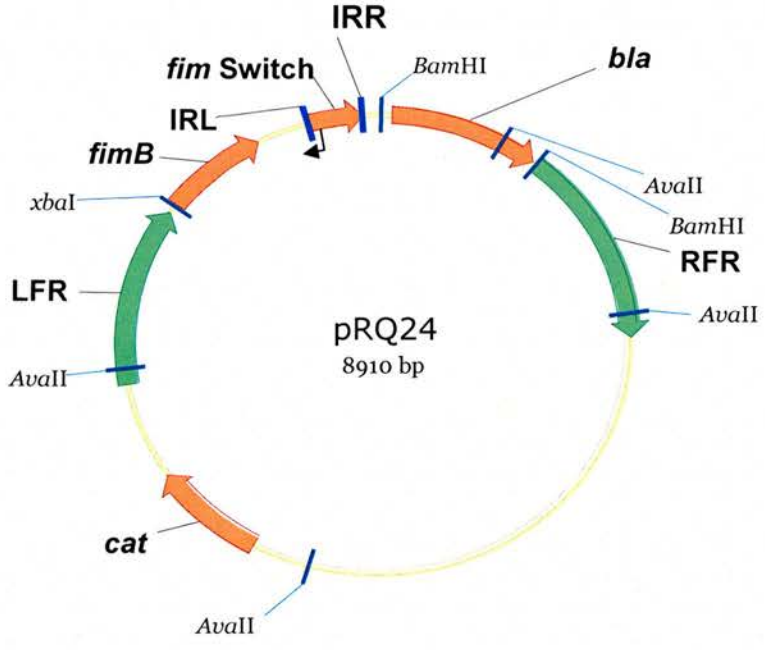

Vector map of pRQ24 showing the *bla* gene cloned downstream of *fimS* to create a *fimS::bla* fusion construct.

Fig 3.17b

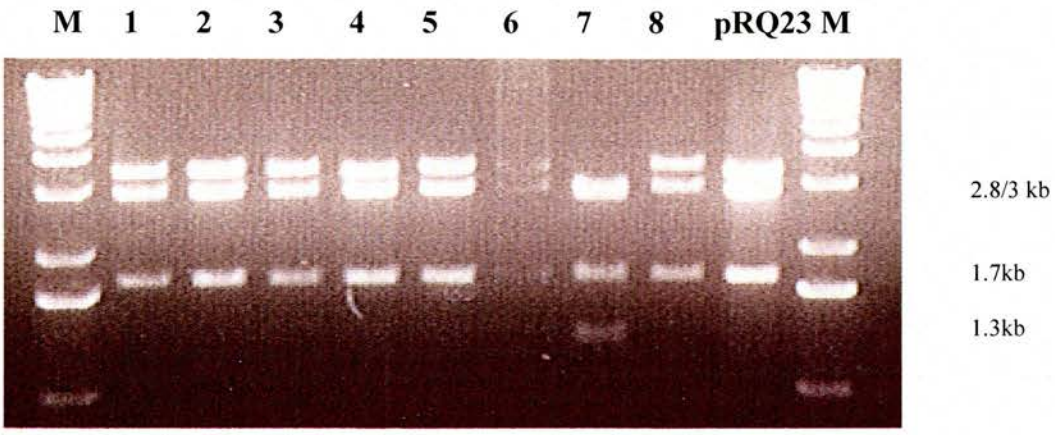

***Ava*II digest on eight putative pRQ23::*bla* clones. #7 produces the expected banding pattern for a *fimS::bla* fusion construct. The 2.8kb and 3kb bands are seen as a doublet, further resolution of the agarose gel would result in the separation of this doublet. M = 1kb ladder.**

Fig 3.17c

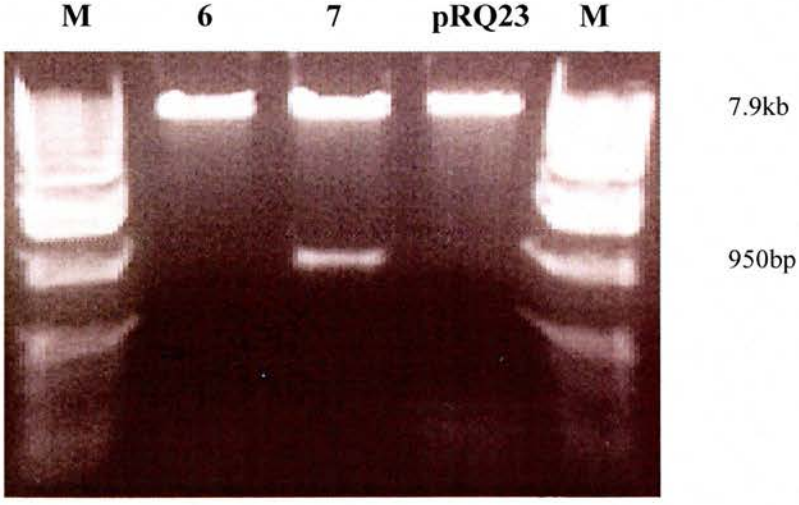

***Bam*HI excision digest on clones #6, #7 and pRQ23. Clone #7 excises a *bla* sized band at 950bp confirming the presence of *bla*. Clone #6 and pRQ23 fail to excise a band and linearize at 7.9kb. M = 1kb Ladder.**

3.18 – Chapter 3 Discussion

The creation of FRIVET strains for use in *in vivo* assays requires the construction of a synthetic operon on an allelic exchange ready, pIB plasmid based background. The backbone of the FRIVET system was constructed using the components: *fimB, bla* and *fimS.*

All FRIVET constructs were to be placed in single copy at the *fim* locus in the ZAP193 background. This was achieved using pRQ40. Plasmid pRQ40 was constructed using ~1kb regions of homology upstream and downstream of the *fim* operon termed the LFR and RFR. These fragments were amplified from ZAP193 and cloned into the temperature sensitive allelic exchange vector pIB307 to create plasmid pRQ4.

Finally the *sac/kan* cassette was cloned between the LFR and RFR to create pRQ40. The *sac/kan* cassette is important in the process as it allows selection of successful exchange strains (Blomfield *et al,* 1991) and as such would be needed for the subsequent exchange of FRIVET strains into the *fim* region. The exchange process was successful and the *fim* region was deleted from ZAP541 and ZAP544 to create ZAP542 and ZAP545. Strains were analysed by their antibiotic sensitivity profile and their growth on sucrose containing media. Additionally a PCR was performed using *fimS* specific primers on two strains of ZAP542. As expected both strains failed to produce a PCR product for *fimS* against a positive control (strain MG1655) indicating the successful deletion of the *fim* region from ZAP541 and the creation of ZAP542.

The *fim* deletion vector pRQ7 was also constructed using the LFR and RFR from ZAP1 for deletion of the *fim* region from ZAP1, a category 3 EHEC strain. However, the exchange process was repeated multiple times yet failed to produce exchange strains with the correct antibiotic resistance profile. A possible explanation for this could be the LFR and/or RFR PCR products containing mismatched bases created at the amplification stage. The standard *Taq* polymerase has a mismatch rate of about 1 base in 1000. The primer sequences were also taken from the sequenced EHEC strain EDL933 (Perna *et al,* 2001) and not from the actual ZAP1 sequence and as such the two EHEC sequences could

differ at the flanking regions, resulting in less homology than is needed for successful allelic exchange.

Due to the successful exchange into the ZAP193 background, it was decided to concentrate on ZAP193 based FRIVET strains and to cease working with the ZAP1 background.

The FRIVET backbone was constructed in a stepwise manner using a pIB307 vector as the starting point. The first step was the cloning of the *fimB* gene from MG1655 in between the LFR and RFR on pRQ4 and the resulting clones were analysed by restriction digest and PCR to confirm the creation of pRQ11. The next cloning step was the insertion of the three *fim* switch variants at the *Bam*HI restriction site downstream of *fimB* on pRQ11. The three *fimS* variants were:

- 'on' orientation from pMM36 – pRQ12
- 'off' orientation from pJL2 – pRQ23
- a slower inversion rate 'on' orientation switch from strain NEC120 – pRQ16

All three switch variants were successfully cloned into the *Bam*HI site downstream of *fimB* and results were verified with restriction analysis and diagnostic PCR.

The final step in creating the FRIVET synthetic backbone was the cloning of the *bla* gene downstream of *fimS* for each of the three *fimS* variant lineages. The cloning of *bla* into pRQ12 allowed us to select putative clones by screening on ampicillin containing media. Clones that were resistant to ampicillin therefore would have contained a functioning *fimS::bla* transcriptional fusion where the promoter in *fimS* drives transcription of the *bla* gene. Subsequent restriction digest and diagnostic PCR confirmed the successful cloning of *bla* into pRQ11. The cloning of the *bla* gene into pRQ23 and pRQ16 was also successful, verified by restriction digest and diagnostic PCR.

The FRIVET system backbone was now constructed. The next step in the construction of FRIVET strains was to clone promoters of choice to drive *fimB* expression and to construct the inhibitory mechanisms needed to control the FRIVET system.

Due to the technical difficulties of constructing the FRIVET operon, many lines of construction had to be 'dropped' after numerous attempts. Whilst it is important to create a functioning FRIVET operon, further efforts must be made to construct the various *fimS* variants and *E. coli* O157:H7 background variants. Without having these variants it will be much harder to create a controllable FRIVET system or to answer specific questions about strain differences in *E. coli* O157:H7 during infection or colonisation.

Chapter 4

Cloning of EHEC promoters into the FRIVET backbone & Construction of FRIVET Control Plasmids

4.1 – Introduction

This chapter will focus on two separate elements:

- The cloning of EHEC promoters upstream of *fimB* into various FRIVET constructs outlined in chapter 3 to create test FRIVET constructs
- The construction of plasmid constructs designed to control the FRIVET operon. These constructs will be placed in single copy at a separate locus to the FRIVET operon.

4.2- Cloning EHEC promoters in front of *fimB* to create FRIVET vectors

The FRIVET backbone consists of a promoterless copy of *fimB* upstream of the *fimS*::*bla* fusion construct. The 5' *fimB* primer contains *Bgl*II and *Xba*I restriction sites as 5' tails (Fig 4.2). The *Bgl*II site will be used to clone the amplified *fimB* into the *Bam*HI site on pRQ4 and the *Xba*I site will be used to clone promoters of choice upstream of *fimB* to create functional transcriptional fusions to *fimB*. Thus *fimB* will be under the transcriptional control of the cloned promoter and consequently *fimS* inversion rates and Bla production.

The promoters were cloned into two lineages of FRIVET backbone: pRQ13 and pRQ24. Both lineages contain wt *fim* switch regions but the orientation of the FRIVET operon differs in each lineage. Our limited knowledge of the behaviour of the FRIVET operon meant a greater chance of successfully creating a working FRIVET construct using two distinct lineages.

Fig 4.2

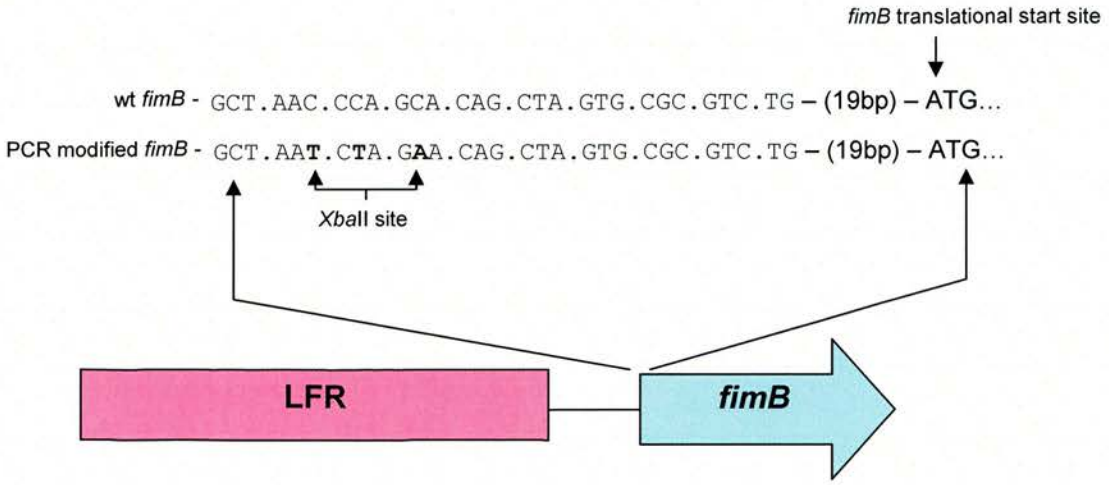

The 5' *fimB* primer introduces a novel *Xba*I site 38bp upsteam of the *fimB* translational start site. 3 bases are modified from wt sequence in the primer to effect this change.

The four EHEC promoters were initially chosen to be cloned were:

- *lee5* – LEE5 (*tir, cesT, eae*) operon control in EHEC
- *fliC* – Flagella regulation
- *lpf1* – controls EHEC long polar fimbriae production
- *loc8* – controls EHEC Loc8 fimbrial production

Our choices reflect a wide variety of EHEC virulence factors. To represent the LEE pathogenicity island we will use the promoter for the LEE5 operon, responsible for transcription of the *tir, cesT* and *eae* genes. The *tir* gene product: the translocated intimin receptor is a translocated effector protein that embeds itself into the host cell membrane

and acts as a receptor for the *eae* gene product: the adhesin Intimin. CesT acts as a chaperone for Intimin.

Bacterial flagella ultrastructure shares many components with type III secretion systems and flagella regulation may be linked to EHEC pathogenesis as part of a global virulence gene cascade. *E. coli* O157:H7 flagella have also been shown to play a role in persistence of infection in chickens (Best *et al*, 2005) and more recently, GrlA, a LEE encoded positive regulator of LEE gene expression, acts as a negative regulator of flagellar gene expression (Iyoda *et al*, 2006).

The promoters for two EHEC specific adhesins will also be studied. The importance of Lpf1 in an EHEC colonisation study is yet to be elucidated but Loc8 was identified in a signature tagged transposon mutagenesis study as a potentially important adhesin for EHEC colonisation (Dziva *et al*, 2004), however studying the activity of these fimbrial promoters *in vivo* will allow us to draw futher conclusions about EHEC pathogenesis and primary attachment.

4.3 - Cloning the *lee5* promoter into pRQ13

The *lee5* promoter from strain ZAP193 was amplified by PCR using primers LEE5 5' and LEE5 3', digested with *Xba*I and ligated with *Xba*I digested pRQ13.

Eleven putative clones were screened by PCR using primers LEE5 5' and *fimB* 3' (Fig 4.3b) to identify *lee5* clones that had inserted in the correct orientation respective to *fimB* to create a *lee5::fimB* transcriptional fusion. The diagnostic PCR yielded one clone, #23, that produced a positive PCR product for the *lee5::fimB* construct. The band on the agarose gel is at the expected size (1.2kb) but is faint. This is due to the two primers not being designed to be used together. As such one of the primers will anneal to the DNA with less specificity leading to a weaker, less defined band when run on an agarose gel.

To confirm the result of the PCR an *Ava*II digest was performed on clone #23 and pRQ13 (Fig 4.3c). The change in banding pattern from 1.7kb, 1.9kb, 2.4kb and 2.8kb for pRQ13 to 1.7kb, 2.4kb, 2.4kb and 2.8kb for pRQ101 is due to the extra *lee5* promoter DNA raising the 1.9kb band to 2.4kb. Clone 23 was subsequently designated pRQ101 (Fig 4.3a)

Fig 4.3a

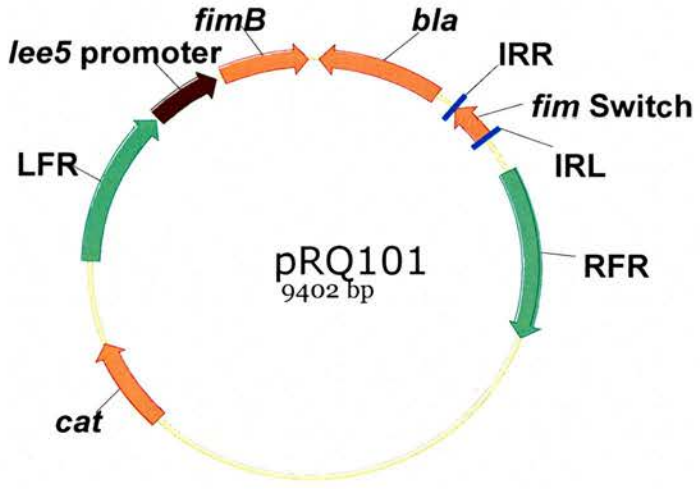

Vector map of pRQ101 showing the *lee5* promoter cloned upstream of *fimB* at the *Xba*I site.

Fig 4.3b

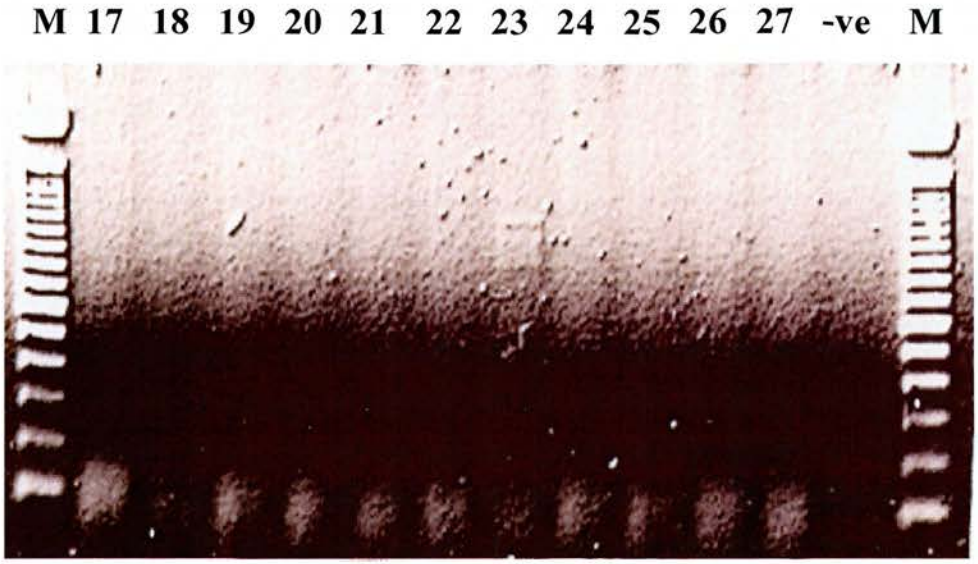

Diagnostic PCR on eleven putative *lee5* clones using 5' *lee5* and 3' *fimB* primer. Clone 23 produces a weak band at the expected size. M = 100bp ladder

Fig 4.3c

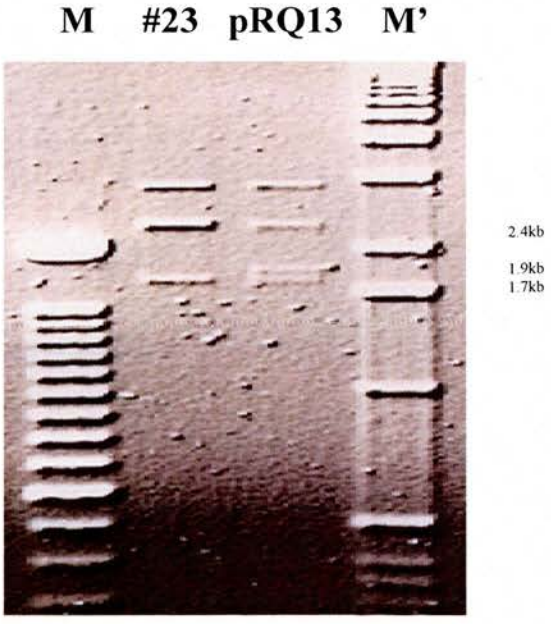

***Ava*II digest of clone 23 against pRQ13. The extra *lee5* DNA raises the 1.9kb band in pRQ13 to 2.4kb, seen as a doublet for clone 23. M = 100bp; M' = 1kb Ladders.**

4.4 – Cloning the *fliC* promoter into pRQ13

The *fliC* promoter region was excised from a lab prepared pTOPO::*fliC* clone using *Xba*I and gel purified according to manufacturer's protocol. The pTOPO clone contained the *fliC* promoter region amplified from ZAP193. The gel purified fragment was ligated with pRQ13 pre-digested with *Xba*I.

Eight putative clones were analysed by *Ava*II restriction digest (Fig 4.4a). The *Ava*II digest of pRQ13 in figure 23b yields a banding pattern of 1.7kb, 1.9kb, 2.5kb and 2.8kb. Of the eight putative clones analysed with *Ava*II, clones #2 and #4 - #8 produced a banding pattern of 1.7kb, 2.2kb, 2.5kb and 2.8kb indicating the insertion of 300bp DNA upstream of *fimB*.

To confirm the presence of *fliC* and to check its orientation with *fimB,* clones #2 and #4-#8, were subject to a diagnostic PCR specific for the *fliC::fimB* fusion using the primers *fliC* 3' and *fimB* 3' (Fig 4.4c). Clone #3 was included as a control. Clones #2, #5, #6 produce a PCR product using the primers for the *fliC::fimB* fusion construct and as expected clone #3 did not produce a PCR product. Clones #4 and #7 also failed to produce a PCR product and it is likely that these clones contain the *fliC* promoter region in the reverse orientation respective to *fimB*. Clone #6 was subsequently designated pRQ102 (Fig 4.4b).

Fig 4.4a

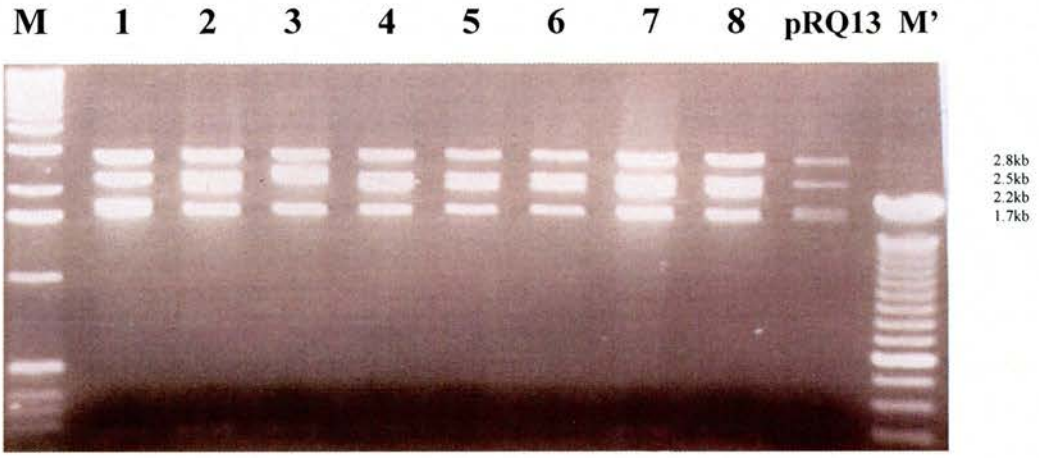

***Ava*II digest of *fliC* clones. #2, #4-#8 produce banding patterns indicating an extra 300bp DNA. M = 1kb ladder; M' = 100bp ladders.**

Fig 4.4b

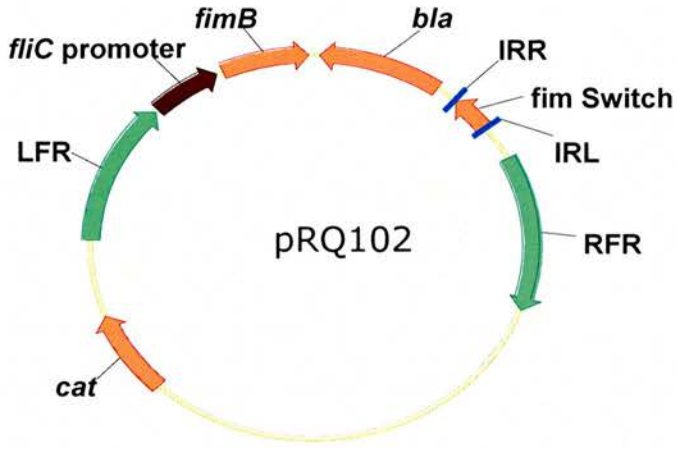

Vector map of pRQ102 showing the *fliC* promoter cloned upstream of *fimB* to create a *fliC::fimB* transcriptional fusion.

Fig 4.4c

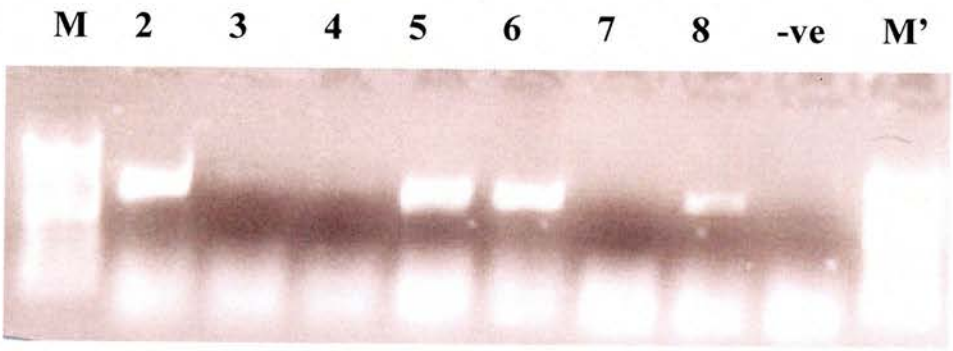

Diagnostic PCR using 5' *fliC* primer and 3' *fimB* primer. Clones #2, #5, #6 and #8 produce PCR products at the expected size of 1kb. Clones #4 and #7 are likely to contain the *FliC* promoter, but in the reverse orientation. M = 1kb; M' = 100bp ladders.

4.5– Cloning the *lee5* promoter into pRQ24

The *lee5* promoter was amplified from ZAP193 using primers LEE5 5' and LEE5 3' and after digestion with *Xba*I was ligated with pRQ24.

Putative clones were analysed by *Ava*II restriction analysis (Fig 4.5b). The pRQ24 banding pattern of 1.3kb, 1.7kb, 2.8kb and 3kb is altered in four of the ten clones: #4, #9, #10 and #12. In these clones' banding patterns the 2.8kb band seen in pRQ24 is raised to 3.3kb confirming the insertion of DNA in between these *Ava*II sites.

To verify the DNA insertion as the *lee5* promoter a PCR was performed on clones #1, #5, #9, #10 and #12 using the *lee5* 5' primer and the *fimB* 3' primer (Fig 4.5c). Clones #9, #10 and #12 produce PCR products at the expected size of 1.2kb confirming the result of the *Ava*II digest. Clones #1 and #5 also produce faint bands in figure 20c. It is possible that clones #1 and #5 are correct and contain the *lee5::fimB* fusion construct. The *Ava*II banding pattern for these clones may not have had the 3kb and 3.3kb bands fully separated on the agarose gel at the time of image capture. Clone #10 was designated pRQ103 (Fig 4.5a).

Fig 4.5a

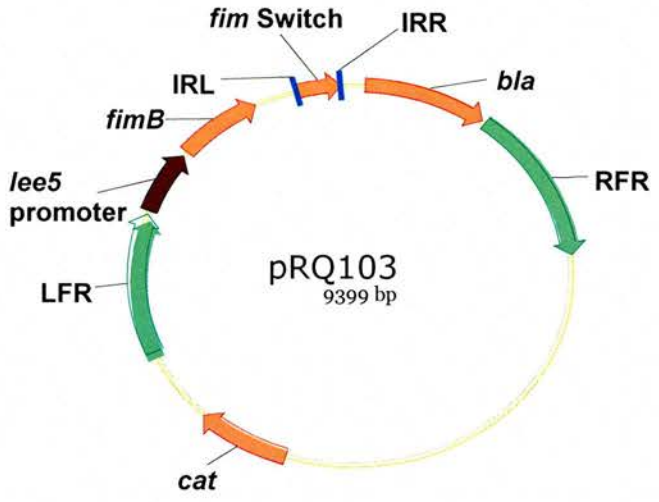

Vector map showing the *lee5*::*fimB* fusion construct in pRQ103.

Fig 4.5b

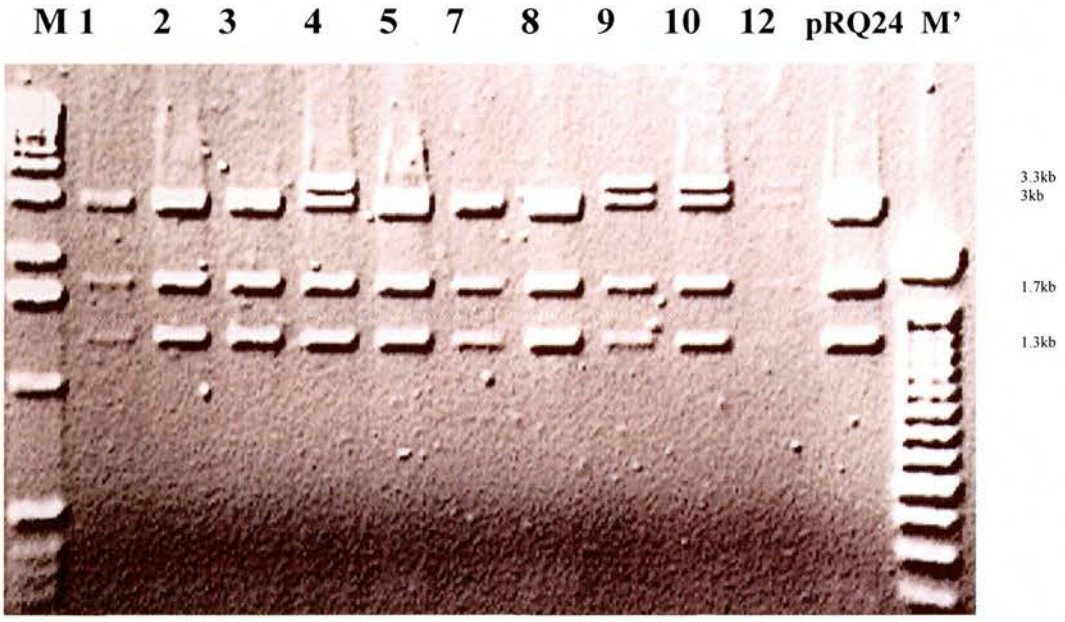

***Ava*II digest of ten putative *lee5* clones. #4, #9, #10 and #12 all exhibit the expected banding pattern indicating DNA insertion between the LFR and *bla*. M = 1kb; M' = 100bp ladders.**

Fig 4.5c

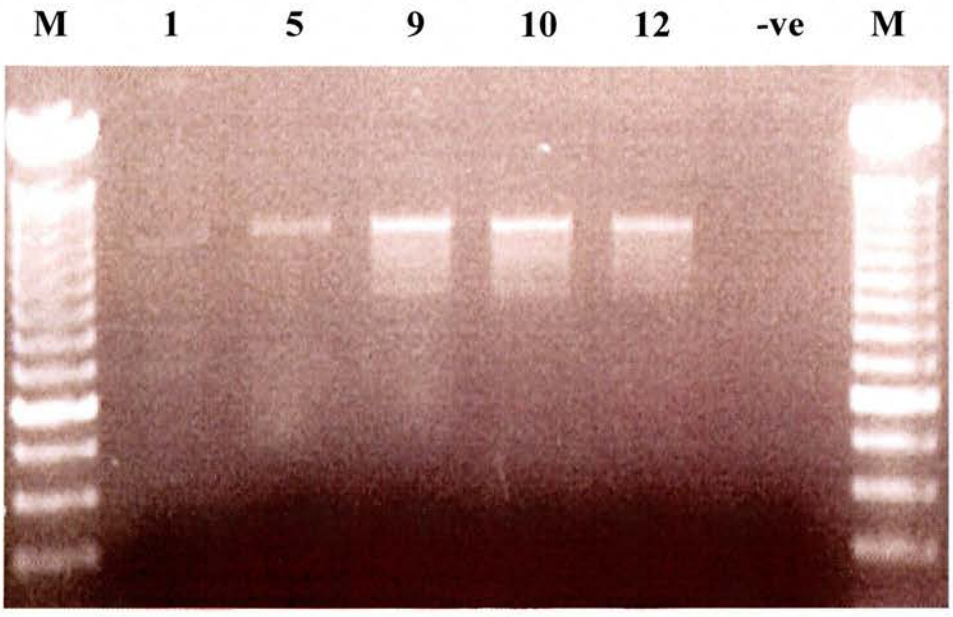

PCR using *lee5* 5' and *fimB* 3' primer. Clones #9, #10 and #12 produce a product at the expected size (1.3kb). Clones #1 and #5 produce faint bands in contrast to a negative *Ava*II digest. The –ve control is water. M = 100bp Ladder.

4.6 – Cloning the *lpf1* promoter into pRQ24

The *lpf1* promoter region was amplified from ZAP193 using the primers LPF1 5' and LPF1 3'. The resultant PCR product was digested with *Xba*I and ligated with pRQ24 upstream of *fimB*.

Clones were analysed by *Ava*II restriction digest (Fig 4.6b). Clones F and G show the 2.8kb band in pRQ24 raised to 3.3kb indicating the insertion of DNA between two *Ava*II sites. To confirm the extra DNA as the *lpf1* promoter region a fusion specific PCR was performed on clone F and pRQ24 using primers LPF1 5' and *fimB* 3' (data not shown). Clone f produced a PCR product of the expected size and was subsequently designated pRQ104 (Fig 4.6a)

Fig 4.6a

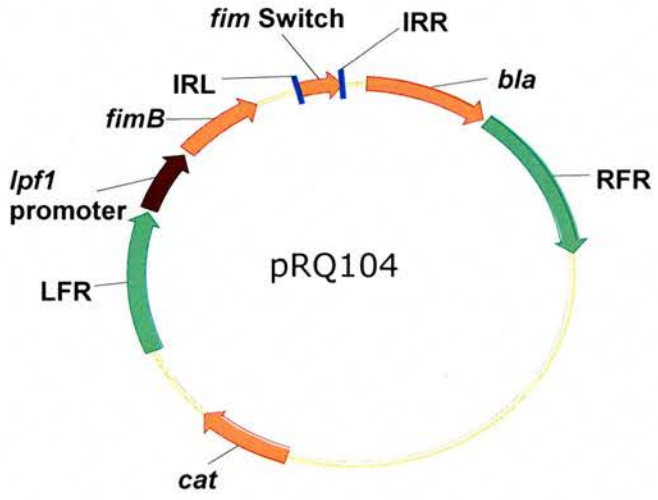

Vector map of pRQ104 showing the *lpf1* promoter upstream of *fimB*.

Fig 4.6b

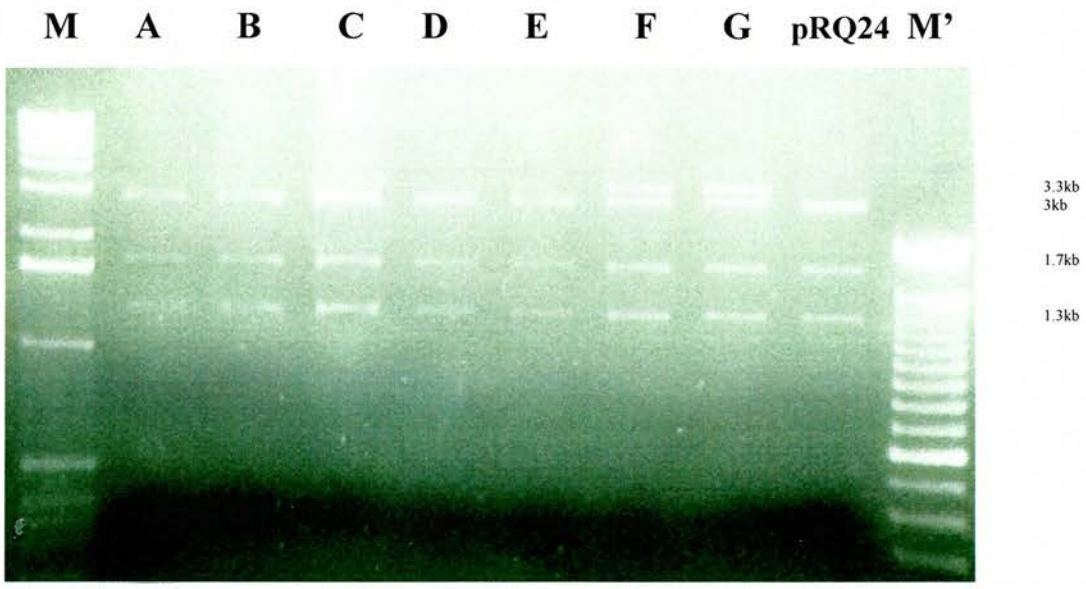

***Ava*II restriction digest on 7 putative *lpf1* clones. Clones F and G exhibit the expected banding pattern of 1.3kb, 1.7kb, 3kb and 3.3kb indicating a DNA insertion of roughly 500bp. Clones A-E exhibited identical banding patterns to wt pRQ24. M = 1kb; M' = 100bp ladders.**

4.7 – Cloning the *loc8* promoter into pRQ24

The *loc8* promoter region was amplified from ZAP193 using primers *loc8* 5' and *loc8* 3' and ligated with pRQ24 upstream of *fimB*.

Of the ten putative clones analysed by *Ava*II restriction digest in Fig 4.7b, clones #1, #4, #7 and #8 produced the expected banding pattern for an insertion of DNA between the LFR and *bla*.

Clones #1, #4, #7 and #8 were subsequently analysed by diagnostic PCR for the *loc8::fimB* fusion construct using the 5' *loc8* primer and the 3' *fimB* primer (Fig 4.7c). Clones #7 and #8 produce positive PCR products using these primers, indicating the correct construction of the *loc8::fimB* fusion. Clones #1 and #4 did not produce PCR products using these primers. It is likely that these clones do contain the *loc8* promoter region but in the reverse orientation. Thus using the 5' *loc8* primer will not yield a positive PCR. Clone #7 was designated pRQ105 (Fig 4.7a)

Fig 4.7a

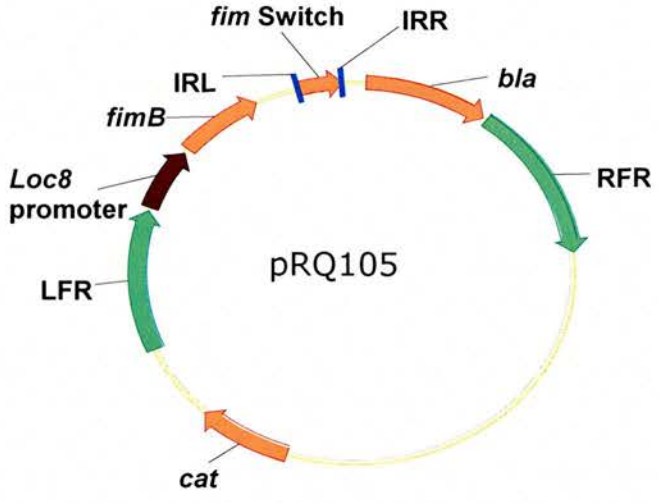

Vector map of pRQ105 showing the *loc8* promoter region cloned upstream of *fimB* on pRQ24 to create a *loc8::fimB* fusion.

Fig 4.7b

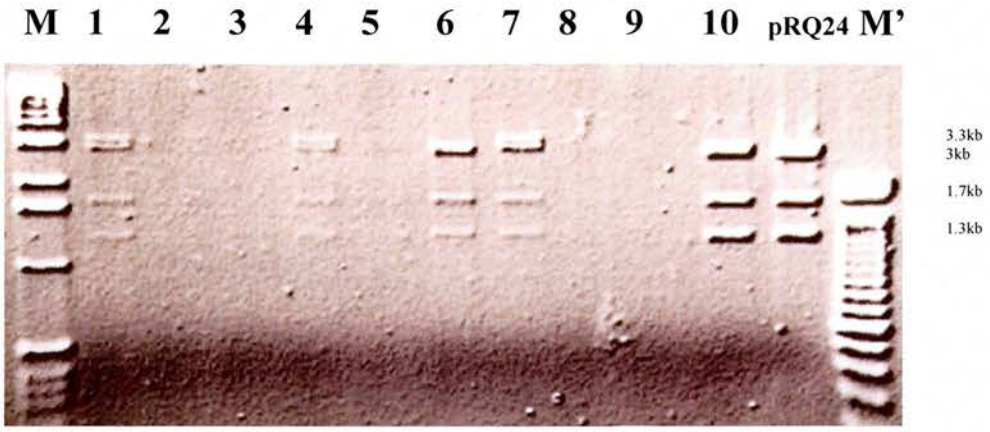

***Ava*II digest on ten putative *loc8* clones. Clones #1, #4, #7 and #8 show the banding pattern: 1.3kb, 1.7kb, 3kb and 3.3kb indicating a DNA insertion between the LFR and *bla* on pRQ24. M = 1kb; M' = 100bp ladders.**

Fig 4.7c

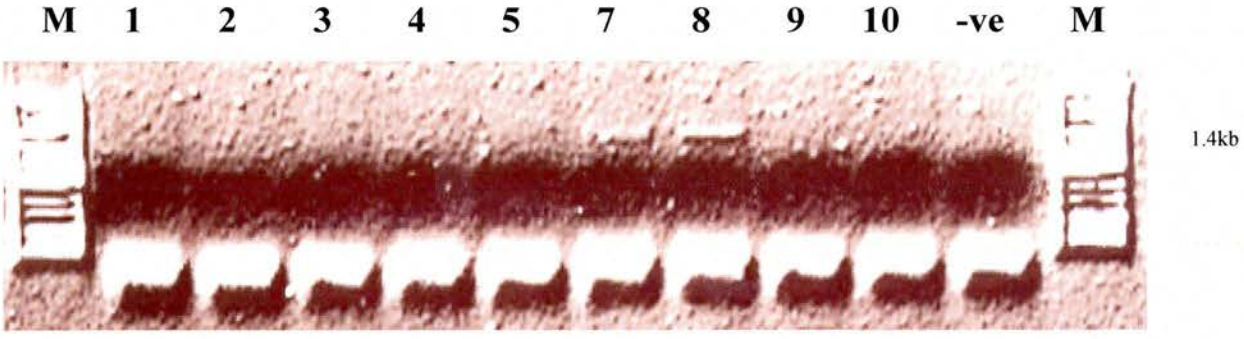

Diagnostic PCR on putative *loc8* clones using 5' *loc8* and 3' *fimB* primer. Clones #7 and #8 produce a PCR product for the *loc8::fimB* fusion construct at the expected size of 1.4kb. M = 1kb ladder.

4.8 - Controlling the FRIVET system

The main aim of each FRIVET experiment is to ascertain the proportion of bacteria that have switched from ampicillin sensitive to ampicillin resistant as a result of *fimS* switching from the 'off' orientation to the 'on' orientation. The inoculum for each experiment therefore has to start with the *fim* switch in the 'off' orientation. To prevent unwanted switching whilst preparing the inoculum and after sampling at the end of the assay, we will use the DNA binding protein PapB to inhibit FimB mediated switching and thus FRIVET induction, during these periods. A regulator of the *pap* operon, PapB has been shown to inhibit the action of FimB on the *fim* switch, although the exact mechanism and binding site is yet to be elucidated.

By placing p*apB* under the control of an IPTG inducible promoter in single copy, we can induce PapB production during inoculum preparation and at the end of the assay during sampling. We can then be confident that any *fimS* switching can only take place during the assay. The control fusions will be placed in single copy at the *lac* locus in our FRIVET test strains. As such we will use the pIB307 plasmid containing the *lacI* and *lacA* genes for allelic exchange into the *lac* locus (pAJR26).

We will use two IPTG inducible promoters of different strengths:

- *lac*UV5 promoter – tight regulation, used to control *papB* in pHMG88
- Ptac promoter – combination of *lac* and *trp* promoter regions, IPTG concentration proportional to Ptac expression

The use of these promoters will provide us with a wide range of potential PapB levels to inhibit FRIVET induction. The level of PapB needed to inhibit the FRIVET system will be defined during FRIVET testing.

In addition an IPTG inducible copy of *fimE* was created on a pACYC vector. The ability of FimE to mediate *fim* switching from the 'on' orientation to the'off' orientation will

also be studied. It will be useful to have two potential inhibitors of *fim* switching as PapB inhibition has been studied on the native type 1 fimbrial operon. The FRIVET system may respond to PapB in a different manner and it may become necessary to deploy a FimE based vector to ensure the inoculum is in the correct *fimS* orientation prior to inoculation.

4.9 - Cloning the *lac*UV5::*papB* fusion into pAJR26

The *lac*UV5::*papB* transcriptional fusion construct was amplified by PCR from pHGM88 with using the primers *lac*UV5 1 and *papB*4. The resultant PCR fragment was ligated with pAJR26 at the intergenic *Bam*HI site.

Three putative clones were analysed by PCR using primers *papB*4 and *lacA* 3' (Fig 4.9b). All three clones produced a band of the expected size (1kb) indicating correct cloning of the *lac*UV5::*papB* fusion construct into pAJR26. Clone #1 was subsequently designated pRQ8 (Fig 4.9a)

Fig 4.9a

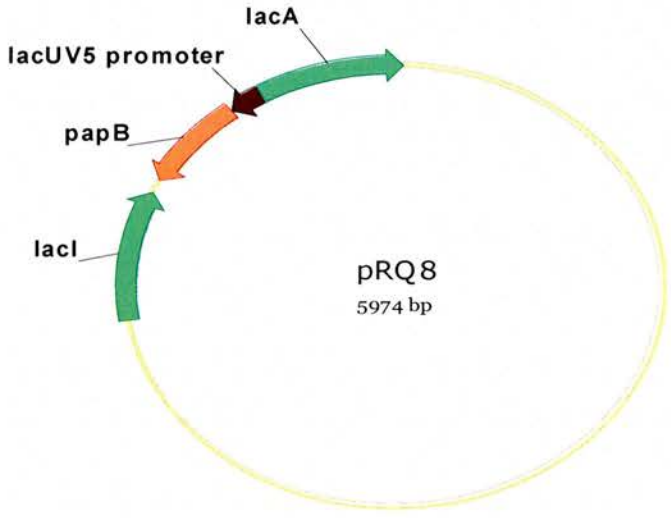

Vector map of pRQ8 showing the *lac*UV5::*papB* fusion construct cloned at the *lac IA* intergenic *Bam*HI site on pAJR26.

Fig 4.9b

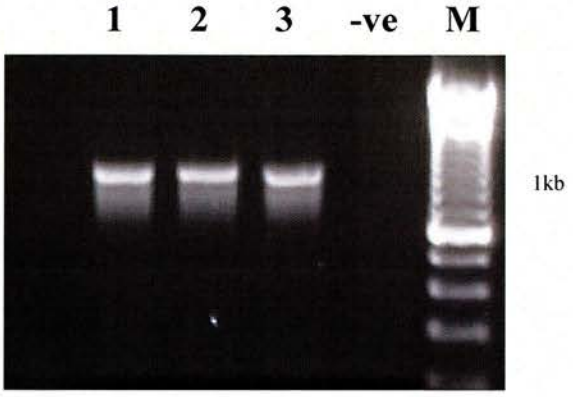

Diagnostic PCR on three putative clones using a 3' *papB* primer and a 3' *lac*A primer. All three clones produce a PCR product at the expected size of 1kb. M = 100bp ladder.

4.10 - Cloning the Ptac promoter into pAJR26

The Ptac promoter region was amplified from the vector pACTAC using primers 5' Ptac *Bgl*II and 3' Ptac *Bam*HI. The resulting PCR product was digested with *Bgl*II and *Bam*HI before ligation with pAJR26 at the intergenic *Bam*HI site.

Nine putative clones were analysed by restriction digest with *Rsa*I (Fig 4.10b). Clones #7 and #8 produced the expected banding pattern for the *Rsa*I digest as the 933bp band seen in the ctrl digest was raised to 1.1kb for #7 and #8, indicating the insertion of DNA between these *Rsa*I sites.

To confirm the orientation of the Ptac promoter a PCR was performed with two sets of primers: (1) *lac*I 5' and 3' Ptac *Bam*HI; (2) *lac*A 3' and 3' Ptac *Bam*HI (Fig 4.10c). Clone #7 produced a strong PCR product using primer set 2 and clone #8 produced a strong PCR product using primer set 1. Clone #9 produced a PCR product with primer set 1 and a weaker 'ghost' band for primer set 2 and may represent a correct clone however the *Rsa*I digest for clone #9 suggests this is not the case. Clone #8 also appeared to produce a PCR product with primer set 2, although it is likely that this is the result of lane bleed through from clone #9 when the agarose gel was loaded, resulting in the false positive. The large ghost band at ~1.5kb seen in lane 1 for clone #7 with primer set1 can likely be attributed to non-specific priming as a result of using non matched primers for PCR. Clone #8 was subsequently designated pRQ19 (Fig 4.10a)

Fig 4.10a

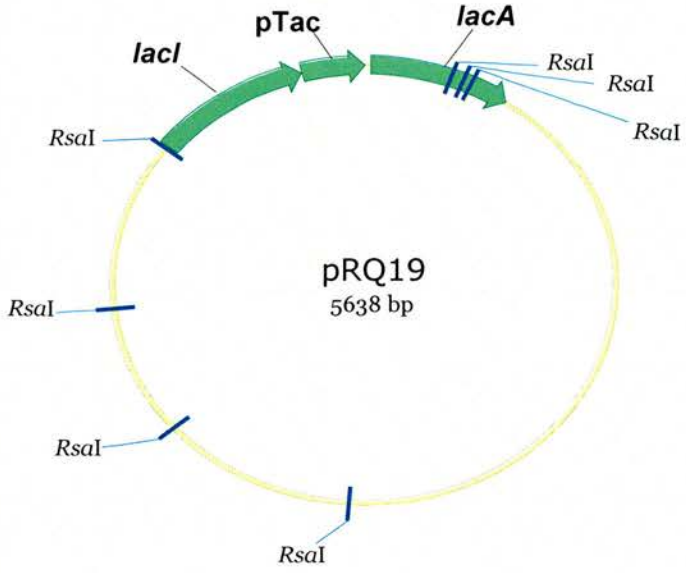

Vector map of pRQ19 showing the Ptac promoter region cloned at the intergenic *Bam*HI site between *lacI* and *lacA* on pAJR26

Fig 4.10b

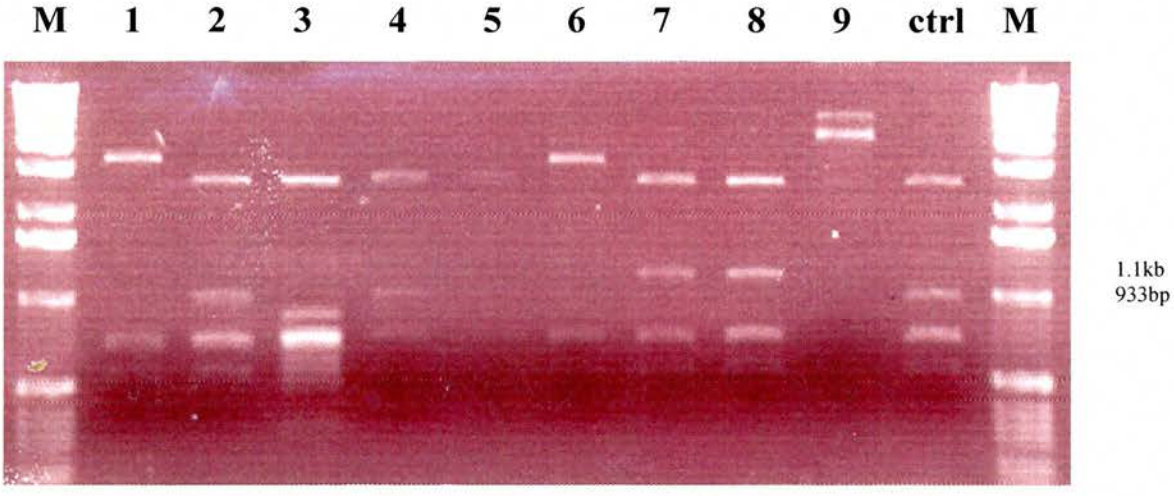

***Rsa*I digest on nine putative clones. Clones #7 and #8 show an increase of 170bp in The 933bp band indicating the insertion of a DNA fragment of that size. The ctrl is pAJR26. M = 1kb ladder.**

Fig 4.10c

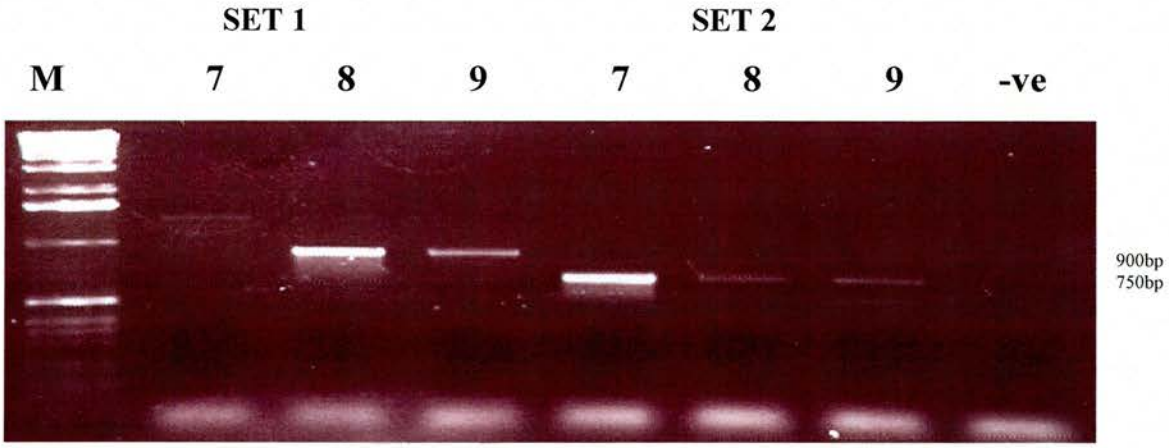

Diagnostic PCR on clones #7, #8 and #9 using two sets of primers: (1) *lac*I 5' and 3' Ptac *Bam*HI; (2) *lac*A 3' and 3' Ptac *Bam*HI. Clone #7 produced a PCR product of the expected size with primer set 2. Clone #8 produced a PCR product with primer set 1. M = 1kb ladder.

4.11 - Cloning the *papB* gene into pRQ19

The *papB* gene was amplified from pHMG88 using primers *papB*3 and *papB*4 and the resulting PCR product was digested with *Bam*HI and ligated with pRQ19.
Twelve putative clones were digested with *Bam*HI in an attempt to excise the cloned *papB* gene (Fig 4.11b). Clones #2, #3, #5-20 and #12 all excised a band at the expected size for *papB*.

To confirm the creation of a Ptac::*papB* transcriptional fusion on pRQ19 a diagnostic PCR was performed on all ten of the *Bam*HI positive clones using a 5' Ptac primer and the *papB*4 primer (Fig 4.11c). Clones #1, #3, #7, #10 and #12 all produced a PCR product at the expected size for the Ptac::*papB* fusion. Clone #12 was subsequently designated pRQ20 (Fig 4.11a)

Fig 4.11a

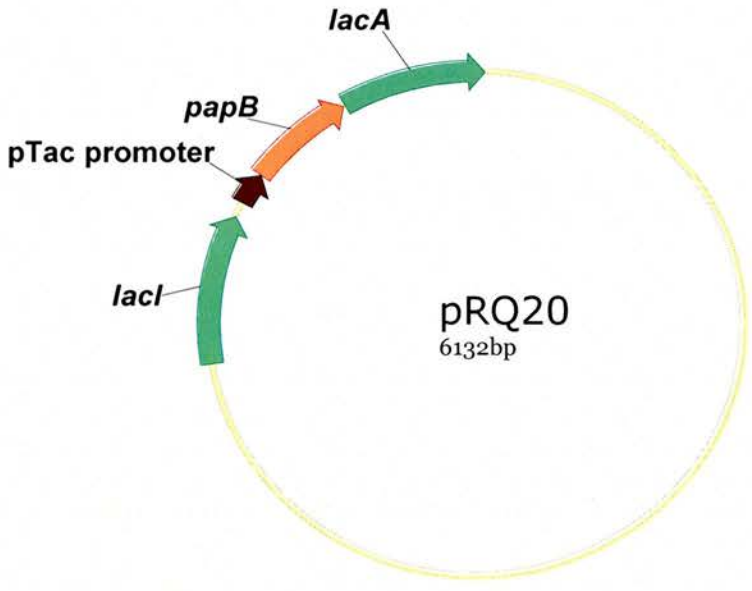

Vector map of pRQ20 showing the *papB* gene cloned upstream of the Ptac promoter to create a Ptac::*papB* transcriptional fusion.

Fig 4.11b

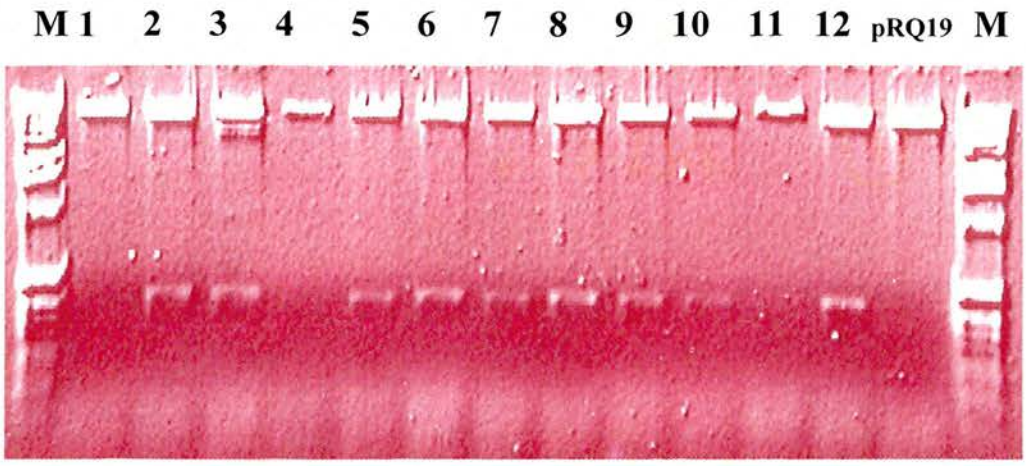

***Bam*HI digest of twelve putative *papB* clones. Clones #2, #3, #5-#10 and #12 all excise a band the size of *papB* (500bp). M = 1kb ladder.**

Fig 4.11c

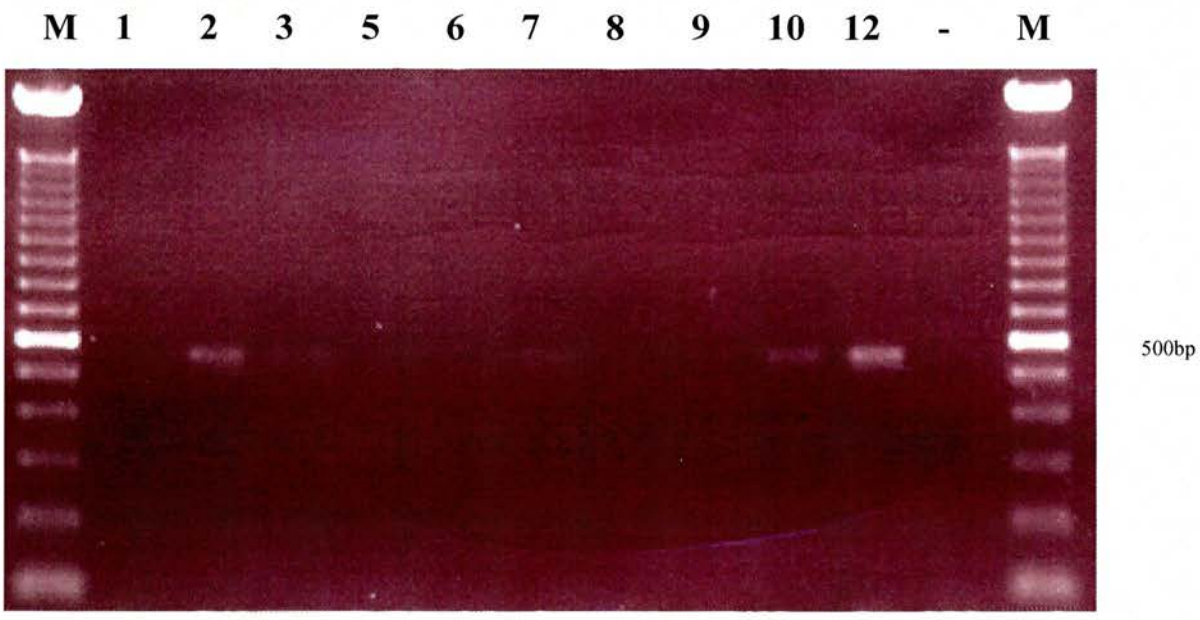

Diagnostic PCR using 5' Ptac primer and *papB*4 to screen putative clones for Ptac::*papB* fusion construct. Clones #2, #3, #7, #10 and #12 all produced PCR products of the expected 550bp size. M = 100bp ladder.

4.12 - Exchanging pRQ8 into a ZAP193 background

Using the allelic exchange vector pRQ8 single copy fusions of *lac*UV5::*pap*B were made in the ZAP193 *sac/kan* background at the *lac* locus. To confirm the allelic exchange process was successful a PCR was performed on six exchange strains using the primers *lacA* 3' down and *papB*4 (Fig 4.12a). All six putative exchange strains produced a PCR product of the expected 800bp size.

To confirm this result was due to the construct being present in single copy on the chromosome and not residual pRQ8, a pIB specific PCR was performed on the six strains using primers specific for pIB backbone sequence Fig 4.12b). Controls used were: pIB *lacIA* (C1), a stx- lysate (C2) and H_2O (C3). All six strains were negative for the PCR and the positive control C1 produced a PCR product as expected. Strain #1 was stored at -70^{0}C and designated ZAP541.

Fig 4.12a

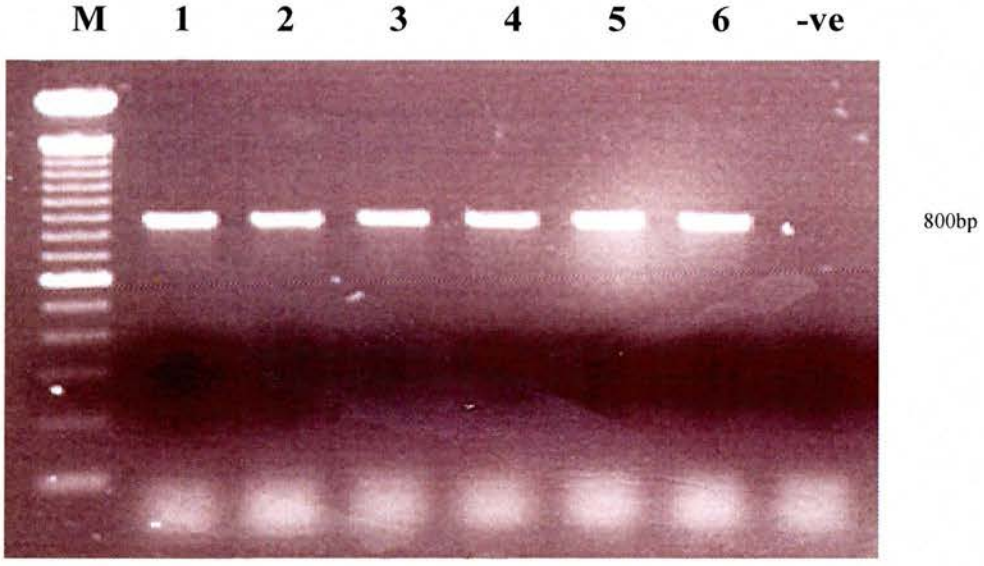

Diagnostic PCR on six exchange strains using primers *lacA* 3' down and *papB4*. All six strains produced an 800bp PCR product. The –ve control in lane 7 is water. M = 100bp ladder.

Fig 4.12b

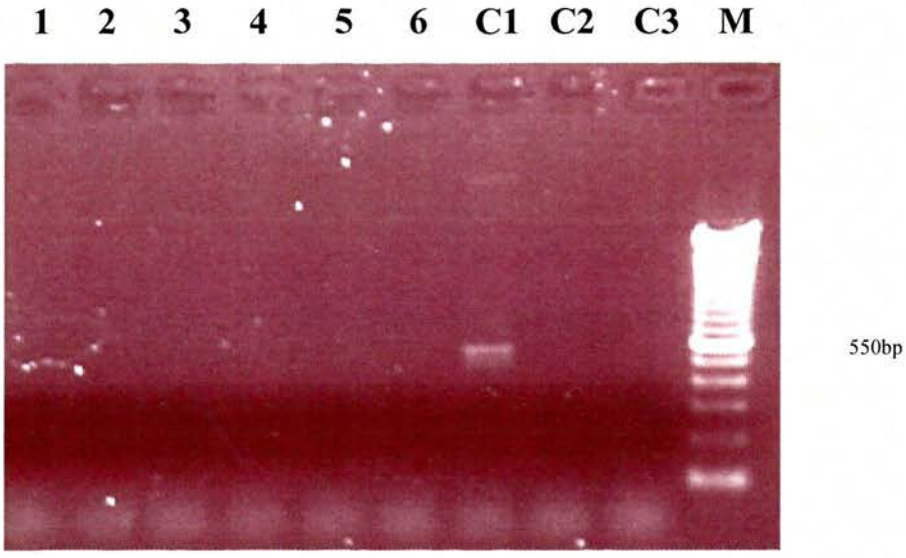

Diagnostic PCR screen on six exchange strains using primers specific for pIB plasmid backbone. Controls: C1 = pAJR26; C2 = ZAP193 lysate; C3 = water. M = 100bp ladder.

4.13 - Exchanging pRQ20 into a ZAP193 background

Strain ZAP193 *sac/kan* was transformed with the temperature sensitive allelic exchange vector pRQ20. After the first 48h of allelic exchange ten kanamycin and chloramphenicol resistant strains were subject to a diagnostic PCR using primers *lacI* up 5' and 3' Ptac *Xba*I (Fig 4.13b). The position of the primers in relation to the primary exchange construct is shown in Fig 4.13ba

Strain A2 produced a positive PCR product at the expected 1.8kb size and was taken forward for the second half of the allelic exchange procedure.
Resultant strains that were kanamycin and chloramphenicol sensitive and grew well on sucrose containing media were designated ZAP544 and stored at -70^{0}C.

Fig 4.13a

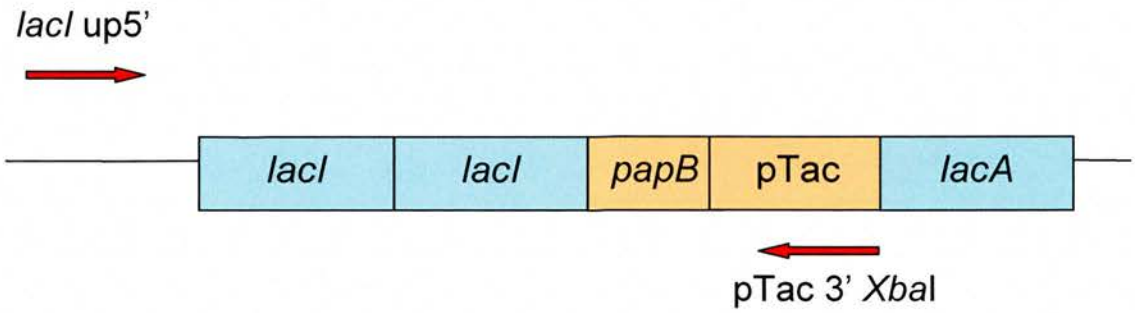

Diagrammatic representation of primer position in Fig 3.29a. The *lacI* up5' primer binds upstream on the chromosome of the primary integrate ensuring the specificity of the PCR for integrated vectors only.

Fig 4.13b

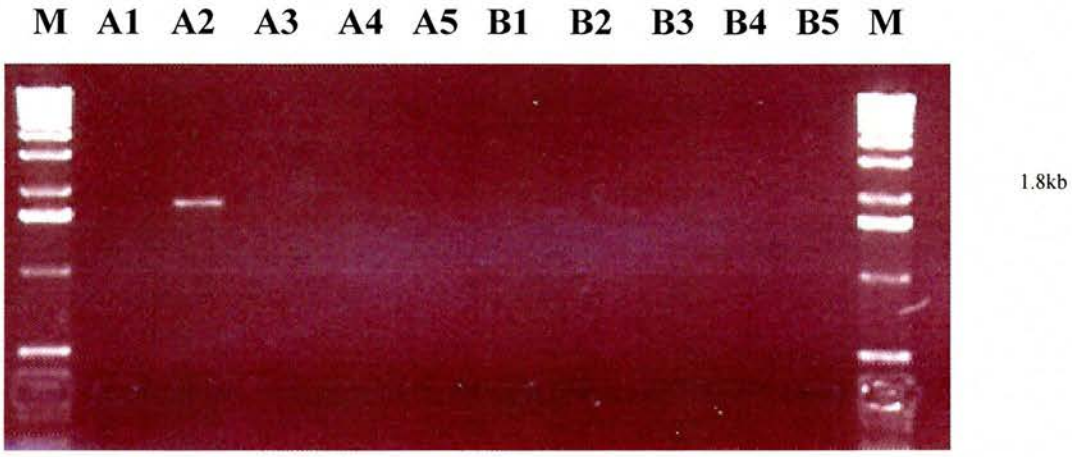

Diagnostic PCR on ten exchange strains using a 5' upstream *lacI* primer and a 3' Ptac primer. Strain A2 produced a PCR product at the expected length of 1.8kb. M = 1kb ladder.

4.14 - Cloning the *fimE* gene into the pACTAC vector

The *fimE* gene was amplified from *E. coli* MG1655 using primers *fimE*1 and *fimE*2. The resulting fragment was digested with *Bam*HI and ligated with the pACYC184 based vector pACTAC downstream of Ptac to create a Ptac::*fimE* fusion.

Eight putative clones were isolated and subjected to restriction digest analysis with *Ava*I (Fig 4.14a). The pACTAC vector contains a single *Ava*I site and will linearize after digestion with *Ava*I at 4.4kb. The cloning of *fimE* introduces a second *Ava*I site and correct clones will produce 2 bands of 1.2kb and 3.7kb after *Ava*I digestion. Of the eight clones analysed only clones #5-#7 exhibit this banding pattern. The smeared bands seen above the 3.7kb band for these clones is likely to be un-digested plasmid at a size of ~5kb.

To verify this result a diagnostic PCR was performed using primers 5' Ptac *Hind*III and FIME2 to identify the clones that contained the Ptac::*fimE* transcriptional fusion construct (Fig 4.14c). The two negative controls were: pACTAC (-ve) and water (MQ). Clones #3-#8 all produce PCR products of the expected 800bp length.

This confirms that clones #5-#7 contain the Ptac::*fimE* fusion construct. Clones #3, #4 and #8 also produce a positive PCR product with these primers yet linearize at 4.4kb after *Ava*I digest in Fig 4.14a. This anomaly cannot be fully explained so these clones were discarded. Clone #7 was taken forward and designated pACTAC::*fimE* (Fig 4.14b).

Fig 4.14a

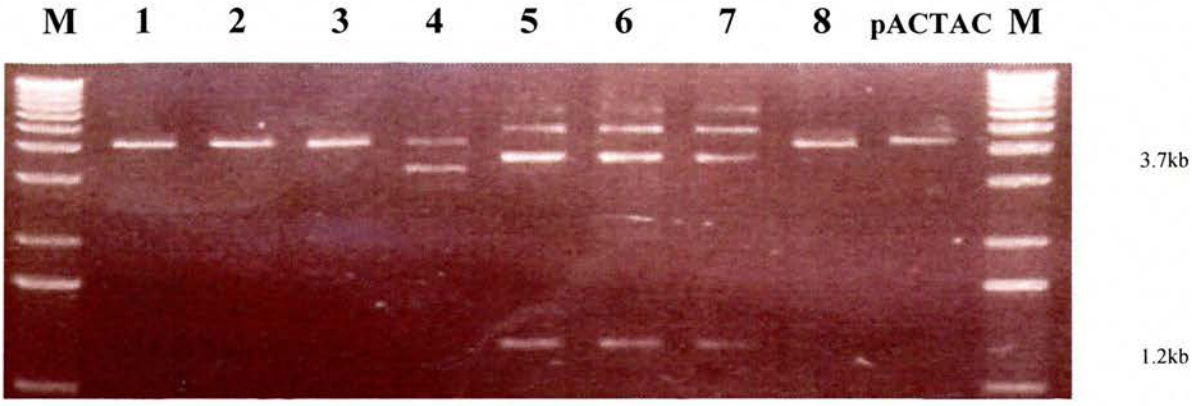

***Ava*I digest of eight putative *fimE* clones. The *fimE* gene introduces a novel *Ava*I site and correct clones will produce two bands at 1.7kb and 1.2kb. Clones #5-#7 produce this banding pattern, indicating the correct cloning of *fimE* downstream of Ptac. M = 1kb ladder**

Fig 4.14b

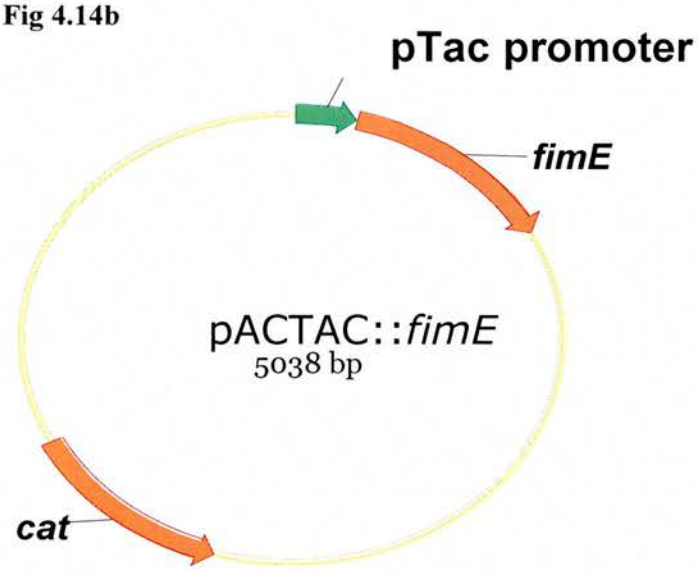

Vector diagram of pACTAC::*fimE* showing the Ptac::*fimE* transcriptional fusion created on a pACYC184 based backbone.

Fig 4.14c

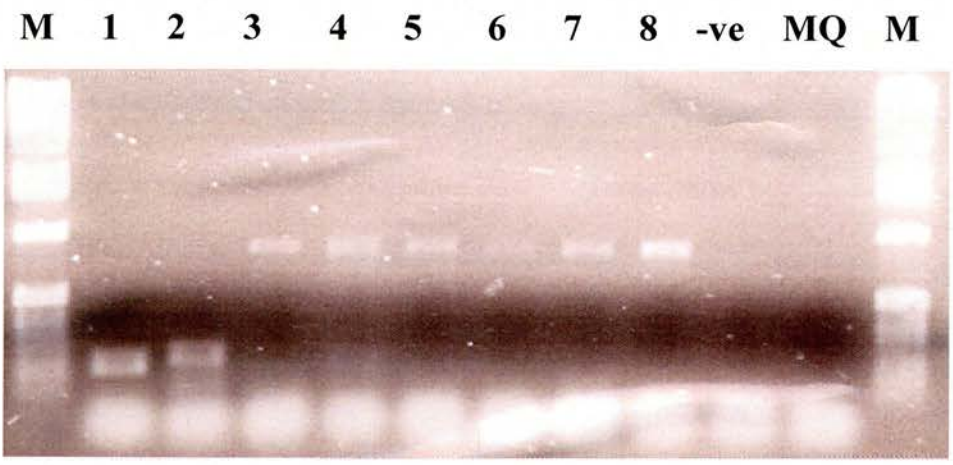

Diagnostic PCR on eight putative *fimE* clones. Clones #3-#8 all produce PCR products at the expected size. The –ve control is pACTAC. M = 1kn ladder.

4.15– Chapter 4 discussion

The first aim once the FRIVET backbone had been constructed was to clone EHEC promoters of choice upstream of *fimB* to create FRIVET constructs ready for allelic exchange into ZAP542. The cloned *fimB* gene from MG1655 used a 5' primer containing a novel *Xba*I site upstream of the *fimB* translational start site. This *Xba*I site was used to clone promoters of choice, thereby creating transcriptional fusions between the cloned promoter and *fimB*. The promoters cloned into the FRIVET backbone vectors were:

- *lee5* – LEE5 (*tir, cesT, eae*) operon control in EHEC
- *fliC* – Flagella regulation
- *lpf1* – controls EHEC long polar fimbriae production
- *loc8* – controls EHEC Loc8 fimbrial production

The *lee5* promoter was cloned into both the pRQ13 and the pRQ24 background and putative clones were analysed by restriction digest and diagnostic PCR. The *fliC* promoter was cloned into the pRQ13 background and the *lpf1* and *loc8* promoters were cloned into the pRQ24 background. Putative clones were again analysed by a mix of restriction digests and diagnostic PCR. Multiple attempts were made to clone the *fliC* promoter into pRQ24 and the *lpf1* and *loc8* promoters into pRQ13 but these attempts failed repeatedly. It was decided that as a FRIVET vector now existed for each promoter, no more effort would be put into creating the full set of FRIVET vectors from the pRQ13 and pRQ24 lineages.

The control of the FRIVET system is of utmost importance to establish a repeating, dependable *in vivo* assay. The initial inocula for each experiment must have the *fimS* set

to 'off' and FRIVET constructs must be locked in their orientations after their recovery so that they can be analysed for 'off' to 'on' switching that took place solely in the assay. It has been established that the *pap* operon regulator: PapB, also acts to inhibit FimB mediated switching of the *fim* switch (Holden *et al*, 2001; Xia *et al*, 2000).

By using PapB at the correct moments in the assay and during the inoculum preparation it should be possible to 'lock' the switch in the orientation at that time. By placing the *papB* gene downstream of an inducible promoter, high concentrations of PapB can be produced, theoretically locking the switch orientation, at will. A series of IPTG inducible promoters (*lac*UV5 and Ptac) was used to create transcriptional fusions with *papB*. The fusions were constructed on the temperature sensitive allelic exchange vector pIB307 and as with the FRIVET operon, the promoter::*papB* construct was placed in single copy on the chromosome of ZAP193 with one difference: the *papB* constructs were placed at the *lac* locus.

Initially, prior to the deletion of the *fim* locus, the *lac* region was deleted from ZAP193 using the vector pAJR26::*sackan*, thereby leaving the *sackan* cassette at the *lac* locus for subsequent exchanges. This strain was then transformed with the *lac*UV5::*papB* (pRQ8) and the Ptac::*papB* constructs (pRQ20) to create strains ZAP541 and ZAP544 respectively. Strains whose antibiotic resistance profiles and sucrose sensitivity assays were correct were subject to diagnostic PCR to confirm the phenotypic results. The *fim* operon was subsequently deleted from these strains to create ZAP542 and ZAP545.

The construction pathway of the two Δ*fim* strains can be seen in Fig 4.15.

Fig 4.15

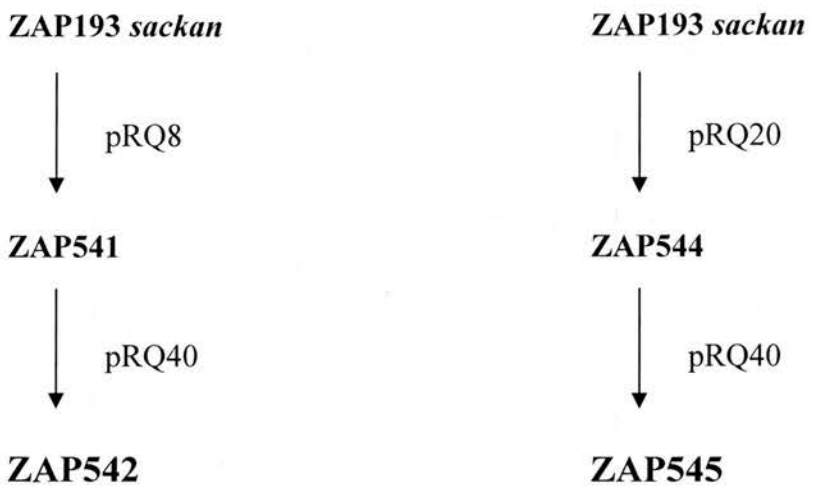

Construction map of the two Δ*fim* strains: ZAP542 and ZAP545. Each strain has a different IPTG inducible promoter at *lac* controlling *papB*. ZAP542 contains the *lac*UV5 promoter and ZAP545 contains the Ptac promoter. Both strains contain the *sackan* cassette at *fim* for subsequent allelic exchange of FRIVET vectors

Prior to exchange at the *fim* locus with FRIVET plasmids, the *fim* region was deleted from strains ZAP541 and ZAP544 using the plasmid pRQ40 (see chapter 3).

The IPTG inducible vector pACTAC and the *fimE* gene from MG1655 were used to create the pACTAC::*fimE* vector. FimE acts to mediate *fim* switching from the 'on' to the 'off' orientation and will be used in inhibitory assays with FRIVET strains.

In total five FRIVET vectors were produced with EHEC promoters and two strains were prepared for FRIVET vector exchange, each strain carrying the *papB* gene under transcriptional control of different IPTG inducible promoters.

However it must be remembered that the exact mechanism for PapB inhibition of the Fim system is not yet known. Without a complete understanding of the mechanism and a working knowledge of the levels of PapB required it will be difficult to gain complete

control over wt *E. coli* O157:H7 promoters unless prior levels of f*imB* transcription are known using RT-PCR or Northern analysis.

Ideally we would have been able to test the level of PapB produced from the two promoters used in the study prior to single copy exchange at the *lac* locus and compare the levels required for inhibition of a native *fim* system using WT *fimB* promoters to that required to block inhibition of FimB action on *fimS* when under control of a particular *E. coli* O157:H7 promoter.

Chapter 5

Testing of the FRIVET system

5.1 – Introduction

The construction of the FRIVET system on a temperature sensitive allelic exchange vector with a promoterless copy of *fimB* allows the cloning of chosen promoters into this plasmid background. The newly created vector can then be exchanged in single copy into an *E coli* O157:H7 stx- background. The FRIVET strain can then be tested *in vitro* before being used *in vivo*.

The aim of the FRIVET system is to provide accurate data for the activity of *E. coli* O157:H7 promoters *in vivo* regarding their timing and expression patterns. However due to the complex nature of the FRIVET 'synthetic operon', testing needs to take place *in vitro* beforehand. We need to understand the dynamics of the FRIVET operon and its levels of tolerance before we deploy the system *in vivo*. The promoter from the arabinose operon will be used as a FRIVET test promoter.

The arabinose operon allows *E. coli* strains to utilize L-arabinose as a carbon source. The genes of the arabinose operon are distributed at three points on the chromosome. The uptake of arabinose into the cell is controlled by *araE,* and at a distinct site on the chromosome *araF, araG* and *araH.* Thus, *araE* is under the control of a single promoter and *araFGH* under the control of a separate promoter. At the third distinct site is the *araC, araBAD* complex. At this site *araC* acts as a positive regulator of the *ara* operon and the *araBAD* genes under the control of the $\boldsymbol{P_{BAD}}$ promoter act on intracellular arabinose, converting it in a stepwise manner to D-xylulose-5-phosphate. The AraC protein acts positively to stimulate transcription at $\boldsymbol{P_{BAD}}$ in the presence of arabinose as well as acting negatively to repress the promoter in the absence of arabinose (Englesberg, E. *et al*, 1969). The AraC protein has also been shown to regulate its own synthesis (Casadaban M.J., 1976) and the *ara* operon is known to be repressed by the addition of glucose due to catabolic repression (Greenblatt and Schleif, 1971). In this instance the addition of glucose lowers the intracellular level of cyclic AMP and cyclic AMP receptor protein (CRP) which is also required for the induction of the *ara* operon. The *araC, araBAD* complex is represented diagrammatically in Figure 5.1. In the presence of

inducer AraC binds two control sites upstream of P_{BAD}. These control sites termed I_1 and I_2 are half sites four bases apart. The homodimeric AraC protein occupies both half sites and transcription occurs from P_{BAD}. However in the absence of inducer only a single subunit of AraC binds to the half site I_1, the other subunit binds to a separate half site termed O_2 at a position upstream of *araC*.

Fig 5.1

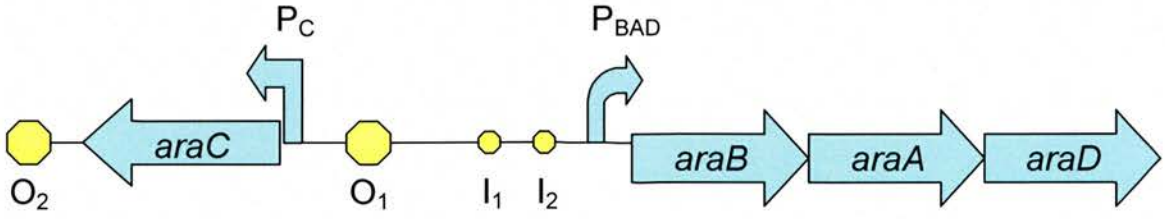

Genetic map of the *ara* operon, showing the organization of the the *araBAD* complex and the O and I half sites.

As can be seen in Figure 5.1, the binding of AraC to the I_1 and O_2 half sites stops RNA polymerase from binding to P_C and P_{BAD} preventing transcription of the *araBAD* complex.

Guzman et al reported the use of the P_{BAD} promoter to modulate the expression of genes over a variety of inducer concentrations (Guzman *et al* 1995). The population expression profile of a gene at subsaturating levels of inducer can have two explanations.

Either:

- The percentage level of P_{BAD} expression in each cell in the population is identical to the percentage expression level in the population as a whole. Each cell is partially induced.
- Each cell in the population is either fully induced or uninduced. The percentage level expression seen in the population is representative of the mixture of induced and uninduced cells

Siegele et al subsequently reported that the expression from the P_{BAD} promoter was 'all or none'. Using GFP as a reporter, individual cells were studied under varying concentrations of inducer. Cells either were fluorescent or not and the proportion of the fluorescent cells grew larger as the concentration of inducer was raised (Siegele and Hu, 1997). The nature of this 'all or none' response to inducer was linked to the arabinose transporter AraE. The *araE* gene is under the transcriptional control of AraC, which itself is induced by the presence of arabinose. In order for *araC* expression to occur there must be a small amount of AraE present to transport inducer inside the cell. If the amount of AraE is above a threshold level, *araC* is expressed, resulting in the expression of the *araBAD* and *araE/araFGH* complexes. More AraE production results in more inducer transported into the cell to further stimulate *araC* transcription. If however, the level of AraE inside the cell is below the threshold level, the amount of inducer transported into the cell is too low to fully activate *araC* expression and the system remains repressed. The result is either a fully induced cell or an uninduced cell. Subsequently researchers have used inducible promoters linked to *araE* to uncouple the AraE/AraC dynamic. The researchers found that P_{BAD} expression level was determined by inducer concentration at an individual cell level (Khlebnikov, *et al*, 2002).

As the FRIVET system is designed to assay individual cells on an 'all or none' basis in the population due to the ampicillin selection, this mode of P_{BAD} expression does not affects its selection as the FRIVET test promoter. The P_{BAD} promoter is still an ideal choice for initial testing of the FRIVET system as it is relatively 'tight' and can be controlled by the addition of arabinose and other sugars.

The first step will be the cloning of the *ara* promoter region from the vector pBAD18 upstream of *fimB* on the FRIVET vectors to create *ara::fimB* transcriptional fusions. These FRIVET test vectors will then be exchanged into the chromosomes of ZAP193 and the existing FRIVET *papB* strains ZAP542 and ZAP544

All three resulting *ara* FRIVET test strains will be induced with high, medium and low levels of arabinose in LB and M9 media at both 30^0C and 37^0C to test the functionality of

the FRIVET system. These initial tests will validate the *ara::fimB* transcriptional fusion construction in the FRIVET vectors as well as indicating the range of induction levels for the FRIVET system in two media and at two temperatures using three concentrations of arabinose.

The FRIVET strains will then be tested for *papB* function. The ability of *papB* to 'lock' the *fim* switch will play a crucial role in the control of the FRIVET system for *in vivo* assays. The testing protocol for the *papB* inhibition assays will use two IPTG inducible promoters of different strengths. Strain ZAP542 contains the *lac*UV5 promoter fused to *papB* in single copy at the *lac* locus and ZAP544 contains the stronger Ptac promoter fused to *papB* in single copy at the *lac* locus. Each construct will be induced with IPTG at a final concentration of 1mM against various concentrations of arabinose.

Additionally *fimE* will be used to verify the ability to turn the system from 'on' to 'off' using the pACTAC::*fimE* vector, and glucose will be used to test the FRIVET *ara* promoter region responds to catabolite repression.

In order to understand more about *ara* promoter strength, the *ara* promoter region will be cloned in front of *gfp+* to create an *ara::gfp+* transcriptional fusion. This will then be used in a series of fluorescence assays designed to assess the population based transcription level using a range of arabinose concentrations. These assays can be seen in Figures 5.3a, 5.3b and 5.3c.

The main aims in testing the arabinose driven FRIVET system are:

- To validate the construction of the FRIVET operon initially – is it functional?
- To validate the ability to create *fimB* based transcriptional fusions
- To define a protocol that is simple and quick to reproduce
- To define the role of PapB in the control of *fimS*
- To check the system can be reversed using *fimE*
- To confirm the *ara* promoter responds to catabolite repression in the FRIVET operon

Finally the FRIVET system will be tested *in vivo* using the sheep gut loop animal model (5.18). In two separate experiments various FRIVET constructs were tested to identify *E. coli* O157:H7 promoter activation of the FRIVET system in an *in vivo* background.

5.2 – Construction of an *ara::gfp+* reporter vector in a pACYC background

The *ara* promoter region from pBAD18 was amplified by PCR using the primers *ara*5' *Xba*I and *ara* 3' *Xba*I. The resulting PCR fragment was digested with *Xba*I and ligated with pACYC::*gfp+* upstream of the *gfp+* gene to create an *ara::gfp+* transcriptional fusion.

Ten putative clones were analysed by *Rsa*I restriction digest (Fig 5.2b). The pACYC::*gfp+* plasmid contains 2 *Rsa*I sites and was used as a comparison to detect clones containing the promoter insert. The *Rsa*I digest of the control pACYC::*gfp+* plasmid results in a banding pattern of 150bp, 550bp, 1.5kb and 2.6kb. The cloning of the 400bp *ara* promoter region into pACYC::*gfp+* would result in the 2.6kb band being raised to 3kb. Clones #2, #3, #5-#10 all show this banding pattern indicating the insertion of a 400bp DNA fragment between these *Rsa*I sites

The *ara* promoter region also introduces a novel *Bam*HI site in its sequence and therefore the correct cloning into pACYC::*gfp+* would give 2 bands when digested with *Bam*HI, as pACYC::*gfp+* already contains one site. Additionally as the *Bam*HI site in the *ara* promoter is near to the 3' end a *Bam*HI digest will confirm the orientation of the *ara* promoter with respect to *gfp+*. The *Bam*HI banding pattern for the *ara::gfp+* fusion construct in the correct orientation will be 4.2kb, 600bp and 500bp, whereas the banding pattern for the incorrect orientation will be 4.2kb, 880bp and 250bp. Clones #4- #10 were digested with *Bam*HI and clones #5 and #7-#10 exhibited the correct *Bam*HI banding pattern for the *ara::gfp+* fusion construct in the correct orientation (Fig 5.2c). Clone #7 was subsequently designated pRQ30 (Fig 5.2a).

Fig 5.2a

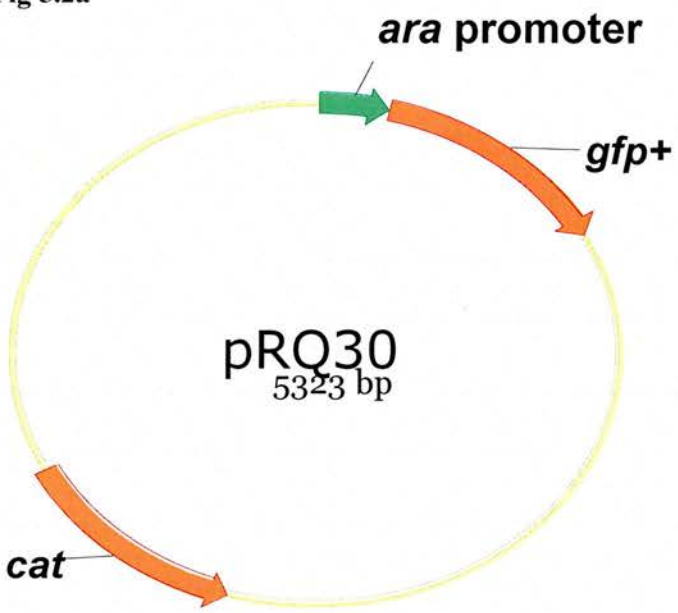

Vector map of pRQ30 showing the *ara* promoter cloned upstream of the *gfp*+ gene to create an *ara::gfp*+ transcriptional fusion.

Fig 5.2b

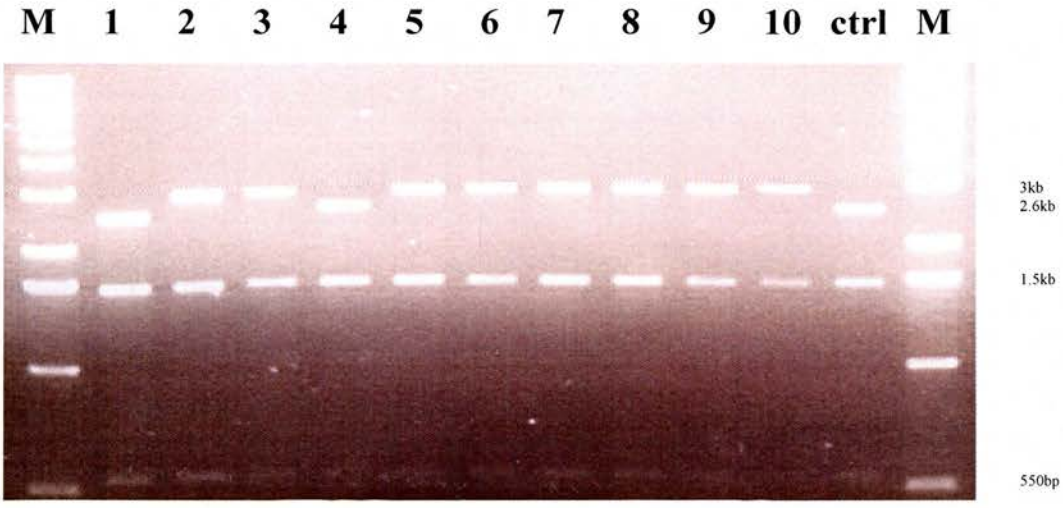

***Rsa*I digest on ten putative pRQ30 clones. The ctrl is pACYC::*gfp*+. Clones #2, #3 and #5-10 exhibit the correct banding pattern for an insertion of 400bp DNA upstream of the *gfp*+ gene. M = 1kb ladder.**

Fig 5.2c

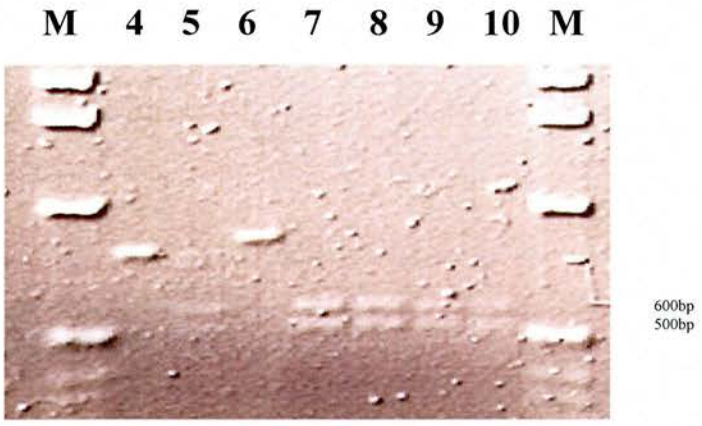

***Bam*HI digest on seven clones to determine the orientation of the cloned *ara* promoter. Clones #5 and #7-10 all exhibit the correct banding pattern for an *ara::gfp*+ transcriptional fusion. M = 1kb ladder.**

5.3 – Testing pRQ30 arabinose induction using a fluorimeter

The *E coli* strain AAEC189 was transformed with pRQ30 and subject to a fluostar assy using a fluorimeter. Three concentrations of arabinose were used to induce pRQ30 at 37^0C. The results can be seen in Figures 5.3a, 5.3b and 5.3c.

Fig 5.3a

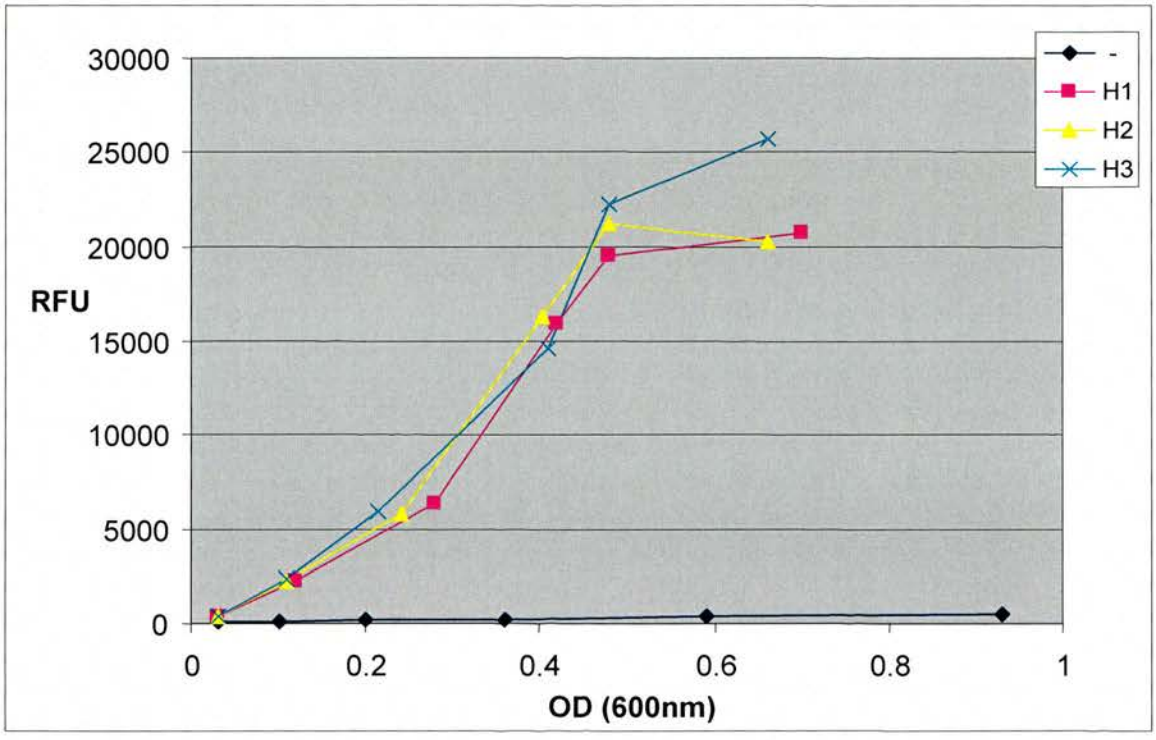

E. coli strain AAEC189 was transformed with pRQ30. 5ml overnight cultures were prepared in M9-C media. Four flasks of M9-C medium were inoculated with the overnight cultures to an optical density of 0.05. Arabinose was added to three of the flasks designated H1, H2 and H3 to a final concentration of 0.02% w/v whilst the fourth flask remained arabinose free (-). At time points throughout the assay 20µl samples were measured for their fluorescence levels using a Fluorimeter. These results were plotted against optical density. All three arabinose flasks produced high levels of fluorescence by mid exponential phase, the negative control flask produced low levels of fluorescence for the duration of the assay.

Fig 5.3b

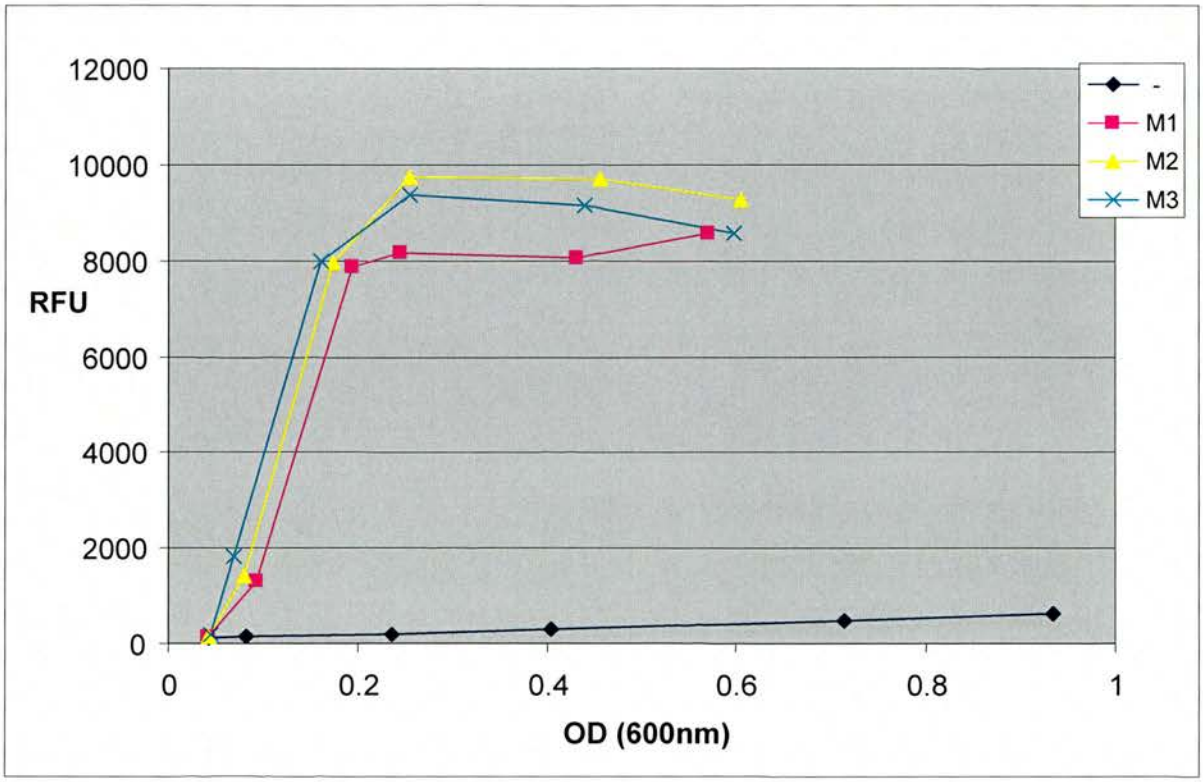

E. coli strain AAEC189 was transformed with pRQ30. 5ml overnight cultures were prepared in M9-C media. Four flasks of M9-C medium were inoculated with the overnight cultures to an optical density of 0.05. Arabinose was added to three of the flasks designated M1, M2 and M3 to a final concentration of 0.002% w/v whilst the fourth flask remained arabinose free (-). All three arabinose flasks reached a fluorescence level of nearly 8000 at an OD of 0.2. Flask M1 remained at this level for the duration of the assay whilst flasks M2 and M3 produced higher levels of fluorescence. The negative control flask produced low levels of fluorescence for the duration of the assay.

Fig 5.3c

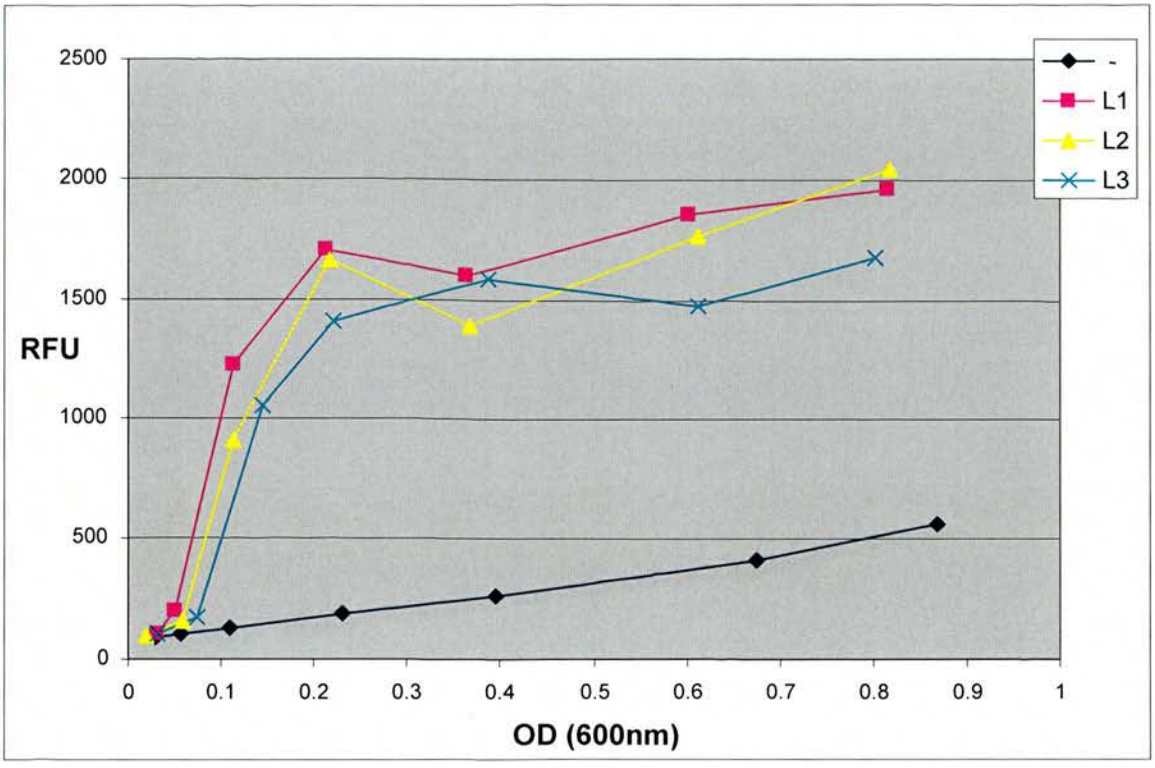

E. coli strain AAEC189 was transformed with pRQ30. 5ml overnight cultures were prepared in M9-C media. Four flasks of M9-C medium were inoculated with the overnight cultures to an optical density of 0.05. Arabinose was added to three of the flasks designated L1, L2 and L3 to a final concentration of 0.0002% w/v whilst the fourth flask remained arabinose free (-). All three arabinose flasks produced low levels of fluorescence compared with higher arabinose concentrations. The negative control flask produced low levels of fluorescence for the duration of the assay.

The results seen in Figures 5.3a, 5.3b and 5.3c show that the population is activated in an inducer concentration dependant manner and that our respective levels of inducer for L, M and H are sufficient to produce distinguishable fluorescence levels. We can know begin to construct the FRIVET test strain using the *ara* promoter.

5.4 – cloning the *ara* promoter into pRQ13

Using pBAD18 as a template the *ara* promoter region was amplified using primers *ara* 5' *Xba*I and *ara* 3' *Xba*I. The resulting PCR product and pRQ13 were digested with *Xba*I and ligated together.

Putative clones were analysed for *ara* promoter insertion by *Ava*II restriction digest (Fig 5.4b). The *ara* promoter PCR product introduces an new *Ava*II site. Therefore positive clones will show a distinct banding pattern of 2.8kb, 2.5kb, 1.7kb, 1.2kb and 1.3kb. Twelve putative clones were digested with *Ava*II as seen in Figure 5.4b. Four of the twelve produced the expected banding pattern: clones #1, #2, #9 and #10.

As the *ara* promoter was cloned using a single *Xba*I site and *Xba*I sites on the 5' and 3' *ara* primers a PCR was performed to confirm the orientation of the promoter respective to *fimB* using two sets of primers. The first PCR used primers LFR 1 and *ara* 5' *Xba*I and represented the reverse (i.e. incorrect) *ara* promoter insertion. The second PCR used primers *ara* 5' *Xba*I and *fimB* 3' and represented the correct orientation for the *ara* promoter to create a transcriptional fusion with *fimB*.

Clones #1, #2. #9 and #10 produced a positive PCR product for both primer sets (data not shown) indicating both variations of construct were present. It is likely that the parent strain has acquired both variants of *ara::fimB* from two separate plasmids, resulting in a double positive PCR.

Using the same sets of primers a further PCR was performed on clones #2, #5, #6, #7 and #8 (Fig 5.4c). There remained a possibility that the 1.2kb and 1.3kb bands had not fully resolved for these clones in the *Ava*II digest. Clone #2 once again produces positive PCR products for both primer sets as does clone #6. Clones #5, #7 and #8 however produce a positive PCR product for primer set 2 only (5' *ara* primer and 3' *fimB* primer) indicating the correct orientational insertion of the *ara* promoter region in pRQ13 to create a *ara::fimB* transcriptional fusion. Clone #8 was subsequently designated pRQ15 (Fig 5.4a)

Fig 5.4a

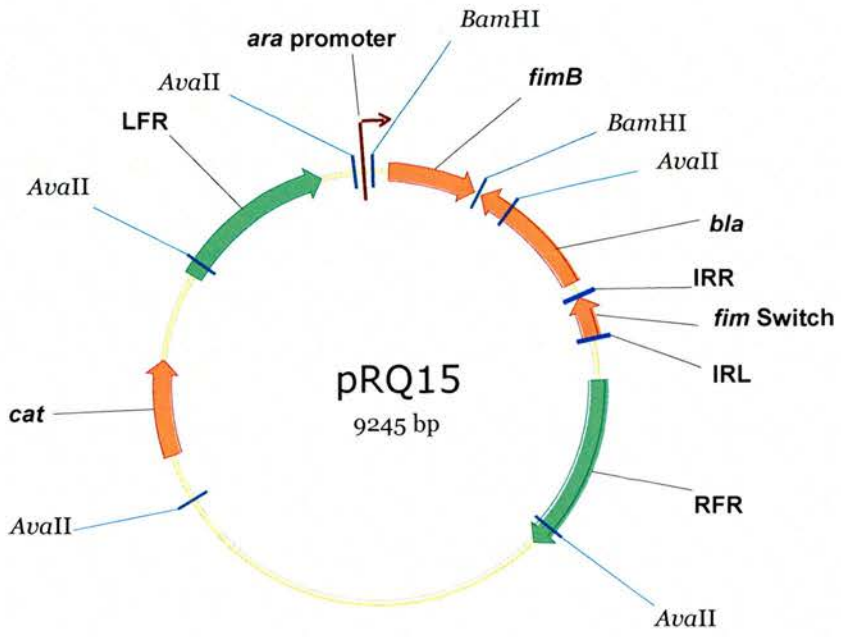

Vector map of pRQ15 showing the *ara* promoter region cloned upstream of *fimB* to create an *ara::fimB* transcriptional fusion.

Fig 5.4b

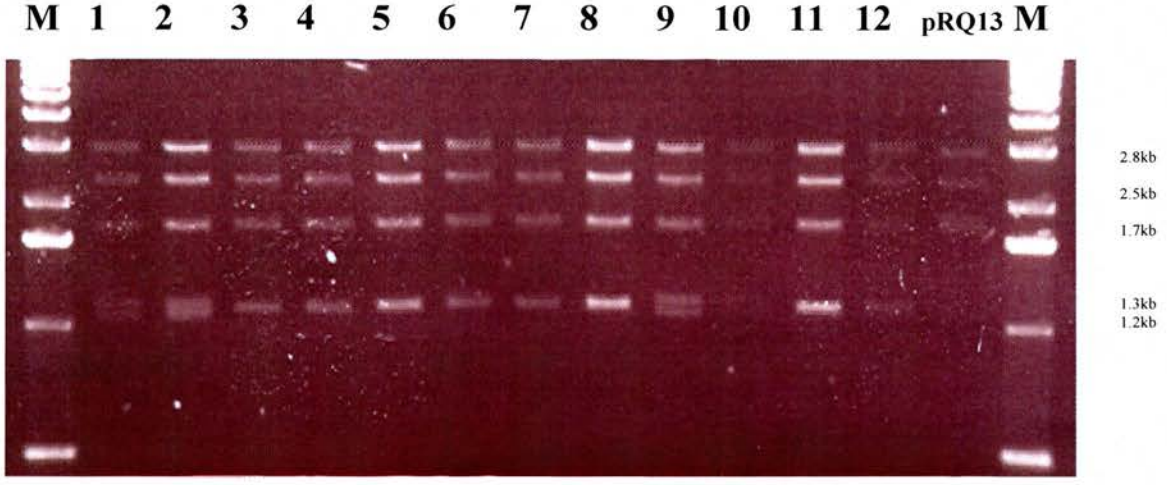

***Ava*II digest on twelve putative clones carrying the *ara* promoter. Clones #1, #2 #9 and #10 all produce the 2.8kb, 2.5kb, 1.7kb, 1.3kb and 1.2kb banding pattern indicating the cloning of the *ara* promoter into pRQ13. M = 1kb ladder.**

Fig 5.4c

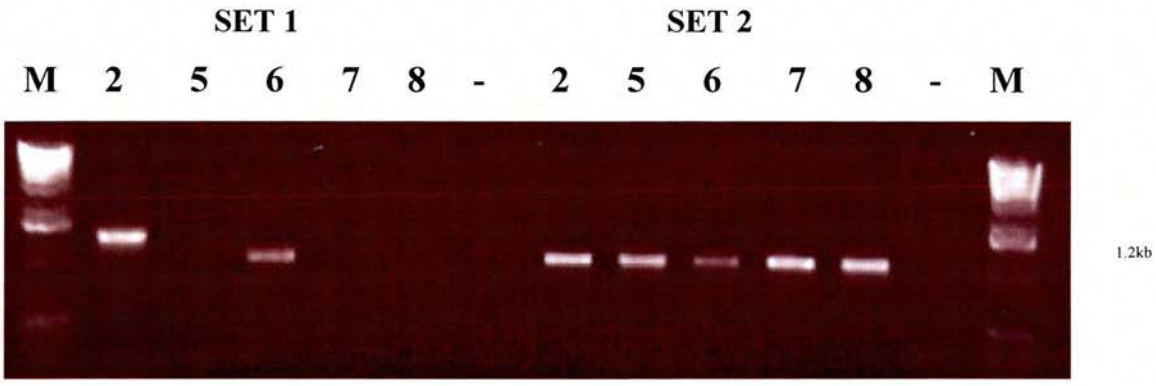

Diagnostic PCR using two primer sets to determine *ara* promoter orientation in five putative clones. Clones #5, #7 and #8 produce positive PCR products using primer set 2 but do not produce PCR products using primer set 1. The control (-) is water. M = 1kb ladder.

5.5 – Cloning the *ara* promoter into pRQ17

Using pBAD18 as a template the *ara* promoter was amplified using primers *ara* 5' *Xba*I and *ara* 3' *Xba*I. The resulting PCR product and pRQ17 were digested with *Xba*I and ligated together.

Ten putative clones containing the *ara* promoter region were analysed by *Ava*II restriction digest and compared to pRQ17 (Fig 5.5b). All ten clones produced a banding pattern of 2.8kb, 2kb, 1.7kb, 1.3kb and 1.2kb. This banding pattern is consistent with the correct cloning of the *ara* promoter into pRQ17 as the *ara* promoter region contains a novel *Ava*II site.

Each of the ten clones was subject to a diagnostic PCR to determine the orientation of the clone *ara* promoter region using a set of primers for forward orientation (correct) and reverse orientation (incorrect) respectively: (1) *ara* 5' *Xba*I and *fimB* 3'; (2) *ara* 3' *Xba*I and *fimB* 3' (Fig 5.5c). Clones B2, C1, C2, D1, D2, E1 and E2 all produced a positive PCR product for the correct *ara::fimB* transcriptional fusion. However clones C2, D1, D2 and E1 also produced a positive PCR result for the reverse orientation, indicating both constructs were present in the same plasmid prep. Clone C1 was taken forward and designated pRQ18 (Fig 5.5a).

Fig 5.5a

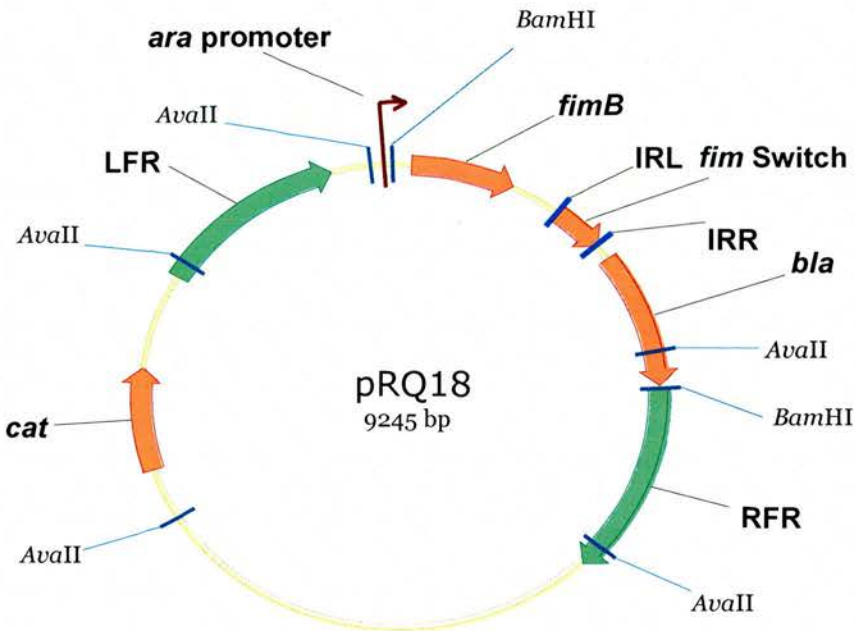

Vector map of pRQ18 showing the *ara* promoter cloned upstream of *fimB* to create an *ara::fimB* transcriptional fusion construct.

Fig 5.5b

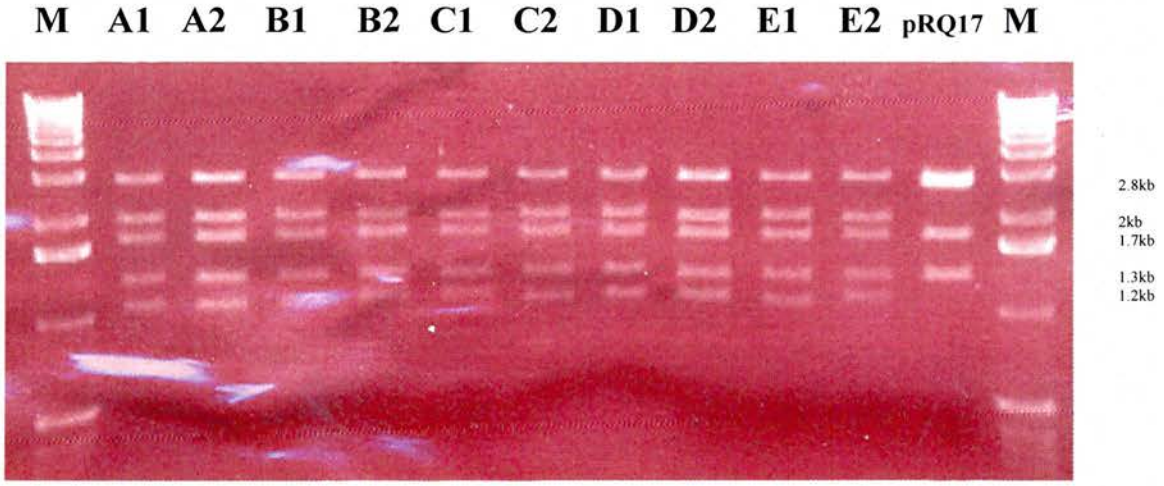

***Ava*II digest on ten putative clones. All ten clones produced the expected banding pattern consistent with the insertion of DNA in pRQ17. M = 1kb ladder.**

Fig 5.5c

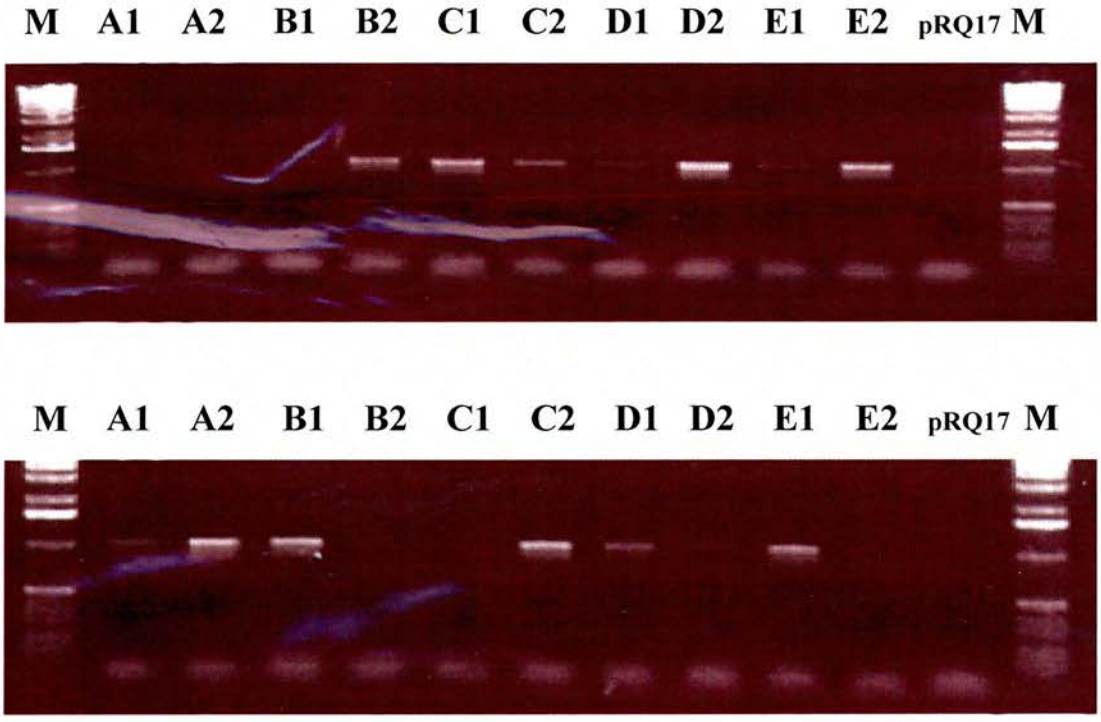

Diagnostic PCR using two primer sets on ten putative clones. Clones B2, C1 and E2 produce PCR products for primer set 1 but not for primer set 2 indicating the correct cloning of the *ara* promoter region into pRQ17. M = 1kb ladder.

5.6 – Exchanging pRQ15 into ZAP542

Strain ZAP542 was transformed with the temperature sensitive allelic exchange vector pRQ15 to create a FRIVET *ara* testing construct with *lac*UV5::*papB* at the *lac* locus. Putative strains that were kanamycin sensitive and grew well on sucrose containing media were stored at -70^{0}C. However for a FRIVET assay to function the *fim* switch must start in the 'off' orientation. As *fimS* on pRQ15 was originally cloned from pMM36 we would expect the *fim* switch in these putative strains to be in the 'on' orientation

The *fim* switch orientation in seven isolates was confirmed as 'on' by PCR using primers *fimS* V1 5' *bla* 3' and digesting the 1.6kb PCR product with *Hinf*I before running on an agarose gel (Fig 5.6). Using arabinose at a concentration of 0.04% w/v an 'on' to 'off' switching assay was performed to isolate an 'off' variant of strain #1. The resultant strain was designated ZAP543 and stored at -70^{0}C.

To ascertain the correct concentration of ampicillin needed for the FRIVET assays a series of LB agar plates were made with varying concentrations of ampicillin. The concentrations were 5μg/ml, 10μg/ml, 15μg/ml, 20μg/ml, 25μg/ml, 30μg/ml, 35μg/ml, 40μg/ml, and 50μg/ml. Serial dilutions of ZAP543 were spread onto these LBA plates and growth recorded. ZAP543 grew at concentrations of 5μg/ml and 10μg/ml but failed to grow at higher ampicillin concentrations. Further plates were made with 7.5μg/ml and 12.5μg/ml ampicillin. ZAP 543 failed to grow on the 12.5μg/ml plate. The experiment was repeated a further two times and the same results were observed. Subsequently the concentration of ampicillin in the FRIVET assays was set at 10μg/ml.

Fig 5.6

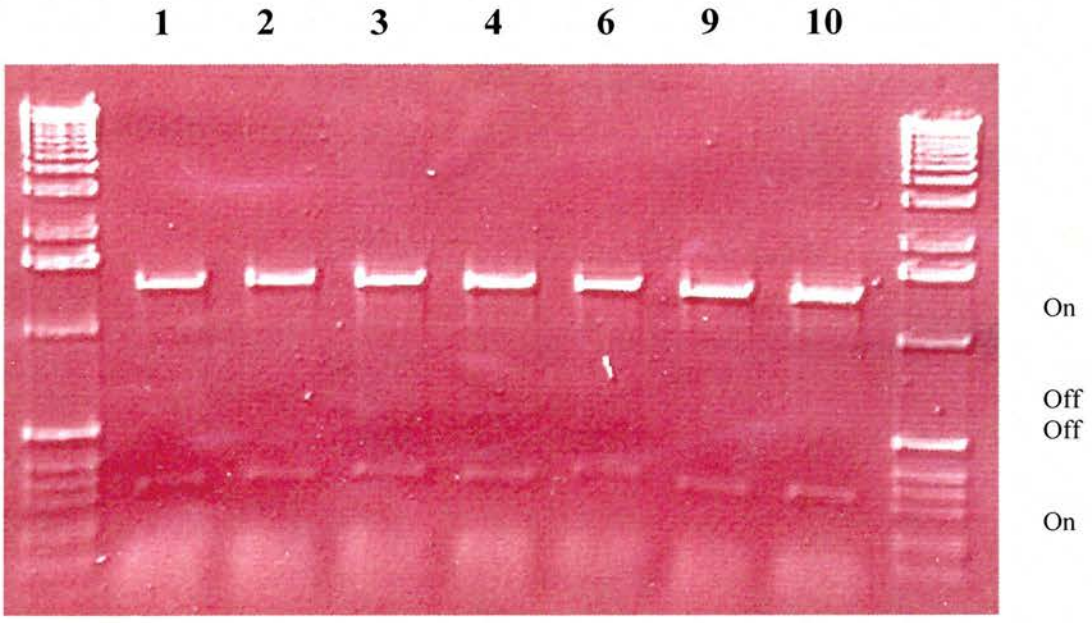

***Hinf*I digestion of 1.6kb PCR product from seven putative pRQ15 exchange strains. All seven strains exhibit *Hinf*I banding pattern for the 'on' orientation. Briefly, the 7 strains were subject to PCR using primers FRIVET *bla* diag and FRIVET *fimS* diag. The resulting 1.1kb PCR product was purified and subject to restriction digest with *Hinf*I. DNA bands at 672bp/182bp indicate *fimS* in the 'on' orientation. Bands at 389bp/466bp indicate *fimS* in the 'off' orientation.**

5.7 – Exchanging pRQ15 into ZAP544

ZAP544 was transformed with the temperature sensitive allelic exchange vector pRQ40 and subjected to allelic exchange. Putative strains confirmed as receiving the *sac/kan* cassette (phenotype Δ*fim sac/kan*) were termed ZAP545 and transformed with pRQ15. After allelic exchange two strains that exhibited kanamycin and chloramphenicol sensitivity and good growth on sucrose containing media were subjected to diagnostic PCR using the LFR up 5' primer and the *ara* 3' primer (Fig 5.7).

Strain #1 produced a PCR product of the expected size (1.5kb) and was subjected to an 'on' to 'off' switching assay: The strain was grown in LB media in the presence of arabinose to an OD of 0.9. The culture was then diluted onto LB agar and incubated overnight. Colonies were subsequently patched onto LB and LBA plates to isolate the 'off' variants. These 'off' variants were designated ZAP 546 and stored at -70^{0}C.

The inhibitory concentration of ampicillin was found to be 10μg/ml and this concentration was used in subsequent FRIVET assays with ZAP546.

Fig 5.7

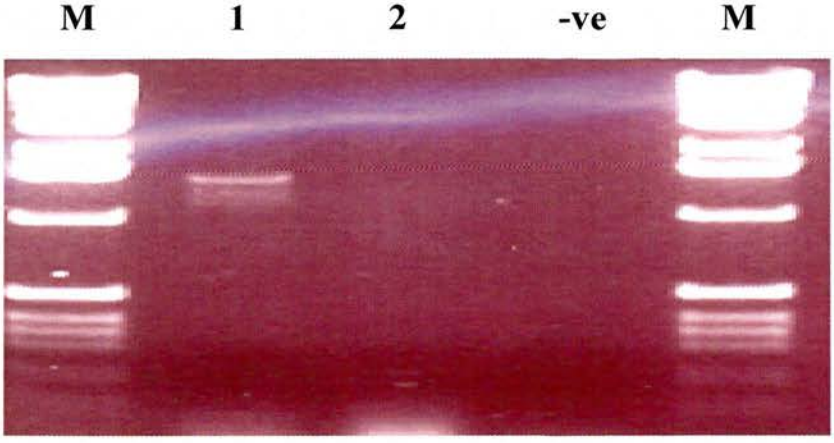

Diagnostic PCR on two putative ZAP546 strains using primers specific for an upstream region of LFR and the 3'*ara* primer. Strain #1 produces a PCR product of the expected 1.5kb size. The –ve control is ZAP545. M = 1kb ladder.

5.8 – Exchanging pRQ15 into ZAP193

ZAP193 was initially transformed with pRQ40 and subjected to allelic exchange to create the Δ*fim sackan* strain: ZAP547. Putative strains were analysed by their antibiotic resistance profile and growth on sucrose containing media. Strains that fit the phenotypic profile were transformed with pRQ15. Again putative strains were analysed by their antibiotic resistance patterns and sucrose growth. Strains that exhibited the correct phenotypic profile were designated ZAP548.

The inhibitory concentration of ampicillin was found to be 10μg/ml and this concentration was used in subsequent FRIVET assays with ZAP548.

5.9 – Induction of ZAP548 with varying concentrations of arabinose at 37^{0}C in M9 media

The FRIVET test strain ZAP548 was subject to FRIVET assays using three levels of arabinose inducer in M9 media at 37^{0}C. The results are shown in Figures 5.9a, 5.9b and 5.9c.

Fig 5.9a

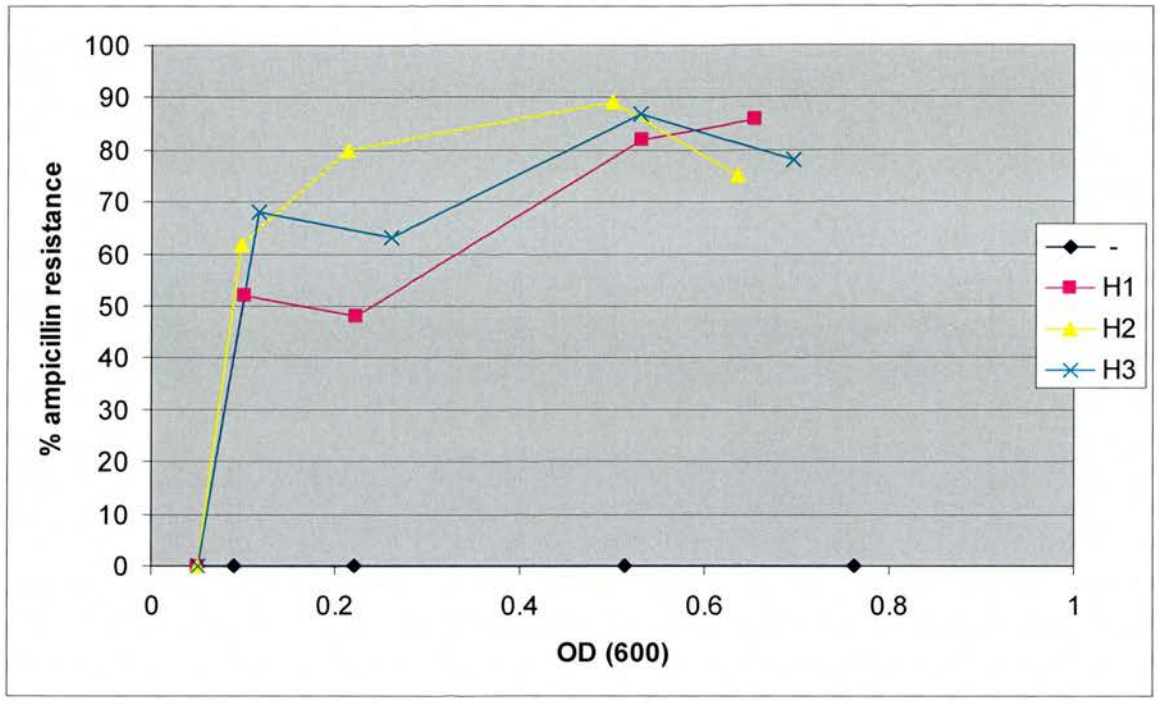

Four flasks of M9 medium were inoculated with overnight cultures of ZAP548 to an optical density of 0.05. Arabinose was added to three flasks designated H1, H2 and H3 to a final concentration of 0.02% w/v. The fourth flask remained arabinose free (-). The % ampicillin resistance exhibited in each culture was plotted against optical density. 100µl aliquots of each culture were removed at multiple time points and the % of ampicillin resistant bacteria in each aliquot determined by direct plating. All three flasks exhibited similar levels of FRIVET induction during the assay. The negative control flask (-) did not exhibit any resistance to ampicillin in the absence of arabinose inducer.

Fig 5.9b

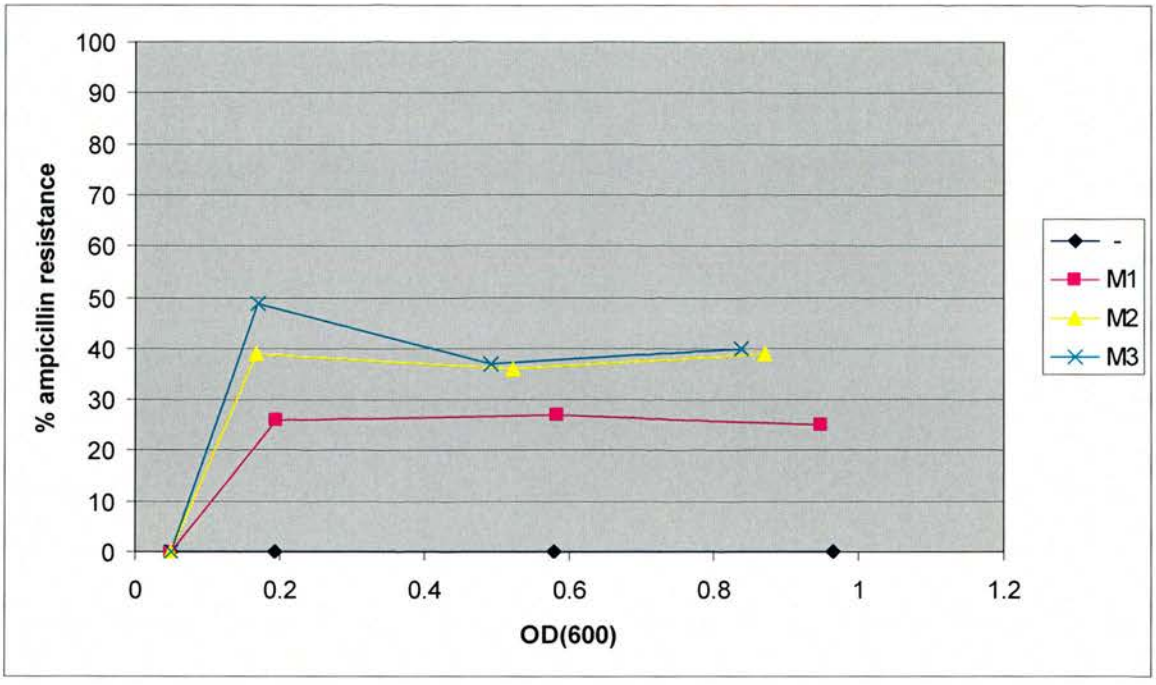

Four flasks of M9 medium were inoculated with overnight cultures of ZAP548 to an optical density of 0.05. Arabinose was added to three flasks designated M1, M2 and M3 to a final concentration of 0.002% w/v. The fourth flask remained arabinose free (-). 100µl aliquots of each culture were removed at multiple time points and the % of ampicillin resistant bacteria in each aliquot determined by direct plating. All three flasks exhibited similar levels of FRIVET induction during the assay. The negative control flask (-) did not exhibit any resistance to ampicillin in the absence of arabinose inducer.

Fig 5.9c

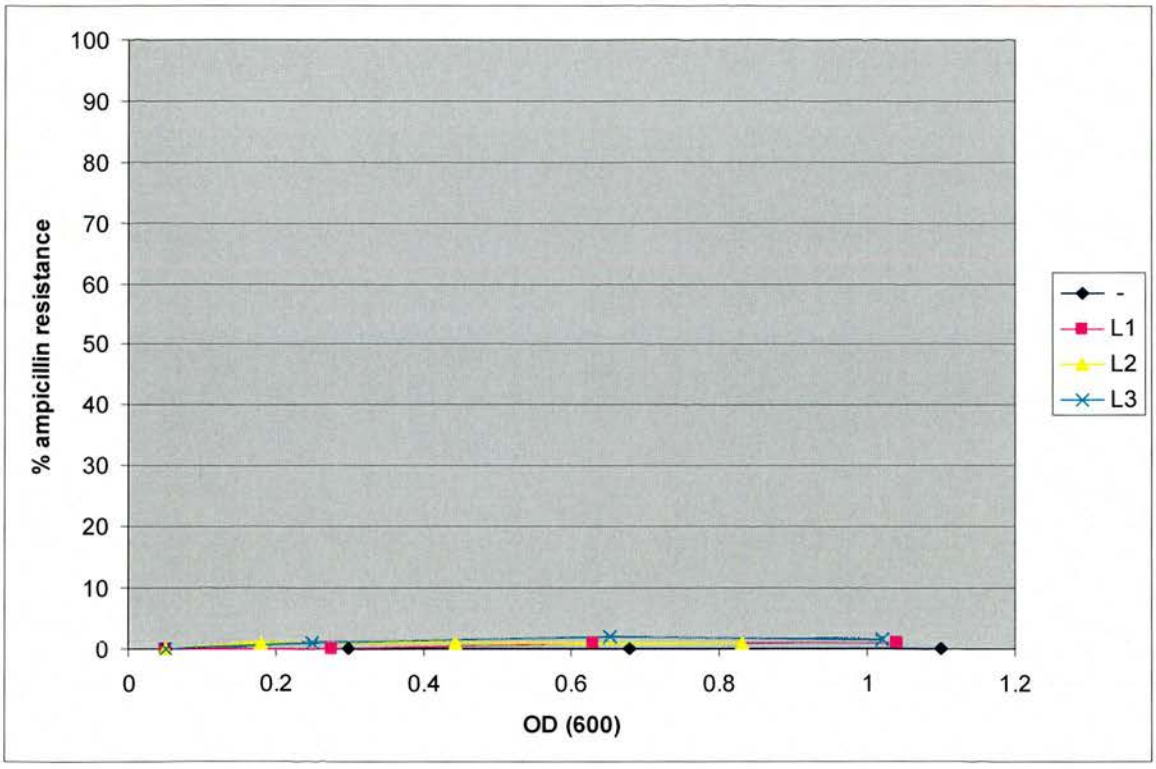

Four flasks of M9 medium were inoculated with overnight cultures of ZAP548 to an optical density of 0.05. Arabinose was added to three flasks designated L1, L2 and L3 to a final concentration of 0.0002% w/v. The fourth flask remained arabinose free (-). 100µl aliquots of each culture were removed at multiple time points and the % of ampicillin resistant bacteria in each aliquot determined by direct plating. All three flasks exhibited very low levels of FRIVET induction with a maximum ampicillin resistance level of 2% reached by flask L3 at an OD of 0.63. The negative control flask (-) did not exhibit any resistance to ampicillin in the absence of arabinose inducer.

The results for these three FRIVET assays for ZAP548 show that the FRIVET operon functions as a synthetic unit when under the control of the *ara* promoter and furthermore seems to be subject to similar population dynamics seen with the pRQ30 testing of the *ara* promoter by responding to a varying concentration of arabinose inducer..

5.10 – Induction of ZAP543 with varying levels of arabinose concentration in LB broth at 37^0C.

ZAP543 (*lac*UV5::*papB* @ *lac*) was induced with three concentrations of arabinose in LB broth in a FRIVET assay. The results can be seen in Figure 5.10.

Fig 5.10

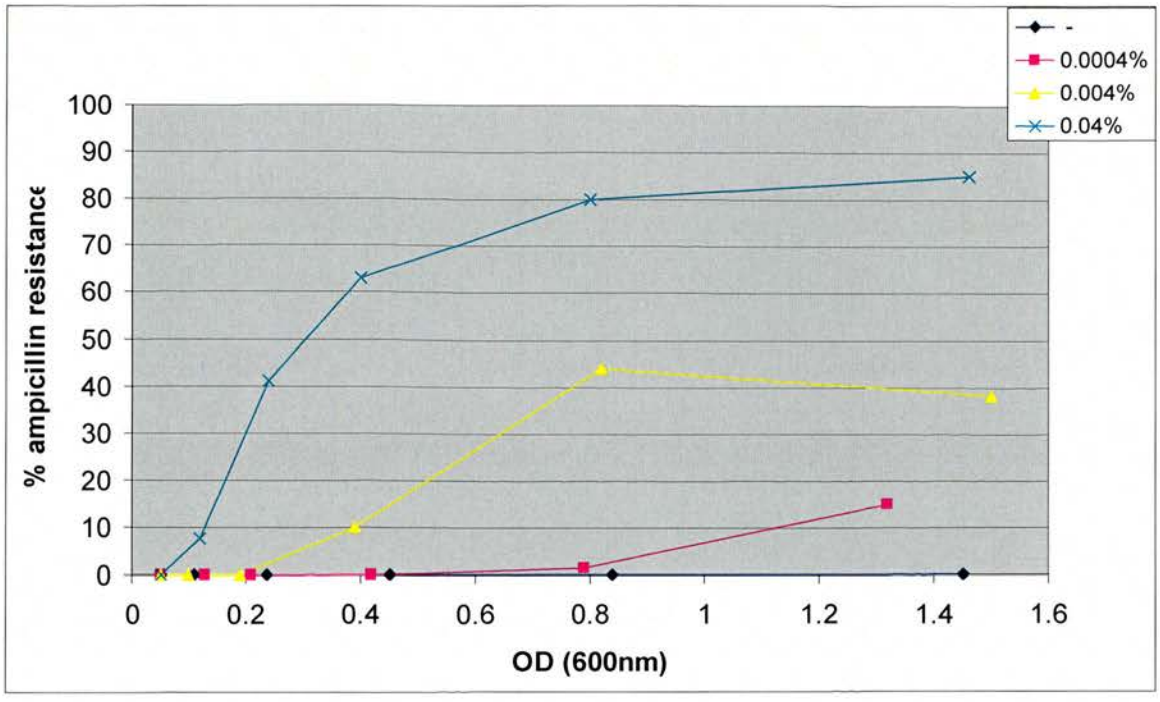

Four LB broths were inoculated with ZAP543 and induced with concentrations of arabinose of 0.0004% w/v, 0.004% w/v, 0.04% w/v and no arabinose (-) at 37^0C. Samples were taken at regular intervals and analysed for proportion of recovered colonies that were resistant to ampicillin. The % ampicillin resistance exhibited in each culture was plotted against optical density. It is evident that as higher concentrations of arabinose were used the proportion of ampicillin resistant bacteria detectable increased. The control flask (-) population did not exhibit any resistance to ampicillin in the absence of arabinose inducer.

5.11 - Induction of ZAP546 with varying concentrations of arabinose at 37^0C and 30^0C.

ZAP546 (Ptac::*papB* @ *lac*) was subject to a FRIVET assay using varying arabinose concentrations in LB broth at 37^0C (Fig. 5.11a) and 30^0C (Fig. 5.11b).

Fig 5.11a

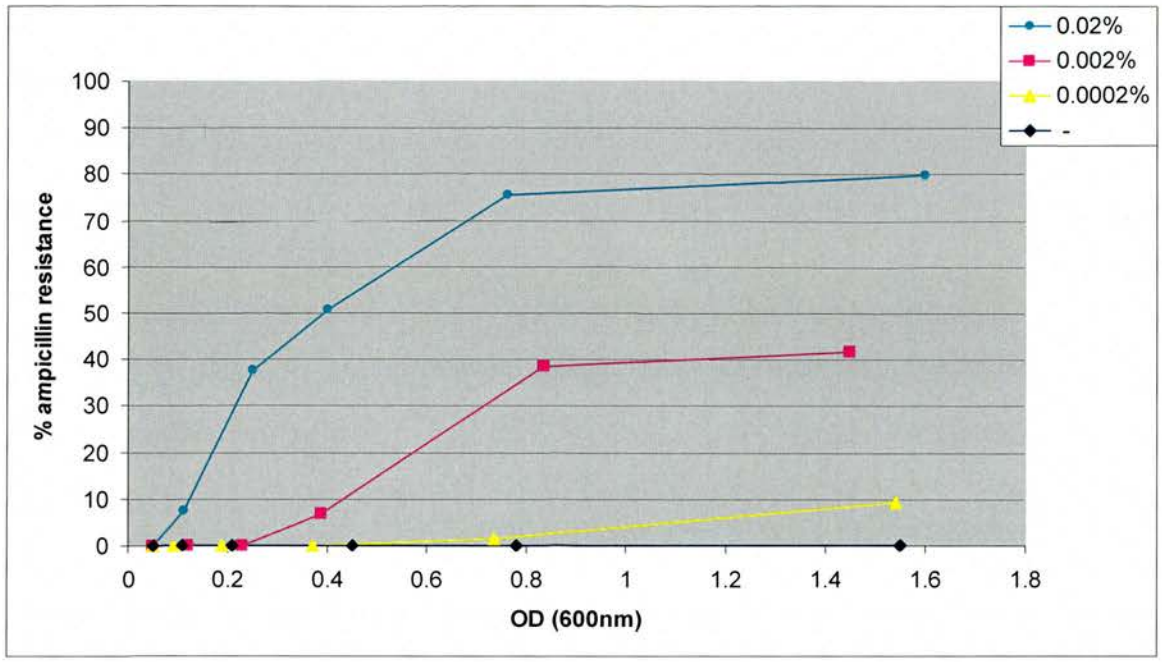

Four LB broths were inoculated with overnight cultures of ZAP546 to an optical density of 0.05. Arabinose was added to a final concentration of 0.02% w/v, 0.002% w/v and 0.0002% w/v to three of the flasks. 100µl aliquots of culture were removed from all flasks at multiple time points and the % of ampicillin resistant bacteria determined by direct plating. The % ampicillin resistance exhibited by each culture was relative to the concentration of arabinose added. The negative control flask (-) population did not exhibit any resistance to ampicillin in the absence of inducer.

Fig 5.11b

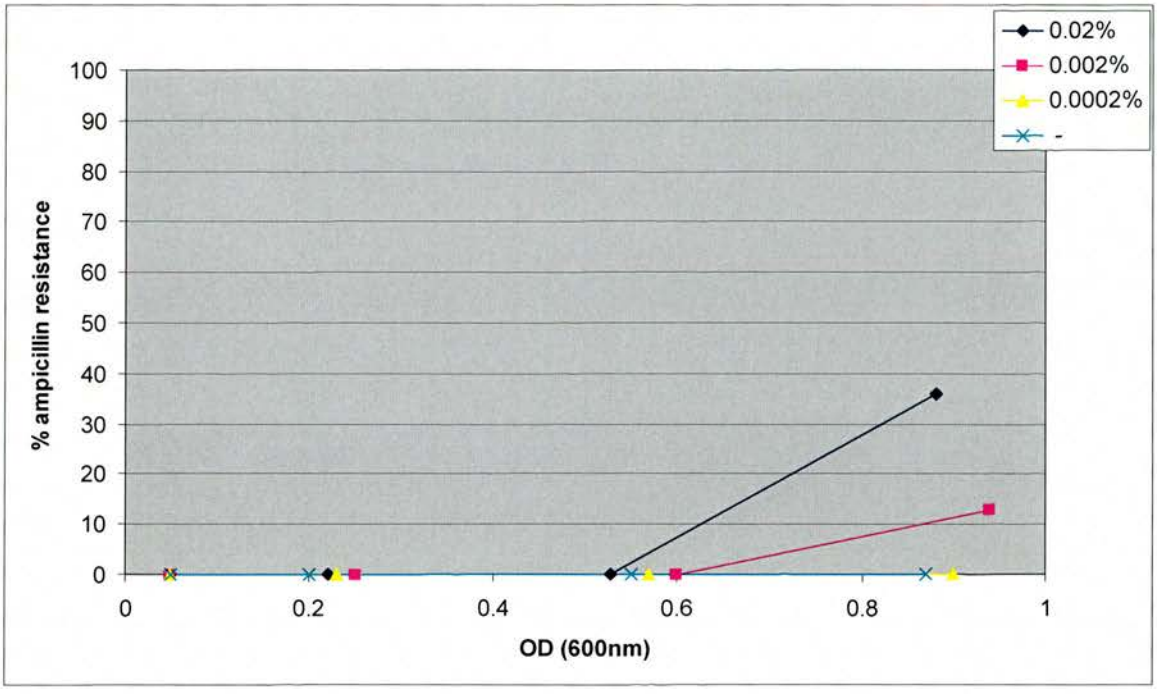

Four LB broths were inoculated with an overnight culture of ZAP546 to an optical density of 0.05. Arabinose was added to a final concentration of 0.02% w/v, 0.002% w/v and 0.0002% w/v in the three flasks. The fourth flask had no arabinose added. 100µl aliquots of each culture were removed at multiple time points and the % of ampicillin resistant bacteria in each aliquot was determined by direct plating. The % ampicillin resistance from each flask remained at 0% until mid exponential phase when the 0.02% w/v and 0.002% w/v flasks showed increased ampicillin resistance. The 0.0002% w/v flask remained 'off' for the duration of the experiment. The negative control flask (-) population did not exhibit any resistance to ampicillin in the absence of arabinose inducer.

5.12 – Induction of ZAP546 with varying concentrations of arabinose at 37^{0}C in M9 media

ZAP546 (Ptac::*papB* @ *lac*) was subject to three FRIVET assays using varying concentrations of arabinose inducer. The results can be seen in Figures 5.12a, 5.12b and 5.12c.

Fig 5.12a

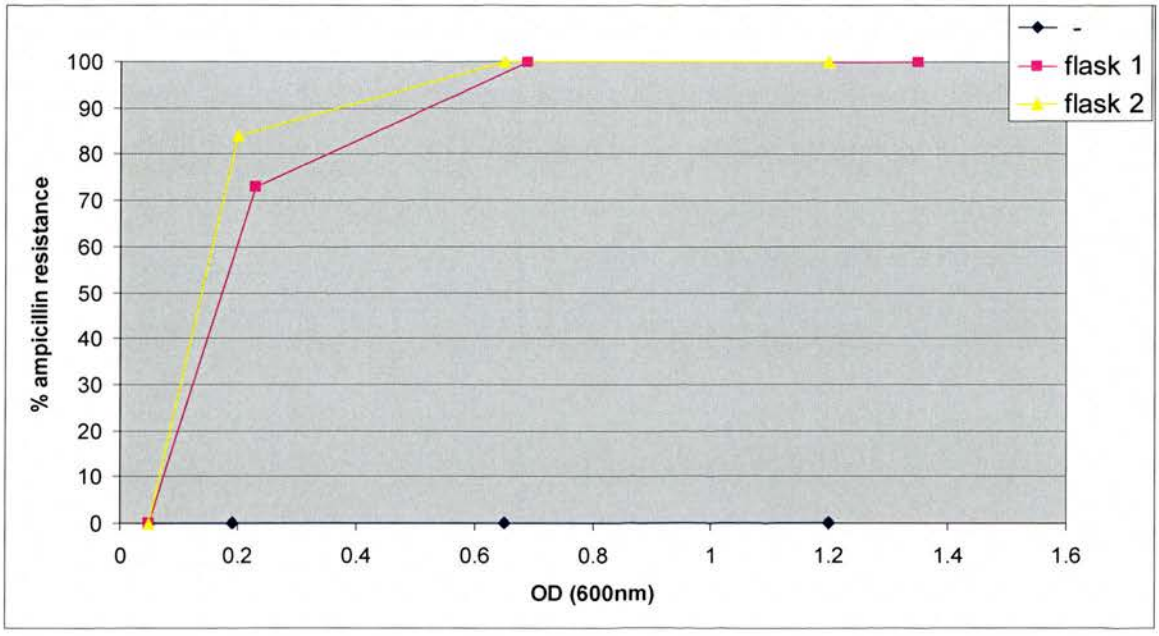

Three flasks of M9 medium were inoculated with overnight cultures of ZAP546 to an optical density of 0.05. Arabinose was added to a final concentration of 0.02% w/v to two flasks. The third had no arabinose added (-). 100µl aliquots of each culture were removed at multiple time points and the % of ampicillin resistant bacteria in each aliquot was determined by direct plating. The % ampicillin resistance increased to 73% and 84% for both flasks by early exponential phase and rose to 100% for both flasks by mid exponential phase until stationary phase. The negative control flask (-) population did not exhibit any resistance to ampicillin in the absence of arabinose inducer.

Fig 5.12b

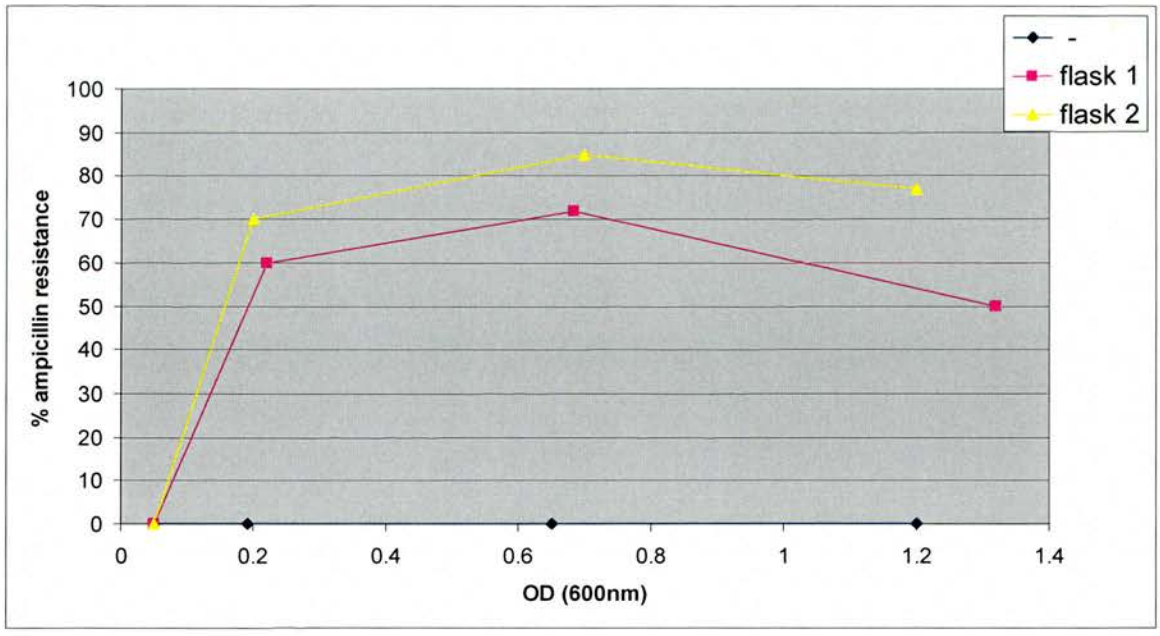

Three flasks of M9 medium were inoculated with overnight cultures of ZAP546 to an optical density of 0.05. Arabinose was added to a final concentration of 0.002% w/v to two flasks. The third had no arabinose added. 100µl aliquots of each culture were removed at multiple time points and the % of ampicillin resistant bacteria in each aliquot was determined by direct plating. The % ampicillin resistance increased to 60% and 70% for both flasks by early exponential phase and rose to 72% and 84% respectively by mid exponential phase. The negative control flask (-) population did not exhibit any resistance to ampicillin in the absence of arabinose inducer.

Fig 5.12c

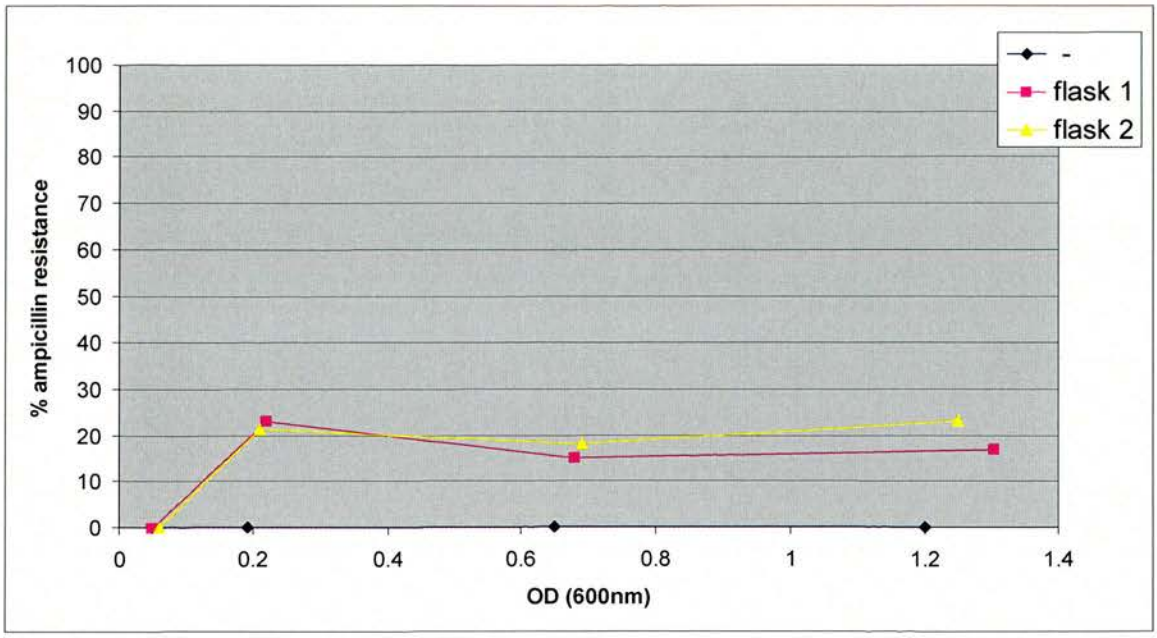

Three flasks of M9 medium were inoculated with overnight cultures of ZAP546 to an optical density of 0.05. Arabinose was added to a final concentration of 0.0002% w/v to two flasks. The third had no arabinose added. 100µl aliquots of each culture were removed at multiple time points and the % of ampicillin resistant bacteria in each aliquot was determined by direct plating. The % ampicillin resistance increased to ~22% for both flasks by early exponential phase and remained at that level until stationary phase. The negative control flask (-) population did not exhibit any resistance to ampicillin in the absence of arabinose inducer.

5.13 – Using PapB to suppress FRIVET induction in ZAP543 at 37^{0}C in LB broth

ZAP543 (*lac*UV5::*papB* @ *lac*) was subject to an FRIVET inhibition assay to measure the effect of PapB on the FRIVET system. IPTG was added to direct the production of PapB from the *lac*UV5::*papB* fusion @ the *lac* locus. The results of this assay can be seen in Figure 5.13.

Fig 5.13

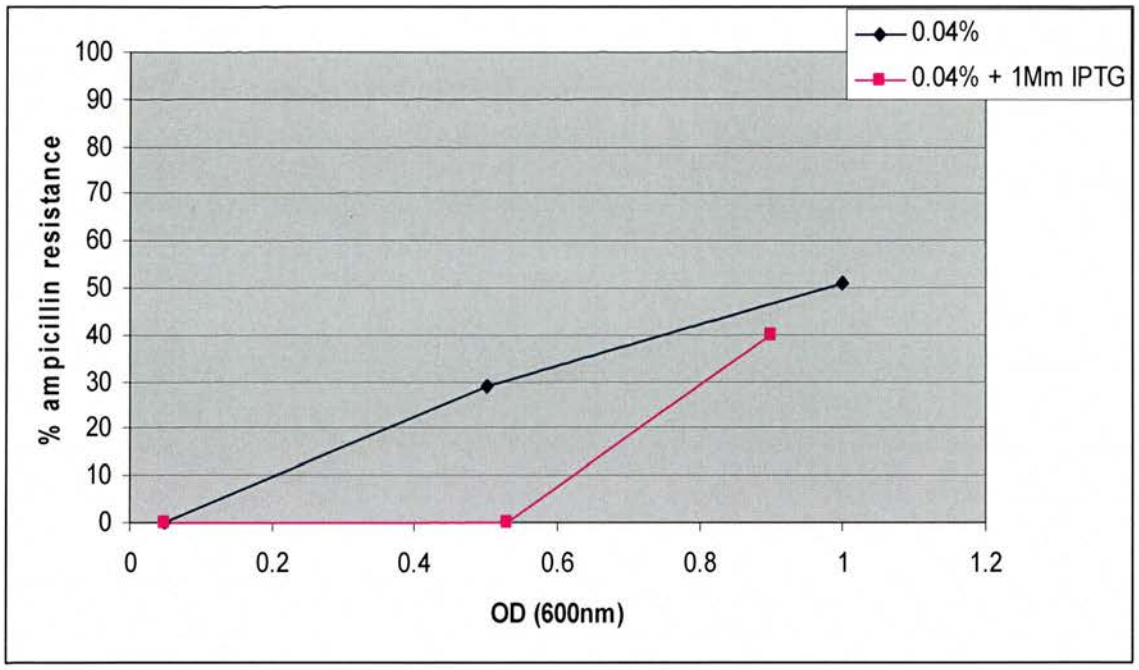

Two LB broths were inoculated from a ZAP543 overnight culture to an optical density of 0.05. Arabinose was added to both flasks to a final concentration of 0.04% w/v. In addition 1mM IPTG (final concentration) was added to one of the flasks to induce the *lac*UV5::*papB* transcriptional fusion at the *lac* locus on ZAP543. The IPTG/arabinose culture demonstrated 'locking' of the FRIVET system until mid exponential phase when inversion of the *fim* switch was detected. The control flask exhibited a steady increase in levels of arabinose mediated FRIVET expression.

5.14 – Suppression of FRIVET induction in ZAP546 at 37^0C

ZAP546 (Ptac::*papB* @ *lac*) was subject to an FRIVET inhibition assay to measure the effect of PapB on the FRIVET system. IPTG was added to direct the production of PapB from the Ptac::*papB* fusion @ the *lac* locus. Figure 5.14a shows the assay as performed in LB broth. The assay was also repeated in M9 media with a lower arabinose concentration (Fig 5.14b).

Fig 5.14a

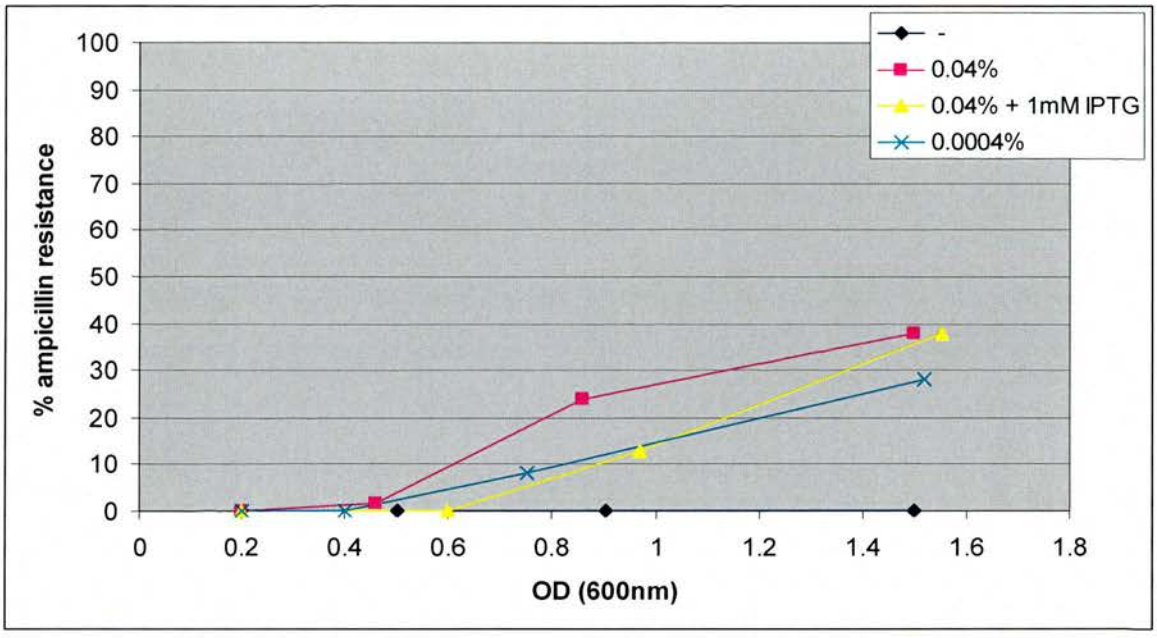

Four LB broths were inoculated with overnight cultures of ZAP546 to an optical density of 0.2. Arabinose was added to a final concentration of 0.04% w/v, 0.04% w/v and 0.0004% w/v to three flasks. The fourth had no inducer added (-). IPTG was added to a flask with 0.04% w/v arabinose to a final concentration of 1mM IPTG. 100µl aliquots of each culture were removed at multiple time points and the % of ampicillin resistant bacteria in each aliquot was determined by direct plating. The two positive control flasks with 0.04% w/v and 0.0004% w/v arabinose exhibited increase in ampicillin resistance relative to the concentration of arabinose. The flask containing 0.04% arabinose and IPTG showed decreased FRIVET induction compared to control until stationary phase at which point cultures from both the arabinose/IPTG flask and the 0.04% arabinose control flasks exhibited similar levels of ampicillin resistance. The negative control flask (-) population did not exhibit any resistance to ampicillin in the absence of arabinose inducer.

Fig 5.14b

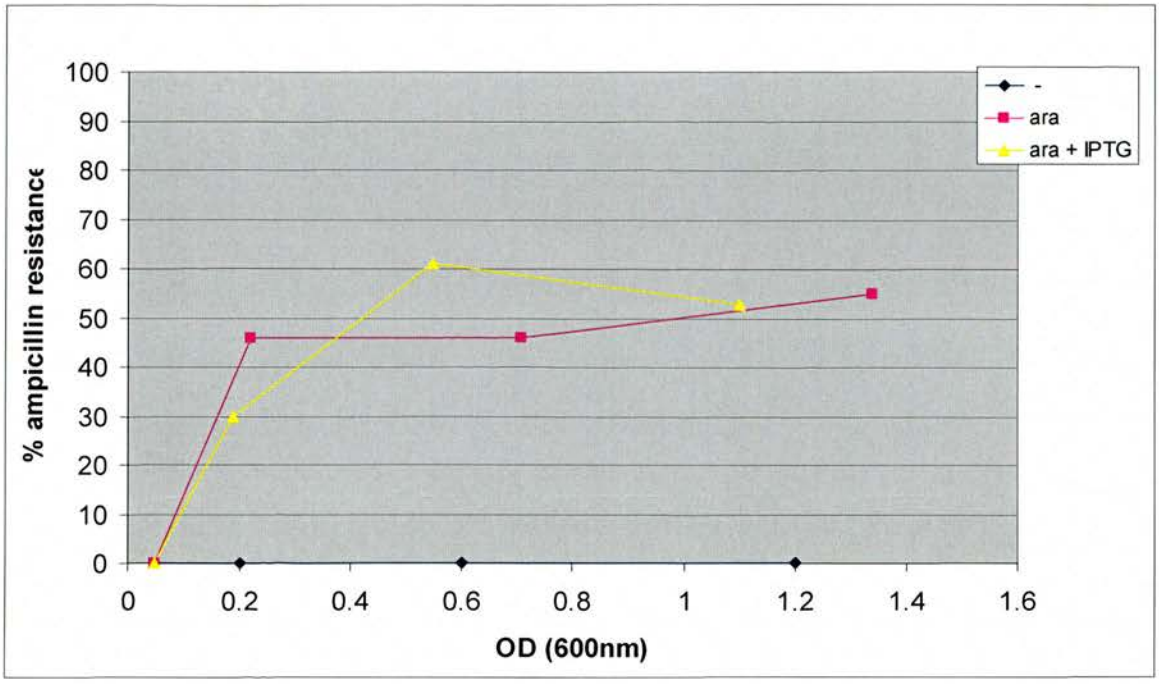

Three flasks of M9 media were inoculated with overnight cultures of ZAP546 to an optical density of 0.05. Arabinose was added to a final concentration of 0.002% w/v to two flasks. The third had no arabinose added (-). IPTG was added to one of the 0.002% w/v arabinose flasks to a final concentration of 1mM. . 100µl aliquots of each culture were removed at multiple time points and the % of ampicillin resistant bacteria in each aliquot was determined by direct plating. The IPTG/arabinose flask exhibited 30% ampicillin resistance at an optical density of 0.2 against 47% for the positive control. However, by mid exponential phase the IPTG/arabinose flask showed a higher ampicillin resistance % than the control although both flasks exhibited similar levels of ampicillin resistance by stationary phase. The negative control flask (-) population did not exhibit any resistance to ampicillin in the absence of arabinose inducer.

5.15 – Transformation of ZAP546 with pHMG88 to suppress FRIVET induction

The results seen in 5.13 and 5.14 show that the level of PapB in these assays failed to suppress the activity of the FRIVET system. The next logical step was to increase the level of PapB in the cell and to observe if the concentration of PapB was the defining factor in the PapB/Fim switch interaction. This was achieved by the transformation of ZAP546 with pHMG88, a medium copy plasmid containing the IPTG inducible *lac*UV5::*papB* transcriptional fusion. By adding IPTG, PapB would be produced both from the chromosomal Ptac::*papB* fusion on ZAP546 and from pHMG88 resulting in high concentrations of PapB in the cell. The assay was performed with three concentrations of arabinose inducer in M9 media at 37^0C. The results can be seen in Figures 5.15a, 5.15b and 5.15c

Fig 5.15a

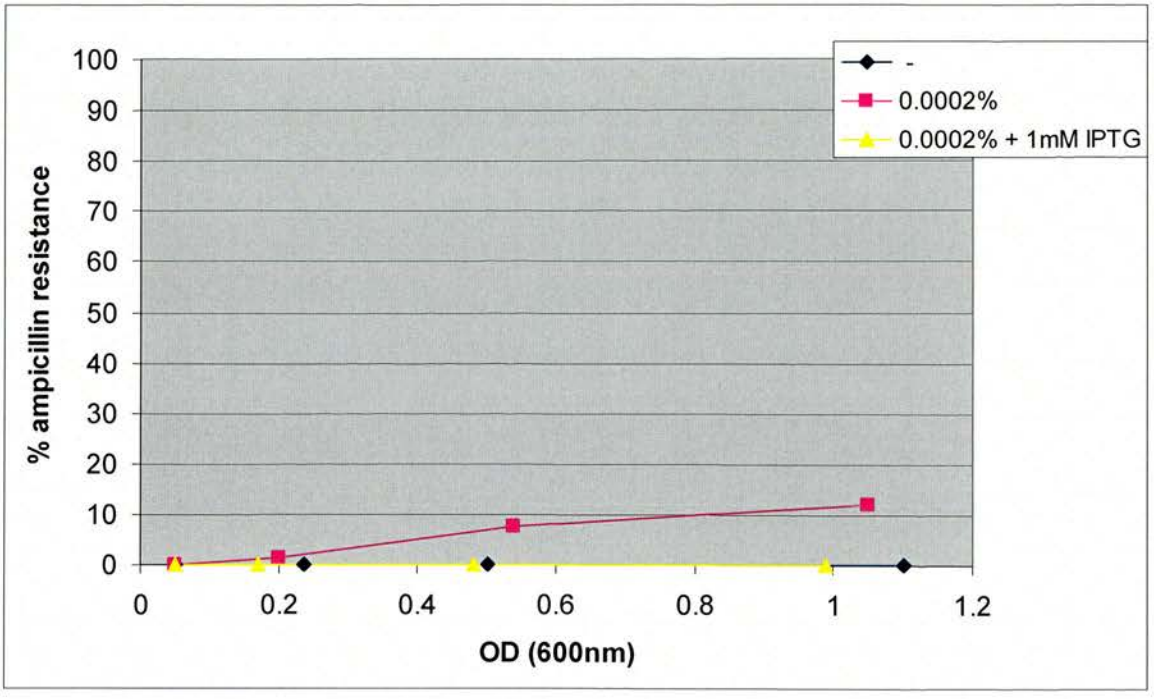

Three flasks of M9-T medium were inoculated with overnight cultures of ZAP546::pHMG88 to an optical density of 0.05. Arabinose was added to a final concentration of 0.0002% w/v to two flasks. The third had no arabinose added (-). IPTG was added to one of the 0.0002% w/v arabinose flasks to a final concentration of 1mM. 100µl aliquots of each culture were removed at multiple time points and the % of ampicillin resistant bacteria in each aliquot was determined by direct plating. The positive control 0.0002% w/v flask reached an ampicilin resistance of 8% at an OD of 0.5 rising to 12% at an OD of 1.05. The IPTG/arabinose culture demonstrated 'locking' of the FRIVET system and remained 'off' for the duration of the assay. The negative control flask (-) population did not exhibit any resistance to ampicillin in the absence of arabinose inducer.

Fig 5.15b

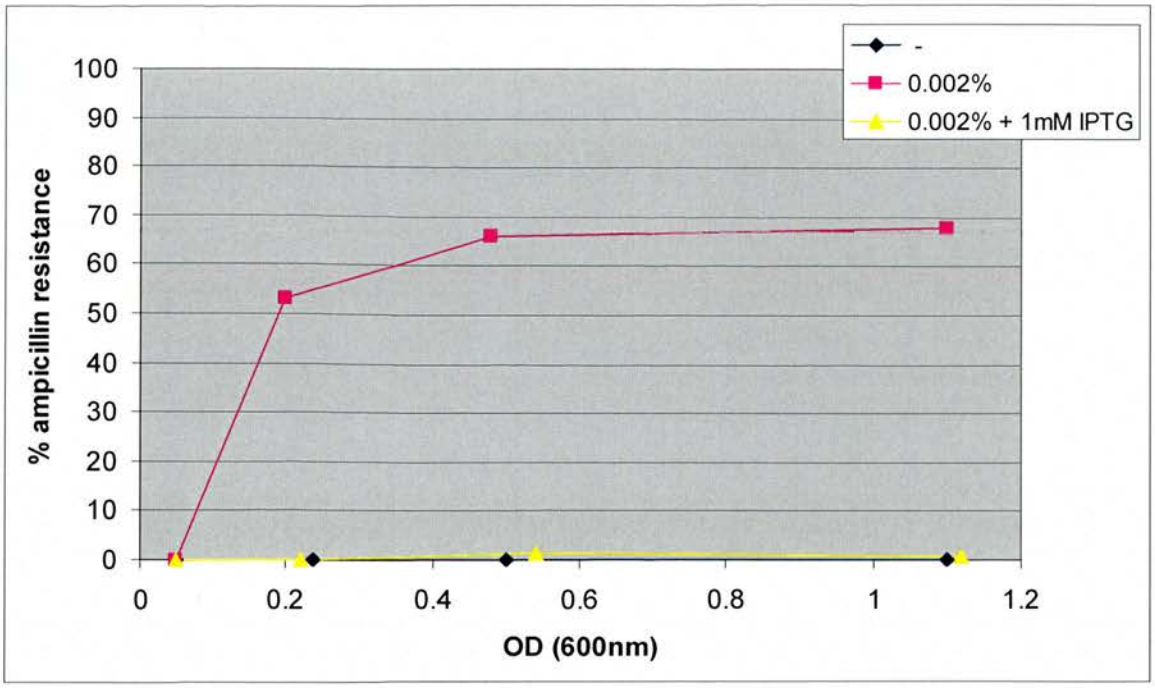

Three flasks of M9-T medium were inoculated with overnight cultures of ZAP546::pHMG88 to an optical density of 0.05. Arabinose was added to a final concentration of 0.002% w/v to two flasks. The third had no arabinose added (-). IPTG was added to one of the 0.002% w/v arabinose flasks to a final concentration of 1mM. 100µl aliquots of each culture were removed at multiple time points and the % of ampicillin resistant bacteria in each aliquot was determined by direct plating. The positive control 0.002% w/v flask reached an ampicilin resistance of 52% at an OD of 0.2 rising to 66% at an OD of 0.48 and 68% at an OD of 1.1. The IPTG/arabinose flask exhibited significantly decreased FRIVET induction and reached a maximum ampicillin resistance percentage of 1.3% during the assay. The negative control flask (-) population did not exhibit any resistance to ampicillin in the absence of arabinose inducer.

Fig 5.15c

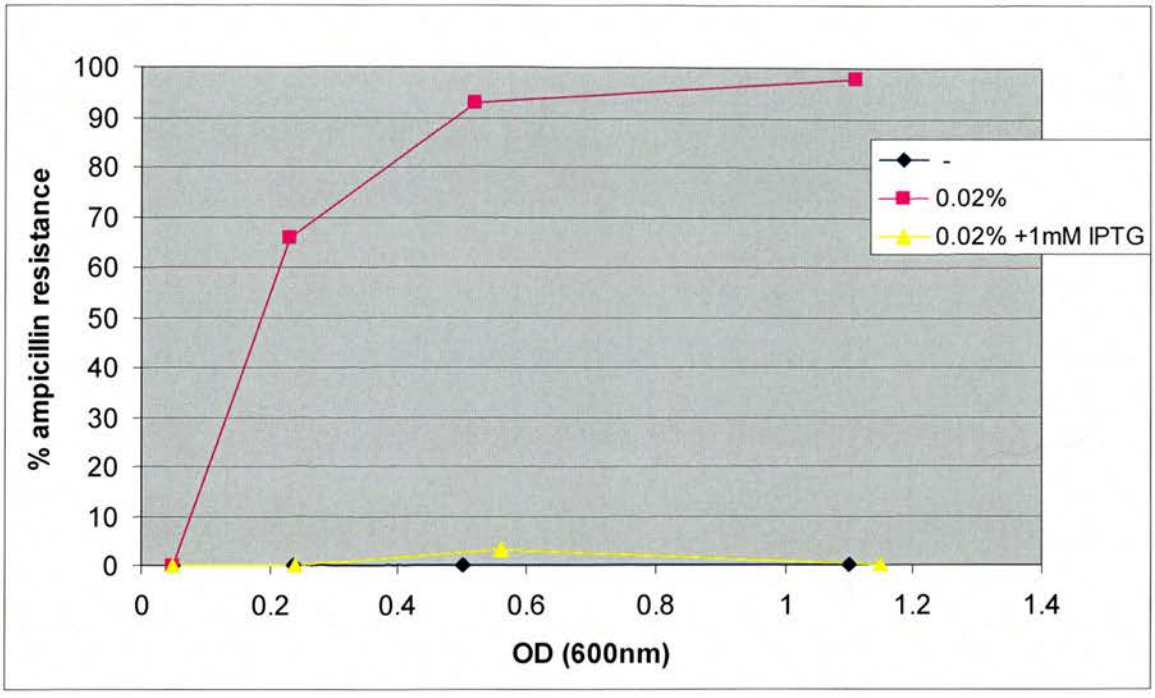

Three flasks of M9-T medium were inoculated with overnight cultures of ZAP546::pHMG88 to an optical density of 0.05. Arabinose was added to a final concentration of 0.02% w/v to two flasks. The third had no arabinose added (-). IPTG was added to one of the 0.02% w/v arabinose flasks to a final concentration of 1mM. 100µl aliquots of each culture were removed at multiple time points and the % of ampicillin resistant bacteria in each aliquot was determined by direct plating. The positive control 0.02% w/v flask reached maximum ampicilin resistance of 98% at an OD of 1.1. The IPTG/arabinose flask exhibited significantly decreased FRIVET induction and only reached a maximum ampicillin resistance percentage of 3.1% during the assay. The negative control flask (-) population did not exhibit any resistance to ampicillin in the absence of arabinose inducer.

The results in Figures 5.17a, 5.17b and 5.17c clearly show the inhibition of FRIVET induction with the addition of pHMG88. To test whether the prescence of the plasmid itself was making a difference ZAP546 was transformed with pACYC184 and the assay from Figure 5.17a repeated (data not shown). No inhibition of FRIVET induction was observed. We can conclude that PapB appears to function to inhibit the FRIVET operon at a threshold level, and that this level is not reached with the use of the *lac*UV5 and Ptac promoters in single copy.

5.16– Inhibition of the FRIVET system using pACTAC::*fimE* at 37^0C in M9-C media

ZAP546 (Ptac::*papB* @ *lac*) was transformed with pACTAC::*fimE* to observe the effects of FimE on the FRIVET system. It was expected that the FRIVET system may need another level of control not using PapB. This pACYC184 based vector contains a Ptac::*fimE* transcriptional fusion. The results of the FRIVET inhibition assay can be seen in Figure 5.16.

Fig 5.16

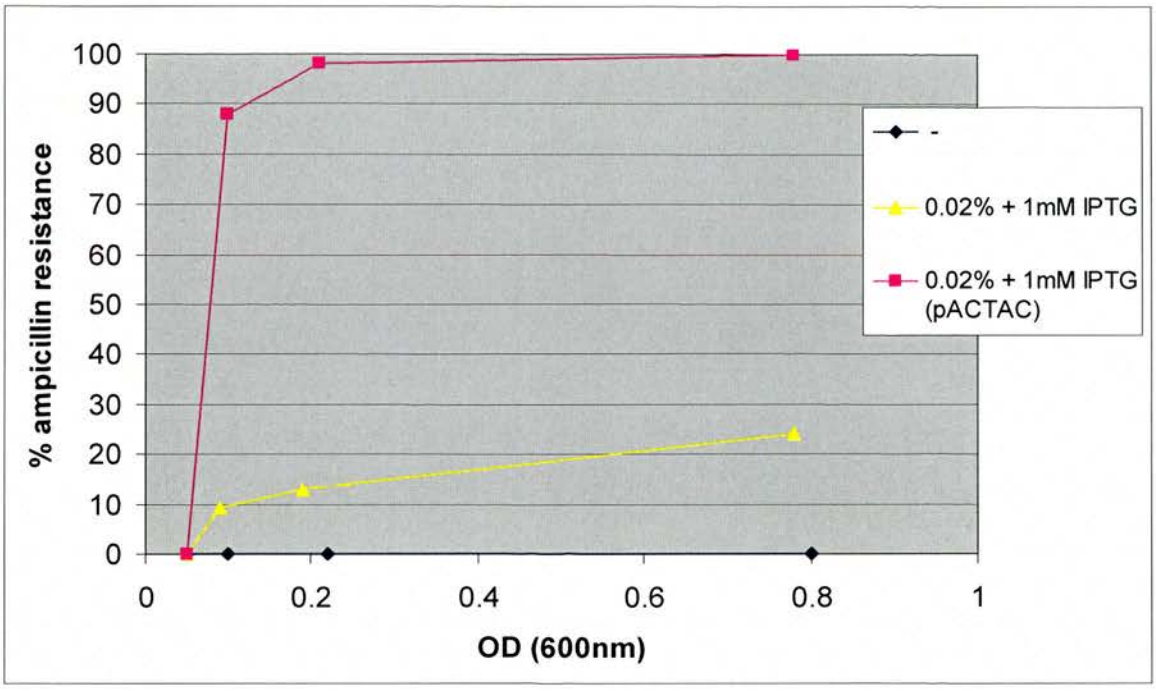

Three flasks of M9-C medium were inoculated with overnight cultures of ZAP546::pACTAC::*fimE* to an optical density of 0.05. The remaining flask was inoculated with an overnight culture of ZAP546::pACTAC to an optical density of 0.05. Arabinose was added to a final concentration of 0.02% w/v to three flasks. The fourth was designated the negative control and remained free of arabinose (-). IPTG was added to two of the 0.02% w/v arabinose flasks to a final concentration of 1mM100µl aliquots of each culture were removed at multiple time points and the % of ampicillin resistant bacteria in each aliquot was determined by direct plating. The positive control 0.02% w/v flask only reached a maximum ampicilin resistance of 29% at an OD of 0.8, however the pACTAC control flask reached a 100% ampicillin resistance level at a similar OD. The pACTAC::*fimE* flask exhibited decreased FRIVET induction compared to the pACTAC control flask reaching a maximum ampicillin resistance percentage of 24% during the assay. The negative control flask (-) population did not exhibit any resistance to ampicillin in the absence of arabinose inducer.

5.17 – Repression of the FRIVET system with supplemental glucose

ZAP546 (Ptac::*papB* @ *lac*) was grown in the presence and absence of glucose to observe the effects of glucose repression on the *ara* based FRIVET test system. The results can be seen in Figure 5.17.

Fig 5.17

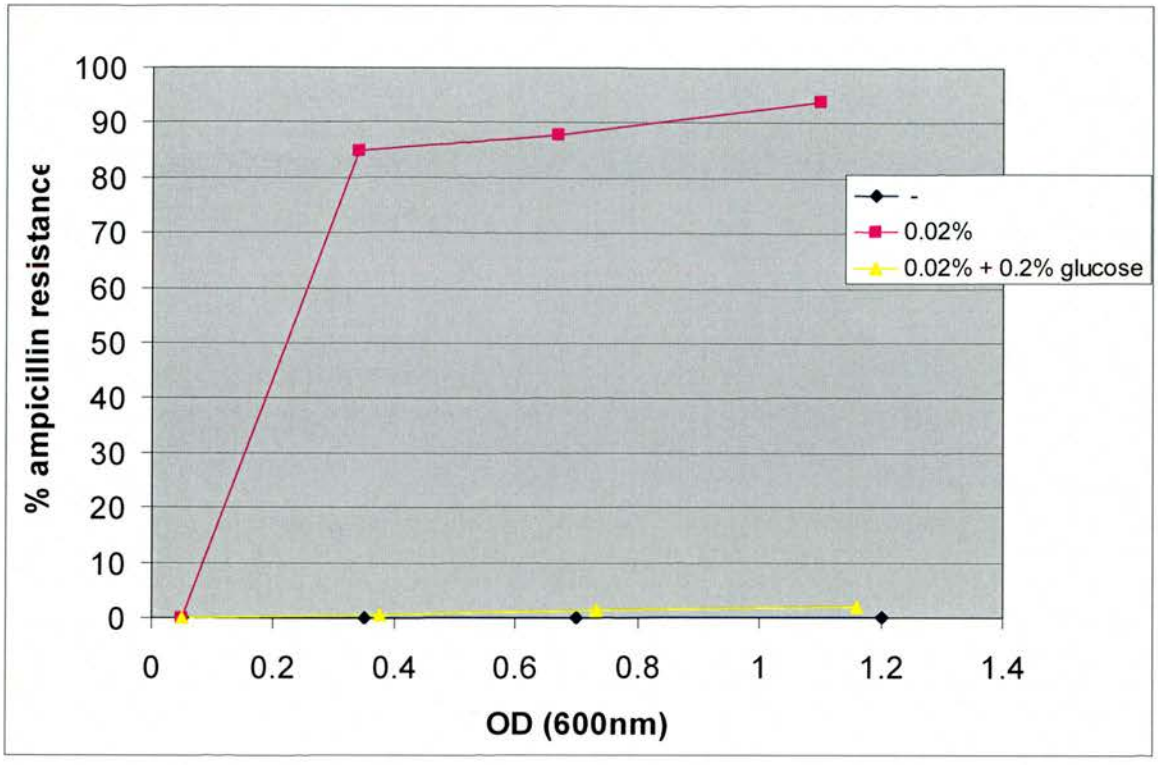

Three flasks of M9 medium were inoculated with overnight cultures of ZAP546 to an optical density of 0.05. Arabinose was added to a final concentration of 0.02% w/v to two flasks. The third was designated a negative control and remained arabinose free (-). Glucose was added to one of the arabinose flasks to a final concentration of 0.2% v/v. 100µl aliquots of each culture were removed at multiple time points and the % of ampicillin resistant bacteria in each aliquot was determined by direct plating. The positive control 0.02% w/v flask reached an ampicilin resistance level of 94% at an OD of 1.1. The arabinose/glucose flask exhibited significantly decreased FRIVET induction levels compared to the arabinose only flask reaching a maximum ampicillin resistance percentage of 1.4% during the assay. The negative control flask (-) population did not exhibit any resistance to ampicillin in the absence of arabinose inducer.

5.18 – Using LEE5 FRIVET constructs in a sheep gut loop animal model of infection

ZAP545 was transformed with the FRIVET plasmids pRQ103, 104 and 105 to create the strains VLAFRIVET::LEE5, VLAFRIVET::*lpf1* and VLAFRIVET::*loc8* respectively. Using the method outlined in chapter 2 a ligated gut loop assays was performed on 2 sheep at the VLA, Weybridge, UK using the three VLAFRIVET strains.

The results of the two assays can be seen in Figures 5.18a – 5.18c.

Fig 5.18a

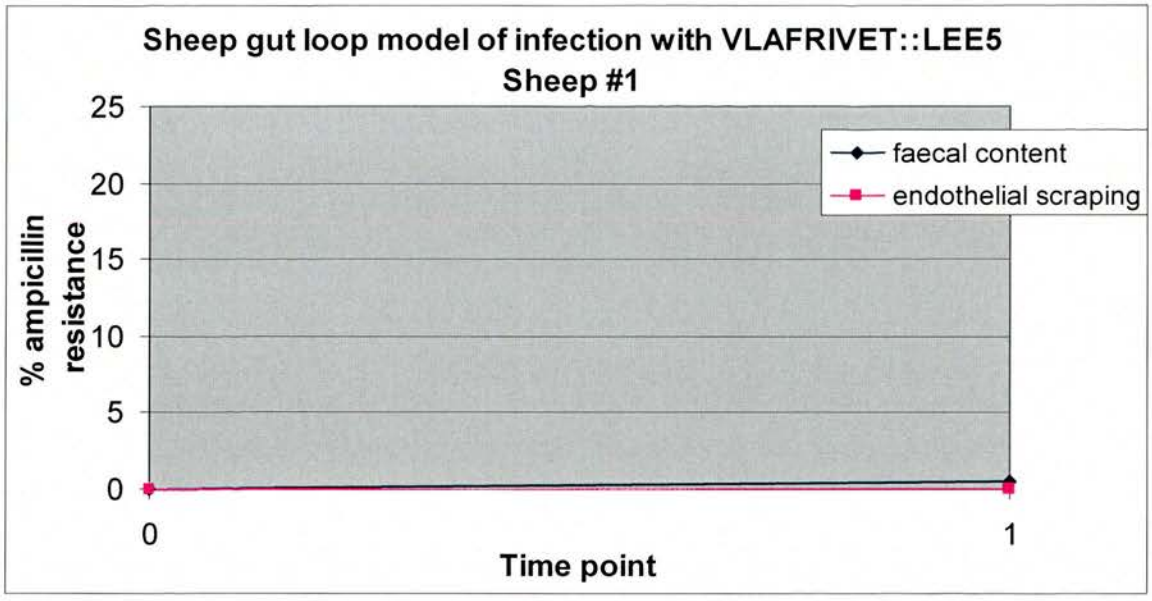

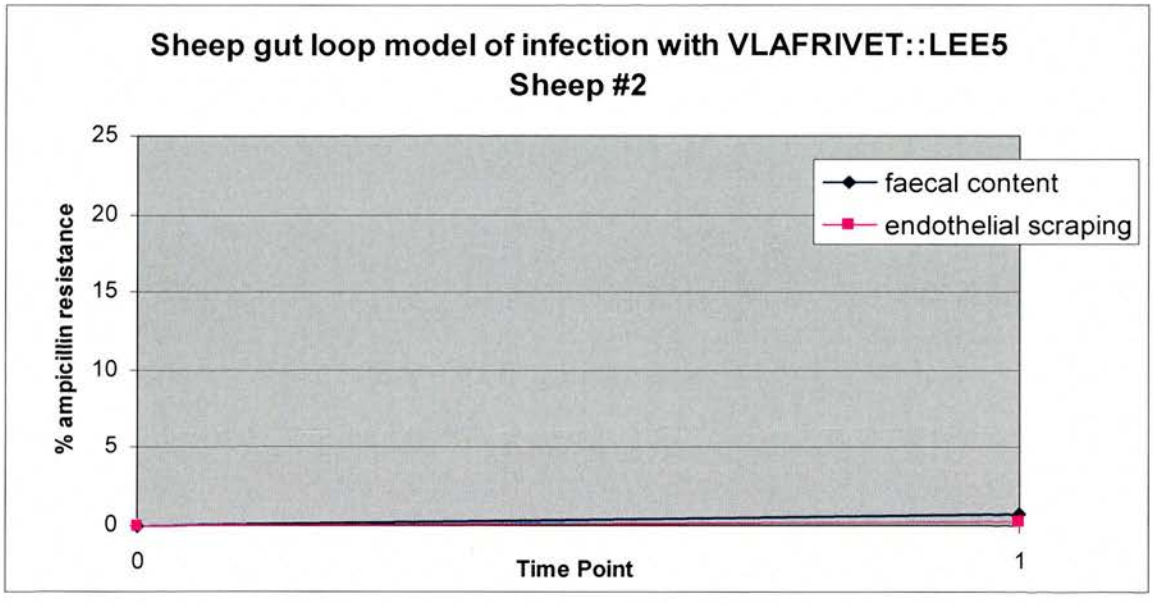

An overnight culture of VLAFRIVET::LEE5 grown in LBNal was used to inoculate a single gut loop segment in sheep #1 and sheep #2. After 6h the segment was excised and cut open. Faecal content and the endothelial lining were processed separately and a FRIVET ampicillin assays was performed on each sample. The results show negligible FRIVET activation for the LEE5 promoter in this assay.

Fig 5.18b

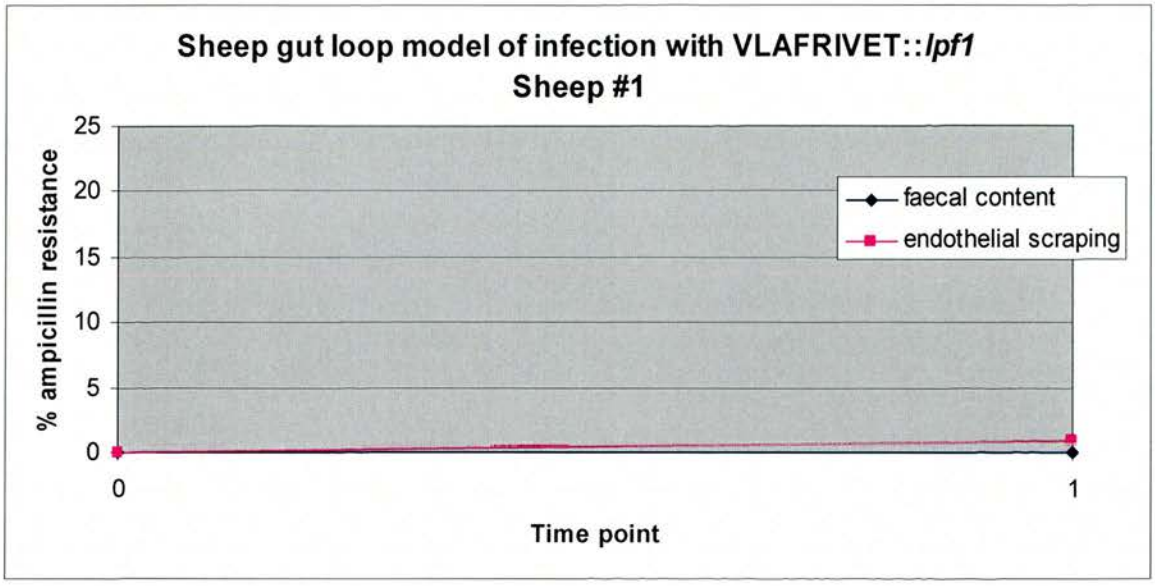

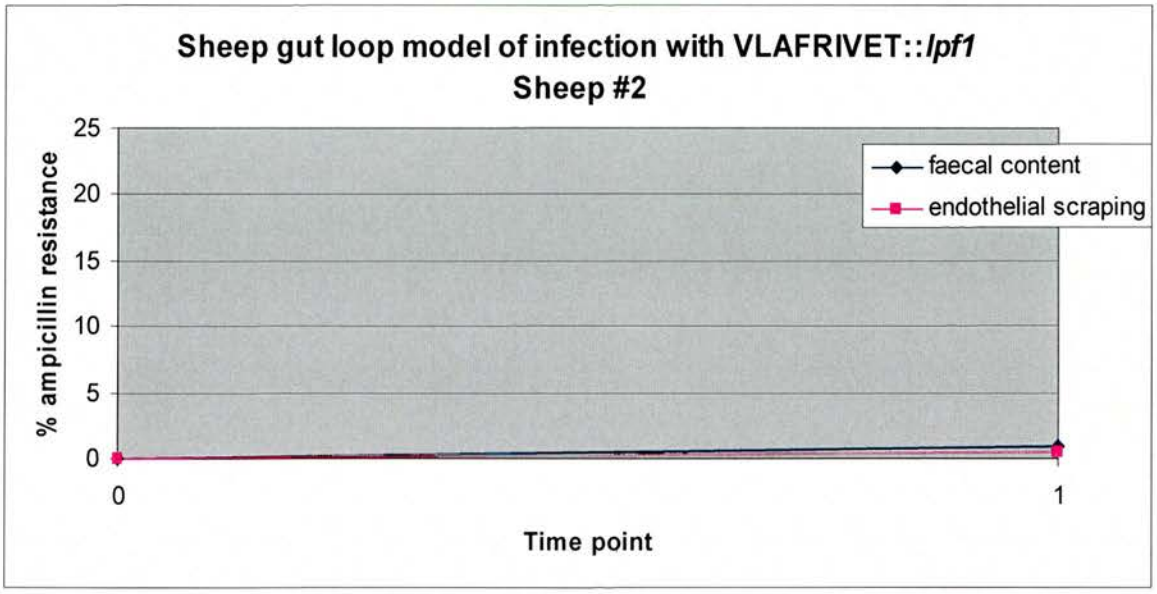

An overnight culture of VLAFRIVET::*lpf1* grown in LBNal was used to inoculate a single gut loop segment in sheep #1 and sheep #2. After 6h the segment was excised and cut open. Faecal content and the endothelial lining were processed separately and a FRIVET ampicillin assays was performed on each sample. The results as shown in Fig 5.18b shows very low FRIVET activation for the *lpf1* promoter in this assay.

Fig 5.18c

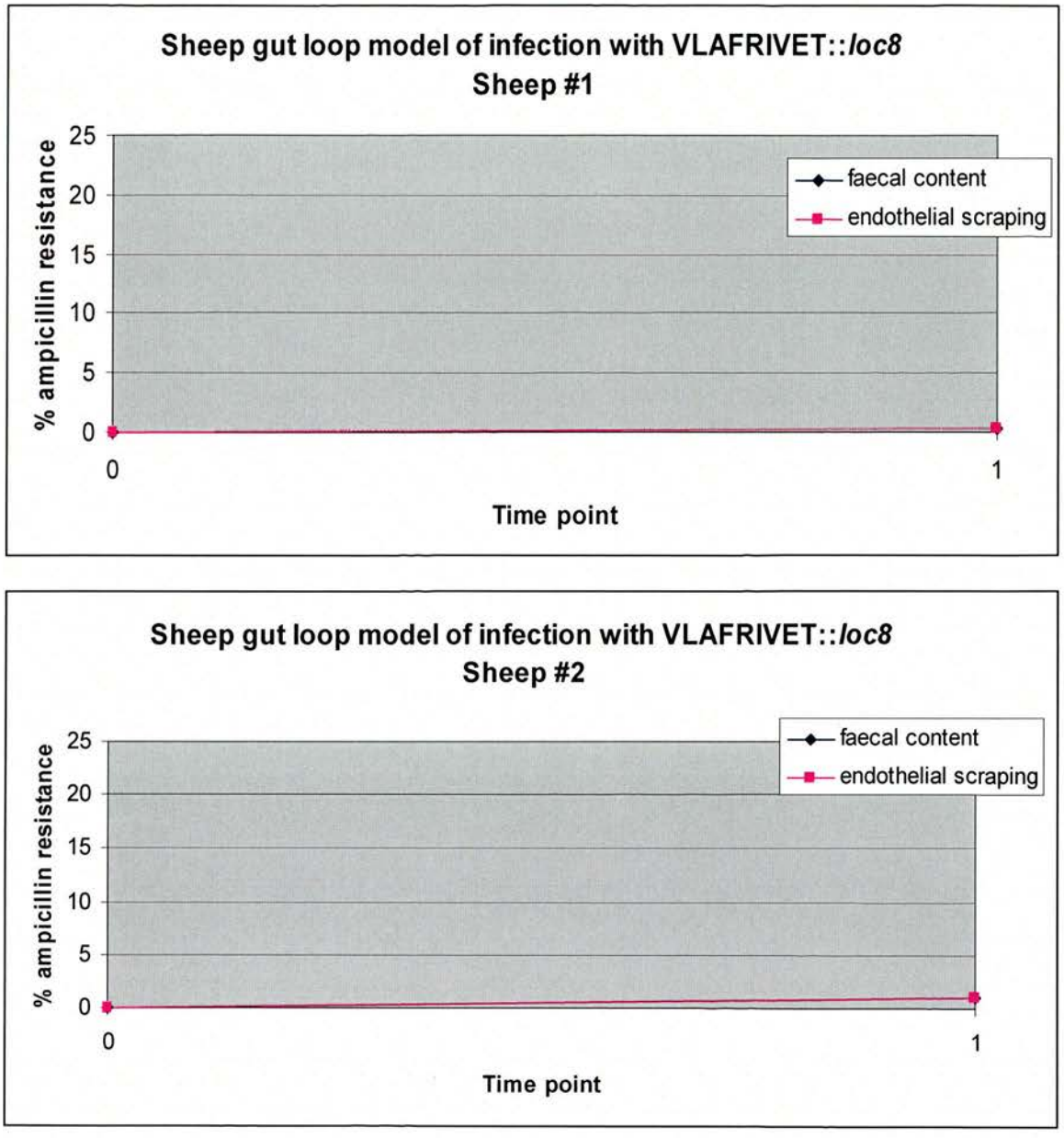

An overnight culture of VLAFRIVET::*loc8* grown in LBNal was used to inoculate a single gut loop segment in sheep #1 and sheep #2. After 6h the segment was excised and cut open. Faecal content and the endothelial lining were processed separately and a FRIVET ampicillin assays was performed on each sample. The results for the two assays show minimal FRIVET activation for the *loc8* promoter in this assay.

5.19 – Chapter 5 discussion

Having chosen the arabinose inducible promoter as the FRIVET test promoter, the first step was to establish a working range of arabinose concentrations to be used in the FRIVET assays. For this an *ara::gfp+* fusion was constructed on a pACYC background, subsequently termed pRQ30. The strain AAEC189 was transformed with pRQ30 and used to inoculate a series of M9-C flasks. Using a Fluorimeter, the fluorescence value of each culture was measured and plotted against optical density. The results demonstrate a good range of values using the arabinose concentrations (final) as follows:

- High (H) – 0.02% w/v
- Medium (M) – 0.002% w/v
- Low (L) – 0.0002% w/v

The negative control also demonstrated the tight regulation of the *ara* promoter in the absence of arabinose inducer. These values were subsequently taken forward for use in the FRIVET assays.

The functional testing of the FRIVET operon was extremely important in order to validate the operon as a working unit and to define the working limits in an *in vitro* assay. Testing *in vitro* at this stage will allow us to predict possible issues with the system and controlling it.

Initially the *ara* FRIVET vectors pRQ15 and pRQ18 were constructed from pRQ13 and pRQ17 respectively. The *ara* promoter region from the arabinose inducible vector pBAD18 was amplified and cloned upstream of *fimB* at the novel *Xba*I site. Putative clones were analysed by restriction digest and diagnostic PCR to confirm the creation of the *ara::fimB* transcriptional fusion.

With the *ara* FRIVET vectors now constructed the next step was the allelic exchange into three Δ*fim* backgrounds:

- ZAP542 – Δ*fim*; *lac*UV5::*papB* at *lac*
- ZAP545 – Δ*fim*; Ptac::*papB* at *lac*
- ZAP547 – Δ*fim*

The *ara* FRIVET vector pRQ15 was exchanged into each background and phenotypic testing confirmed the creation of new FRIVET strains for each background. Additionally diagnostic PCR was carried out on ZAP546 strains to confirm the results of the phenotypic analysis. As the orientation of the *fim* switch in pRQ15 is 'on' (*fimS* from pMM36) arabinose was used to induce *fim* switching and 'off' strains were reovered and stored for subsequent *in vitro* testing. The resulting FRIVET test strains were:

- ZAP543 – *ara::*FRIVET at *fim*; *lac*UV5::*papB* at *lac*
- ZAP546 – *ara::*FRIVET at *fim*; Ptac::*papB* at *lac*
- ZAP548 – *ara::*FRIVET at *fim*

Each Δ*fim* strain was also transformed with pRQ18 and subjected to allelic exchange. No strains were recovered in the first attempt and due to the success with the exchange of pRQ15 into the Δ*fim* backgrounds it was decided to halt allelic exchange of pRQ18 into the Δ*fim* backgrounds.

Initial arabinose testing used three concentrations of arabinose termed low (L), medium (M) and high (H) as previously defined using the *ara::gfp+* fusion. These arbitrary concentrations equated to a final arabinose concentration of 0.0002% w/v (L), 0.002% w/v (M) and 0.02% w/v (H). The one exception was Figure 5.10. In this assay ZAP543 was induced with levels of arabinose equating to final concentrations of 0.0004% w/v (L), 0.004% w/v (M) and 0.04% w/v (H).

ZAP548 was induced with arabinose in M9 medium alone, ZAP546 was induced in M9 medium and LB medium and ZAP543 was induced in LB medium alone. For the

majority of assays the change in the media showed a negligible change in results, both media produced consistent reproducible results with all three strains. However there were some inconsistencies with using LB medium. In some assays, very low levels of ampicillin resistance were seen, even with high levels of inducer. As LB medium can differ from supplier to supplier and each component may differ in composition, each batch of LB medium used in an assay may be subtlety different and could affect arabinose induction levels, especially if other carbon sources are present in the medium. For this reason LB was not used for subsequent FRIVET testing, even though it provides a distinct time advantage over M9 medium for bacterial growth.

As expected ZAP548 produced ampicillin resistance levels in proportion to the level of inducer added. Each assay was carried out in triplicate, and the results indicate reproducible consistent results for each arabinose concentration. Also importantly in the absence of inducer the FRIVET operon remained 'silent', that is, no induction was observed. This suggests that without promoter led *fimB* activation, *fimS* does not invert, and is not under the control of other unknown regulators or recombinases that may affect *fimS* switching.

It is clear from these results however that whilst the FRIVET system always responded to arabinose as an inducer, it was difficult to obtain completely reproducible results. Two reasons for this are: FRIVET tests were performed in 2 types of media: LB and M9. The results from the LB assays demonstrated a degree of variation in ampicillin resistance levels over a number of individual assays. The relative benefits of using LB for the FRIVET assays seem to be outweighed by the variation we see in arabinose induction using different batches of LB and as mentioned previously FRIVET assays were performed in M9 media as well. However there was still a degree of variability in the percentage of the population that were ampicillin resistant as demonstrated in Figs 5.9a and 5.9b. In these assays ZAP548 was induced with two concentrations of arabinose: 0.02% and 0.002% respectively. Three flasks were used in each assay and we noted variation in the percentage of ampicillin resistance over the course of the assay for each flask. In fig 5.9a, there was a 30% range difference in ampicllin resistance at TP2

(OD600=~0.2), a difference that dropped to 10% by TP4 (OD600=~0.7). As the media used was defined M9 there must be other reasons for the variability we see in the *in vitro* FRIVET assays other than the presence of alternative carbon sources in the medium.

Another reason for the variability seen could be the FRIVET sampling method. The method used to measure the percentage ampicillin resistance could have generated a degree of variability with the counting of ampicillin resistant colonies on the LBA plates. The presence of 'satellite' ampicillin sensitive colonies growing in close proximity to ampicillin resistant β-lactamase producing colonies may have provided false positives. The overall ampicillin resistance percentage in the population will therefore be artificially high. Moreover the extent of this false positive will be different for each individual plate and flask, furthering the chance of wide variability in the results of a FRIVET assay using the same concentration of inducer. Great care was taken to count only fully mature colonies (satellite colonies can exhibit a "sick" phenotype on plates). Analysis of the *fimS* orientation in each individual colony would give us an accurate readout of the ampicillin resistance levels in the population.

ZAP543 and ZAP546 were also both induced with L, M, and H levels of arabinose in LB medium. Both strains produced very similar results for each arabinose level as seen in Figure 5.10 and Figure 5.11a. At this stage we can be confident therefore that the Ptac promoter is at least as 'tightly' regulated as the *lac*UV5 promoter. If the Ptac promoter was driving low level constitutive expression of *papB* we would expect to see a decrease in FRIVET induction for ZAP546 relative to ZAP543. There was a concern that the Ptac promoter might be 'leaky' as other studies in the laboratory had indicated such a finding (Dai Wang, personal communication).

To see the effects of low temperature on the FRIVET system, ZAP546 was induced at 30^0C using the three levels of inducer. Overall induction levels were much delayed, each flask not responding to inducer levels until an OD~0.5 as opposed to 0.1 for 37^0C (Figure 5.11b). This result indicates a lower level of induction from the *ara* promoter at lower temperatures.

The induction of ZAP546 in M9 medium produced a different set of results to ZAP548 in the same medium at the same arabinose inducer levels. Overall, the level of induction was higher in the ZAP546 flasks than in the ZAP548 flasks. The assays were repeated again to verify these results and the same difference was observed (data not shown). The main difference between ZAP546 and ZAP548 is the Ptac::*papB* construct at *lac* in ZAP546. We would not expect the difference between the two strains to be as a result of PapB being produced from a 'leaky' Ptac promoter in M9 medium. If PapB was being produced we would expect a slightly lower induction level in ZAP546 than in ZAP548 which is not the case. It is likely that the differences are strain dependent; however it was decided to continue with arabinose testing and IPTG inhibition assays.

ZAP543 was induced with 0.04% w/v arabinose and 1mM IPTG to ascertain the inhibitory effects of PapB when induced from the *lac*UV5 promoter. Looking at Figure 5.13 we see that PapB appears to have a strong inhibitory action on FimB mediated switching until mid exponential phase (OD~ 0.5). At this point induction inhibition appears to be lifted and the rate of induction becomes faster than the un-inhibited control flask. This result suggests that the levels of PapB were initially high enough to inhibit the actions of FimB. However as the assay continued FimB levels were high enough to overcome PapB inhibition and switching started. This result suggests that PapB can work to inhibit the FRIVET operon from switching if it can occupy the preferential binding site prior to FimB levels becoming high, and if PapB levels can remain at a high level.

When ZAP546 was tested in a similar IPTG inhibition assay to ZAP543, the result was similar, if not to the same level. Induction levels were lower at mid and late exponential phase for the IPTG flask against the positive control, and ampicillin resistance levels eventually reached the same point at an OD~1.5. This result is not as expected. The Ptac promoter driving *papB* expression in ZAP546 should provide a higher level of free PapB than the *lac*UV5 promoter in ZAP543. Accordingly, there should be more evidence of FRIVET inhibition for ZAP546. A possible explanation was the LB broth used having a subtlety different composition for each assay. The same assay was repeated for ZAP546

in M9 medium (Figure 5.14b). The result shows no inhibitory effect by PapB after early exponential phase.

Given the dynamics of the *ara* promoter in populations, it was hypothesised that the levels of FimB in each cell induced by arabinose was too high for the levels of PapB in that cell expressed from the Ptac promoter. It was decided to transform ZAP546 with pHMG88, a pACYC based plasmid carrying the *lac*UV5::*papB* fusion. This plasmid had been successful in UPEC type 1 fimbriae inhibition assays in the laboratory (N. Holden, personal communication) and was initially used to study *pap* operon regulation (Forsman *et al*, 1989).

The transformed ZAP546 strain was grown in the presence of arabinose at the three predefined concentrations and IPTG was added to a final concentration of 1mM. The results in Figures 5.15a, 5.15b and 5.15c clearly show the 'locking' of the FRIVET system in the 'off' orientation when measured against a positive control. This set of results seems to confirm our hypothesis based on a 'threshold' level for PapB in an *ara* based FRIVET system. By inducing pHMG88, the combined levels of PapB from the plasmid and the single copy Ptac::*papB* fusion at *lac* were enough to competitively inhibit FimB mediated switching. However, if PapB levels dropped below the threshold, FimB mediated switching can occur, as seen in Figures 5.13 and 5.14b.

Whilst this observation is important with regards to initial *ara* testing of the FRIVET system, we do not expect the same issues with EHEC promoters. The population based nature of the *ara* promoter in each cell results in an articially high concentration of PapB needed to inhibit FRIVET induction. Further testing using FRIVET test strains containing EHEC promoters will be carried out to ascertain the levels of promoter induction.

The FRIVET system was also tested for its response to FimE and glucose. The *fimE* gene from MG1655 was cloned into the IPTG inducible vector pACTAC downstream of the Ptac promoter. In a FRIVET assay using ZAP546, the results indicate that FimE acts

to inhibit *fimS* switching when compared to a positive control transformed with the pACTAC vector only (Figure 5.16). Similarly, the addition of glucose to the FRIVET assay to a final concentration of 0.2% w/v significantly inhibits FRIVET induction when compared to a positive control (Figure 5.17).

Figures 5.18a, 5.18b and 5.18c show the results of a sheep ligated gut loop experiment carried out on two sheep with three FRIVET strains using the LEE5, *lpf1* and *loc8* promoters. As we see there is little to no FRIVET activation seen in these assays. The PBS serial dilutions for each assay were carried to the 10^{-5} plate and the 10^{-3}, 10^{-4} and 10^{-5} dilutions were plated onto LBNalAmp and LBNal plates. The results shown are for the 10^{-4} dilution plate. However the 10^{-3} and 10^{-5} plates were also counted and the results were similar to those shown in Figures 5.18a, b and c with little or no activation seen for the FRIVET system (data not shown).

There are a number of reasons as to the relative failure of these assays to validate the FRIVET system as a novel *in vivo* technology. The first is that the animal model and method chosen was not ideal for the purpose of elucidating the role of these *E. coli* O157:H7 promoters in its natural bovine host. Previous studies has shown the site of colonisation of *E. coli* O157:H7 to be the terminal recto anal junction (Naylor *et al*, 2005). The tissue types at this site differ markedly from those in the ascending spiral colon used for the ligated gut loops. A study using *E. coli* O157:H7 in the same animal model showed sparse and small A/E lesions as determined by microscopy. No change in this result was found with increasing bacterial cell density or pre-inoculation growth conditions (Wales *et al*, 2002).

Additionally the VLAFRIVET strains were tested *in vitro* at the same time using a variety of media in an attempt to prove the *E. coli* O157:H7 promoters driving the FRIVET operon in these strains was functionally operating and responding to environmental signals. None of the VLAFRIVET strains exhibited any FRIVET activation in these assays. Fluoremeter assays using a LEE5::*gfp*+ fusion on a pACYC backbone showed enhanced fluorescence when transferred from an LB overnight culture

to an MEM media (data not shown). However, VLAFRIVET::LEE5 failed to respond to the same media change to any significant degree.

Without fully understanding the nature of the FRIVET operon when driven by a wild type *E. coli* O157:H7 promoter the FRIVET system will be unable to answer many of the questions about the biology of *E. coli* O157:H7 in an *in vivo* environment. Combining the issues seen with FRIVET strains based on *E. coli* O157:H7 promoters and the FRIVET operon and a lack of reproducibility in the results seen in the *ara in vitro* assays we can conclude that much more work is needed to establish a solid FRIVET operon that functions *in vitro* and a choice of *E. coli* O157:H7 promoters that allow us to fully test a FRIVET strain prior to expensive and technically challenging *in vivo* experiments.

Chapter 6

Conclusion

The aims of this thesis were fourfold:

1) To construct a working FRIVET operon containing the invertible *fim* element that is able to direct transcription of the downstream *bla* gene and respond to FimB.
2) To test the limits of the FRIVET operon using a suitable test promoter and appropriate control points and to define a reproducible experimentally robust screening method
3) To construct *E coli* O157:H7 promoter based FRIVET constructs for use in *in vitro* and *in vivo* assays to enable us to understand *E coli* O157:H7 promoter activity in an animal model
4) To use constructed FRIVET strains in an *in vivo* experiment. The animal model and strain to be used will be decided closer to the time. Current animal models such as the sheep gut loop (ligated chambers in the ascending spiral colon) may be deployed.

Although there were numerous technical difficulties in creating the synthetic FRIVET operon, the first two aims were completed successfully. The FRIVET operon was tested using the arabinose inducible promoter: *ara*. With hindsight, the population induction patterns of the *ara* promoter was not ideal for measuring promoter activation levels at a cellular level and for defining the appropriate levels of any control gene needed (in this case *papB*). However, the *ara* promoter was chosen in lieu of an IPTG inducible promoter.

Ideally I would have used Ptac or *lac*UV5 as a FRIVET test promoter. However, knowing that a *papB* based control fusion would be needed at *lac*, and that control fusion would need to be quiescent in the *in vivo* assays, it was decided to use an IPTG inducible promoter for this role, disallowing it as a FRIVET test promoter.

PapB failed to 'lock' to inversion of *fimS* as a single copy fusion construct with the pTac promoter but increasing the levels of PapB by adding pHMG88, a pACYC based vector containing a *lac*UV5::*papB* fusion, exhibited the locking of the *fim* switch, validating our hypothesis that PapB acts as a competitive inhibitor of FimB mediated switching at a certain threshold level. Evidently the level produced by the single copy pTac::*papB* fusion at *lac* in the FRIVET strain was sub-threshold. Introducing more PapB into the system pushed the PapB levels over this threshold, resulting in the 'locking' of the *fim* element. EHEC promoters that provided a lower threshold for PapB inhibition may have been controllable from a single copy *papB* construct however I was unable to test this hypothesis as no functional *in vivo* FRIVET strains were constructed.

The ability to control the FRIVET system, specifically the orientation of the *fim* switch, after collection from the *in vivo* system is vital for reproducible results and an accurate record of promoter activation in the animal model. To this end for the FRIVET system to work, PapB must be able to function against a particular *E coli* O157:H7 promoter. The inability to produce a single copy *papB* control system for the FRIVET system was a major problem and further work will need to be carried out in order to provide a means of controlling FRIVET induction.

The failure to create functional and stable single copy fusions using *E coli* O157:H7 promoters was largely due to technical difficulties and time constraints. In the future alternative allelic exchange methods could be attempted to create single copy *E coli* O157:H7 FRIVET strains.

Once this technical hurdle has been overcome however, the FRIVET system is well placed to produce original and exciting data concerning *E. coli* O157:H7 virulence gene activity in an *in vivo* environment. The first step towards the success of the FRIVET system is to understand the working parameters of the *E. coli* O157:H7 FRIVET strains, such as those used in the VLA sheep assays. Results from these assays make it clear that more initial work is needed on the strains to fully understand their range of dynamics *in vitro*, before *in vivo* work can commence. The initial experiments using this strain would

focus on testing the functional limits of this promoter in response to known environmental conditions *in vitro* such as MEM medium and aerobic/anaerobic conditions. Once a degree of control is achieved with this strain then the functionality of PapB can be assessed. It is my expectation that PapB should function to inhibit FimB mediated switching in the LEE5::FRIVETstrain, and that *papB* can be placed under control of an IPTG or arabinose inducible promoter for this to occur.

Research in our laboratory confirms that LEE5 is upregulated on cell contact with Hela cells, and as such the LEE5::FRIVET strain would be tested using a similar experimental design and setup. Temporal control of multiple promoters can be tested at this juncture using multiplt FRIVET strains.

Data recorded at this stage will allow us to ascertain the suitability of the LEE5 and other FRIVET strains for animal experiments. Whilst the *in vitro* experiments cannot accurately reproduce the environmental signals present in the animal, we can hope to gain an understanding of the promoter fired FimB levels during FRIVET assays. There is a risk that the FRIVET system is too sensitive and operates on a 'hair trigger', that is, small levels of promoter activation will be enough to mediate switching in the majority of cells.

The ability to 'tune' RIVET systems has been demonstrated before (Lee *et al*, 1999). We would be able to utilise a unique *cla*I restriction site within *fimB* to introduce changes to the *fimB* shine-dalgarno site. By modifying the *fimB* Shine-dalgarno site, we can bring FimB levels down and add further control to the FRIVET system.

The FRIVET system was also tested in an animal model using the ligated gut loop method on adult sheep. The results of the assay using key *E. coli* O157:H7 promoters indicated little or no FRIVET activation. The same strains also failed to exhibit any FRIVET induction in a series of *in vitro* assays using permissible media and growth conditions. The animal model used was also likely to be not ideal for *E. coli* O157:H7 virulence gene activation. Previous studies had shown the ligated sheep gut loops as a poor model for *E. coli* O157:H7 A/E lesion formation (Wales *et al*, 2002).

Once a more suitable animal model is found and we have a greater understanding of the *E. coli* O157:H7 FRIVET strains and the variability seen in the *ara in vitro* assays, a range of *in vivo* assays can be performed using the FRIVET constructs. In its most basic guise, a FRIVET experiment would start with the oral inoculation of the animal model and the collection of faecal samples for FRIVET analysis after suitable time has elapsed. This assay will allow us to ascertain whether the promoter being tested was activated at any timepoint during the colonisation process, a 'history' or 'memory' of gene activity will be retained by the cell for future analysis. Promoters that are known to have an active role in colonisation of the bovine GI TR such as LEE5 and LEE4 would be expected to show ampicillin resistant populations for their respective FRIVET strains. Other promoters such as *fliC* and *lpf*, have a less than clear role in bovine colonisation, and as such FRIVET analysis would prove extremely useful in unravelling the initial factors responsible for *E. coli* O157:H7 persistance in the bovine host.

However it must be noted that the FRIVET system can only provide a yes/no for promoter activation in the animal model. Specific controls would have to be employed to discount the global gene activation or false positives during the infection and sampling process. The use of a *fimS* orientation PCR on individual colonies from sampling plates would give a clear result of the percentage of the population that have exhibited FRIVET activation. However, this PCR screening method increases the complexity and the time of the assay. One of the advantages of FRIVET was a simple, quick and reproducible screening method.

Additionally the FRIVET system would likely have to be 'tuned' for each *E. coli* O157:H7 promoter to achieve the correct 'trigger pressure' for the promoter *in vivo*. Without extensive *in vitro* workup, the FRIVET system could either be too 'soft' for the promoter, leading to false positives as very low levels of environmental signals could activate the FRIVET system even if they were biologically irrelevant to the promoters role in *E. coli* O157:H7 infection. Conversely the FRIVET system could be too 'hard', leading to low or zero levels of FRIVET activation and false negatives. These specific

issues cannot be controlled for at the time of the assay. They need to be unravelled during the *in vitro* workup for each *E. coli* O157:H7 FRIVET promoter.

The natural evolution of the basic FRIVET assay would involve analysis of bacteria recovered from different sites along the GI tract via post-mortem processing. This will allow us to analyse the timing of individual *E. coli* O157:H7 gene expression. By subjecting multiple *E. coli* O157:H7 FRIVET strains to this assay we can build a solid picture of how *E. coli* O157:H7 regulates its virulence genes in a colonisation model. For example: are LEE4 and LEE5 co-ordinately regulated *in vivo* as *in vitro* and is the T3SS basal apparatus present prior to LEE4/LEE5 activation; does *E. coli* O157:H7 use Lpf as an initial adhesin and is FliC involved in the attachment process? By analysing FRIVET activation levels at various points in the GI tract we can link the yes/no answers the FRIVET system gives us to build a better view of *E. coli* O157:H7 pathogenesis in the host.

Whilst the FRIVET system is a novel and potentially powerful tool for elucidating bacterial *in vivo* gene dynamics, it is not the 'all in one' *in vivo* tool for answering all the key *in vivo* questions for *E. coli* O157:H7 infection or colonisation process. The power in the FRIVET system will lie in its use in conjunction with other *in vivo* and *in vitro* methods such as micro-arrays and fluorescence microscopy. These methods could potentially be employed directly from bacterial samples during post mortem or from faeces. Micro-array data allows us to see the upregulation of any number of genes during an infection process or at a particular juncture in the GI tract. Additionally the use of fluorescence microscopy to analyse *E. coli* O157:H7 promoters linked to fluorescence proteins such as *gfp* and *rfp* can be used to measure gene activation in a population, or to identify A/E lesion formation on tissue samples taken during post-mortem.

It was postulated during the research phase of this thesis to integrate our knowledge of fluorescence reporter systems and the FRIVET system to build a modified FRIVET operon that could be analysed by fluorescence microscopy. This operon, named the 'traffic light' FRIVET system, uses two fluorescence proteins: *gfp* and *rfp* either side of

the fim switch in place of *bla*. As *fimS* contains a promoter that can direct upstream transcription when in the 'off' orientation (no FimB production) and downstream transcription when in the 'on' orientation (FimB produced) we can analyse the activation of the FRIVET system by noting the switch from cells fluorescing red to fluorescing green under microscopy. The traffic light FRIVET system is outlined in Figure 6.1.

Fig 6.1 – Proposed traffic light FRIVET model

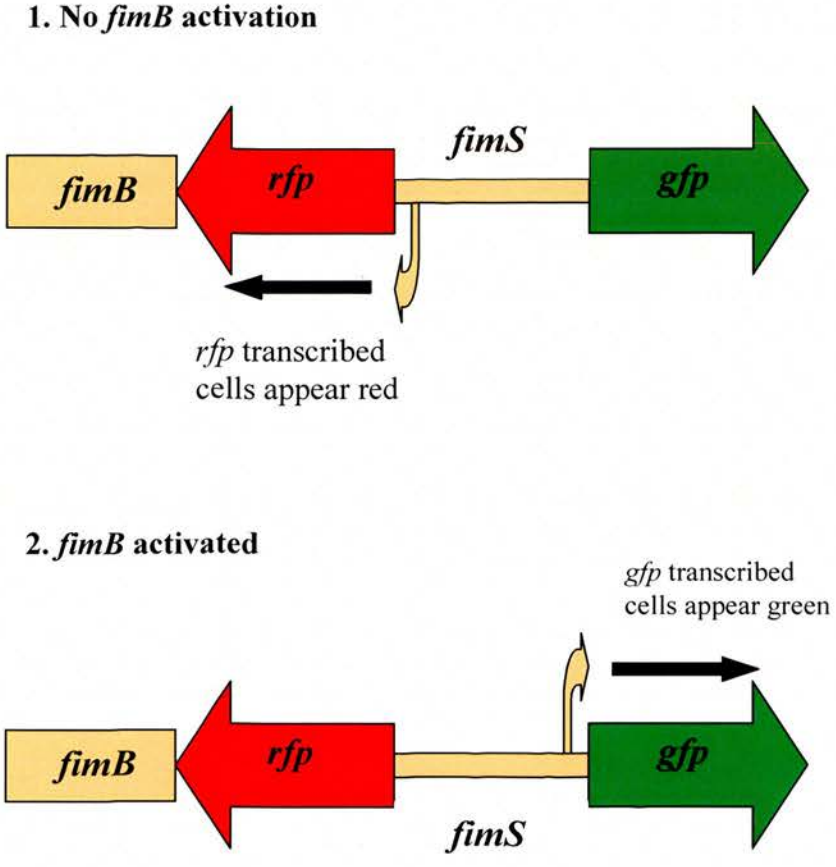

The FRIVET traffic light model is based on the promoter in *fimS* driving transcription in either direction depending on its orientation. At that start of the experiment *fimS* is in the 'off' orientation, the *fimS* promoter will direct transcription of *rfp* and the cells will be red under fluorescence microscopy. During the assay *fimB* will be activated leading to the invesion of *fimS*. The promoter now directs the downstream transcription of *gfp* and the cells appear green under fluorescence microscopy. By taking timepoint samples during the assay we can measure the induction of *fimB* at a single cell level in a population.

The use of the FRIVET system in conjunction with other *in vivo* methods will allow a clearer picture of the virulence gene dynamics of *E. coli* O157:H7 in the host to be

formed. Modifications to the basic FRIVET model to incorporate other reporter genes such as fluorescence proteins as seen in traffic light FRIVET allow us to gain further understanding of the promoter being investigated.

FRIVET on its own will help to answer some basic *in vivo* questions, but to gain the greatest understanding of *E. coli* O157:H7 biology, it must be used in tandem with other *in vivo* systems.

Chapter 7

References

Adu-Bobie, J., Trabulsi, L.R., Carneiro-Sampaio, M.M., Dougan, G. and Frankel, G.
Identification of immunodominant regions within the C-terminal cell binding domain of intimin alpha and intimin beta from enteropathogenic *Escherichia coli*.
Infect Immun. (1998) (12):5643-9

Angelini, F., Menard, A., Asencio, C., Marais, A. and Megraud, F.
Construction of replicative and integrative plasmids for setting up the in vivo expression technology in *Helicobacter pylori*.
Plasmid (2004) 51(2):101-7

Ball, H.J., Finlay, D., Burns, L. and Mackie, D.P.
The detection of verocytotoxins in bacterial cultures from human diarrhoeal samples with monoclonal antibody-based ELISAs.
Res Vet Sci (1994) 57(2):225-32

Bartoleschi, C., Pardini, M.C., Scaringi, C., Martino, M.C., Pazzani, C. and Bernardini, M.L.
Selection of *Shigella flexneri* candidate virulence genes specifically induced in bacteria resident in host cell cytoplasm.
Cell Microbiol (2002) 4(9):613-26

Baumler, A.J. and Heffron, F.
Identification and sequence analysis of *lpfABCDE*, a putative fimbrial operon of *Salmonella typhimurium*.
J Bacteriol (1995) 177(8):2087-97

Baumler, A.J., Tsolis, R.M. and Heffron, F.
The lpf fimbrial operon mediates adhesion of *Salmonella typhimurium* to murine Peyer's patches.
PNAS (1996) 9;93(1):279-83

Best, A., La Ragione, R.M., Sayers, A.R. and Woodward, M.J.
Role for flagella but not intimin in the persistent infection of the gastrointestinal tissues of specific-pathogen-free chicks by shiga toxin-negative *Escherichia coli* O157:H7.
Infect. Immun. (2005) 73(3):1836-46

Blomfield, I.C., McClain, M.S., Princ, J.A., Calie, P.J. and Eisenstein, B.I.
Type 1 fimbriation and *fimE* mutants of *Escherichia coli* K-12
J. Bacteriol. (1991) 173: 5298-307

Blomfield, I.C., Calie, P.J., Eberhardt, K.J., McClain, M.S. and Eisenstein, B.I.
Lrp stimulates phase variation of type 1 fimbriation in *Escherichia coli* K-12
J. Bacteriol. (1993) 175: 27-36

Blomfield, I.C., Kulasekara, D.H. and Eisenstein, B.I.
Integration host factor stimulates both FimB- and FimE- mediated site specific DNA inversion that controls phase variation of type 1 fimbriae expression in *Escherichia coli*
Mol. Microbiol. (1997) 23: 705-17

Blomfield, I.C.
The regulation of pap and type 1 fimbriation in Escherichia coli
Adv. Microbial Physiol. (2001) 45: 1-27

Boudeau, J., Barnich, N. and Darfeuille-Michaud, A.
Type 1 pili-mediated adherence of *Escherichia coli* strain LF82 isolated from Crohn's disease is involved in bacterial invasion of intestinal epithelial cells.
Mol Microbiol. (2001) 39(5):1272-84.

Burns, L.S., Smith, S.G.J. and Dorman, C.J.
Interaction of the FimB integrase with the *fimS* invertible DNA element in *Escherichia coli in vivo* and *in vitro*
J. Bacteriol. (2000) 182: 2953-9

Bustamante, V.H., Santana, F.J., Calva, E. and Puente, J.L.
Transcriptional regulation of type III secretion genes in enteropathogenic *Escherichia coli*: Ler antagonizes H-NS-dependent repression.
Mol Microbiol. (2001) 39(3):664-78.

Camilli, A. and Mekalanos, J.J.
Use of recombinase gene fusions to identify *Vibrio cholerae* induced during infection
Mol. Microbiol. (1995) 18: 671-83

Campellone, K.G., Rankin, S., Pawson, T., Kirschner, M.W., Tipper, D.J. and Leong, J.M.
Clustering of Nck by a 12-residue Tir phosphopeptide is sufficient to trigger localized actin assembly.
J Cell Biol. (2004) 164(3):407-16.

Casadaban, M.J.
Regulation of the regulatory gene for the arabinose pathway, *araC*
J Mol Biol, (1976) Jul; 104 (3):557-66

Cornick, N.A., Booher, S.L. and Moon, H.W.
Intimin facilitates colonization by *Escherichia coli* O157:H7 in adult ruminants. Infect Immun. (2002) 70(5):2704-7.

Chiu, H-J. and Syu, W-J.
Functional analysis of EspB from enterohaemorrhagic *Escherichia coli*
Microbiology (2005) 151: 3277-86

Creasey, E.A., Delahay, R.M., Bishop, A.A., Shaw, R.K., Kenny, B., Knutton, S. and Frankel, G.
CesT is a bivalent enteropathogenic *Escherichia coli* chaperone required for translocation of both Tir and Map.
Mol Microbiol (2003) 47(1):209-221

Dahan, S., Wiles, S., La Ragione, R.M., Best, A., Woodward, M.J., Stevens, M.P., Shaw, R.K., Chong, Y., Knutton, S., Phillips, A. and Frankel, G.
EspJ is a prophage-carried type III effector protein of attaching and effacing pathogens that modulates infection dynamics.
Infect Immun (2005) 73(2):679-686

Daniell, S.J., Delahay, R.M., Shaw, R.K., Hartland, E.L., Pallen, M.J., Booy, F., Ebel, F., Knutton, S. and Frankel, G.
Coiled-coil domain of enteropathogenic *Escherichia coli* type III secreted protein EspD is involved in EspA filament-mediated cell attachment and hemolysis.
Infect Immun (2001) 69(6):4055-4064

Dean-Nystrom, E.A., Bosworth, B.T., Cray, W.C.Jr. and Moon, H.W.
Pathogenicity of *Escherichia coli* O157:H7 in the intestines of neonatal calves.
Infect Immun (1997) 65(5):1842-1848
Dean-Nystrom, E.A., Bosworth, B.T., Moon, H.W., and O'Brien, A.D.
Escherichia coli O157:H7 requires intimin for enteropathogenicity in calves.
Infect Immun (1998) 66(9):4560-4563

Dviza, F., van Diemen, P.M. Stevens, M.P., Smith, A.J. and Wallis, T.S.
Identification of *Escherichia coli* O157:H7 genes influencing colonisation of the bovine gastrointestinal tract using signature-tagged mutagenesis
Microbiology (2004) 150: 3631-45

Dubnau, E., Fontan, P., Manganelli, R., Soares-Appel, S. and Smith, I.
Mycobacterium tuberculosis genes induced during infection of human macrophages.
Infect Immun (2002) 70(6):2787-2795

El-Labany, S., Sohanpal, B.K., Lahooti, M., Akerman, R. and Blomfield, I.C.
Distant *cis*-active sequences and sialic acid control the expression of *fimB* in *Escherichia coli* K-12
Mol. Microbiol. (2003) 49: 1109-18

Elliott, S. J., Wainwright, L. A., McDaniel, T. K., Jarvis, K. G., Deng, Y. K., Lai, L. C., McNamara, B. P., Donnenberg, M. S. and Kaper, J. B.
The complete sequence of the locus of enterocyte effacement (LEE) from enteropathogenic *Escherichia coli* E2348/69.
Mol Microbiol (1998) 28:1-4

Elliott, S. J., Yu, J. and Kaper, J. B.
The cloned locus of enterocyte effacement from enterohemorrhagic *Escherichia coli* O157:H7 is unable to confer the attaching and effacing phenotype upon *E. coli* K-12.
Infect Immun (1999) 67:4260-4263.

Elliot, S.J., Sperandio, V., Giron, J.A., Shin, S., Mellies, J.L., Wainwright, L., Hutcheson, S.W., McDaniel, T.K. and Kaper, J.B.
The Locus of Enterocyte Effacement (LEE)-Encoded Regulator Controls Expression of Both LEE- and Non-LEE-Encoded Virulence Factors in Enteropathogenic and Enterohemorrhagic *Escherichia coli*
Infect Immun (2000) 68(11):6115-6126

Forsman, K., Goransson, M. and Uhlin, B.E.
Autoregulation and multiple DNA interactions by a transcriptional regulatory protein in *E. coli* pili biogenesis
EMBO J. (1989) 8: 1271-7

Frankel, G., Phillips, A.D., Rosenshine, I., Dougan, G., Kaper, J.B. and Knutton, S.
Enteropathogenic and enterohaemorrhagic *Escherichia coli*: more subversive elements
Mol. Microbiol. (1998) 30: 911-21

Friedberg, D., Umanski, T., Fang ,Y. and Rosenshine I.
Hierarchy in the expression of the locus of enterocyte effacement genes of enteropathogenic *Escherichia coli.*
Mol Microbiol. (1999) 34 : 941-52.

Gahan, C.G. and Hill, C.
The use of listeriolysin to identify in vivo induced genes in the gram-positive intracellular pathogen *Listeria monocytogenes*.
Mol Microbiol. (2000) (2):498-507.

Gally, D.L., Bogan, J.A., Eisenstein, B.I. and Blomfield, I.C.
Environmental regulation of the *fim* switch controlling type 1 fimbrial phase variation in *Escherichia coli* K-12: Effects of temperature and media
J. Bacteriol. (1993) 175: 6186-93

Gally, D.L., Leathart, J. and Blomfield, I.C.
Interaction of FimB and FimE with the *fim* switch that controls the phase variation of type 1 fimbriation in *Escherichia coli*
Mol. Microbiol. (1996) 21: 735-38

Gammage, S.D., Patton, A.K., Strasser, J.E., Chalk, C.L. and Weiss, A.A.
Commensal bacteria influence *Escherichia coli* O157:H7 persistence and shiga toxin production in the mouse intestine
Infect Immun. (2006) 74: 1977-83

Garmendia, J., Phillips, A.D., Carlier, M.F., Chong, Y., Schuller, S., Marches, O., Dahan, S., Oswald, E., Shaw, R.K., Knutton, S. and Frankel,. G.
TccP is an enterohaemorrhagic *Escherichia coli* O157:H7 type III effector protein that couples Tir to the actin-cytoskeleton.
Cell Microbiol. (2004) 6(12):1167-83.

Garmendia, J., Frankel, G. and Crepin, V.F.
Enteropathogenic and enterohaemorrhagic *Escherichia coli* infections: translocation, translocation, translocation
Infect Immun. (2005) 73: 2573-85

Godaly, G., Frendeus, B., Proudfoot, A., Svensson, M., Klemm, P. and Svanborg, C.
Role of fimbriae-mediated adherence for neutrophil migration across *Escherichia coli*-infected epithelial cell layers.
Mol Microbiol. (1998) 30(4):725-35.

Greenblatt, J. and Schleif, R.
Arabinose C protein: regulation of the arabinose operon *in vitro*
Nat New Biol. 1971 Oct 6; 233 (40) : 166-70

Gruenheid, S., Sekirov, I., Thomas, N.A., Deng, W., O'Donnell, P., Goode, D., Li, Y., Frey, E.A., Brown, N.F., Metalnikov, P., Pawson, T., Ashman, K. and Finlay, B.B.
Identification and characterization of NleA, a non-LEE-encoded type III translocated virulence factor of enterohaemorrhagic *Escherichia coli* O157:H7.
Mol Microbiol. (2004) 51:1233-49.

Gunther, N.W. 4th, Lockatell, V., Johnson, D.E. and Mobley, H.L.
In vivo dynamics of type 1 fimbria regulation in uropathogenic *Escherichia coli* during experimental urinary tract infection.
Infect Immun. (2001) 69(5):2838-46.

Guzman, L. M., Belin, D., Carson, M. J., and Bewick, J.
Tight regulation, modulation and high level expression vectors containing the arabinose pBAD promoter.
Journal of Bacteriology (1995) 177: 4121-4130.

Handfield, M., Lehoux, D.E., Sanschagrin, F., Mahan, M.J., Woods, D.E. and Levesque, R.C.
In vivo-induced genes in *Pseudomonas aeruginosa*.
Infect Immun. (2000) 68(4):2359-62.

Hayashi, T., Makino, K., Ohnishi, M., Kurokawa, K., Ishii, K., Yokoyama, K., Han, C.G., Ohtsubo, E., Nakayama, K., Murata, T., Tanaka, M., Tobe, T., Iida, T., Takami, H., Honda, T., Sasakawa, C., Ogasawara, N., Yasunaga, T., Kuhara, S., Shiba, T., Hattori, M. and Shinagawa, H.
Complete genome sequence of enterohemorrhagic *Escherichia coli* O157:H7 and genomic comparison with a laboratory strain K-12.
DNA Res. (2001) 28;8(1):11-22. Erratum in: DNA Res (2001) 27;8(2):96.

Hensel, M., Shea, J.E., Gleeson, C., Jones, M.D., Dalton, E. and Holden, D.W.
Simultaneous identification of bacterial virulence genes by negative selection
Science (1995) 269(5222):400-3

Holden, N.J., Uhlin, B.E. and Gally, D.L.
PapB paralogues and their effect on the phase variation of type 1 fimbriae in *Escherichia coli*.
Mol Microbiol. (2001) 42(2):319-30.

Holden, N.J. and Gally, D.L.
Switches, cross-talk and memory in *Escherichia coli* adherence
J. Med. Microbiol. (2004) 53: 585-93

Holden, N.J., Totsika, M., Mahler, E., Roe, A.J., Catherwood, K., Lindner, K., Dobrindt, U. and Gally, D.L.
Demonstration of regulatory cross-talk between P fimbriae and type 1 fimbriae in uropathogenic *Escherichia coli*
Microbiology (2006) 152: 1143-53

Hoey, D.E., Currie, C., Else, R.W., Nutikka, A., Lingwood, C.A., Gally, D.L. and Smith, D.G.
Expression of receptors for verotoxin 1 from *Escherichia coli* O157 on bovine intestinal epithelium.
J Med Microbiol. (2002) 51(2):143-9.

Iyoda, S., Koizumi, N., Satou, H., Lu, Y., Saitoh, T., Ohnishi, M. and Watanabe, H.
The GrlR-GrlA Regualtory System Coordinately Controls the Expression of Flaggelar and LEE-Encoded Type III Protein Secretion Systems in Enterohemorrhagic *Escherichia coli*
J. Bacteriol 2006 188 16 p 5682-5692

Iwanaga, M., Yamamoto, K., Higa, N., Ichinose, Y., Nakasone, N. and Tanabe, M.
Culture conditions for stimulating cholera toxin production by *Vibrio cholerae* 01 El Tor
Microbiology and Immunology (1986) 30: 1075-83

Kanack, K.J., Crawford, J.A., Tatsuno, I., Karmali, M.A. and Kaper, J.B.
SepZ/EspZ is secreted and translocated into HeLa cells by the enteropathogenic
Escherichia coli type III secretion system.
Infect Immun. (2005) 73(7):4327-37.

Kaper, J.B.
Enterohaemorrhagic *Escherichia coli*
Curr. Op. in Microbiol. (1998) 1:103-8

Kenny, B., DeVinney, R., Stein, M., Reinscheid, D.J., Frey, E.A. and Finlay, B.B.
Enteropathogenic *E. coli* (EPEC) transfers its receptor for intimate adherence into
mammalian cells.
Cell. (1997) 91(4):511-20.

Kenny, B. and Jepson, M.
Targeting of an enteropathogenic *Escherichia coli* (EPEC) effector protein to host
mitochondria.
Cell Microbiol. (2000) (6):579-90.

Khan, A., Datta, S., Das, S.C., Ranamurthy, T., Khanam, J., Takeda, Y., Bhattacharya, S.K. and Nair, G.B.
Shiga toxin producing *Escherichia coli* infection: current progress and future challenges
Indian J. Med. Res. (2003) 118: 1-24

Khlebnikov, A., Skaug, T. and Keasling, J.D.
Modulation of gene expression from the arabinose-inducible araBAD promoter.
J. Ind Microbiol Biotechnol. (2002) (1):34-7.

Klemm, P.
Two regulatory *fim* genes, *fimB* and *fimE* control the phase variation of type 1 fimbriae in *Escherichia coli*
EMBO J. (1986) 5, 1389-93

Knutton, S., Rosenshine, I., Pallen, M.J., Nisan, I., Neves, B.C., Bain, C., Wolff, C., Dougan, G. and Frankel, G.
A novel EspA-associated surface organelle of enteropathogenic *Escherichia coli* involved in protein translocation into epithelial cells.
EMBO J. (1998) (8):2166-76.

Kresse, A.U., Rohde, M. and Guzman, C.A.
The EspD protein of enterohemorrhagic *Escherichia coli* is required for the formation of bacterial surface appendages and is incorporated in the cytoplasmic membranes of target cells.
Infect Immun. (1999) (9):4834-42.

Kulasekara, D.H. and Blomfield, I.C.
The molecular basis for the specificity of *fimE* in the phase variation of type 1 fimbriae of *Escherichia coli* K-12
Mol. Microbiol. (1999) 31: 1171-81

Laaberki, M-H., Janabi, N., Oswald, E. and Repoila, F.
Concert of regulators to switch on LEE expression in enterohaemorrhagic *Escherichia coli* O157:H7: Interplay between Ler, GrlA, HNS and RpoS
Int. J. Med. Microbiol. (2006)

Lai, Y.C., Peng, H.L. and Chang, H.Y.
Identification of genes induced in vivo during *Klebsiella pneumoniae* CG43 infection.
Infect Immun. (2001) (11):7140-5

Leathart, J.B.S. and Gally, D.L.
Regulation of type 1 fimbrial expression in uropathogenic *Escherichia coli*: heterogeneity of expression through sequence changes in the *fim* switch region
Mol. Microbiol. (1998) 28: 371-81

Lee, S.H., Butler, S.M. and Camilli, A.
Selection for *in vivo* regulators of bacterial virulence
PNAS (2001) 98: 6889-94

Lee, S.H., Hava, D.L., Waldor, M.K. and Camilli, A.
Regulation and temporal expression patterns of Vibrio cholerae virulence genes during infection
Cell, (1999) 99: 625-34

Lingwood, C.A.
Role of verotoxin receptors in pathogenesis.
Trends Microbiol. (1996) (4):147-53

Livny, J. and Friedman, D.I.
Characterising spontaneous induction of Stx encoding phages using a selectable reporter system
Mol. Microbiol. (2004) 51: 1691-704

Low, A.S., Holden, N., Rosser, T., Roe, A.J., Constantinidou, C., Hobman, J.L., Smith, D.G.E., Low, J.C. and Gally, D.L.
Analysis of fimbrial gene clusters and their expression in enterohaemorrhagic *Escherichia coli* O157:H7
Env. Microbiology (2006)

Low, A.S., Dziva, F., Torres, A.G., Martinez, J.L., Rosser, T., Naylor, S., Spears, K., Holden, N., Mahajan, A., Findlay, J., Sales, J., Smith, D.G.E., Low, J.C., Stevens, M.P. and Gally, D.L.
Cloning, expression and characterisation of fimbrial operon F9 from enterohaemorrhagic *Escherichia coli* O157:H7
Infection and Immunity (2006) 74: 2233-44

Lowe, A.M., Beattie, D.T. and Deresiewicz, R.L.
Identification of novel staphylococcal virulence genes by in vivo expression technology.
Mol Microbiol. (1998) (5):967-76.

Mahan, M.J., Slauch, J.M. and Mekalanos, J.J.
Selection of bacterial virulence genes that are specifically induced in host tissues.
Science. (1993) (5095):686-8.

Marches, O., Nougayrede, J.P., Boullier, S., Mainil, J., Charlier, G., Raymond, I., Pohl, P., Boury, M., De Rycke, J., Milon, A. and Oswald, E.
Role of tir and intimin in the virulence of rabbit enteropathogenic *Escherichia coli* serotype O103:H2.
Infect Immun. (2000) (4):2171-82.

Marches, O., Ledger, T.N., Boury, M., Ohara, M., Tu, X., Goffaux, F., Mainil, J., Rosenshine, I., Sugai, M., De Rycke, J. and Oswald, E.
Enteropathogenic and enterohaemorrhagic *Escherichia coli* deliver a novel effector called Cif, which blocks cell cycle G2/M transition.
Mol Microbiol. (2003) (5):1553-67.

Marches, O., Wiles, S., Dziva, F., La Ragione, R.M., Schuller, S., Best, A., Phillips, A.D., Hartland, E.L., Woodward, M.J., Stevens, M.P. and Frankel, G.
Characterisation of two non-locus of enterocyte effacement-encoded type-III translocated effectors, NleC and NleD, in attaching and effacing pathogens
Infection and Immunity (2005) 73: 8411-7

Martinez, J.J., Mulvey, M.A., Schilling, R.D., Pinker, J.S. and Hultgren, S.J.
Type 1 pilus-mediated invasion of bladder epithelial cells
EMBO J (2000) 19:2803-2812

McClain, M.S., Blomfield, I.C. and Eisenstein, B.I.
Roles of *fimB* and *fimE* in site specific DNA inversion associated with phase variation of type 1 fimbriae in *Escherichia coli*
J. Bacteriol. (1991) 173: 5304-14

McDaniel, T.K., Jarvis, K.G., Donnenberg, M.S. and Kaper, J.B.
A genetic locus of enterocyte effacement conserved among diverse enterobacterial pathogens.
Proc Natl Acad Sci U S A. (1995) 28;92(5):1664-8

Mead, P.S., Slutsker, L., Dietz, V., McCaig, L.F., Bresee, J.S., Shapiro, C., Griffin, P.M. and Tauxe, R.V.,
Food-related illness and death in the United States
Emerging Infectious Disease 1999 5, 607-625

Mellies, J.L., Elliott, S.J., Sperandio, V., Donnenberg, M.S. and Kaper, J.B.
The Per regulon of enteropathogenic *Escherichia coli*: identification of a regulatory cascade and a novel transcriptional activator, the locus of enterocyte effacement (LEE)-encoded regulator (Ler).
Mol Microbiol. (1999) (2):296-306.

Merrell, D.S. and Camilli, A.
Detection and analysis of gene expression during infection by in vivo expression technology
Phil. Trans. R. Soc. Lond. B (2000) 355: 587-99

Michino, H., Araki, K., Minami, S., Takaya, S., Sakai, N., Miyazaki, M., Ono, A. and Yanagawa, H.
Massive outbreak of *Escherichia coli* O157:H7 infection in schoolchildren in Sakai City, Japan, associated with consumption of white radish sprouts.
Am J Epidemiol. (1999) (8):787-96.

Mundy, R., Jenkins, C., Yu, J., Smith, H. and Frankel, G.
Distribution of espI among clinical enterohaemorrhagic and enteropathogenic *Escherichia coli* isolates.
J Med Microbiol. (2004) (Pt 11):1145-9.

Nataro, J.P. and Kaper, J.B.
Diarrheagenic *Escherichia coli.*
Clin Microbiol Rev. (1998) (1):142-201. Review. Erratum in: Clin Microbiol Rev (1998) (2):403.

Naylor, S.W., Low, J.C., Besser, T.E., Mahajan, A., Gunn, G.J., Pearce, M.C., McKendrick, I.J., Smith, D.G. and Gally, D.L.
Lymphoid follicle-dense mucosa at the terminal rectum is the principal site of colonization of enterohemorrhagic *Escherichia coli* O157:H7 in the bovine host.
Infect Immun. (2003) (3):1505-12.

Naylor, S.W., Gally, D.L. and Low, J.C.
Enterohaemorrhagic *E. coli* in veterinary medicine.
Int J Med Microbiol. (2005) (6-7):419-41. Review.

Naylor, S.W., Roe, A.J., Nart, P., Spears, K., Smith, D.G.E., Low, J.C. and Gally, D.L.
Escherichia coli O157:H7 forms attaching and effacing lesions at the terminal rectum of cattle and colonisation requires the *LEE4* operon
Microbiology (2005) 151: 2773-81

O'Connell, C.B., Creasey, E.A., Knutton, S., Elliott, S., Crowther, L.J., Luo, W., Albert, M.J., Kaper, J.B., Frankel, G. and Donnenberg, M.S.
SepL, a protein required for enteropathogenic *Escherichia coli* type III translocation, interacts with secretion component SepD
Mol. Microbiol. (2004) 52: 1613-25

O'Gara, J.P. and Dorman, C.J.
Effects of local transcription and H-NS on inversion of the *fim* switch of *Escherichia coli*
Mol. Microbiol. (2000) 36: 457-66

O'Loughlin, E. V., and Robins-Browne, R. M. (2001).
Effect of Shiga toxin and Shiga-like toxins on eukaryotic cells.
Microbes and Infection. 3: 493-507.

Olsen, P.B. and Klemm, P.
Localisation of promoters in the fim gene cluster and the effect of H-NS on the transcription of *fimB* and *fimE*
FEMS Microbiol. Lett. (1994) 116: 95-100

Olsen P.B., Schembri, M.A., Gally, D.L. and Klemm, P.
Differential temperature modulation by H-NS of the *fimB* and *fimE* recombinase genes which control the orientation of the type 1 fimbrial phase switch
FEMS Microbiol. Lett. (1998) 162: 17-23

Osbourn AE, Barber CE, Daniels MJ.
Identification of plant-induced genes of the bacterial pathogen *Xanthomonas campestris* pathovar campestris using a promoter-probe plasmid.
EMBO J. (1987) (1):23-8.

Oshima, T., Ito, K., Kabayama, H. and Nakamura, Y.
Regulation of lrp gene expression by H-NS and Lrp proteins in *Escherichia coli*: dominant negative mutations in lrp.
Mol Gen Genet. (1995) (5):521-8.

Osorio, C.G., Crawford, J.A., Michalski, J., Martinez-Wilson, H., Kaper, J.B. and Camilli, A.
Second generation recombination based *in vivo* expression technology for large scale screening for *Vibrio cholerae* genes induced during infection of the mouse small intestine
Infect Immun. (2005) 73: 972-80

Quitard, S., Dean, P., Maresca, M. and Kenny, B.
The enteropathogenic*Escherichia coli* EspF effector molecule inhibits PI-3 kinase-mediated uptake independently of mitochondrial targeting
Cell Microbiol. (2006) 8(6), 972-981

Perna, N.T., Mayhew, G.F., Posfai, G., Elliott, S., Donnenberg, M.S., Kaper, J.B. and Blattner, F.R.
Molecular evolution of a pathogenicity island from enterohemorrhagic *Escherichia coli* O157:H7.
Infect Immun. (1998) (8):3810-7.

Perna, N.T., Plunkett, G. 3rd, Burland, V., Mau, B., Glasner, J.D., Rose, D.J., Mayhew, G.F., Evans, P.S., Gregor, J., Kirkpatrick, H.A., Posfai, G., Hackett, J., Klink, S., Boutin, A., Shao, Y., Miller, L., Grotbeck, E.J., Davis, N.W., Lim, A., Dimalanta, E.T., Potamousis, K.D., Apodaca, J., Anantharaman, T.S., Lin, J., Yen, G., Schwartz, D.C., Welch, R.A. and Blattner, F.R.
Genome sequence of enterohaemorrhagic *Escherichia coli* O157:H7.
Nature. (2001) 409(6819):529-33. Erratum in: Nature (2001) 410(6825):240.

Phillips, A.D., Navabpour, S., Hicks, S., Dougan, G., Wallis, T. and Frankel, G.
Enterohaemorrhagic *Escherichia coli* O157:H7 target Peyer's patches in humans and cause attaching/effacing lesions in both human and bovine intestine.
Gut. (2000) (3):377-81.

Rediers, H., Rainey, P.B., Vanderleyden, J. and de Mot, R.
Unravelling the secret lives of bacteria: Use of *in vivo* expression technology and differential fluorescence induction promoter traps as tools for exploring niche-specific gene expression
Microbiol. Mol. Biol. Rev. (2005) 69: 217-61

Reece, S., Simmons, C.P., Fitzhenry, R.J., Matthews, S., Phillips, A.D., Dougan, G. and Frankel, G.
Site-directed mutagenesis of intimin alpha modulates intimin-mediated tissue tropism and host specificity.
Mol Microbiol. (2001) (1):86-98.

Riley, L.W., Remis, R.S., Helgerson, S.D., McGee, H.B., Wells, J.G., Davis, B.R., Hebert, R.J., Olcott, E.S., Johnson, L.M., Hargrett, N.T., Blake, P.A. and Cohen, M.L.
Hemorrhagic colitis associated with a rare *Escherichia coli* serotype.
New England Journal of Medicine (1983) 308:681-5

Ritchie, J.M., Thorpe, C.M., Rogers, A.B. and Waldor, M.K.
Critical roles for stx2, eae, and tir in enterohemorrhagic *Escherichia coli*-induced diarrhea and intestinal inflammation in infant rabbits.
Infect Immun. (2003) (12):7129-39.

Robinson, C. R., Sinclair, J.F., Smith, M.J. and O'Brien, A.D.
Shiga toxin of enterohemorrhagic *Escherichia coli* type O157:H7 promotes intestinal colonisation
PNAS (2006) 103:25, 9667

Roe, A.J. and Gally, D.L.
Enteropathogenic and enterohaemorrhagic *Escherichia coli* and diarrhoea
Curr. Opin, Infect, Dis. (2000) 13: 511-7

Roe, A.J., Currie, C., Smith, D.G.E. and Gally, D.L.
Analysis of type 1 fimbriae expression in verotoxigenic *Escherichia coli*: A comparison between serotypes O157 and O26
Microbiology (2001) 147: 145-52

Roe, A.J., Yull, H., Naylor, S.W., Woodward, M.J., Smith, D.G. and Gally, D.L.
Heterogeneous surface expression of EspA translocon filaments by *Escherichia coli* O157:H7 is controlled at the posttranscriptional level.
Infect Immun. (2003) (10):5900-9.

Roe, A.J., Naylor, S.W., Spears, K.J., Yull, H.M., Dransfield, T.A., Oxford, M., McKendrick, I.J., Porter, M., Woodward, M.J., Smith, D.G.E. and Gally, D.L.
Co-ordinate single-cell expression of *LEE4*- and *LEE5*- encoded proteins of *Escherichia coli* O157:H7
Mol. Microbiol. (2004) 54: 337-52

Roesch, P.L. and Blomfield, I.C.
Leucine alters the interaction of the leucine-responsive regulatory protein (Lrp) with the *fim* switch to stimulate site-specific recombination in *Escherichia coli*
Mol. Microbiol. (1998) 27: 751-61

Sambrook, J., Fritsch, E.F., and Maniatis, T. (1989).
Molecular Cloning: A Laboratory Manual, 2nd edition (New York: Cold Spring Harbour Laboratory Press).

Sanchez-SanMartin, C., Bustamante, V.H., Calva, E. and Puente, J.L.
Transcriptional regulation of the orf19 gene and the tir-cesT-eae operon of enteropathogenic *Escherichia coli*.
J Bacteriol. (2001) (9):2823-33.

Schwan, W.R., Seifert, H.S. and Duncan, J.L.
Growth conditions mediate differential transcription of *fim* genes involved in phase variation of type 1 pili
J. Bacteriol. (1992) 174: 2374-5

Schwan, W.R., Seifert, H.S. and Duncan, J.L.
Analysis of the fimB promoter region involved in type 1 pilus phase variation in *Escherichia coli*.
Mol Gen Genet. (1994) (5):623-30.

Sharma, V.K. and Zuerner, R.L.
Role of hha and ler in transcriptional regulation of the esp operon of enterohaemorrhagic *Escherichia coli* O157:H7
J. Bacteriol. (2004) 186: 7290-301

Shaw, R.K., Smollett, K., Cleary, J., Garmendia, J., Straatman-Iwanowska, A., Frankel, G. and Knutton, S.
Enteropathogenic Escherichia coli type III effectors EspG and EspG2 disrupt the microtubule network of intestinal epithelial cells.
Infect Immun. (2005) (7):4385-90.

Siegele, D.A. and Hu, J.C.
Gene expression form plasmids containing the *araBAD* promoter at subsaturating inducer concentrations represents mixed populations
PNAS (1997) 94 (15) : 8168-72

Sinclair, J.F. and O'Brien, A.D.
Cell surface-localized nucleolin is a eukaryotic receptor for the adhesin intimin-gamma of enterohemorrhagic *Escherichia coli* O157:H7.
J Biol Chem. (2002) 277(4):2876-85. Epub 2001 Nov 9.

Smith, D.G.E., Naylor, S.W. and Gally, D.L.
Consequences of EHEC colonisation in humans and cattle
Int. J. Med. Microbiol. (2002) 292: 169-83

Smith, S.G.J. and Dorman, C.J.
Functional analysis of the FimE integrase of *Escherichia coli* K-12: Isolation of mutant derivatives with altered DNA inversion preferences
Mol. Microbiol. (1999) 34: 965-79

Snyder, J.A., Haugen, B.J., Buckles, E.L., Lockatell, C.V., Johnson, D.E., Donnenberg, M.S., Welch, R.A. and Mobley, H.L.
Transcriptome of uropathogenic *Escherichia coli* during urinary tract infection.
Infect Immun. (2004) (11):6373-81.

Snyder, J.A., Haugen, B.J., Lockatell, C.V., Maroncle, N., Hagan, E.C., Johnson, D.E., Welch, R.A. and Mobley, H.L.
Coordinate expression of fimbriae in uropathogenic *Escherichia coli*.
Infect Immun. (2005) (11):7588-96.

Snyder, J.A., Lloyd, A.L., Lockatell, C.V., Johnson, D.E. and Mobley, H.L.
Role of phase variation of type 1 fimbriae in a uropathogenic *Escherichia coli* cystitis isolate during urinary tract infection.
Infect Immun. (2006) (2):1387-93.

Sohanpal, B.K., El-Labany, S., Lahooti, M., Plumbridge, J.A. and Blomfield, I.C.
Integrated regulatory responses of *fimB* to H-acetylneuraminic (sialic) acid and GlcNAc in *Escerichia coli* K-12
PNAS (2004) 101: 16322-7

Spears, K.J., Roe, A.J. and Gally, D.L.
A comparison of enteropathogenic and enterohaemorrhagic *Escherichia coli* pathogenesis
FEMS Microbiol. Lett. (2006) 255: 187-202

Spears, P.A., Schauer, D.A. and Orndorff, P.E.
Metastable regulation of type 1 piliation in *Escherichia coli* and isolation and characterisation of a phenotypically stable mutant
J. Bacteriol. (1986) 168: 179-85

Sperandio, V., Li, C.C. and Kaper, J.B.
Quorum-sensing *Escherichia coli* regulator A: a regulator of the LysR family involved in the regulation of the locus of enterocyte effacement pathogenicity island in enterohemorrhagic *E. coli*.
Infect Immun. (2002) 70(6):3085-93.

Stevens, M.P., Roe, A.J., Vlisidou, I., van Diemen, P.M., La Ragione, R.M., Best, A., Woodward, M.J., Gally, D.L. and Wallis, T.S.
Mutation of toxB and a truncated version of the efa-1 gene in *Escherichia coli* O157:H7 influences the expression and secretion of locus of enterocyte effacement-encoded proteins but not intestinal colonization in calves or sheep.
Infect Immun. (2004) (9):5402-11.

Tatsuno, I., Horie, M., Abe, H., Miki, T., Makino, K., Shinagawa, H., Taguchi, H., Kamiya, S., Hayashi, T. and Sasakawa, C.
toxB gene on pO157 of enterohemorrhagic *Escherichia coli* O157:H7 is required for full epithelial cell adherence phenotype.
Infect Immun. (2001) (11):6660-9.

Toru Tobe, Scott A. Beatson , Hisaaki Taniguchi, Hiroyuki Abe, Christopher M. Bailey, Amanda Fivian, Rasha Younis, Sophie Matthews, Olivier Marches, Gad Frankel, Tetsuya Hayashi, and Mark J. Pallen
An extensive repertoire of type III secretion effectors in *Escherichia coli* O157 and the role of lambdoid phages in their dissemination
PNAS (2006) 103: 40, 14941-14946

Tu, X., Nisan, I., Yona, C., Hanski, E. and Rosenshine, I.
EspH, a new cytoskeleton-modulating effector of enterohaemorrhagic and enteropathogenic *Escherichia coli*.
Mol Microbiol. (2003) (3):595-606.

Viswanathan, V. K., Koutsouris, A., Lukic, S., Pilkinton, M., Simonovic, I., Simonovic, M. and Hecht, G.
Comparative Analysis of EspF from Enteropathogenic and Enterohemorrhagic *Escherichia coli* in Alteration of Epithelial Barrier Function
Infec Immun. (2004) 72: 3218-3227

Vlisidou, I., Dziva, F., La Ragione, R.M., Best, A., Garmendia, J., Hawes, P., Monaghan, P., Cawthraw, S.A., Frankel, G., Woodward, M.J. and Stevens, M.P.
Role of intimin-tir interactions and the tir-cytoskeleton coupling protein in the colonisation of calves and lambs by *Escherichia coli* O157:H7
Infect Immun. (2006) 74: 758-64

Wachter, C., Beinke, C., Mattes, M. and Schmidt, M.A.
Insertion of EspD into epithelial target cell membranes by infecting enteropathogenic *Escherichia coli*.
Mol Microbiol. (1999) (6):1695-707.

Wolff, C., Nisan, I., Hanski, E., Frankel, G. and Rosenshine, I.
Protein translocation into host epithelial cells by infecting enteropathogenic *Escherichia coli*.
Mol Microbiol. (1998) (1):143-55.

Woodward, M.J., Best, A., Sprigings, K.A., Pearson, G.R., Skuse, A.M., Wales, A., Hayes, C.M., Roe, J.M., Low, J.C. and La Ragione, R.M.
Non-toxigenic *Escherichia coli* O157:H7 strain NCTC12900 causes attaching-effacing lesions and eae-dependent persistence in weaned sheep.
Int J Med Microbiol. (2003) (4):299-308.

Wray, C., McLaren, I.M., Randall, L.P. and Pearson, G.R.
Natural and experimental infection of normal cattle with *Escherichia coli* O157.
Vet Rec. (2000) 147(3):65-8.

Wu, Y., Lee, S.W., Hillman, J.D. and Progulske-Fox, A.
Identification and testing of *Porphyromonas gingivalis* virulence genes with a pPGIVET system.
Infect Immun. (2002) (2):928-37.

Xia, Y., Gally, D., Forsman-Semb, K. and Uhlin, B.E.
Regulatory cross-talk between adhesin operons in *Escherichia coli*: inhibition of type 1 fimbriae expression by the PapB protein.
EMBO J. (2000) (7):1450-7.

Xie, Y., Yao, Y., Kolisnychenko, V., Teng, C-H. and Kim, K.S.
HbiF regulates type 1 fimbriation independently of FimB and FimE
Infect Immun. (2006) 74: 4039-47

Yanisch-Perron, C., Vieira, J. and Messing, J.
Improved M13 phage cloning vectors and host strains: nucleotide sequences of the M13mp18 and pUC19 vectors.
Gene 1985; 33 (1): 103-19

Young GM, Miller VL.
Identification of novel chromosomal loci affecting *Yersinia enterocolitica* pathogenesis.
Mol Microbiol. (1997) (2):319-28.

Zhang, L., Chaudhuri, R.R., Constantinidou, C., Hobman, J.L., Patel, M.D., Jones, A.C., Sarti, D., Roe, A.J., Vlisidou, I., Shaw, R.K., Falciani, F., Stevens, M.P., Gally, D.L., Knutton, S., Frankel, G., Penn, C.W. and Pallen, M.J.
Regulators encoded in the *Escherichia coli* type III secretion system 2 gene cluster influence expression of genes within the locus for enterocyte effacement in enterohemorrhagic *E. coli* O157:H7.
Infect Immun. (2004) (12):7282-93.

Appendix I

EHEC O157:H7 – getting to the bottom of the burger bug

Robert J. O. Quantrell, Stuart W. Naylor, Andrew J. Roe, Kevin Spears & David L. Gally

E. coli O157:H7 is a nasty human pathogen, yet it does not harm its cattle host. Dave Gally and his colleagues are finding out why.

Enterohaemorrhagic *E. coli* (EHEC) emerged as a human pathogen in the 1980s through a series of food-borne outbreaks. Its notoriety stems from the severe disease it can cause, especially in the very young and the elderly. EHEC contain integrated bacteriophage genomes capable of expressing a potent toxin known as verotoxin (VT) or shiga-like toxin (SLT) that destroys blood vessels by killing endothelial cells. Damage to blood vessels in the gastrointestinal tract leads to the characteristic bloody diarrhoea associated with this infection. Kidney damage and failure can also be precipitated by the toxin and the very young are more susceptible, due in part to a higher toxin receptor level in the kidney. Fig. 1 outlines the key virulence-associated factors produced by the organism.

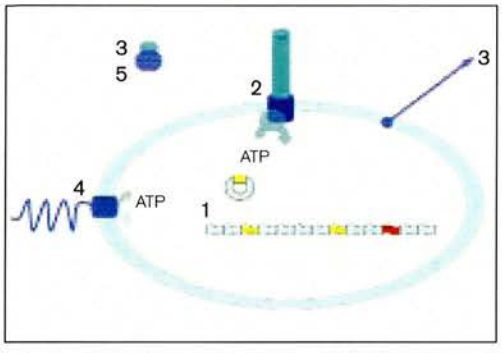

RIGHT (TOP DIAGRAM):
Fig. 1. Diagram illustrating some of the major virulence factors of EHEC O157. (1) Chromosomal DNA contains pathogenicity islands (red and yellow) such as the locus for enterocyte effacement (LEE) that is largely responsible for the attaching and effacing phenotype. Additional virulence traits are carried by the large pO157 plasmid. (2) The LEE encodes a type III secretion system that allows the injection of bacterial proteins into target cells, thereby allowing intimate attachment. (3) Initial bacterial binding to host cells or bacterial spread following attachment may be mediated by fimbriae. (4) Bacterial motility is driven by the presence of flagellae that may enhance penetration of host defences, including mucus, thereby aiding initial attachment to host tissue. (5) Finally, *E. coli* O157 carries a phage-encoded AB toxin known as Shiga-like toxin (SLT) or verotoxin (VT), which can have multiple effects dependent on host and cell type. These include inhibition of pro-inflammatory responses and apoptosis.
COURTESY D.L. GALLY

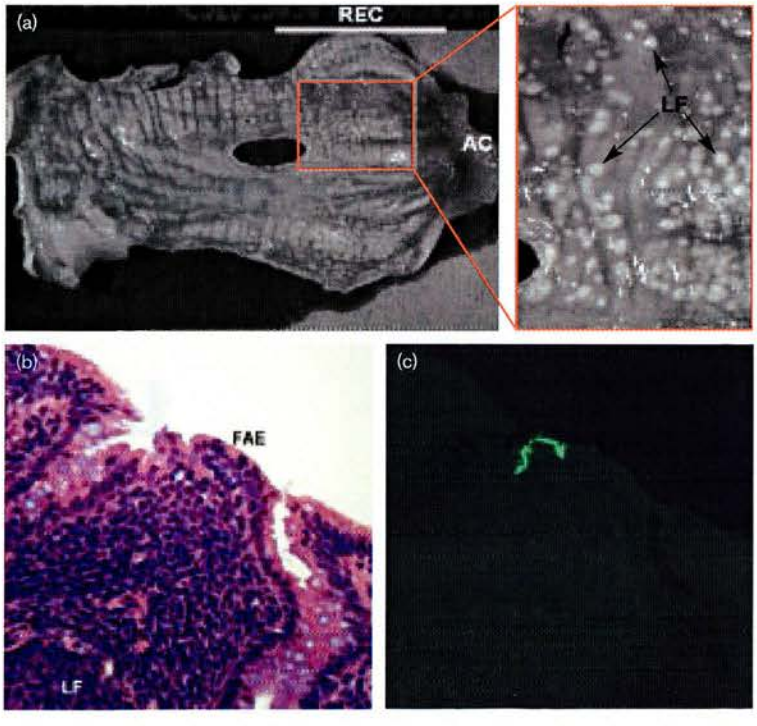

RIGHT:
Fig. 2. Lymphoid follicles at the bovine terminal rectum. (a) Location of lymphoid follicles (LF) after acetic acid treatment of terminal rectal mucosa. AC, anal canal; REC, region of bacterial colonization. (b) H&E stain of a lymphoid follicle (LF) and follicle-associated epithelium (FAE) at the terminal rectum. (c) Microcolony of EHEC O157:H7 (green) situated on FAE.
COURTESY D.L. GALLY

EHEC in cattle

There is now considerable evidence that ruminants, particularly cattle, are the direct or indirect source of most human infections. In the UK, North America and Japan, the main serogroup associated with disease is EHEC O157:H7. Unlike in humans, EHEC O157:H7 does not cause overt disease in cattle and can be considered a commensal. The overall aim of our research is to understand how EHEC O157:H7 colonizes cattle so that interventions can be designed to remove it from this primary host and therefore prevent transmission to humans. A key requirement is to determine where and how EHEC O157:H7 persists in the bovine gastrointestinal tract, as this is a prerequisite to finding the factors involved in bacterial persistence and designing interventions.

The bottom line

Cattle orally dosed with 10^9 EHEC O157:H7 shed up to 10^6 bacteria per gram faeces for at least 4 weeks. In our work to localize the bacterium in cattle, the first few post-mortems of animals shedding high levels of EHEC O157:H7 in their faeces failed to find significant levels at any site within the gastrointestinal tract, including the contents. As a result of this observation, attention turned to the terminal rectum of the animal, with subsequent work demonstrating that the bacteria were really only colonizing the final few centimetres of the gut at the terminal rectum adjacent to the anal canal. EHEC O157:H7 was coating the faeces as the animal defaecated and this was proven by sampling the surface versus the core of the faecal stool (when such separation is possible). The bacteria are therefore being taken in orally and more or less ignore metres of gastrointestinal tract and then colonize in a narrow band adjacent to the anus (this research was supported by a Veterinary Fellowship from DEFRA and was subsequently known as *The Fellowship of the Ring*!). This remarkable tropism explained why others had missed the site in the past and opened up the possibility of simple interventions to remove the bacteria from colonized animals.

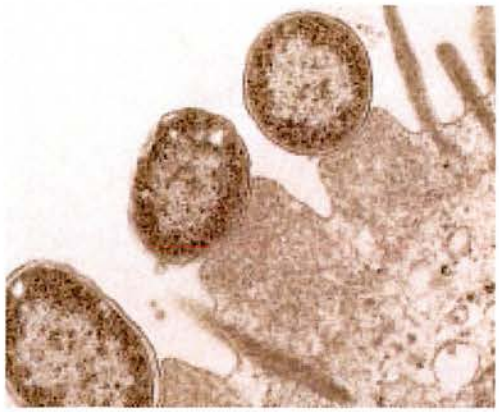

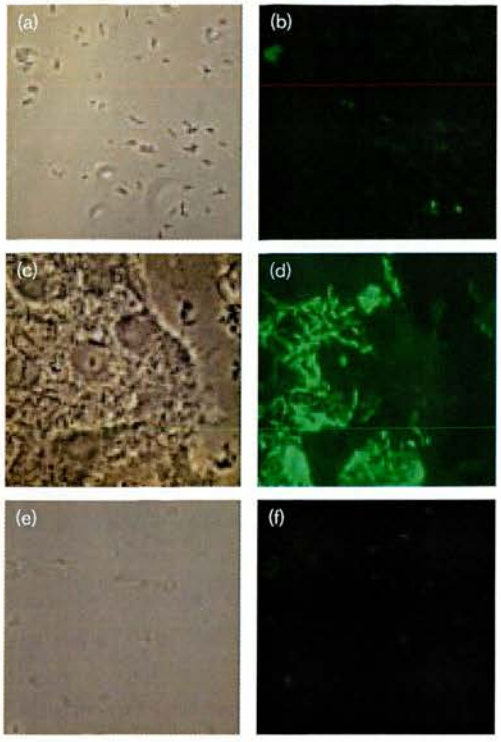

TOP LEFT:
Fig. 3. A/E lesions in the bovine spiral colon induced by a human EHEC O111:H- strain (E43035N) at 4 days post-inoculation.
REPRODUCED WITH PERMISSION FROM *MICROBIOLOGY* **148**, 3767-3778.

LEFT:
Fig. 4. Expression of *tir*::*egfp* in *E. coli* O157:H7 on contact with cultured EBL cells. Cells were incubated with bacteria before fixation at the time points indicated. (b), (d) and (f) show expression of *tir*::*egfp* at 0 min (b), 15 min with EBL contact (d) and 15 min without EBL contact (f). (a), (c) and (e) show bacterial phase contrast images at 0 min (a), 15 min with EBL contact (c) and 15 min without EBL contact (e).
COURTESY D.L. GALLY

The molecular basis of colonization

Attention then turned to the molecular basis of this tropism. Examination of the site of EHEC O157:H7 colonization was not shared by the generic *E. coli* population and revealed a region containing a high concentration of sub-mucosal lymphoid follicles (Fig. 2a). These follicles contain B and T lymphocytes that signal alterations to the epithelium above these structures. This follicle-associated epithelium (FAE) is characterized by a reduction in the levels of mucus-secreting goblet cells and the presence of cells with shortened microvilli. These cells are similar to M-cells found in the small intestine that sample lumenal antigens. In conjunction with work carried out using human gastrointestinal explants, this research indicates that EHEC O157:H7 is likely to interact initially with M or M-like cells in both humans and cattle. Similarly, members of the *Enterobacteriaceae* – *Salmonella*, *Shigella* and other pathotypes of *E. coli* – have been shown to use M-cells as an initial point of interaction with their host.

The obvious downside to contacting M-cells is that their usual function is to take up foreign particles. Bacteria such as *Salmonella* have the capacity to take advantage of this internalization, but this does not appear to be the case for EHEC O157:H7 as it is predominantly extracellular. In common with these other enteric pathogens, EHEC has a type III secretion system that enables the injection of bacterial proteins into host cells (see Figs 1, 5 and 6). The most obvious consequence of this is the formation of attaching and effacing lesions (Fig. 3) and this secretion system is essential for colonization and persistence in cattle. Another fundamental role for this system could be in disabling the M-cell on contact to then allow colonization of the epithelium in that area. This is analogous to the type III secretion system of *Yersinia* spp. that is able to rapidly disable macrophages and prevent phagocytosis. One hypothesis to explain the EHEC O157:H7 tropism is that the type III secretion system is only primed for action by signals present in the lower gastrointestinal tract, thus allowing this specific region to be colonized rather than FAE at higher sites in the gastrointestinal tract. Subsequent spread and persistence of the bacteria at the terminal rectal site will require other components such as flagellae and fimbriae as well as the capacity to multiply in the mucus layer.

EPEC vs EHEC in cattle

In contrast to the related but non-toxigenic enteropathogenic *E. coli* (EPEC), EHEC O157:H7 does not cause disease in cattle and can colonize and potentially recolonize animals for long periods (weeks). This long-term shedding relies on preventing both an

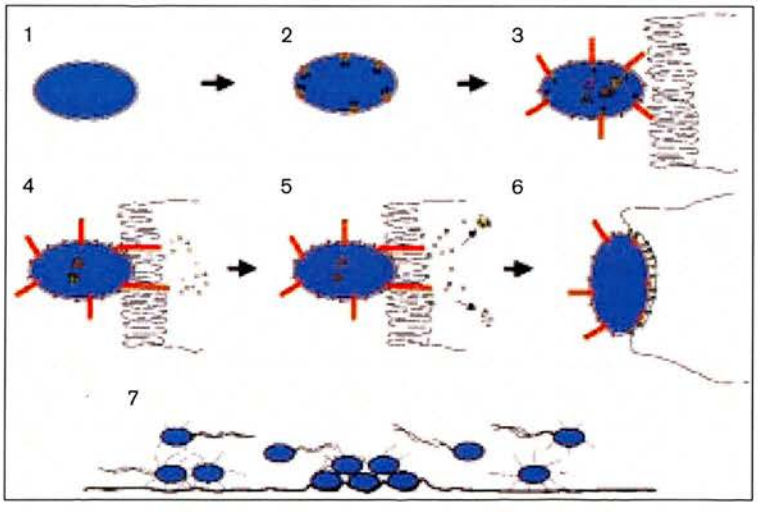

LOWER LEFT:
Fig. 5. Model illustrating primed expression of type III secretion on colonization of the bovine terminal rectum. (1) Transition through the majority of the bovine gastrointestinal tract without epithelial interaction. (2) In the lower gastrointestinal tract a combination of environmental cues, including higher bacteria levels and quorum sensing, lead to expression of the basal type III secretion apparatus. At this time the mRNA for the EspADB translocon may also be produced. (3) With a further signal, such as cell contact, the mRNA is translated and EspA filaments are produced. Transcription of certain type III secreted effector proteins occurs and intimin is expressed and inserted into the bacterial outer membrane (4 & 5). Secretion of effector proteins may occur in a co-ordinated manner, controlled by both expression patterns and differential affinities of effector proteins for shared chaperones that escort the secreted proteins to the apparatus and out of the bacterial cell. (6) Cytoskeletal rearrangements occur as a consequence of the activities of the injected effector proteins and the interaction of intimin with the translocated intimin receptor (Tir). The result is an intimately attached bacterium and an attaching and effacing (A/E) lesion. (7) From this initial binding site the bacteria spread to colonize the surrounding epithelium using a combination of flagellae, fimbriae and type III secretion. This includes possible bacterium–bacterium binding via type IV pili.
COURTESY D.L. GALLY

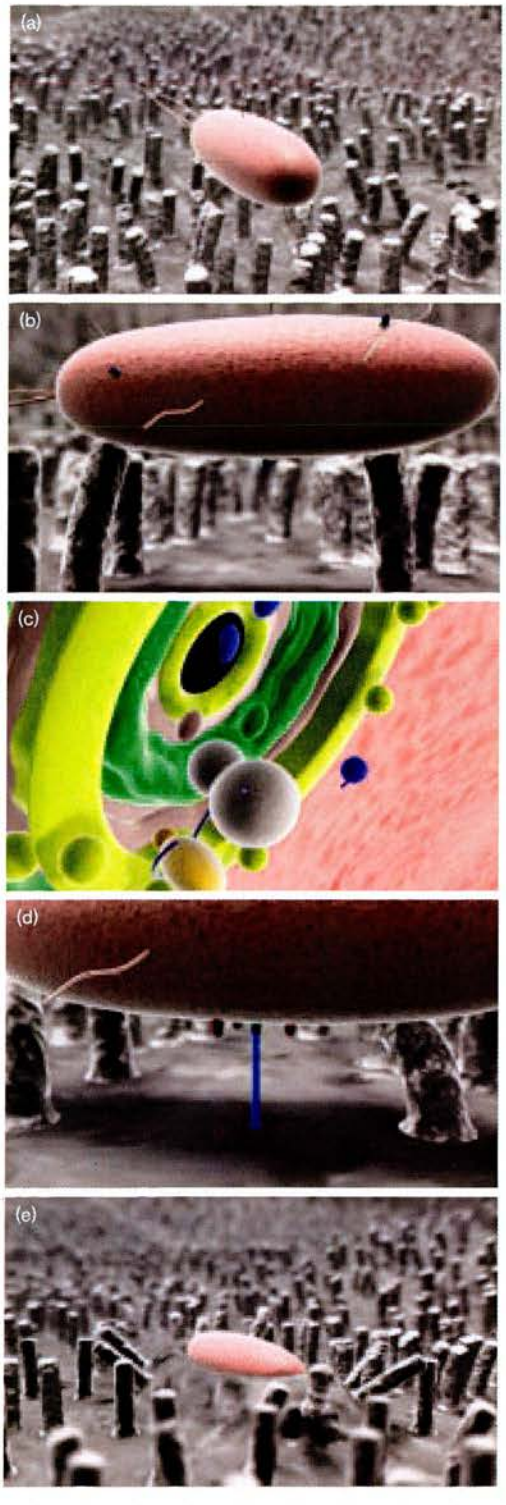

RIGHT:
Fig. 6. (a) EHEC O157:H7 responds to host environmental signals and expresses adhesins on its outer membrane. (b) EHEC O157:H7 binds to microvilli on the host-cell surface. (c) LEE4 (EspADB translocon) mRNA (shown in blue) is translated *in situ* at the inner membrane of the TTSS. The resultant Esp proteins are then exported through the needle complex. In this way translation and secretion are coupled. (d) EHEC O157:H7 produces a long EspA filament that allows the injection of the translocated intimin receptor (Tir) into the host cell where it inserts into the membrane. EHEC O157:H7 then binds tightly to the host cell via this Tir–intimin interaction. (e) Host-cell cytoskeletal rearrangements result in EHEC O157:H7 embedding in the host-cell membrane as part of the formation of an attaching and effacing (A/E) lesion.
COURTESY BIOVISUAL

Further reading

Cornelis, G. (2002). The *Yersinia* YSC-YOP 'type III' weaponry. *Nat Rev Mol Cell Biol* 3, 742–752.

Knutton, S., Rosenshine, I., Pallen, M. J. & others (1998). A novel EspA-associated surface organelle of enteropathogenic *Escherichia coli* involved in protein translocation into epithelial cells. *EMBO J* 17, 2166–2176.

Naylor, S. W., Low, J. C., Besser, T. E. & others (2003). Lymphoid follicle-dense mucosa at the terminal rectum is the principal site of colonization of entero-hemorrhagic *Escherichia coli* O157:H7 in the bovine host. *Infect Immun* 71, 1505–1512.

Stevens, M. P., van Diemen, P. M., Dziva, F., Jones, P. W. & Wallis, T. S. (2002). Options for the control of enterohaemorrhagic *Escherichia coli* in ruminants. *Microbiology* 148, 3767–3778.

inflammatory response and an adaptive immune response on colonization. Multiple factors contribute to this biology.

1. The very restricted site of colonization may limit responses in comparison to generalized colonization of the gut, or gastrointestinal tract.
2. *In vitro*, most EHEC isolates limit expression of important surface antigens such as the type III translocation filaments and intimin; this is in stark contrast to EPEC strains characterized to date that show less restricted expression.
3. The regulation in EHEC O157:H7 has evolved to allow rapid expression of these type III secretion-related factors on contact with host cells (Fig. 4).
4. Other EHEC factors such as VT/SLT appear to inhibit pro-inflammatory cytokine expression.

Having described EHEC O157:H7 as a commensal in cattle earlier in the article, it is clear that this belies a complex multifactorial interaction with the bovine host that leads to colonization by stealth. Transfer this bacterium to humans as an incidental host and the consequences can be devastating. This difference primarily lies with the receptor distribution for the VT/SLT in the two hosts, but also is likely to reflect their differences in colonization patterns, gene expression and signalling pathways. Fig. 5 illustrates the initial sequential interactions envisaged currently

EHEC O157:H7 – the movie

We have worked with a UK-based animation company Biovisual (www.biovisual.co.uk) to produce a full-length animation representing the key stages of EHEC O157:H7 interaction with the host. Biovisual produces custom animations that aim to summarize complex microbiological processes in a 3D environment. Still images illustrating steps in the process are shown in Fig. 6 and the full animation can be viewed at the Biovisual website or at our laboratory homepage (www.vet.ed.ac.uk/zap/research/movie.htm).

Acknowledgments

Research discussed in this article was predominantly funded by a DEFRA Research Fellowship to D. G. and was carried out in a consortium with Professor David G. E. Smith at the Moredun Research Institute, Penicuik and Dr J. Christopher Low at the Scottish Agricultural College (SAC) Veterinary Sciences Division. R. Q. & A. R. are based at UoE and funded by DEFRA. K. S. is based at UoE and funded by the BBSRC. S. N. is funded by DEFRA and based at SAC.

● *Dr David Gally, Zoonotic and Animal Pathogens Research Laboratory, Division of Veterinary Biomedical Sciences, University of Edinburgh, Teviot Place, Edinburgh EH8 9AG, UK.*
Tel. 0131 651 1342; Fax 0131 650 6531
email dgally@ed.ac.uk